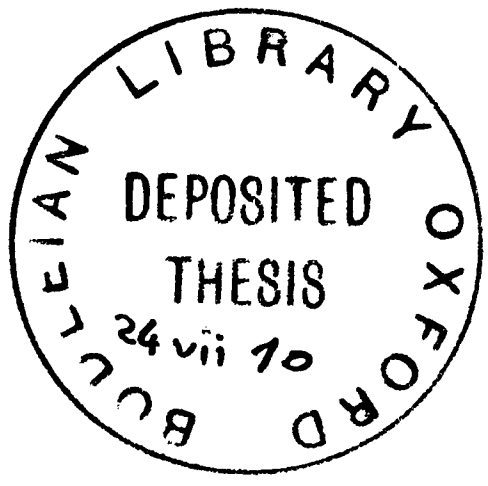
THE PETROLOGY AND GEOCHEMISTRY OF THE BIG SPRUCE LAKE SYENITE COMPLEX N.W.T. CANADA.

BY

MICHAEL PETER MARTINEAU

ORIEL COLLEGE



Thesis submitted for the degree of Doctor of Philosophy in the University of Oxford.

February, 1970.

LIST OF CONTENTS.

Page

ABSTRACT

PREFACE

CHAPTER 1. INTRODUCTION 1
Rock - types 1
Location 1
Previous work 2
Field mapping 4
Analyses 4

CHAPTER 2. GENERAL GEOLOGY OF THE COMPLEX 5
Country Rock 5
Subdivision of the complex 5
Centre 1 6
Centre 2 6
Centre 3 7
Centre 4 7
Centre 5 8
Magma Types 8
Relationship to faulting 9

CHAPTER 3. THE NORTHERN BASIC AND ULTRAMAFIC CENTRE 1 11
General 11
The alkali diorite 12
The marginal diorite 12
The laminated diorites 13
The sequence of crystallization 14
The mineralogy a) Feldspar 14
b) Pyroxene 14
c) Amphibole 15
d) Biotite 15
e) Oxides 15
f) Quartz 15
g) Other minerals 15
The chemistry 16
The relationship to the gabbro and syenites 16
The alkali gabbro 17
General 17
The marginal gabbro 17
The Big feldspar gabbro 18
The Leucocratic Laminated gabbro 18
The Rythmic Banded gabbro 19
The mineralogy 20
The chemical composition 20
The relationship of the units 21
The intrusive olivine magnetite pyroxenites 21
The composition of the pyroxenites 22
Remobilization at the outer contact 22
Remobilization of the gabbros and diorites 23
The mineralogy 23
Detailed mineralogy a) Olivine 24
b) Pyroxene 24
c) Opaque minerals 25
d) Plagioclase 25
e) Biotite and barkevikite 25
f) Apatite 25

	Page
Chemistry	25
The origin of the pyroxenites	26
The associated metasomatism	26
The temperature of crystallization	27
The Alaskan and Ural pyroxenites	27
The relationship of the pyroxenites to the alkali gabbro	27
CHAPTER 4. THE SYENITES OF CENTRE 2	28
Pre-syenite metasomatism	28
Pre-syenite faulting	28
Pre-syenite porhyry dykes	29
Other porphyry dykes	29
The syenites	
General	29
Syenite 1	30
Syenite 2	30
Syenite 3	31
Syenite 4	32
The chemistry	33
Differentiation	34
Relationship to Centre 1	34
Relationship to Centre 2	35
CHAPTER 5. CENTRE 3 ALKALINE UNDERSATURATED ROCKS	36
Porphyry dykes	36
Plagioclase porphyries a) Ultramafic	36
b) Gabbro	36
c) Syenite	36
d) Comendite	37
Anorthoclase and sanidine porphyries	37
a) Rhomb feldspar - pyroxene	37
b) Rhomb feldspar - nepheline	37
c) Nepheline - sanidine	38
Chemistry	38
Conclusions	38
The nepheline syenites	39
General	39
Subdivision of the foyaites	40
Intrusive form	41
Mineral textures	41
Evidence of layering	42
Mineralogy a) nepheline	43
b) feldspar	44
c) aegirine	44
d) other minerals	44
Ijolites	45
Tinguaites	45
Chemistry of the alkaline rocks	46
Agpaitic versus miascitic syenites	46
Relationship to the carbonatites	47
Relationship to centres 1 and 2	48
Origin of the ijolites	49
Layering in the foyaites	50
Nature and formation of the fenites	50
Southern foyaite fenite	51
Northern foyaite fenite	52
Biotite - pyroxenite fenite	52
Composition of the fenites	53
Composition of the fenitizing agent	54

	Page
CHAPTER 6. THE HIGH POTASSIC ROCKS	56
General	56
Moose island centre	56
Magnetic anomaly pattern	56
Shonkinite	57
Minette	58
Biotite - pyroxenite	58
Mineralogy	59
a) Pyroxene	60
b) Olivine	60
c) Biotite	60
d) Feldspar	61
e) Zeolite	61
f-j) Other minerals	61-62
Other high potassic rocks	62
Pseudo - leucite porphyry	62
Biotite - peridotites	62
Lamprophyres	63
Chemistry	63
Differentiation	64
Other biotite-pyroxenites	66
Possible modes of origin of the high potassic rocks	67
1) assimilation	68
2) zone melting	68
3) fractionation	68
CHAPTER 7. CARBONATITE CENTRE 5	70
General	70
Location and rock types	70
Association metasomatism	71
Gas escape vents	71
The carbonatites	72
The dolomitic pipe	73
Dolomite dykes	73
The carbonated biotite-peridotite	74
The calcite carbonatites	74
The mineralogy a) calcite	76
b) biotite	76
c) fluorite	76
d) bastnäsite	76
e-j) other minerals	77
The Bigspruce island pegmatites	77
The metasomatism	77
The carbonatite pegmatites	78
The chemistry of the carbonatites	79
Origin	79
Age and location	81
CHAPTER 8. THE REGIONAL GEOLOGY, GEOCHEMISTRY, AND GENERAL CONCLUSIONS	83
General	83
The Yellowknife subprovince	83
The Great Bear subprovince	85
Post Snare regional geology	86
The relationship of Bigspruce lake to the regional geology	86
Geochemical trends and the magma series	88
Physical conditions of intrusion a) depth	91
b) temperature	91
Comparisons with other alkaline provinces	92
APPENDIX	
LIST OF REFERENCES.	

LIST OF FIGURES

FIG.		PAGE
3-1	Modal Variation in the Alkali Diorite showing the Cryptic Layering	14
3-2	Modal Variation in the Alkaline Gabbro	18
3-3	Chemical Variation in the Alkaline Gabbro	18
3-4	Modal Composition in the Intrusive Pyroxenites	24
3-5	Analyses of Co-Existing Pyroxenes and Olivines from the Olivine-Magnetite Pyroxenites	25
5-1	Normative Trends for the Saturated and Under-saturated Porphyry Dyke Series	38
5-2	Normative Compositions of the Foyaites, Tinguaites and Ijolites	47
5-3	Normative Compositions of the Foyaite Fenites in Comparison to the Compositions of the Granodiorite and Chilled Foyaite	55
6-1	Subtraction Diagram to Illustrate the Composition of the Material Removed in the Formation of the Biotite Pyroxenite from the Shonkinite	66
7-1	Sketch Map of the Cone Sheets and Radial Dykes Surrounding the Dolomitic Breccia Pipe.	74
7-2	Sketch Map of the Distribution of Calcitic Carbonatites Marginal to the Bigspruce Island Pegmatite Centre.	74
7-3	Distribution of the North American Carbonatites and Kimberlites	81
7-4	Distribution of the North American Carbonatites and Kimberlites in Comparison with the Region of High Mean Crustal Velocity	81
7-5	Equilibrium Curves for the Co-Existing Phases Tremolite + Calcite + Quartz	82
8-1	Summary of the Geochemical Trends from Centres 1-4. a) $CaO-Na_2O-K_2O$ diagram	89
8-2	Summary of the Geochemical Trends from Centres 1-4. b) $MgO-FeO-(Na_2O+K_2O)$ diagram	89

LIST OF PLATES

PLATE		PAGE
1-1	Aerial Photograph of Bigspruce Lake	2
2-1	Aeromagnetic Intensity Map of the Bigspruce Lake and Moose Island Areas	6
3-1	Contact between Cumulus and Chilled Diorite	13
3-2	Acicular Hollow Apatite in Chilled Diorite	13
3-3	Lamination and Whispy Banding in Diorite	14
3-4	Persistant Mafic Mineral Banding in Diorite	14
3-6	Cumulus Plagioclase, Texture of the B.F.G.	21
3-7	Mafic Aggregate in the Big Feldspar Gabbro	21
3-8	Lamination in the lower Leucocratic Gabbro	21
3-9	Mafic mineral banding in the Lower L.L.G.	21
3-10	Cross-bedding of the Mafic Mineral Bands	21
3-11	Persistant Rhythmic Bands in the Lower R.B.G.	21
3-12	Complementary Magnetite-Pyroxenite, and Anorthosite Bands. Middle R.B.G.	21
3-13	Impersistant Trough Banding, Middle R.B.G.	21
3-14	Cumulus Magnetite-Pyroxenite, Middle R.B.G.	21
3-15	Magnetite-Pyroxenite Dyke Crosscutting L.L.G. Banding	28
3-16	Texture of the Chilled Magnetite-Pyroxenite	28
3-17	Detail of Chill Margin to Olivine-Magnetite-Pyroxenite Dyke	28
3-18	Hybridization and Remobilization of the L.L.G.	28
3-19	Texture of the Olivine-Magnetite-Pyroxenite	28
3-20	Oscillatory Zoned Pyroxene, and Barkevite	28
3-21	Pyroxenite Dyke Intruding the Fault A-A, Arete Lake	28
3-22	Pyroxenite Dykes Displaced Along Shear Zones	28
4-1	Spalling of the Diorite at the Ring Syenite Contact S_3	36
4-2	Zoning of Rhombic Feldspar, Mafic Quartz Syenite S_4	36
4-3	Interstitial Quartz and Amphibole, Syenite S_2	36
4-4	Perthite Texture in Peralkaline Syenite Dyke	36

LIST OF PLATES

PLATE		PAGE
5-1	Multiple Porphyry Dyke, Associated with Pre-syenite Faulting	39
5-2	Sanidine and Nepheline Phenocrysts in a Porphyry Dyke	39
5-3	Vertically Laminated Sanidine Phenocrysts Southern Foyaite Chill	43
5-4	Foyaite-Urtite Transition Southern Foyaite	43
5-5	Feldspathic Foyaite-Pulaskite Contact. Southern Foyaite	43
5-6	Urtite Xenolith in Pulaskite. Southern Foyaite	43
5-7	Detail of Fine-Scale Silica Zoning in Nepheline Northern Foyaite	46
5-8	Fractured Nepheline Xenocrysts in Ijolite	46
5-9	Texture of the Unalterred Granodiorite	54
5-10	Biotite Coated Fracture. Outer Southern Foyaite Fenite	54
5-11	Albite and Arfvedsonite Reaction Rims Around Quartz	54
5-12	Biotite, Albite, and Arfvedsonite Reaction Rims	54
5-13	Pseudomorph of Quartz Patch in Syenite Fenite	54
5-14	Aegirine Replacing Arfvedsonite, Syenite Fenite Northern Foyaite	54
5-15	Mesoperthite Replacing Sericitized Feldspar, Biotite-Pyroxenite Fenite.	54
5-16	Crystal Settling of Apatite in a Layered Calcite vesicle	54
5-17	Fenitized Fracture in Granodiorite. Termination of a Minette Dyke. Moose Island	54
5-18	Fenite Margined Veinlets in Granodiorite. Syenite Filled Fractures Radiating from the Northern Foyaite	54
6-1	Biotitic Reaction Rim Around Granodiorite Xenolith.	56
6-2	Pyroxene and Magnetite Phenocrysts, Chilled Shonkinite	56
6-3	Sub-Angular Xenoliths in Shonkinite Breccia-Pipe	56
6-4	Olivine Phenocrysts with Biotite Reaction Rims, Breccia Pipe	56
6-5	Coarse Shonkinite with Biotite-Pyroxenite Schlieren	56
6-6	Pyroxene and Olivine in Coarse Shonkinite	56
6-7	Pyroxene and Biotite Phenocrysts in Minette	58
6-8	Zoned Biotite Phenocrysts in Minette	58

LIST OF PLATES

PLATE		PAGE
6-9	Mineral Texture of the Bictite-Pyroxenite	58
6-10	Drill-Core Sections from the Biotite-Pyroxenites	58
6-11	Calcite rhombs in Aegirine. Sövite vein in Biotite-Pyroxenite	58
6-12	Pseudoleucite Phenocrysts in a Porphyry Dyke	58
7-1	Sövite Pegmatite centre, Bigspruce Island, Aerial Photograph	78
7-2	Margin of the Magnetite-Dolomite Breccia Pipe	73
7-3	Outer Cone-Fracture of Gas Escape Vent B.	73
7-4	Calcite Vesicle in chilled Biotite-Peridotite	74
7-5	Carbonate-Biotite-Fluorite Replacement of Chilled Biotite Peridotite	74
7-6	Interstitial Calcite in Coarse Biotite Peridotite	74
7-7	Serpentine Pseudomorph after Biotite, Dolomite Breccia Plug	74
7-8	Stellate Apatite, Dolomite Breccia Plug	74
7-9	Dolomite-Plate Phenocrysts, Chilled Dolomite Dyke	74
7-10	Biotite-Sövite Breccia Pipe	77
7-11	Biotite Phenocrysts in a Biotite Sövite Dyke	77
7-12	Quartz Veins in a Bastnasite Sövite ?Plug	77
7-13	Globular Intergrowths of Fluorite and Calcite in Fluorite-Sövite	77
7-14	Foliated Bastnäsite-Sövite Dyke	77
7-15	Bastnäsite Aggregate in a Sövite Dyke	77
7-16	Quartz-Sericite Gneiss, Shear Zone in Sövite Fenite	77
7-17	Pyrochlore Bordering Titanomagnetite. Sövite-Pegmatite. Big Spruce Island	77

LIST OF MAPS

MAPS		PAGE
1-1	Locality Map for Bigspruce Lake	2
1-2	Previously Known and Inferred Geology of Bigspruce Lake	4
2-1	Outline Sketch Map of the Intrusive Centres and of the Main Intrusive Units	6
2-2	Sketch Map of the Faults and Lineaments Surrounding Bigspruce Lake	9
3-1	Distribution of the Rock Types within Centre 1	12
3-2	Distribution of the Magnetite Pyroxenites and of the Divisions of the Alkaline Gabbro	18
3-3	Second Derivative of the Aeromagnetic Anomaly for Centre 1	22
6-1	Distribution of the Rock Types in theHigh Potassic Centre 4	56
6-2	Second Derivative of the Aeromagnetic Anomaly for Centre 4	57
6-3	Radial Joint System, and Minette Dykes Around the Shonkinite Pipes	58
7-1	Photogeology of Centre 5	71
8-1	Faults Lineaments and Structural Provinces in the Northwest Canadian Shield	84
8-2	Sketch Map of the Structure and Facies of the Snare Metasedimentary Belt	86

LIST OF TABLES

TABLE		PAGE
2-1	The Intrusive Form and Sequence	6
3-1	Analyses of the Alkali Diorites	16
3-2	Analyses of the Alkali Gabbro	20
3-3	Analyses of the Intrusive Pyroxenites	25
4-1	Analyses of Syenites 1 and 3	33
4-2	Analyses of Syenites 2 and 4	33
4-3	Analyses of peralkaline Syenite Dykes	33
5-1	Porphyry Dykes Analyses	38
5-2	Analyses of the Northern Foyaites and Southern Foyaites	46
5-3	Analyses of the Tinguaites and Ijolites	46
5-4	Analyses of the Granodiorites and Fenites	55
6-1	Analyses of the High Potassic Rocks	63
6-2	Modes of the High Potassic Rocks	63
7-1	Trace Element Content of the Carbonatites	79

A B S T R A C T.

The aeromagnetic anomaly high at Bigspruce lake N.W.T. is located over an alkaline and carbonatite complex. Approximately two-thirds of this complex is submerged, but sufficient rock is exposed on the shores and islets to reconstruct the original intrusive form and sequence.

The rock-types are distributed in five geographic and petrographic centres showing a successive southerly migration. These are -

Centre 1 - saturated diorite, gabbro, olivine-magnetite-pyroxenite.
Centre 2 - saturated and oversaturated syenites.
Centre 3 - undersaturated foyaites and ijolites.
Centre 4 - saturated (high potassic) shonkinites, minettes, biotite-pyroxenites.
Centre 5 - silico-carbonatite and carbonatite, sovite and dolomite carbonatite.

Centre 1 is located to the northeast of the main lake. It is composed of an outer diorite, and a later inner gabbro,layered intrusion, surrounded by arcs of olivine - magnetite - pyroxenite, and syenite intruded along a marginal ring fracture.

Both the diorite and the gabbro possess broad wall-rock zones in rapid gradational contact with central laminated differentiates. The diorite lacks significant cryptic variation, but the gabbro is divided into anorthositic and gabbroic series showing the crystal accumulation of olivine, apatite and calcic plagioclase towards the base of the intrusion. The operation of continuous convection currents is evidenced by the radial dip of the lamination and the winnowing of the mafic minerals. Stronger intermittant currents in the gabbro are evidenced by radial trough banding, and rhythmic banding.

The olivine-magnetite-pyroxenites are composed of olivine Fo_{66-63}, clinopyroxene $Ca_{44.6}\ Mg_{55.8}\ Fe_{9.6}$, magnetite and ilmenite in the approximate modal proportions 19: 59: 17: 5. Minor barkevikite, biotite and apatite occur as an alkaline matrix. Quenching to magnetite-pyroxenite at the margins, remobilization of the contact granite or gabbro, and comparison of the modal composition with the field boundaries in the synthetic system ol - cpx - iron oxide demonstrate that these rocks crystallized from an ultramafic magma containing a small percentage of olivine and pyroxene phenocrysts. A temperature of intrusion of 1100 - 1200° is deduced. Although no descriptions of comparable rocks have been found these are regarded as the alkaline, ilmenite-rich,equivalents of the Alaskan-type zoned ultramafic intrusions.

Centre 2 spans the northern half of the lake. It contains two concentric ring dykes of quartz syenite to the south, and two quartz free syenites around the margin of centre 1. The intrusion of these syenites followed an episode of transcurrent faulting which bisected centre 1.

Mineralogically and in geochemistry the syenite series forms a continuation of the gabbro-diorite series, and spans the transitions pyroxene -

alkali amphibole, and plagioclase→alkali feldspar ($An_{52}\rightarrow An_{28}\rightarrow Or_{38}$). A few late syenite dykes are peralkaline, and include aegirine bearing comendites.

Centre 3 occupies the southern half of the lake. It is dominated by a 3·4 x 2·1km body of pegmatitic foyaite rimmed by chilled vertically laminated foyaite, and 10 - 100m of zoned fenite. A finer grained more mafic foyaite covers Bigspruce and Littlespruce islands. Both foyaites are composed of cryptoperthite Or_{66}, nepheline Ne_{69}, and aegirine and show a differentiation into feldspathic, nephelinic, and ijolitic horizons with low angle contacts, and a concentric distribution. This form is interpreted in terms of the preferential crystal settling of feldspar plates in the absence of convection currents. Both the foyaites show a chill composition lying within the low temperature "foyaite sink" in the system Qtz - Ne - Ks. Breccia pipes of sodic ijolite transitional into cancrinite foyaite are marginal to the carbonatite pegmatite focus of Bigspruce island. A possible origin through breccia - fluid exchange reactions involving the loss of K_2O and SiO_2 in the presence of abundant H_2O and Na_2CO_3 is suggested.

High potassic rocks occur predominantly within a subsiduary complex 5km to the southeast of the lake, but identical types occur in close association with the carbonatites. They are composed of pyroxene, olivine, biotite, oxide, apatite and cryptoperthite Or_{50}, with a maximum feldspar content of circa 50%. The shonkinite forms dykes and breccia pipes of similar form and composition to those of the Navajo area, Arizona. The biotite-pyroxenites also form pipes, are transitional into shonkinite through the loss of feldspar, and are surrounded by zoned fenites. They are closely comparable to the stock of Libby, Montana, and to the "O.B.P." nodules found in the East African potassic provinces. Comparisons of the volume and composition of the fenite, pyroxenite and shonkinite are used to show that the biotite-pyroxenite may have originated from the shonkinite through the loss of normative feldspar to the wall rock in a fluoride-rich aqueous fluid phase.

Both the foyaite and pyroxenite fenites resemble those of Fen, Alno and Chishanya, with concentric zones of aegirine-perthite-syenite, arfvedsonite-albite-quartz-syenite and biotite microgranite. The principal geochemical changes are the transfer of silica into the microgranite, and the transfer of feldspar with similar K : Na, ratio to the foyaite or "shonkinite" magma into the syenites.

The carbonatites of centre 5 outcrop within two cone sheet and radial dyke foci of dolomitic and calcitic composition respectively. The dolomite focus lies on the east side of the lake within a fault bound structure. It consists of a central breccia plug of biotite-ankerite carbonatite surrounded by inwardly dipping sheets of dolomite defining a focus $>$ 300m deep. The silicate content of the rock and iron content of the dolomite decrease away from the centre. There is a complete transition within these rocks from calcite bearing biotite-peridotite to carbonatite. On the basis of these replacement reactions a temperature

of intrusion of 500 -560°C is deduced.

The sovite focus lies on the west side of Bigspruce island. It shows a well-defined radial dyke and cone-sheet distribution of silicate-calcite pegmatites associated with Fe, Ti, Ca, Nb, R.E., CO_2, H_2O, Cl metasomatism. Multiple fracturing and intrusion within these pegmatites shows a sequence of-Aegirine + magnetite + calcite; Biotite + magnetite + calcite + pyrochlore; Biotite + calcite + bastnasite. Biotite carbonatite, fluorite carbonatite, and bastnasite carbonatite occur as peripheral satellite bodies.

Mineral textures in the carbonatites give evidence of chilling, quenching and the crystal settling of apatite within the magmas. The close similarity of the trace element content and volatile content support the derivation of the carbonatites from the high potassic parent magma. The $Sr^{87/86}$ ratio of 0.7020 from the calcite and dolomite supports a mantle derivation for this parent.

Within the exposed rock types three main differentiation trends may be distinguished. These are -

1. Alkali gabbro - alkali diorite - syenite - quartz syenite-comendite.
2. Alkali gabbro - rhomb syenite - sanidine syenite - foyaite.
3. Biotite peridotite - shonkinite - biotite pyroxenite.

The geochemical series 1 and 2, as illustrated by the Ca: Na: K and Mg: Fe: Alk diagrams, more closely resemble those of the Gardar province than those of the Oslo or Monteregian provinces but show a lesser degree of iron enrichment, and a greater enrichment in soda relative to Ca and K. These differences are thought to be due to the early disappearance of olivine as a fractionating phase, and to the dominating influence of feldspar fractionation in both series.

Although both the saturated and undersaturated trend may ultimately be derived from the same parent and the composition of the magnetite-pyroxenite shows that it is related, the potassic series is believed to be derived from a distinct high potassic peridotitic parent of mantle origin.

The differentiation of these magmas is believed to have taken place simultaneously in a series of independent magma chambers located within the prism of shattered rock at the intersection of a system of N-S and E-W transcurrent faults. The intrusion of the derived magmas was closely related to movement on the N-S fault system.

On a regional scale the complex is located at the centre of a dome of granitic rocks close to the border between the Slave and Bear provinces. The age of the complex at 1820 m.y. is similar to the age of uplift of the neighbouring Snare orogenic belt. At the present time these rocks form the oldest known alkali-carbonatite centre.

P R E F A C E .

This thesis would not have been possible without the willing help of many people at Yellowknife, and at Bigspruce Lake. In particular thanks are due to E. Newcombe, and to C. Calland C.M. of the North Canada Power Commission for providing and servicing a canoe, for stores, for air transport at minimal rates and for much advice on working around Bigspruce Lake.

M.B. Roberts acted as field assistant in 1967 mapping singlehanded most of the northern centre. This help is very much appreciated.

In the spring of 1968 Giant Yellowknife Mines staked most of the complex. Dr. G.P. Legagneur and R.W. Spence of the company generously supported a second field season and also made available the results of subsequent mapping, and drilling within parts of the complex. C. Lamb, L. Burgess, and G. Hildebrandt, working for G.Y.M. gave valuable field assistance in 1968. In particular they located the outlying high potassic and dolomite centres which might otherwise have been missed.

Dr. R. St.J. Lambert has supervised the thesis, given much relevant discussion of the conclusions and made available his rocks and maps from a 1963 visit to the lake.

R. Goodwin determined K-Ar ages on 2 biotites, Dr. R.J. Pankhurst determined the $Sr^{87/86}$ ratios of 2 carbonates, C. Fagg analysed by microprobe 5 pyroxenes and olivines, Mrs. J. Wigley analysed 4 rocks for comparison with the X.R.F. analyses.

Prof. E.A. Vincent, Dr. J.D. Bell, T. Deans, Dr. D.C.R. Kempe, Dr.R.St.J.Lambert, Dr.G.Muecke, Dr.R.J.Pankhurst and Dr.B.G.J. Upton supplied analysed powders for use as standards in the X.R.F analysis.

Finally, I express my sincere thanks to Mrs. G. Fawcett for typing an illegible manuscript, to Mrs. J. Martineau for copying diagrams and to R.. Holland for numerous thin sections.

CHAPTER I. INTRODUCTION.

Rock-types.

Bigspruce Lake overlies a plutonic complex of quite remarkable diversity. The rock types include two basic alkaline layered intrusions, a group of syenite ring dykes, two stocks of foyaite, pipes of ijolite, shonkinite, biotite-pyroxenite and carbonatite, and several accompanying dyke swarms. These rock types belong to ultramafic, saturated alkaline, peralkaline, undersaturated alkaline, high potassic basic, and carbonatite suites, and are usually represented in significant quantity.

Location.

The complex is centred at 63°33'N, 115°56'W nine miles south of Kwejinne Lake, and ninety miles north-west of Yellowknife.

Yellowknife, the capital of the North-west Territories, Canada, is a gold-mining town with circa 5,000 population, on the north shore of the Great Slave Lake. It is situated about 750 miles due north of Edmonton, to which it is linked by regular air and road services. The railway, built for the Pine Point ore-body, links with a ferry service across the lake at Hay River.

Bigspruce Lake may be reached by hired float plane from Yellowknife, or on the fortnightly plane supplying one of the two dam-sites lower down the Snare River. Transport around the lake is best provided by a light canoe powered by an outboard motor, which can easily be beached on the shelving shoreline.

The country around shows a typical subdued shield topography. The present lake level lies at 740 ft., whilst the average height of the surrounding plateau is 810 ft. There is a gentle slope south-west towards the shield margin.

In 1946, as a result of the development of the goldmines near Yellowknife, and of the Uranium mines near Port Radium on the Great Bear Lake, two hydro-electric plants were begun on the Snare River rapids. The upper-most of these lay in the south arm of Bigspruce Lake, and raised the lake level by forty feet. Although much marshy ground was submerged, together with some low reefs, the loss of rock exposure was probably slight. The main effect was to cause all shores to be rimmed with a dangerous swathe of dead submerged pine logs, which may make landing difficult. Ice erosion, combined with fluctuating lake level, has cleared a six foot rock band around most shores. About sixty percent of the complex now lies under water.

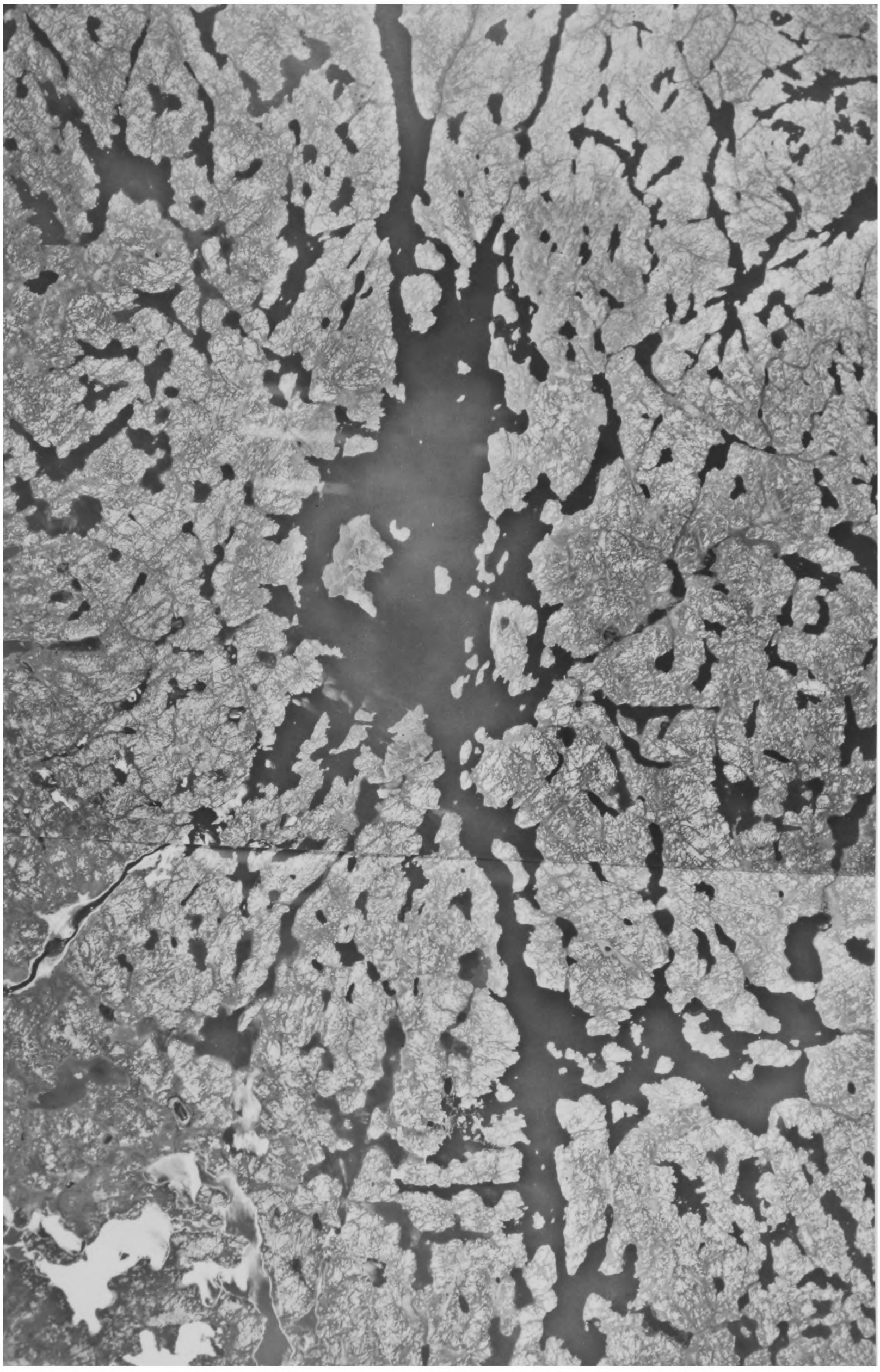
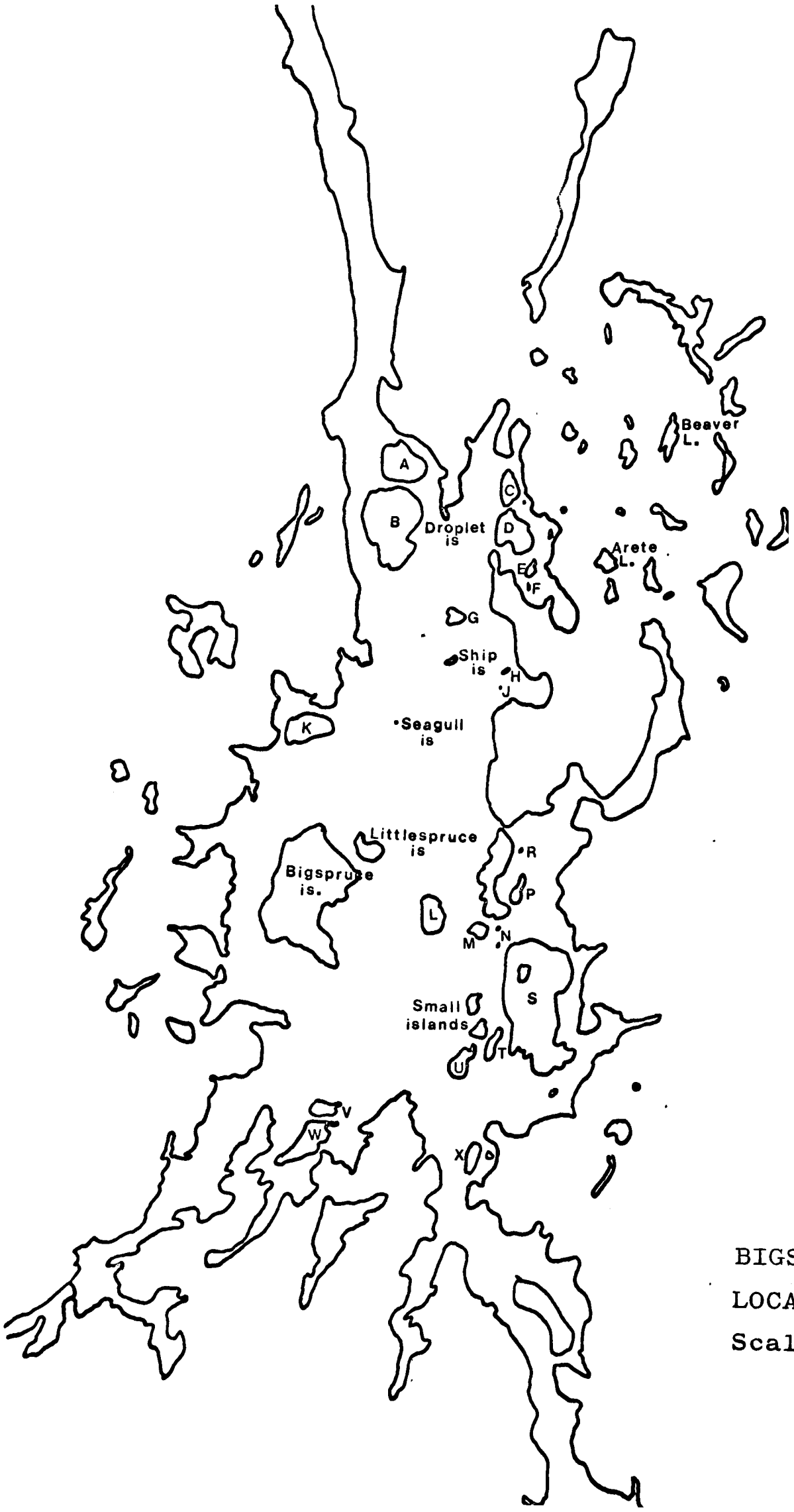


PLATE 1 - 1 Aerial photograph of the Big Spruce Lake and Moose island complex areas. The margin of the complex is outlined by the edge of the darker, more densely forested intrusive rocks. The N-S transcurrent fault A - A the East coast lineament B - B the N. Snare river fault C - C, and the south Snare fault D - D form strong linear, eroded features. The cone - fractures, and radial fractures of the gas escape vents (A), (B), (H), (C), and (J) (see Map 7 - 1) can also be distinguished.

MAP 1 - 1 LOCALITY MAP FOR BIGSPRUCE LAKE



BIGSPRUCE LAKE

LOCALITY MAP

Scale 1 inch to 1 mile

The intrusive rocks stand out on aerial photographs by virtue of their denser vegetation. Granodiorite supports a thin cover of stunted spruce, white birch, aspen and jackpine; the complex supports dense stands of jackpine, spruce and wide areas of muskeg. Ultrabasic and ijolitic rocks are particularly densely covered, owing to their ready breakdown on weathering.

In 1964 a forest fire swept down the east side of the Snare River, from north to south, stripping the tree cover from the complex on the east side of the lake. Subsequent erosion has removed much of the remaining moss or lichen cover. It is doubtful whether adequate field mapping could have been done in these areas without this help. This may be the reason why many of the features, particularly layering in the basic rocks, passed unnoticed by previous visitors to the complex.

Previous Work.

Mapping in the North-West Territories has been extensively dependant on the incentive of mineral exploration. The early explorers, such as Sir John Franklin, noted salt springs and mineral stains of copper and cobalt on their route from the Great Slave Lake up the Mackenzie River to the Great Bear Lake and the Coppermine River. However, Dr.R.Bell, exploring the region around the Great Slave Lake in 1900, could still conclude that "The region.....has remained practically unknown geologically and to a great degree geographically." (R.Bell 1900)

By 1920 veins of cobalt, copper, and pitchblende ores had been found around the Great Bear Lake, and down the western margin of the shield. D.F.Kidd reported on these areas in 1933 and 1936. In 1935 gold was discovered on the west side of Yellowknife bay, and in 1938 further promising discoveries were found to the east of Yellowknife. At the same time gold was found on the Snare River, and at Mosher, Russel, Slemon and Indin Lakes, in the Snare River-Ingray Lake map areas. These districts were explored by C.S.Lord, J.T. Wilson and others, between 1938 and 1940 (Lord 1942). During this mapping the alkaline complex at Bigspruce Lake was discovered. Lord's two-page account is the only pre-flooding description of the area. He noted the occurrence of a variety of syenitic rocks, mostly nepheline bearing, but including diorite, nordmarkite, and amphibolite. He noted that the basic rocks occurred mainly in the area north-east of the lake and, tantalizingly, described how the rocks of the complex appeared to intrude,

> "a small body of white crystalline banded limestone, of probably snare age" on the north-west shore.

The surrounding granites he divided into two series, Proterozoic and Archean, associated with the Snare and the Yellowknife metasediments or metavolcanics respectively. The complex was seen to intrude Archean granodiorites, and, on the basis of the "limestone", was assumed to be of Snare age.

Subsequent age work of the Canadian Geological Survey has confirmed his mapping in all but a few details. Granodiorites in his Archean areas yield ages in excess of 2400 m.y.,whilst those from the Proterozoic yield ages in the vicinity of 1800 m.y. A biotite age from the northern foyaite (centre 3-2) gave an age of 1785 m.y. (Leech et al 1963 - G.S.C. 62 - 92), which is similar to ages from small intrusives in the neighbouring Bear (Proterozic) province.

Baragar (in Leech et al 1963) noted a complete transition from nepheline syenite to granite in what is now recognised as a fenitized granodiorite zone.

By 1963 several carbonatites were known in eastern Canada, and the characteristic high magnetic anomaly resulting from the associated magnetite-rich rocks had been noted. When the aeromagnetic map of the area (G.S.C. geophysical paper No.2966 1963) (Map 1-3)was seen to show a prominent positive anomaly over the north-east segment of the complex, Kennco prospected the area for a possible carbonatite, but without success (Deans and Gittins pers comm). Subsequently, and for a similar reason, Giant Yellowknife Mines began an investigation (1968). It is ironical that in both cases the main interest focused on the northern centre in which no carbonatites are known.

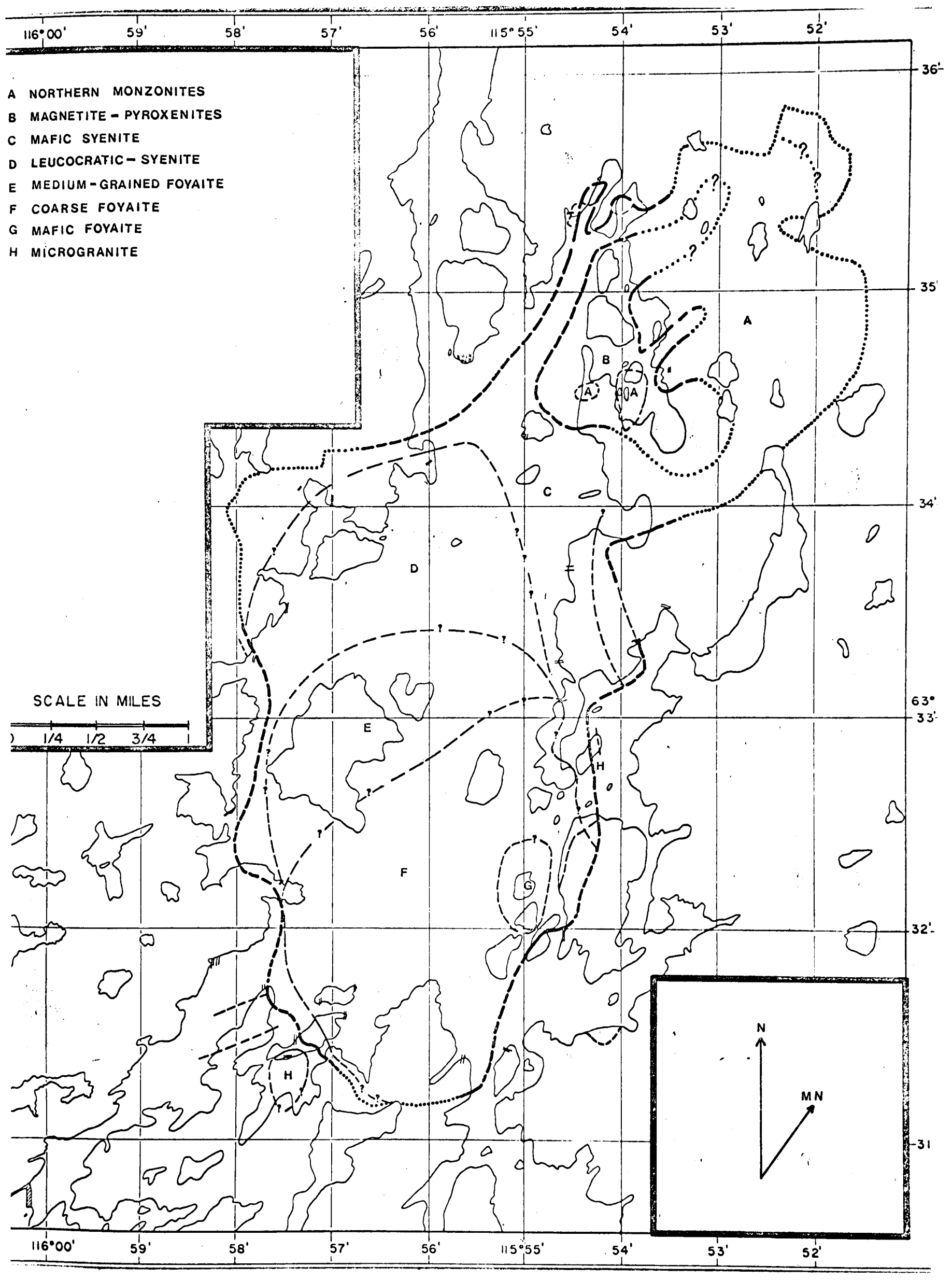
Amongst other features, Kennco noted the occurrence of a ring of quartz-syenite separating the (northern) intrusives from the granitic rocks. This ring dyke belongs to the syenitic centre (2-3).

At the suggestion of Professor R.E.Folinsbee, Dr.R.St.J.Lambert visited the complex for four days in 1964. From the aerial photographs, field notes, and collected specimens, he drew up a map (map 1-2) which bears many resemblances to the present geological map (map 2-1). He stressed (Lambert 1964) the division into two segments, as recognized by Lord, a northern segment containing diorites and magnetite-rich pyroxenites and a southern segment dominated by foyaites.

Between the two, and assigned to the southern segment, he recognised a lunate zone of quartz bearing syenites. He was unable to observe any significant internal contacts, and was therefore forced to conclude that

MAP 1 - 2 PREVIOUSLY KNOWN AND INFERRED GEOLOGY OF BIGSPRUCE LAKE

(LAMBERT 1964)



"the various members of the complex were emplaced closely upon one another with, presumably the outer (syenitic) members first, followed by the nepheline-bearing rocks".

This lack of internal exposed contacts remains a problem even away from the shore, but for the most part, appears to result from the erosion of the interface rather than through hybridization.

Field Mapping.

This thesis results from two visits to the complex, of one month each, in the summers of 1967 and 1968. In 1967, Mr.M.B.Roberts acted as field assistant, mapping - often single-handed - most of the area of centre 1. The difficulty of this task may be appreciated from the aerial photograph and the photographs of the exposure in centre 1. In 1968 field work was carried out in co-operation with two students working for Giant Yellowknife mines; Dr.R.St.J.Lambert accompanied the party for part of the stay. The work concentrated on detailed mapping in centre 1, in the marginal carbonatite areas, and in the two areas of "diabase" located by L.Burgess working for G.Y.M. The first of these was the vent of magnetite-dolomite carbonatite; the second was the Moose Island centre (centre 4) composed of shonkinite, minette, and biotite-pyroxenite. The extensive help received from G.Y.M. is gratefully acknowledged, as is access to the results from two drill holes they have since completed.

Mapping was carried out on foot or by canoe, on a base map of approx 1:10,000 derived from pre-flooding 1:25,000 aerial photographs. Coastlines were drawn by eye from 1:50,000 post flooding aerial photographs. For the Moose Island complex, 1:20,000 base maps were used, derived from post-flooding aerial photographs. No attempt to remove the resulting distortion has been made. Aeromagnetic survey maps have been used to extrapolate submerged contacts.

Analyses.

In order to adequately cover the very wide range of rock types a reconnaissance survey of .200 x-ray fluorescence analyses of whole-rocks has been made. The results have been used to trace chemical variation within the rock series, and to investigate possible connections between the groups. Alkaline rocks of comparable composition from Ascension Island, West Greenland, and Skye have been used as standards. Whilst the results cannot be regarded as fully comparable with good wet

chemical analyses the information gained is believed to fully justify the method used. Several discrepancies in the wet chemical analyses were also revealed.

Unfortunately, many mineral analyses by probe could not be made. This would provide a very interesting further project on the rocks from the complex.

CHAPTER II GENERAL GEOLOGY OF THE COMPLEX.

Country Rock.

The complex intrudes porphyritic granodiorites of the Yellowknife sub-province.

These granodiorites contain a variable proportion of 1-5 cm. microcline phenocrysts in a matrix composed of clouded plagioclose, quartz, biotite and muscovite, and with accessory apatite and zircon. The phenocrysts frequently outline a vertical flow foliation in a generally north-east direction. Altération away from the complex is slight, but locally the rocks have been sheared with the development of chlorite and of a gneissose texture.

Along the south-east margin, muscovite-rich tourmaline pegmatites become abundant in a rather more quartzose hololeucocratic facies of the grandodiorite.

This granodiorite has been variously affected by the intrusion of the complex. Around the northern portion - centres 1 and 2 (Map 2-1) - the country rock is visibly recrystallized for up to 50m, with local re-mobilization, and formation of hybrid diorites in contact with the intrusive ultramafics. Around the peralkaline rocks and carbonatites - centres 3, 4 and 5 (Map 2-1), up to 200 m. of fenite has been formed in which the outermost zone has the appearance of a pale pink slightly crushed microgranite and the innermost is a quartz free syenite.

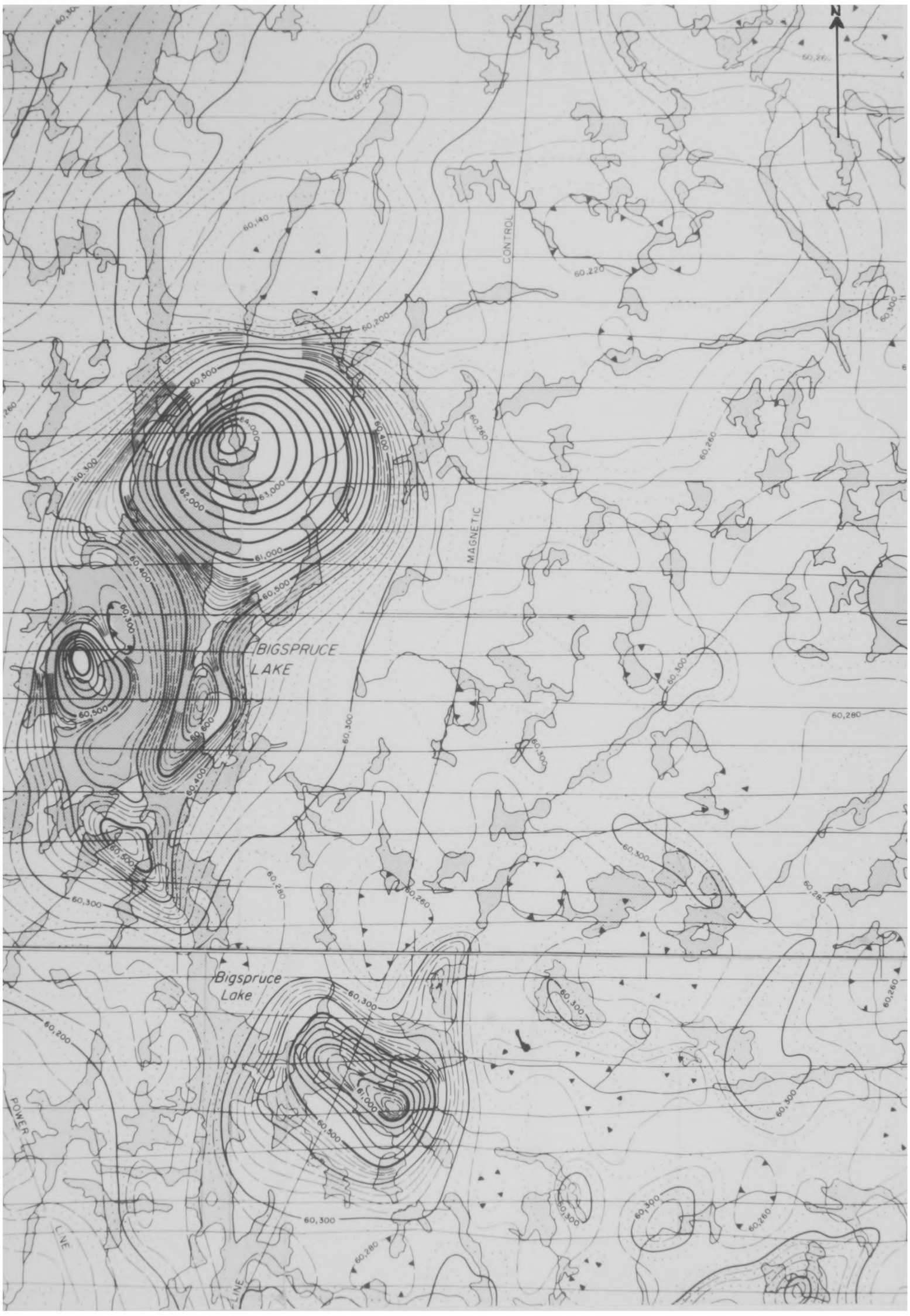
Subdivision of the Complex.

Field mapping of the complex has shown that five intrusive centres may be recognised with an initial migration of intrusive centre in a north to south direction. This intrusive sequence is summarised in Table 2-1 and Map 2-1.

From these it can be seen that each centre is geographically, petrologically, and in intrusive form, a distinct entity. Some degree of overlap, however, does occur, particularly in the location of the ring syenite 2-3

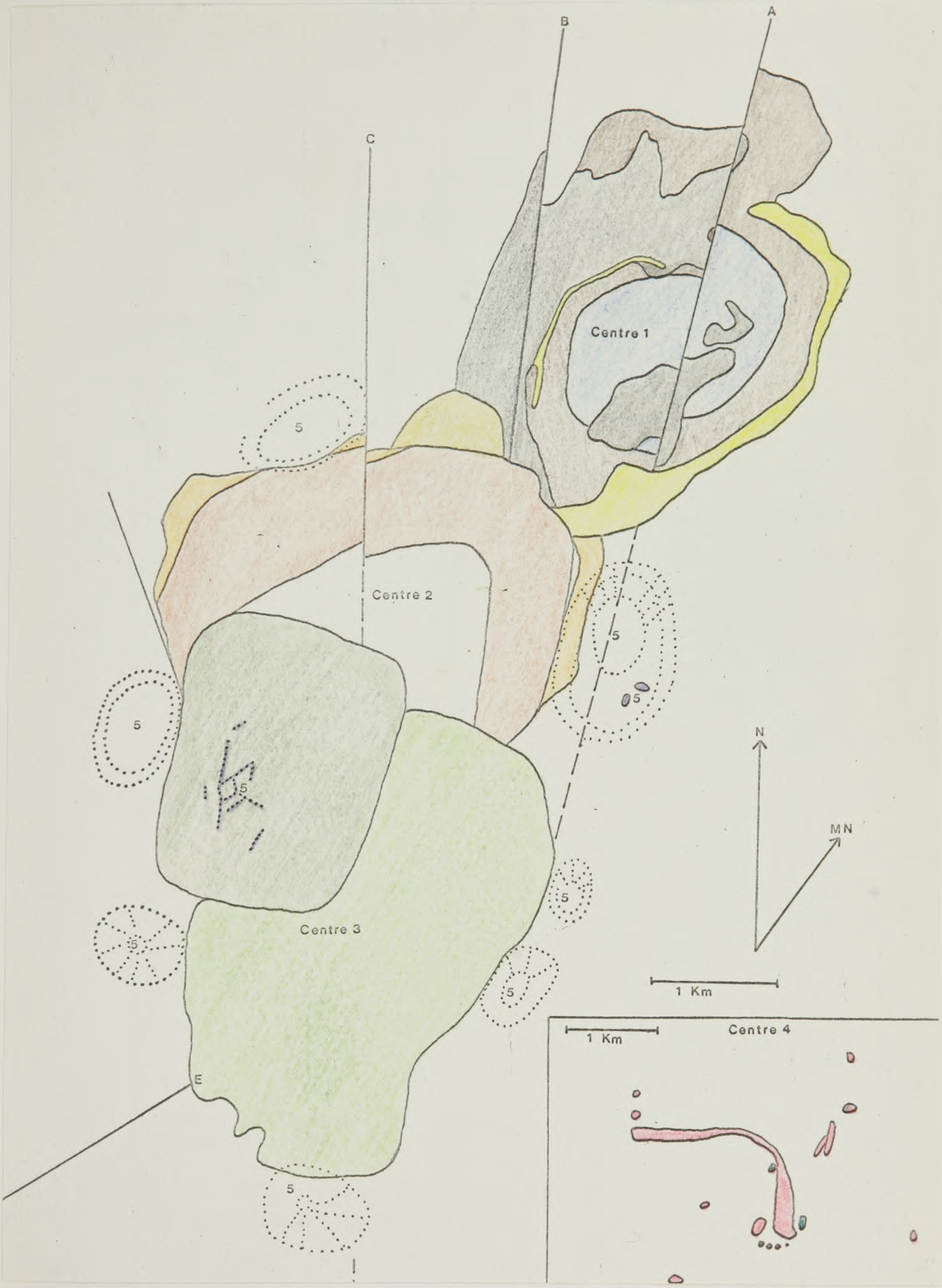
PLATE 2 - 1

AEROMAGNETIC INTENSITY MAP OF THE BIGSPRUCE LAKE AND MOOSE ISLAND AREAS



The complex has intruded a granodiorite batholith with little magnetic intensity variation. The main intensity anomalies are (1) Magnetite - pyroxenites and gabbros, (2) Carbonatite pegmatite centre of Bigspruce island, (3) Shonkinites, minettes etc, Moose island centre. Note the magnetic expression of the East coast lineament, forming an intensity low to the North of the complex and an intensity high along the margin of the lake.

MAP 2 - 1 OUTLINE SKETCH MAP OF THE INTRUSIVE CENTRES AND THE MAIN INSTRUSIVE UNITS



Diorite, dark brown; gabbro, blue; pyroxenites, black; syenites, yellow to brown; foyaites, green; shonkinite, red; biotite-pyroxenite, deep green; carbonatite purple.
Note the southern migration of centres 1-4, the repeated use of the same ring fractures in centres 1 and 2, and the ring of elliptical cone-fractures around the rim of centres 2 and 3. Each centre is of a distinct petrographic type. Faults A, B, and C show syn-intrusion displacement.

TABLE 2 - 1. THE INTRUSIVE SEQUENCE

ROCK TYPE	INTRUSIVE FORM.
CENTRE 1.	
1. Alkali diorite	Layered intrusion
2. Alkali gabbro	Layered intrusion
3. Magnetite-pyroxenite	Massive arc dykes.
4. Biotite-peridotite and Porphyry dykes	Dyke swarms (C.1,2,3,4)
	Displacement 650m on fault A-A.
CENTRE 2.	
1. Pyroxene syenite	? plug
2. Quartz syenite	Ring dyke
3. Northern ring syenite	Ring dyke
4. Comendites and rhomb porphyries	Dykes (C.3.)
5. Mafic quartz syenite	Ring dyke
6. Nepheline-sanidine porphyries	Dyke swarm (C.3.)
CENTRE 3.	
1. Pegmatitic southern foyaite (F)	Layered intrusion
2. Mafic northern foyaite (F)	Layered intrusion.
3. Ijolites	Breccia pipes
4. Tinguaites	Dyke swarm
5. Augite kersantites	Dyke swarm (C.4)
CENTRE 4.	
1. Shonkinites	Dykes and pipes
2. Minettes (F)	Dykes
3. Biotite-pyroxenites (F)	Pipes
CENTRE 5.	
1. Carbonated biotite-peridotite and biotite pyroxenite(F)	Dykes and breccia pipes
2. Biotite-apatite silico-carbonatites (F)	Dykes
3. Sovites and dolomite-carbonatites (F) (M)	Dykes
4. Aegirine-biotite-magnetite-calcite pegmatites (M)	Radial and trangential dykes
5. Fenitized elliptical fracture patterns	Gas escape vents

C.3 = chemically related to Centre 3.

F = associated with fenitization.

M = associated with Fe, Ti, Nb and R.E Metasomatism.

around centre 1, and of the carbonatites and "gas escape vents" of centre 5 over centres 1 and 2. The nepheline-sanidine porphyry dykes of centre 3, and the minette dykes of centre 4, are the only rocks to occur throughout the area of the complex.

Centre 1.

The rocks of centre 1 are all saturated in the sense that they contain normative hypersthene. The diorite additionally contains modal quartz. Both diorite and gabbro show concentric, inwardly inclined banding, cumulus crystal textures, and slight cryptic variation typical of layered intrusions. Trough banding, cross-lamination, and lineation indicative of strong currents, are also present.

They are composed of clinopyroxene, labradorite (An 52) magnetite, and ilmenite, with minor interstitial amphibole, apatite and alkali feldspar. The mafic minerals and apatite are generally aggregated interstitially to feldspar.

The ultramafic rocks vary from olivine-magnetite-clinopyroxenite to magnetite-clinopyroxenite. Texturally they resemble the Alaskan ultramafics but are greatly enriched in magnetite and ilmenite relative to these (Taylor 1967). They form an arcuate mass concentric about the mid-point of centre 1, and several small bodies within the central gabbro. The margins are chilled and flow banded, The contact rocks are often hybridized or remelted. Olivine has been concentrated by flowage at the centres of the larger bodies.

Specific features of the centre are the concentric banding of the bodies about a single point, the presence of cumulus mineral textures, and the trend from intermediate, through basic to ultramafic rock types.

Centre 2.

Centre 2 consists of saturated and oversaturated syenites, in ring dyke form, containing alkali feldspar, green amphibole and quartz, with minor quantities of magnetite, ilmenite, apatite and pyroxene. Most feldspars are of rhombic habit, with oscillatory zoning and rare plagioclase cores and perthite rims. The shape of these feldspars, together with narrow granitic screens, distinguish the separate intrusive phases. A very few dykes are peralkaline with modal aegirine and hematite.

Mineralogically the syenites 1-4 resemble the interstitial phase of the alkali diorite (centre 1-1). Their composition lies along the same

geochemical trend as the diorite, gabbro, and pyroxenite.

Although the main centre of intrusion had shifted towards the south-west, one of the syenites - 2-3 - intruded the ring fracture marginal to the alkali diorite and magnetite-pyroxenites. This syenite cross-cuts, without displacement, the transcurrent fault (A-A) which bisects and shifts the rocks of centre 1.

Centre 3.

Centre 3 is composed of peralkaline nepheline syenites and ijolites in stock or pipe-like form. The rocks contain microcline-microperthite (Or 66), nepheline (Ne 69), and aegirine, with minor quantities of albite, biotite, and andradite garnet. Cancrinite, analcite and sodalite, formed through late stage alteration, are common. However, melanite garnet, niobium minerals and complex zirconium silicates are not present. The ijolites show mineralogical and geochemical differences from the miascites usually associated with carbonatites e.g. East Uganda province (King 1965).

The Centre is surrounded by a fenite zone up to 100m wide characteristic ofthe individual intrusive units. Mineralogical changes involve the growth of perthite around plagioclase cores, the formation of arfvedsonite or aegirine, and the resorbtion of biotite, potash feldspar and quartz. The zone is surrounded by recrystallised microgranite enriched in silica. A complete transition from granodiorite to syenite with preservation of phenocrysts can be traced.

Remobilized fenites are rare.

Centre 4.

The main Moose Island centre lies about 6 miles (9.5 km) S.S.E. of the midpoint of centre 3. All the rock types are mafic and potassic, ranging from shonkinites, with 50% titanaugite and biotite in a matrix of cryptoperthite (Or50), to biotite - pyroxenite. Minette dykes are common. Both shonkinite and biotite pyroxenite may contain modal quartz or zeolite.

The minettes occur as narrow cross-cutting dykes with reddened margins, following the franture pattern within the basement. The shonkinites occur as similar although broader (5-100m) dykes, as a semi-circular ring dyke, and as several small elliptical breccia pipes (30-100m).

The biotite-pyroxenites occur only as pipes, or as schlieren within

shonkinite. Abundant rounded xenoliths of country rock, as well as rounded xenoliths of shonkinite and biotite-pyroxenite, but no deep - seated nodules, occur within the shonkinite vents. Several are surrounded by a hybrid "biotite - diorite" zone grading into reddened granodiorite. In contact with the biotite-pyroxenites this zone is fenitized for a distance of tens of metres.

Centre 5.

Centre 5 is outlined by a discontinuous ring of reddened,elliptical fracture patterns (A-H) believed to be gas-escape-vents. Within the area outlined, carbonatites, carbonatite breccias, and silico-carbonatite dykes sporadically occur, in addition to two or three small inclusion rich breccia pipes, and the pegmatite centre of Bigspruce Island.

Two carbonatite types can be recognised -

a) Ankerite-dolomite type, confined to a narrow (600m) fault bound belt east of centre 3.

b) Biotite-calcite type found throughout centre 5 but particularly in the vicinity of Bigspruce Island.

In eachcase there is complete transition from carbonate vesicles in little altered silicate parent - biotite peridotite and minette respectively - through replacive rocks to silico-carbonatite breccias and magmatic carbonatites.

The carbonatites typically show chilled margins surrounded by narrow shattered fenite zones. In a few cases flow foliation of the fenite has produced a gneissose texture.

The mineralogy is exceedingly varied. Type (a) contains dominantly ankerite, dolomite, apatite, magnetite, quartz and serpentine.
Type (b) contains abundant calcite, biotite, apatite, fluorite, with lesser amounts of bastnasite, quartz, zircon and tremolite.

Magma Types.

The petrology, described above, and the geochemistry, suggest three magma types. Type A is a saturated mildly alkaline type giving rise to the rocks of centres 1 and 2 and the equivalent porphyry dykes.
Type B is sodic and undersaturated giving rise to the foyaites and ijolites of centre 3 and the nepheline-sanidine-porphyry dyke swarm.
Type C is saturated, alkaline and potassic, giving rise to the rocks of centre 4, the biotite - peridotite and minette dyke swarms, and both types of carbonatite.

MAP 2 - 2 SKETCH MAP OF THE FAULTS AND LINEAMENTS SURROUNDING BIGSPRUCE LAKE


E
E
E

Gabbros, syenites and nepheline syenites similar to those found at Bigspruce Lake are commonly associated, for instance in the West Greenland (Watts 1966) Damaraland (Martin etal 1960) or Monteregian (Gold 1967) provinces. However, the potassic types are rare. Almost identical intrusions to those of centre 4 are found in the Navajo area Arizona (Williams 1936), and comparison may be made with the Bearpaw mountains, Montana (Pecora 1956) or the Toro-Ankole region East Africa (Holmes and Harwood 1933: Higazy 1954). The association of so strong a development of both types is possibly unique.

Relationship to faulting.

The position of each centre within the complex shows a close relationship to faulting. Map 2-2 illustrates this influence.

The complex is seen to lie at the centre of a lobe of granitic rocks, surrounded on three sides by metasediments and metavolcanics. The structure is post-Snare, since onlapping Snare sediments are deflected parallel, and a few kilometres west, of the same boundary. It is, therefore, tentatively interpreted as a doming of the basement produced during, or immediately preceding the intrusion of the complex.

This lobe is crosscut by a system of splaying north-south transcurrent faults, dominantly sinistral, extending for a total length of at least 125 km. For 50 km north of the dome these faults form the Snare (1800 m.y.) - Slave (2,400 m.y.) boundary.

Bigspruce Lake lies athwart this system, at its intersection with a group of northeast - southwest or E.N.E. - W.S.W. dextral faults. The line of one of these E-E, E' - E' enters through the south-west arm of the lake formed by the Snare River.

CHAPTER III.

THE NORTHERN. BASIC AND ULTRAMAFIC CENTRE I.

GENERAL.

Map 3-1 shows the known distribution of the main intrusive units of centre 1, together with their inferred extension beneath the lake, and their former extensions beneath the syenites of centre 2. The extrapolation is based in part upon the aeromagnetic intensity map (G.S.C. Geophysical Paper 2966, 1963) and its second derivative, and in part upon xenoliths within the syenites, and upon screens between them. The pyroxenite-granodiorite, and pyroxenite-diorite contacts are sharply delineated by the magnetic maps by virtue of the strong susceptibility contrast.

The main exposed units are -

1. Alkali diorite
2. Alkali gabbro.
3. Magnetite-pyroxenite.

There are also small bodies of late gabbro, and numerous porphyry dykes. The diorite and gabbro form almost concentric layered intrusions with a consistent inward dip of $35^{+}2^{o}$. The diorite is an andesine-oligoclase-clino-pyroxene-oxide-apatite rock with minor quartz, green amphibole, microcline, and zircon. The intrusion shows no consistent variation in the rock composition and only slight cryptic variation in the proportion of quartz and amphibole, and the core composition of the feldspar (An_{51}-An_{34}). The central 500m of the preserved diorite shows a weak lamination defined by the platey feldspar, and impersistent concentrations of pyroxene, apatite and oxide. There is no density stratification or rhythmic banding.

The gabbro is a labradorite-andesine-clinopyroxene-oxide-apatite rock with minor brown amphibole. It is termed a gabbro by virtue of the labradorite feldspar (An_{52}) within the chill, although many of the differentiates are properly ferrodiorites (An_{43-46}) The intrusion shows strong mineral layering. The lower rocks are mafic, apatite-rich gabbros; the central division is formed by laminated leucocratic feldspar cumulates; the upper division is formed by mafic, apatite-poor, rhythmic banded gabbros (ferrodiorites). There is cryptic variation with the loss of cumulus apatite following the crystallization of the lower division, and with the change in composition of the first formed feldspar (An_{52-43}). The uppermost division may represent a new pulse of basic magma.

The pyroxenites are olivine-clino-pyroxene-magnetite-ilmenite rocks closely associated, in distribution, with the gabbro. They are found as dykes within the gabbro, and as a broad, arcuate mass following the outer margin of the diorite west of A-A. The larger masses are flow-banded, with a central concentration of olivine, and chilled magnetite-pyroxenite margins. Associated with the intrusion of the pyroxenites is the saussuritization of the gabbros, and diorites.

MAP 3 - 1 DISTRIBUTION OF THE ROCK TYPES WITHIN CENTRE 1.



Note how the diorite, and gabbro layered intrusions, and the olivine -magnetite-pyroxenite mass, are practically concentric about a common centre in Arete Lake, and how the intrusions are bisected by the fault A-A. The pyroxenite mass has been extrapolated across the syenites of centre 2.

During, and following the intrusion of the pyroxenites, there was 350 metres displacement on the fault A-A, and displacement on several other smaller, sub-parallel or N-W, or N-E, faults. These fractures have been intruded by pyroxenite, and by feldspar-porphyry dykes of gabbro, diorite, mafic syenite, undersaturated syenite, and biotite-pyroxenite composition.

The activity of the centre was terminated by the shift of the intrusive locus to centre 2.

THE ALKALI DIORITE.

The alkali diorite is a white or pink weathering rock of medium grain size, with a pitted surface due to the preferential weathering of the mafic minerals.

The exposed intrusion forms an ellipse 4,200m x 2,700m diameter cored by gabbro so as to define a hollow ring of circa 500m width and 1,500m internal diameter. The centre, as defined by the lamination, lies 500m south of the present geographical centre owing to the removal of some of the marginal diorites along the syenite 2-3 ring fracture.

The diorite is in contact with the granodiorite along the entire northern margin, and for short distances along the eastern, and southern margin where chilled diorite forms screens between the syenite and the granodiorite. Along the majority of the western, southern, and eastern sides the diorite is in gradational contact with syenite 2-3. Along the entire western boundary pyroxenite separates the syenite from the granodiorite. Short screens of chilled diorite have been found between the amphibolitized pyroxenite, and the remobilized granodiorite on the exposed north-east shore contact. The diorite, pyroxenite, and syenite were thus intruded up the same vertical ring fractures.

The contact between the gabbro and the diorite is sharp and vertical. It is formed by porphyritic mafic gabbro chilled against leucocratic, laminated diorite.

THE MARGINAL DIORITE.

The diorite contact against the granodiorite is sharp, chilled and vertical. For 2-5 m either side of the contact the rocks are granulated due to later movements along the ring fracture. The granodiorite is reddened and the quartz recrystallized for 20-50m from the margin.

The chilled diorite is composed of coarse 1-2cm oscillatory zoned feldspar, and pyroxene phenocrysts in a matrix of untwinned alkali feldspar, perthite, green hornblende, quartz and zircon. This phenocrystic chill zone passes gradationally into the medium grained diorite with a decrease in quartz, amphibole and zircon, and the homogenization of the feldspar composition. The feldspar phenocrysts within the chill have cores of An_{51} and rims of perthite. The normal diorite has slightly zoned feldspars of An_{36-28}. The normative composition of the feldspar is practically constant. Also within the marginal rocks are found hollow acicular apatite, and skeletal magnetite and ilmenite. The phenocrysts, and the quenched crystal forms extend for 100-150m from the contact.



PLATE 3 - 1 Contact between the cumulus and chilled diorite. Loose block near the southern margin. The contact is unusually sharp in this block.

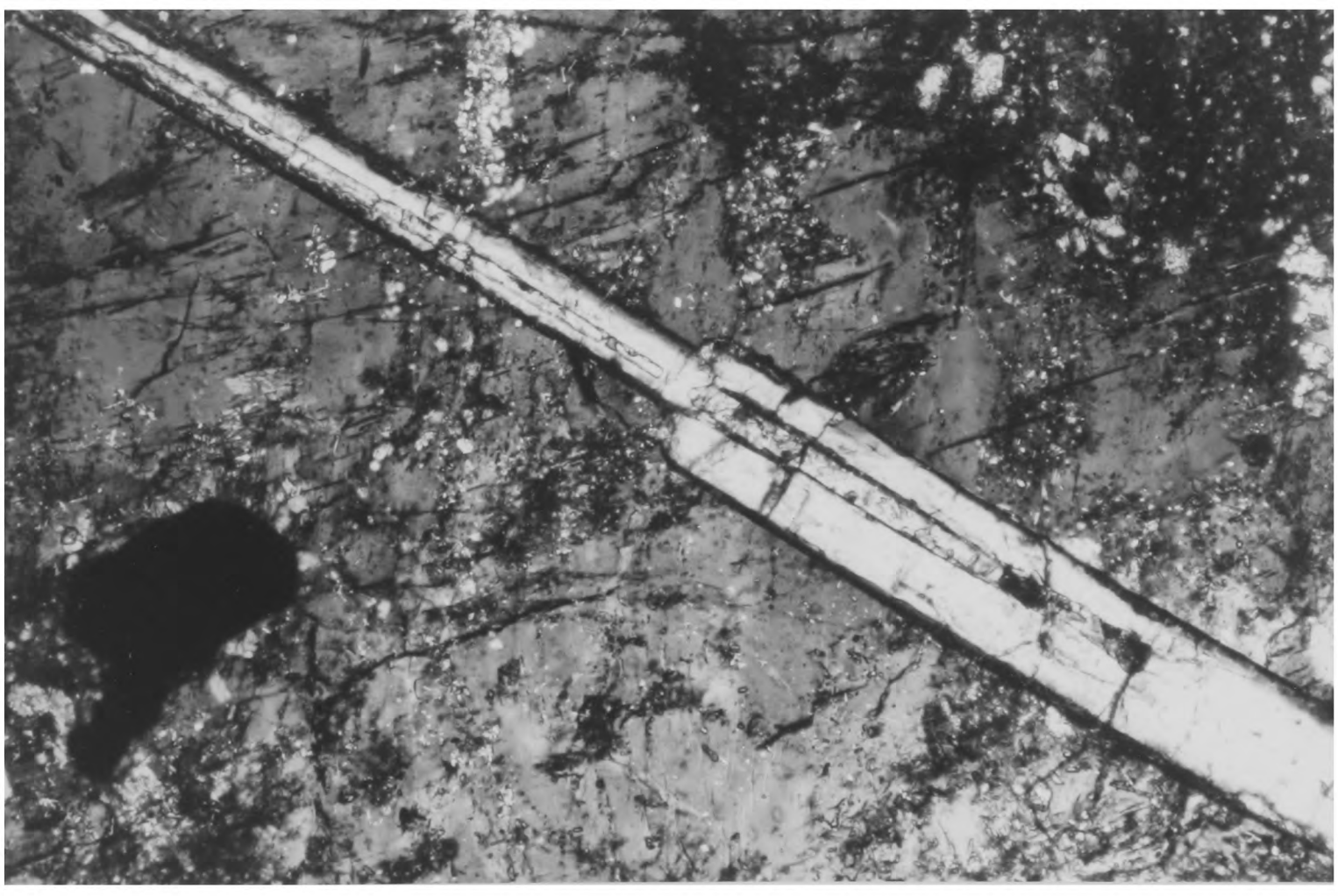


PLATE 3 - 2 Acicular hollow apatite in chilled diorite. 10m from N.W. contact spec. 67313. x 40

At 100-150 m from the original outer contact north of Beaver lake, southeast of Arete lake and in a screen on island H is found a sharp contact between mafic platey feldspar diorite, and leucocratic blocky feldspar diorite. This contact is believed to represent the contact between diorites crystallizing parallel to the chamber walls, and the diorites formed through crystal settling on to the magma chamber floor (plate 3-1). Outside this contact is found a vertical banding defined by thin (0.5 -1cm) corrugated mafic laminae; within the contact is found a low angle (35 ± 2^{o}) inwardly dipping lamination defined by the platey feldspars. Outside the contact the diorite contains phenocrysts, quench textures, and platey feldspars in a syenite matrix of alkali feldspar, quartz, amphibole and poikilitic biotite; inside it the feldspars show post cumulus overgrowths; the pyroxene, and amphibole may be poikilitic; biotite is rare; and quartz is virtually confined to myrmekitic intergrowths with microcline,or clear feldspar, at the crystal boundaries.

THE LAMINATED DIORITES.

Between the northern contact and the innermost diorites a total thickness of about 800m of diorite is exposed, of this approximately 300m shows whispy lamination, and 50m mafic banding. Within the banded diorite there are a few poorly developed troughs. These troughs, and the lamination are taken as evidence of continuous (convective) currents.

The laminated diorites grade imperceptibly into the leucocratic diorite described above. The first detected lamination is found 750m from the northern contact 200m west of Beaver lake. The platey cores of the feldspar are aligned within the plane of the lamination, together with pyroxene, apatite, and oxide, and enclosed by alkali feldspar, myrmekite, pyroxene, oxide and amphibole. The mafic minerals may show a weak lineation of the elongate pyroxenes, and are concentrated in thin short lenticles (plate 3-3) within the same plane. On ascending the sequence these lenticles show a tendency to coalesce, and so to define a mafic banding (plate 3-4). This is not a rhythmic banding since there are no complementary feldspathic bands. Their formation is thought to result from the winnowing of the crystal mush under the action of continuous convection currents. Individual bands are laterally impersistent on a scale of a few metres. Pyroxenite xenoliths have occasionally been found resting on the plane of the lamination.

The innermost diorite, exposed along the west shore west of island E is a laminated feldspar adcumulate without interstitial alkali feldspar, quartz or amphibole. If this diorite is representative of the missing layered series then the final residual liquid should have been syenitic, and should have overlain andesine-pyroxene-oxide cumulates. There is thus a possible direct link between the diorite and the syenite-type magma. These hypothetical central units have been removed by the intrusion of the later gabbro.



PLATE 3 - 3 Lamination, and whispy banding in diorite. The lamination results from the orientation of platey feldspars; the banding from the winnowing out of the denser mafic minerals. 600m S.E. of Arete Lake.

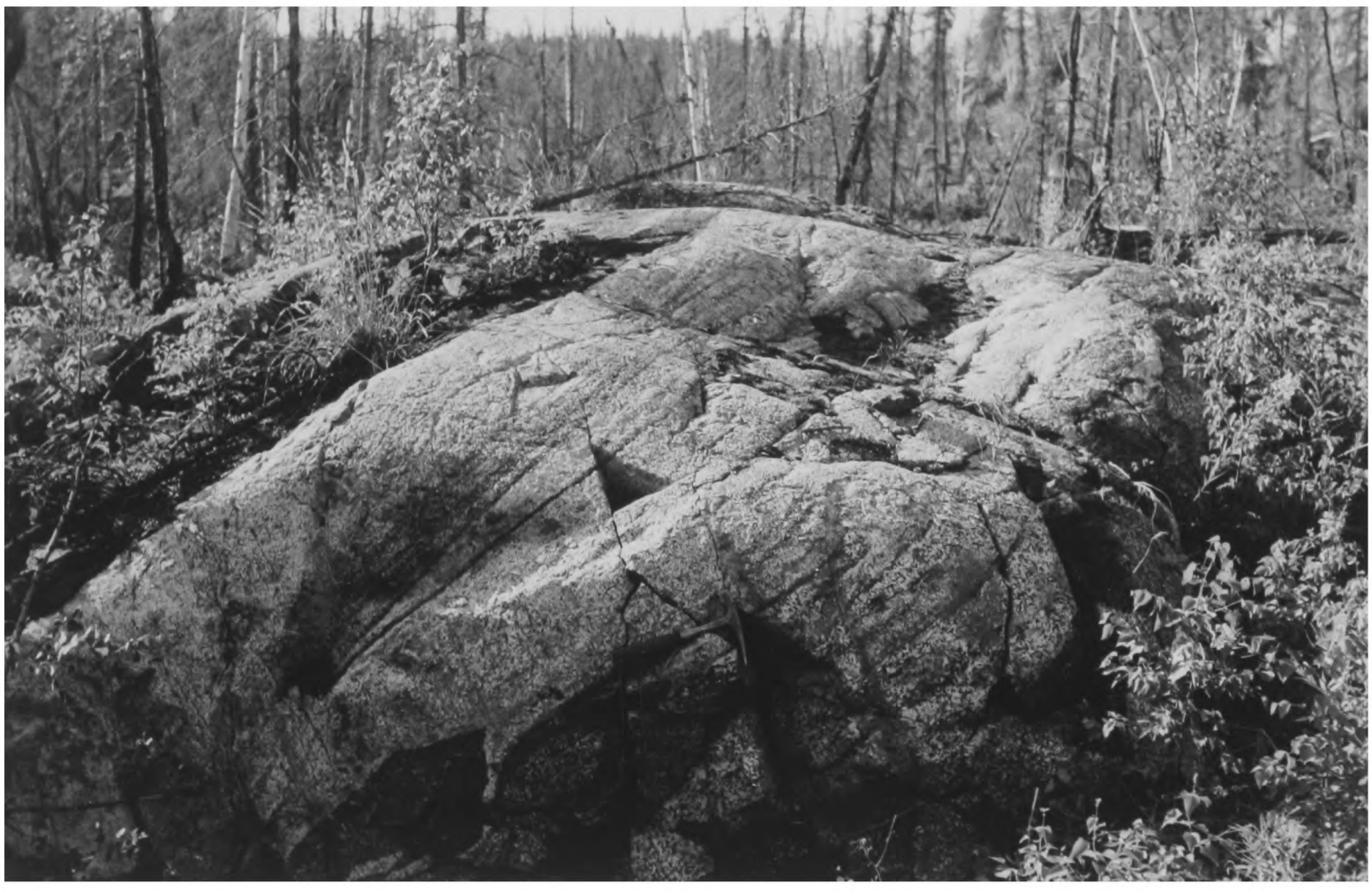
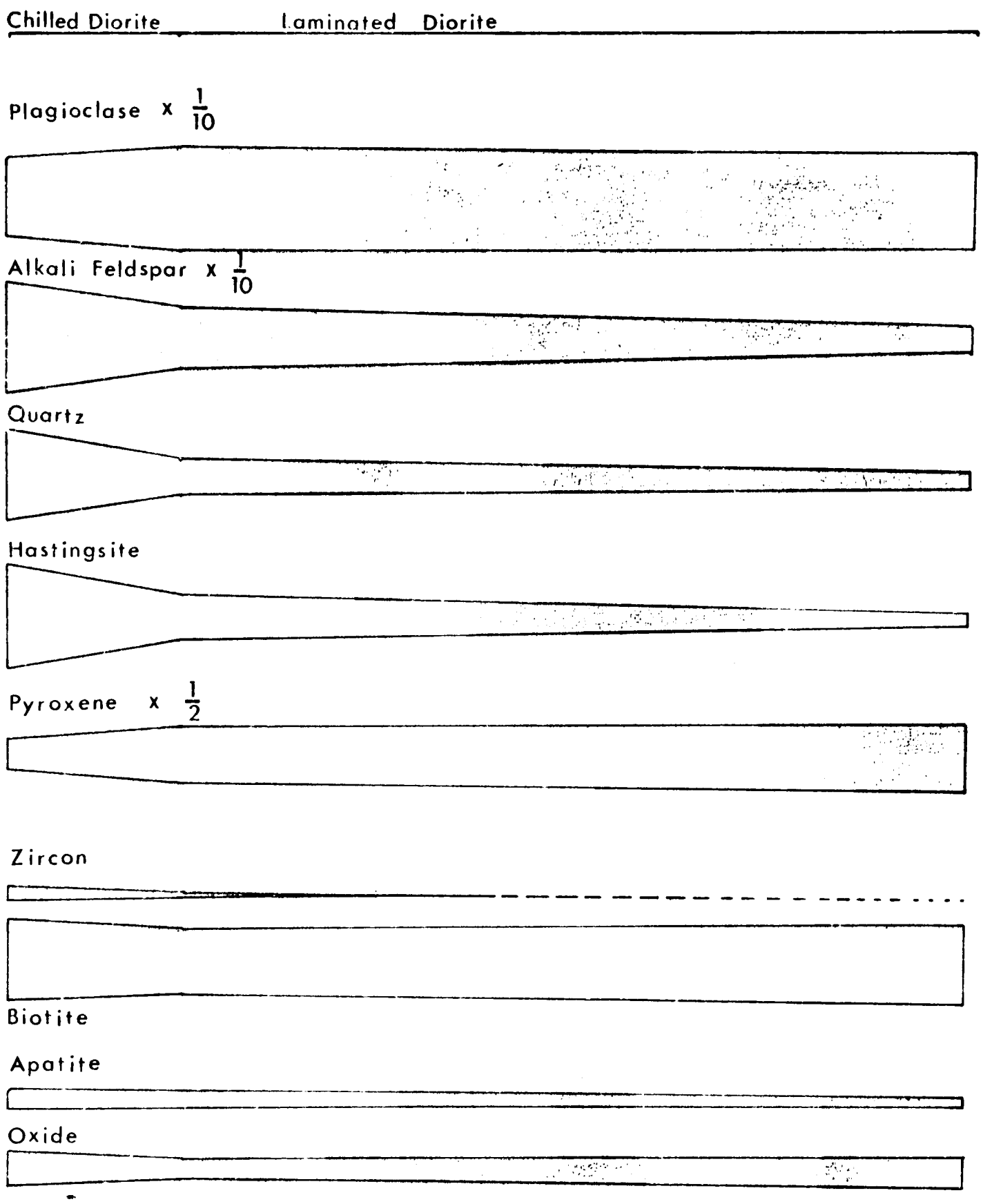


PLATE 3 - 4 Persistant mafic mineral banding in the laminated diorite. There is a common tendency to cross-banding as on the far side of this outcrop. 400m S. of Arete Lake.

FIG 3 - 1 MODAL VARIATION IN THE ALKALI DIORITE SHOWING THE CRYPTIC LAYERING



THE SEQUENCE OF CRYSTALLIZATION.

There is a constant sequence of crystallization throughout the diorite. Labradorite or andesine, and pyroxene crystallized early and as phenocrysts within the chill. Andesine, pyroxene, magnetite, ilmenite, and apatite crystallized together over the bulk of the crystallization interval. Oligoclase or perthite, quartz, biotite, amphibole, and zircon crystallized from the trapped interstitial liquid. The chilled diorite is free of normative quartz and so the proportion of modal quartz is directly proportional to the quantity of modal amphibole crystallizing in place of pyroxene.

The start of convection currents, in the exposed diorites caused little fractionation. The textures are not adcumulus . The main effect was to homogenize the crystal phases through the mixing of the parent magma, and to inhibit the formation of amphibole, probably by transporting away the volatiles.

THE MINERALOGY.

a) Feldspar.

Within the extreme chill (1-10m) 1-3cm plates of labradorite form up to 15% of the rock. The phenocryst cores (An_{51}) are unzoned but show narrow rims of alkali feldspar and exsolved ropy perthite. The matrix consists of 0.5 - 1mm clouded rhombic alkali feldspar, perthite, granophyric quartz-alkali feldspar intergrowths, and euhedral biotite, amphibole, apatite, and oxide.

Away from the chill the phenocrysts are partially resorbed, and show broad oscillatory zoned rims; the granophyric intergrowths become rare; groundmass platey andesine and oligoclase appears.

Outside the 100-150m chill zone the feldspars contain 8-12m tabular cores of An_{34} with overgrowths zoned to An_{28}. Many of these feldspars are clear, and untwinned, show lobate intergrown margins, and swapped rims, and have exsolved patches of microcline. Myrmekitic intergrowths of quartz, and microcline replace the margins of some crystals, and replace the poikilitic feldspar. Myrmekite forms 5-10% of most of the laminated diorites.

The innermost laminated diorite contains unzoned andesine of An_{39}.

b) Pyroxene.

The clinopyroxene is a pale pink weakly pleochroic titanaugite. It occurs within the chill as 1-2mm corroded phenocrysts rimmed by primary green hornblende. Pyroxene within the unchilled diorites is subhedral, or poikilitic to plagioclase. In most of the diorites the mafic minerals are aggregated, a typical aggregate consisting of one or two sub-hedral pyroxene grains, associated with a few grains of magnetite and ilmenite, and enclosed within a single plate of biotite. All the mafic minerals enclose abundant stubby apatite. Within the laminated rocks these aggregates may be strung together with the exclusion of feldspar forming pyroxenite bands and lenticles.

c) Amphibole.

The primary green hornblende occurs rimming pyroxene, and as euhedral crystals in the chilled matrix with quartz, alkali feldspar, and zircon. Within the chill 0.5-3mm amphibole encloses corroded pyroxene cores but in the majority of the diorites the amphibole crystallized following pyroxene without significant reaction as thin rims to the mafic aggregates within the biotite. This amphibole is similar to that found in the quartz free syenites. It is strongly pleochroic

β = Deep brownish green
γ = Deep green
α = Pale straw yellow.

with more intense green rims.

The pyroxene is flecked with red brown barkevikite, and partially replaced by secondary pale green amphibole.

d) Biotite.

Primary biotite is found within the chill as 0.5-1mm hexagonal plates within the quartz rich matrix, and in the laminated diorites as poikilitic 0.5-2cm plates. It is amongst the last minerals to crystallize enclosing amphibole. It is pleochroic from

α = pale yellow
$\beta = \gamma$ = deep olive green

e) Oxides.

Ilmenite is 3-4 times as abundant as magnetite both occurring as subhedral grains within the mafic aggregates. Faint discontinuous lamellae of hematite in ilmenite are common. Magnetite contains broad exsolution blades of ilmenite. Within the chill both oxides form skeletal crystals of euhedral form which may be enclosed without corrosion in amphibole or biotite There are rare spherules of sulphides, dominantly pyrite within the oxide minerals.

Alteration to goethite, limonite, and sphene is common.

f) Quartz.

Although the normative composition of the chilled diorite lacks quartz, modal quartz is present within all the rocks except the innermost laminated diorite. Within the chill it forms granophyric intergrowths with alkali feldspar; within the laminated diorites it forms myrmekitic intergrowths; in both it forms angular crystals filling the final interstices. The quartz content of a rock is directly related to the proportion of primary amphibole. Conditions favouring the crystallization of the amphibole in place of pyroxene would therefore appear to favour the formation of a quartz bearing syenite residual liquid similar to the matrix of the chilled diorite, and similar to syenites 2 and 4.

g) Other minerals.

Apatite occurs in almost constant proportion in all the diorites. Within the chill the apatite shows an extreme acicular form up to 1cm long and under 0.1mm across. Many of the crystals show a hollow central axis. These features have also been noted from quenched (carbonate-rich) liquids by Wyllie, Cox and Biggar (1960). The acicular form of the apatite, and the skeletal oxide are not found outside the wall-rock zone. Elsewhere the apatite is stubby and euhedral. In contrast to the gabbro, it is not

TABLE 3 - 1. ANALYSES OF THE ALKALI DIORITES.

—	67338	67336	67326	67347	67340	68164	68331	67137	68250	67217	67111	67251	SHEFFORD ESSEXITE A	BIG FELDSPAR DYKE ISORTOQ B	OLIGOCLASE BASALT KERGUELEN C
	WALL ROCK DIORITES					LAMINATED DIORITES									
SiO_2	50.70	54.81	54.65	54.60	54.32	53.04	54.18	52.05	55.36	53.73	53.67	51.18	53.15	51.01	50.41
Al_2O_3	17.17	14.86	15.07	14.94	16.76	17.44	16.88	16.74	18.09	16.64	16.53	18.66	17.64	16.27	16.26
Fe_2O_3	-	3.36	3.26	3.10	4.27	4.32	3.34	3.61	3.12	3.33	-	-	3.10	2.57	3.95
FeO	10.43	6.87	7.70	7.43	5.15	5.17	6.56	6.84	4.19	6.67	9.22	8.55	4.65	8.36	7.08
MgO	3.56	3.77	2.93	2.90	2.73	2.78	2.76	3.56	2.16	2.97	3.46	3.07	2.94	4.03	3.22
CaO	8.05	6.18	5.96	6.16	6.59	7.58	6.65	6.97	7.00	6.32	6.30	8.51	5.66	6.71	6.67
Na_2O	4.53	4.79	5.21	5.05	4.72	4.58	4.45	4.60	5.35	4.62	4.59	4.48	5.00	4.31	3.63
K_2O	1.62	2.61	2.52	2.53	2.53	2.08	2.26	2.59	2.31	2.54	2.64	2.01	3.10	2.28	2.28
TiO_2	3.18	2.04	2.40	2.26	1.99	2.13	1.85	2.30	1.64	2.11	2.18	2.10	1.52	2.00	1.63
MnO	0.09	0.19	0.14	0.14	0.13	0.10	0.13	0.13	0.08	0.14	0.13	0.07	0.46	0.16	1.10
P_2O_5	0.32	0.38	0.05	0.74	0.63	0.62	0.81	0.47	0.52	0.77	0.61	0.80	0.65	0.56	1.01

A. Dresser and Denis (1944)

B. Watts (1966 analysis 73)

C. Edwards (1938)

TABLE 3 - 1 TRACE ELEMENTS

	67338	67336	67326	67347	67340	68164	68331	67137	68250	67217	67111	67251	SHEFFORD ESSEXITE	BIG FELD-SPAR DYKE ISORTOQ	OLIGOCLASE BASALT KERGUELEN
													A	B	C
Rb	34	73	-	-	51	-	-	58	-	43	-	-	-	-	-
Ba	1,240	1,050	-	-	2,530	-	1,830	-	-	2,560	-	1,230	- -	-	-
Sr	1,580	962	-	1,230	1,600	-	1,360	1,620	-	1,640	-	2,030	-	-	-
La	-	-	-	-	-	-	-	-	-	-	-	-	-	-	-
Ce	-	--	-	-	-	-	-	-	-	-	-	-	-	-	-
Y	13	-	-	-	-	-	-	-	-	20	-	-	-	-	-
Zr	164	217	-	322	105	-	-	106	-	127	-	102	-	-	-
Nb	27	30	-	39	34	-	-	25	-	33	-	21	-	-	-
		WALL ROCK DIORITES					LAMINATED DIORITES								

concentrated within the mafic aggregates. Zircon occurs as rectangular multiple zoned crystals in the quartz rich interstitial phase. The proportion of zircon decreases with that of amphibole, quartz and alkali feldspar. The concentration of Zr in a diorite is thought to give an indication of the proportion of trapped volatite rich residual liquid.

THE CHEMISTRY.

X-ray fluorescence analyses of twelve of the diorites are listed in Table 3-1. The lack of significant fractionation based on the mineralogical evidence is demonstrated by the lack of variation of the

$\frac{Fe}{Fe + Mg}$, $\frac{Mg}{Mn}$ and $\frac{Na + K}{Na+K+Ca}$ ratios.

The composition of the chill is similar to that of many oligoclase andesites or mugearites. Although most rocks lack normative quartz they contain normative hypersthene, and hence differ from the essexites of the Monteregian province e.g. Mt. St Hilaire or Mt.Johnson which contain modal and normative olivine and nepheline.

The range of variation seen in the analyses reflects the variation in the concentration of the phenocrysts, mafic lenticles, and trapped interstitial liquid, apparent also in the sections, and in the hand specimens. There is no consistent pattern apparent.

THE RELATIONSHIP TO THE GABBRO AND SYENITES.

Although the diorite forms the earliest exposed intrusion of centre 1 the chemistry and mineralogy, particularly the $\frac{Fe}{Fe+Mg}$, $\frac{Mg}{Mn}$, $\frac{Na+K}{Na+K+Ca}$, $\frac{Ba}{K}$, $\frac{Zr}{Nb}$ are intermediate between those of the Big-feldspar gabbro and the quartz free syenite (Fig 5-1, 8-1 and 8-2). The composition of the first formed feldspar (An_{51}) is similar to that found in the gabbros (An_{52}) The chilled matrix is indistinguishable from the quartz bearing syenites 2 and 4. Further evidence of a close genetic link is given by the common centre of the pyroxenite, gabbro, diorite and syenite 3, and by the simultaneous intrusion of pyroxenite, gabbro, diorite and syenite multiple prophyry dykes. All the chills and porphyry dykes contain predominantly feldspar, with minor pyroxene, olivine and magnetite phenocrysts.

Taken together these and other lines of evidence suggest that -

1. the gabbro, diorite, syenites 1 and 3, and syenites 2 and 4 represent distinct stages in the fractionation of the same parent magma.
2. the diorite may be derived from the gabbro through the fractionation of calcic plagioclase , magnesian olivine and pyroxene, and magnetite.
3. the syenites 1 and 3 (quartz free) may be derived from the diorite through the fractionation of plagioclase (andesine), pyroxene and possibly oxide.
4. the syenites 2 and 4 (quartz bearing) may be derived from the diorite through the fractionation of plagioclase (andesine) amphibole and possibly oxide.

5. the magmas were tapped in order of increasing basicity, and density; each magma type could exist independently and simultaneously.
6. hence the magmas were derived from independant batches of the parent magma and must be derived from different magma chambers, within the same geographical area.
7. each batch of magma was tapped along the same set of ring fractures centred on the fault A-A. The magma chambers are therefore thought to be located in a stratified pipe, bounded by the fractures. Successive emplacement may be by a pistonlike subsidence. The layered intrusions are probably fed by ring dyke intrusions.
8. since xenoliths of pyroxenite are found in the diorite, and the gabbro, earlier intrusions may be found at depth, or have existed higher in the pipe. No xenoliths of granite have been found within the pipe.
9. under these conditions the predominant direction for the heat loss should be through the pipe walls. This may explain the comparatively thick vertically laminated division of 100-150m.

THE ALKALI GABBRO.

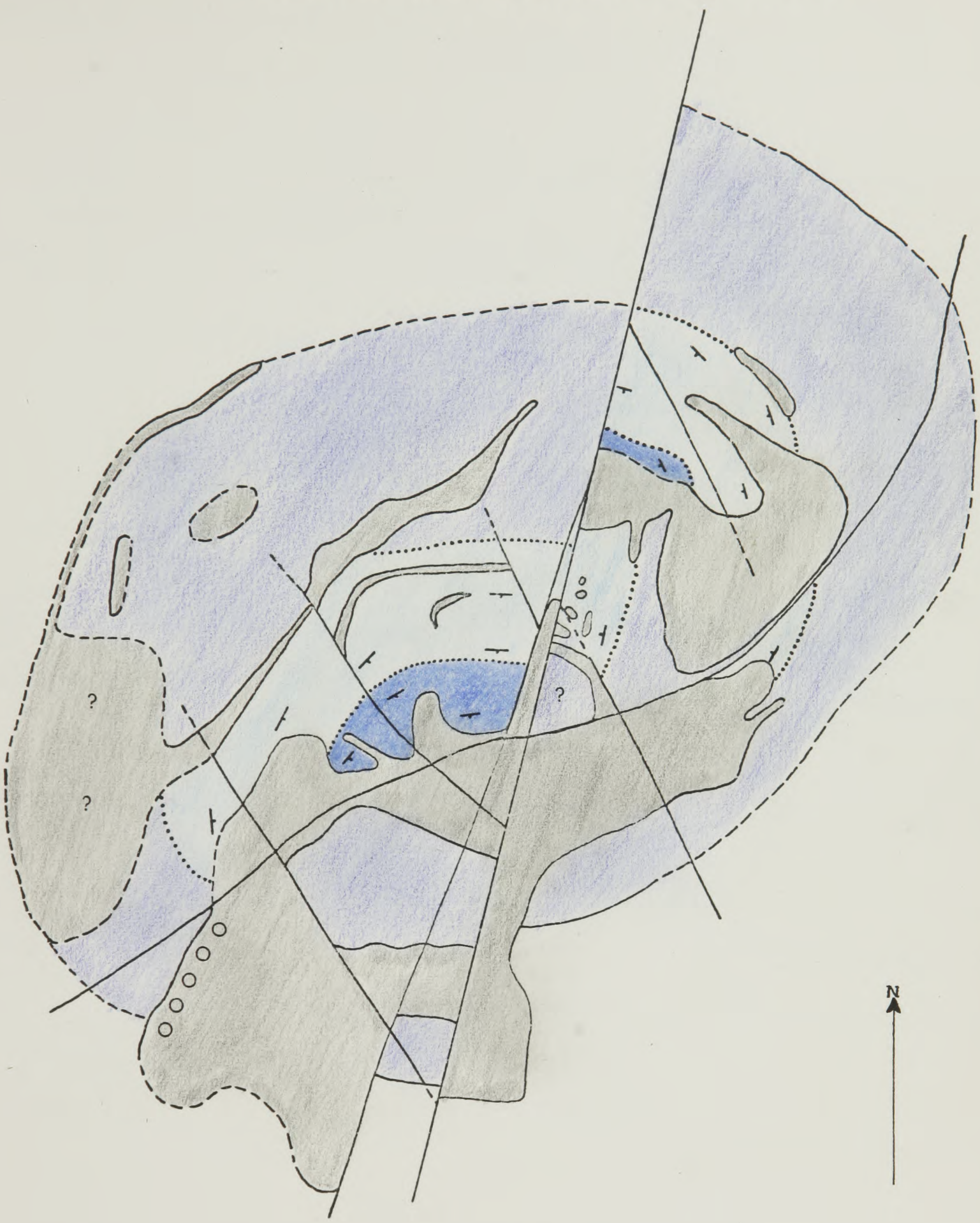
General. The alkali gabbro forms the two displaced segments of a nearly circular intrusion originally 1,200m in diameter. It is central to, and chilled against the laminated diorite.

The intrusion may be subdivided in the field in a similar manner to the diorite, into a marginal mafic porphyritic coarse grained division, the Big-feldspar gabbro (B.F.G), a central division of medium grained laminated, and banded leucocratic diorite, the Leucocratic laminated gabbro (L.L.G.), and an upper division of mafic ferro-diorite with rhythmic banding, the Rhythmic banded gabbro (R.B.G.).
The original form of the intrusion is thought to have been similar to that of the diorite. The B.F.G. contains an alkali matrix, and crystallized parallel to the chamber walls. There is a rapid but gradational change into the L.L.G., which shows lamination, defined by the feldspars, dipping inwards at $35^{+}_{-}2^{o}$, and formed through crystal cumulation on the chamber floor under the influence of continuous convection currents. The separation of feldspar cumulates more leucocratic than the parent led to a trend of iron enrichment and hence to more mafic cumulates. The influence of intermittent rapid flowing crystal-laden density currents is thought to have resulted in the formation of rhythmic banded units in the R.B.G., and to the formation of trough banding. The uppermost, and central differentiates have been removed by the intrusion of the pyroxenites, and by erosion.

THE MARGINAL GABBRO.

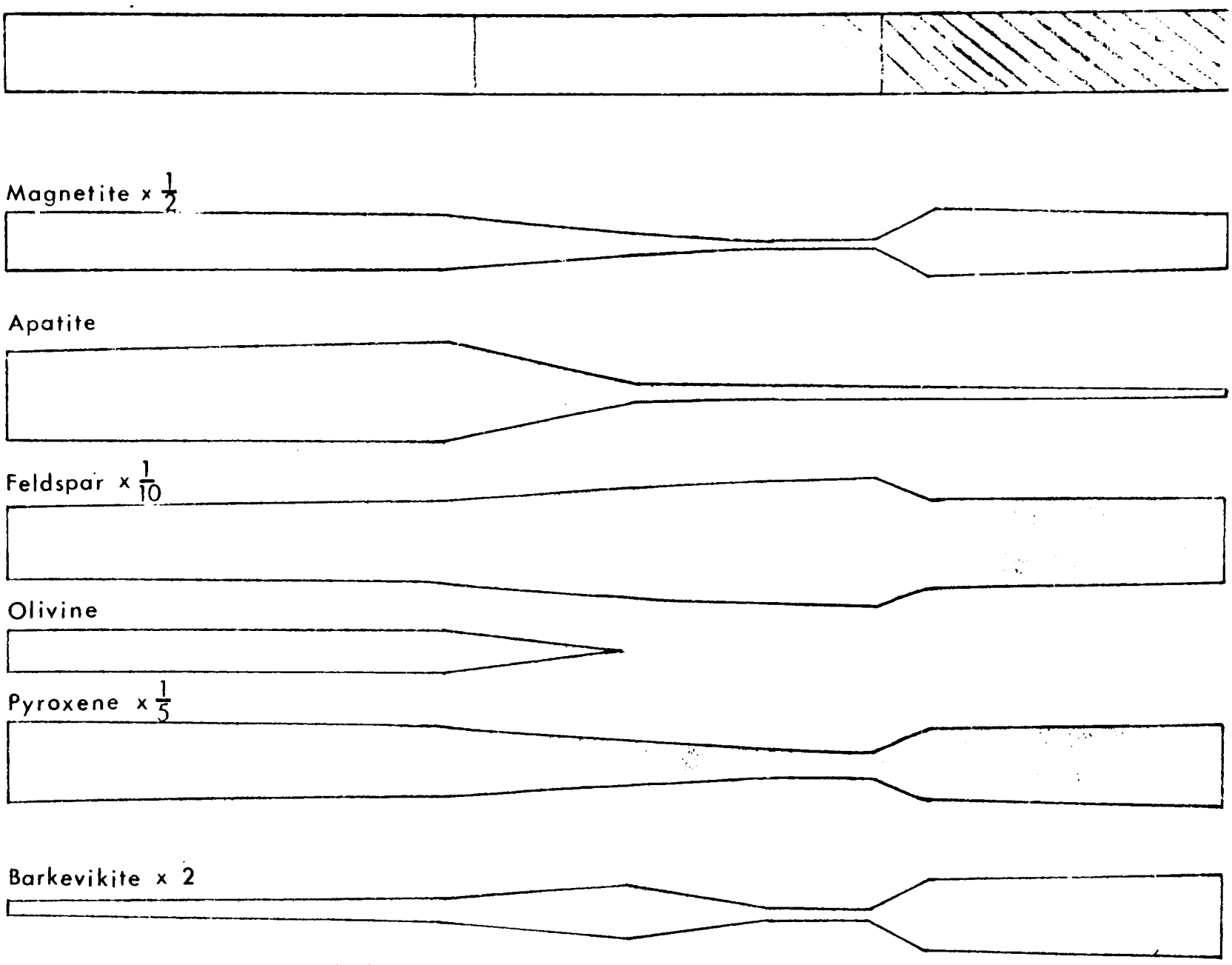
Chilled gabbro is well exposed around much of the contact east of A-A. It contains 25% thin plates 1-2cm of labradorite (An_{52}), and 5% of 1-2cm prismatic titanaugite, in a matrix of more sodic feldspar, poikilitic pyroxene and aggregated pyroxene, oxide, amphibole and apatite. The chill contact is vertical and for 50m is rich in hornfelsed xenoliths of

MAP 3 - 2 DISTRIBUTION OF THE MAGNETITE-PYROXENITES WITHIN THE GABBRO



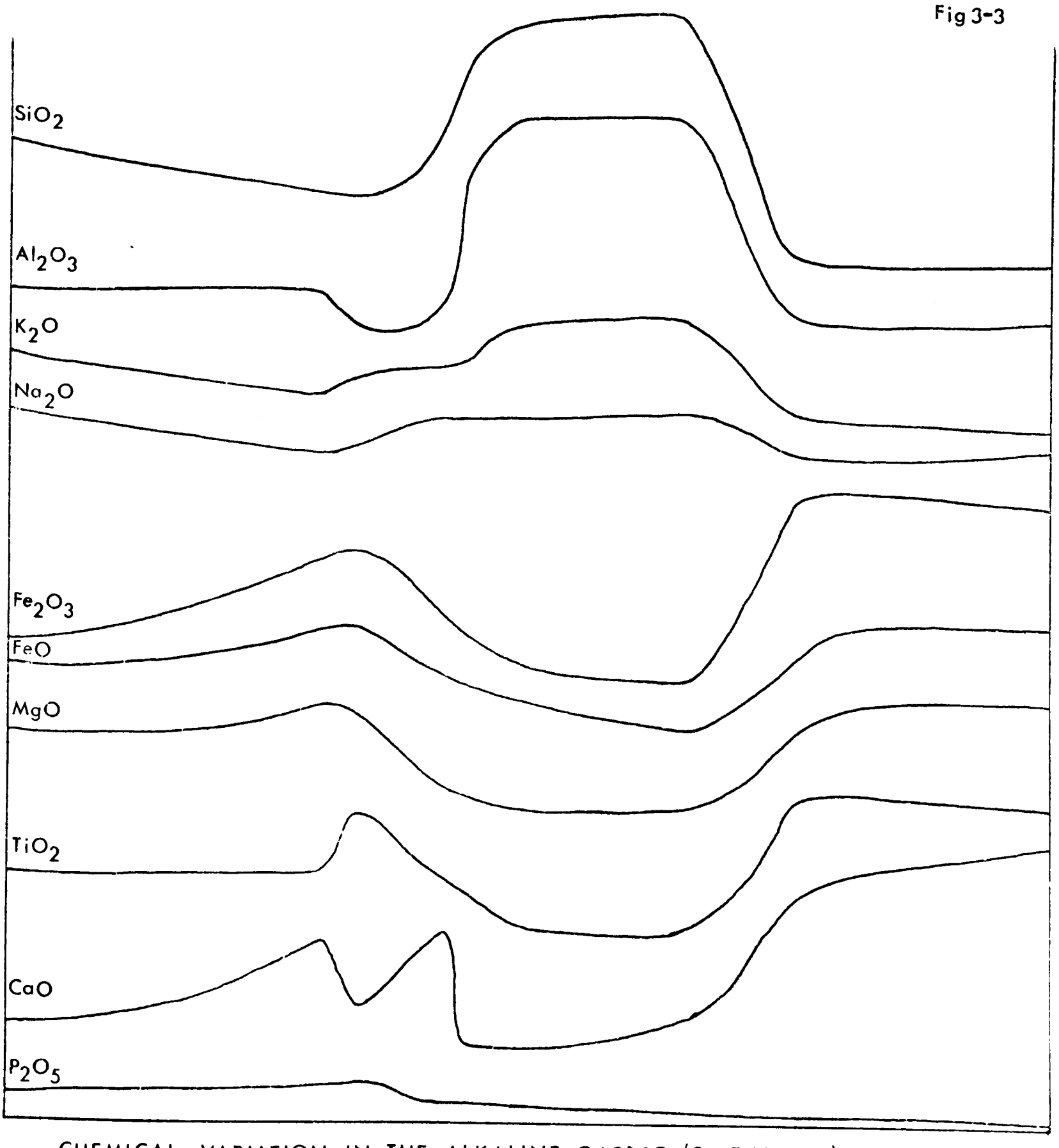
The gabbro is layered, with a border group of Big-feldspar gabbro (deep blue), a zone of feldspathic laminated gabbro (light blue), and a central zone of mafic rhythmic banded gabbro (medium blue). The magnetite-pyroxenites are practically confined to the area of the gabbro; most are fault bound. In addition there are several prominant N-W shear-zone lineaments, and numerous N-E and N-W minor sericitized shears. Many of these are intruded by porphyry dykes. The sinuous N-E fault downthrows to the north-west. This faulting is pre-or almost synchronous with the displacement on the fault A-A and associated with extensive hydrous metasomatism.

Fig 3-2



MODAL VARIATION IN THE ALKALINE GABBRO

Fig 3-3



CHEMICAL VARIATION IN THE ALKALINE GABBRO (See Table 3-2)

diorite.

Along the northwest margin Y-Y, and on the islands and reefs Z-Z, the chill gabbro and the B.F.G. invade dyke-like masses of olivine-magnetite pyroxenite breaking them down into closely packed xenoliths in a gabbroic matrix. The majority of the remaining pyroxenites within the area of the gabbro are intrusive into it.

THE BIG FELDSPAR GABBRO.

The Big feldspar gabbro is a striking rock (plate 3-6), consisting of euhedral 1-2cm andesine tablets in a matrix of pyroxene, magnetite, ilmenite, apatite, and barkevikite. The feldspars are continuously zoned, with broad cores of An_{46-43} and narrow alkali feldspar rims. Most containone or two bands of included pyroxene and oxide. The matrix consists of 60% rounded pyroxene grains poikilitically enclosed within magnetite and ilmenite (20%). The aggregates are rimmed by barkevikitic amphibole (15%). Both the oxide and the amphibole contain abundant stocky apatite (5%). In reflected light the oxides may be seen to include subhedral magnetite and ilmenite cores. The sequence of crystallization was

i) Andesine + apatite

ii) Andesine + pyroxene + magnetite + ilmenite + apatite

iii) Oligoclase + magnetite + ilmenite + barkevikite + apatite.

The lack of feldspar within the mafic aggregates, the euhedral form of the feldspar, and the narrow oligoclase rims show that the trapped interstitial liquid was alkaline, volatile rich, and exceedingly mafic. Olivine, pseudomorphed by tremolite, magnetite, and hematite is found only in the B.F.G. It is euhedral, 0.5-1mm and enclosed within pyroxene in the mafic aggregates. In the cumulus layered rocks its place is presumably taken by the amphibole. Olivine forms under 2% of any slide.

The B.F.G. shows a rapid gradational increase in the proportion of feldspar from 55-65% on approaching the L.L.G. without change in the crystal size or in the texture.

THE LEUCOCRATIC LAMINATED GABBRO.

The transition to medium grained L.L.G. takes place over 10m. The tabular phenocrysts disappear and the feldspar becomes platey and 3-5mm across. Zoning is less common, the majority of the crystals being unzoned and of An_{46} composition. The mafic minerals become disaggregated Pyroxene, and oxide are subhedral and cumulus with the feldspar. Apatite, oxide, barkevikite, and oligoclase are interstitial, intercumulus , and poikilitic. The proportion of the interstitial mafic matrix decreases on ascending the series.

The platey feldspars show a well developed lamination dipping towards the centre of 35 ± 2^{o}. In the marginal L.L.G. the feldspar phenocryst tablets are also aligned parallel to the lamination, concentrated into anorthositic bands, and banked against the B.F.G.

The pyroxene and oxide outline the lamination in the field. They are concentrated within short discontinuous lenticles, which, on ascending

the series into the more feldspathic L.L.G., tend to coalesce into thick sharply bounded bands. Many of these bands are undulose, bifurcating and impersistent. They lack an overlying feldspathic horizon. They appear to have been formed through the winnowing of cumulus pyroxene, and oxide, at the crystal-cumulate - liquid interface.

The proportion of feldspar, and of cumulus to intercumulus crystals, increases continuously on going up the sequence. Within the middle and upper part of the L.L.G. the pyroxene shows a weak radial lineation apparent on the fissile planes of the lamination.

The textures, lamination and lineation are consistent with a formation through the crystal settling of andesine, titanaugite, magnetite and ilmenite under the influence of continuously acting convection currents. The lamination shows that the floor of the magma chamber was inclined at $\sim 35^{\circ}$ and graded abruptly into near vertical wall rock.

The thickness of the exposed L.L.G. is .130m. It must be underlain by a hidden layered series, of unknown thickness, corresponding, approximately, in composition to the B.F.G. to L.L G. transition zone.

THE RHYTHMIC BANDED GABBROS.

The rhythmic banded gabbro consists of 5-10cm complementary magnetite-pyroxenite and anorthosite layers in a relatively thick homogeneous laminated mafic gabbro. The number of rhythmic banded units per metre is variable, but increases on going up the sequence.

The mafic laminated host rock contains similar mineral proportions to the B.F.G. but is relatively impoverished in apatite and oligoclase and enriched in barkevikite. The cumulus crystal phases are andesine, titanaugite, magnetite and ilmenite; both oxides, barkevikite, apatite and minor oligoclase are interstitial. Apatite becomes a rare cumulus phase in the upper third of the sequence.

The transition from the L.L.G. occupies a thickness of ~15m, The increase in the proportion of mafic minerals is abrupt but there are 3 or 4 narrow L.L.G. bands within the transition zone. Rhythmic banding appears immediately above the transition.

The relative mineral proportions in the B.F.G. L.L.G. and R.B.G. are -

	67293	67317	67320A	67320B
Plag.	51.9	73.2	54.8	0.0
Px.	22.8	14.8	26.2	62.2
Bi.	10.5	4.9	9.8	0.0
Ox.	7.8	3.5	6.2	30.3
Am.	0.6	1.7	2.6	3.6
Ap.	6.5	1.9	0.4	3.9

The lamination in the mafic gabbro of the feldspars is accompanied by a lineation of the prismatic pyroxenes. The intercumulus oxides and amphibole through growing on cumulus oxide and pyroxene produce an apparent segregation of the mafic and leucocratic componants.

The rhythmic bands are formed by a lower sharply bounded layer of magnetite-pyroxenite (with the mineral proportions of 67320B), and an upper layer of anorthosite (~85% andesine) in the approximate proportions to

TABLE 3 - 2. ANALYSES OF THE ALKALI GABBRO.

	67144	67293	68260	68263	67296	67297	67346	67320	GABBRO TUGTUTOQ	ESSEXITE YAMASKA	AV.LAVA MID.VAL. SCOT.
									A.	B	C.
SiO_2	48.43	46.92	46.65	49.62	51.20	52.65	44.60	44.21	45.10	43.91	47.1
Al_2O_3	16.60	16.50	15.18	20.43	20.23	22.07	15.76	15.56	16.36	19.63	15.8
Fe_2O_3	3.65	4.22	-	-	2.32	2.71	-	4.45	1.55	4.16	4.0
Fe O	7.37	8.60	12.74	7.55	5.89	2.53	13.69	8.65	12.30	5.55	8.3
MgO	4.96	5.74	5.43	2.87	2.95	2.42	4.82	4.76	6.60	5.20	7.4
CaO	8.57	9.79	8.69	9.94	8.23	8.81	10.39	11.20	7.93	9.49	9.4
Na_2O	4.34	2.99	3.22	4.14	3.99	4.36	2.81	3.08	3.22	4.49	3.1
K_2O	1.81	1.16	1.48	1.57	1.62	2.35	0.88	0.67	1.14	1.51	1.3
TiO_2	3.68	3.46	5.56	3.29	3.27	1.83	5.85	5.38	2.66	3.80	2.9
MnO	o.13	0.14	0.12	0.06	0.11	0.10	0.11	0.13	0.18	0.07	0.2
P_2O_5	0.20	0.32	0.29	0.17	0.14	0.10	0.08	1.32	0.85	0.32	0.5

A. Chill of Giant dyke. Watts (1966 anal.110).

B. Essexite Dresser & Denis (1944)

C. Average olivine basalt of the Scottish Carboniferous (Tomkeieff 1937)

TABLE 3 - 2. T R A C E E L E M E N T S.

	67144	67293	68260	68263	67296	67297	67346	67320
Rb	-	20	-	-	20	32	-	10
Ba	-	593	-	-	-	1,810	572	-
Sr.	-	1,870	-	-	2,530	2,310	-	568
La	-	-	-	-	-	-	-	-
Ce	-	-	-	-	-	-	-	-
Y	-	14	-	-	-	-	-	-
Zr	-	87	-	-	52	54	-	59
Nb	-	20	-	-	9	5	-	14

WALL ROCK GABBRO

LEUCOCRATIC LAMINATED GABBRO

RHYTHMIC BANDED GABBRO.

form the mafic gabbro. A very few layers lack either the magnetite-pyroxenite, or the anorthosite layer. A few bands are 2-3m wide bow shaped troughs 30 - 40cm deep at right angles to the strike of the banding. The persistent rhythmic banded units truncate the troughs.

The trough bands, the complementary nature of the layers, and the irregular distribution of the rhythmic units in the homogeneous laminated gabbro all support an origin through the crystal sorting of the laminated gabbro cumulates under the action of strongly flowing currents. Such currents may be crystal-density currents, analogous to turbidity currents, triggered through fault movements (? fault A-A) and the foundering of crystal cumulates from the chamber walls. The same sequence of bands may be recognised on either side of this fault. Such currents therefore must have affected the majority of the crystallization surface, and cannot be due to local slumping (cf upper ferrodiorites of Skaergard and Kiglapait). These rapid currents are therefore envisaged as violent convective overturns superimposed on the slow continuous convection currents of the lower sequence.

The exposed thickness of the R.B.G. is 57m. The central units, which should lie on the east side of fault A-A north of Arete Lake, and on the plateau south-west of it, have been removed by faulting accompanying the intrusion of the pyroxenites.

THE MINERALOGY.

The chief mineralogical changes, and chemical changes accompanying them are shown on figs.3-2 and 3-3. The cryptic variation includes the loss of cumulus olivine and apatite in the B.F.G. and the feldspar variation from An_{52} - An_{43} on ascending the sequence.

The main characteristics of the rock forming minerals have been described above. The pyroxene is a pale pink titanaugite optically similar to that of the pyroxenite or diorite. The proportion of magnetite to ilmenite is 1:1 in strong distinction from the .3:1 of the pyroxenite and 1:3 of the diorite.

The amphibole is a deep red brown strongly pleochroic barkevikite similar to that of the pyroxenite and in contrast to the green primary hornblende of the diorite.

The biotite is entirely secondary rimming the pyroxene and oxide.

THE CHEMICAL COMPOSITION.

The variations in chemical composition are shown in Table 3-2 and Fig 3-3. The cryptic variation is seen to be slight. P_2O_5 shows an abrupt decrease as expected from the mineralogy. Fe_2O_3, CaO and TiO_2 show an overall increase whilst SiO_2, K_2O and possibly Na_2O and Al_2O_3 show a net decrease. These changes and the much stronger variation in the L.L.G. reflect the mineralogical variations.

The initial composition of the intrusive magma if taken as similar to the B.F.G. is similar to a slightly differentiated alkali basalt or syenogabbro particularly in the high $\frac{Fe}{Fe+Mg}$, high total alkalis, high Ti

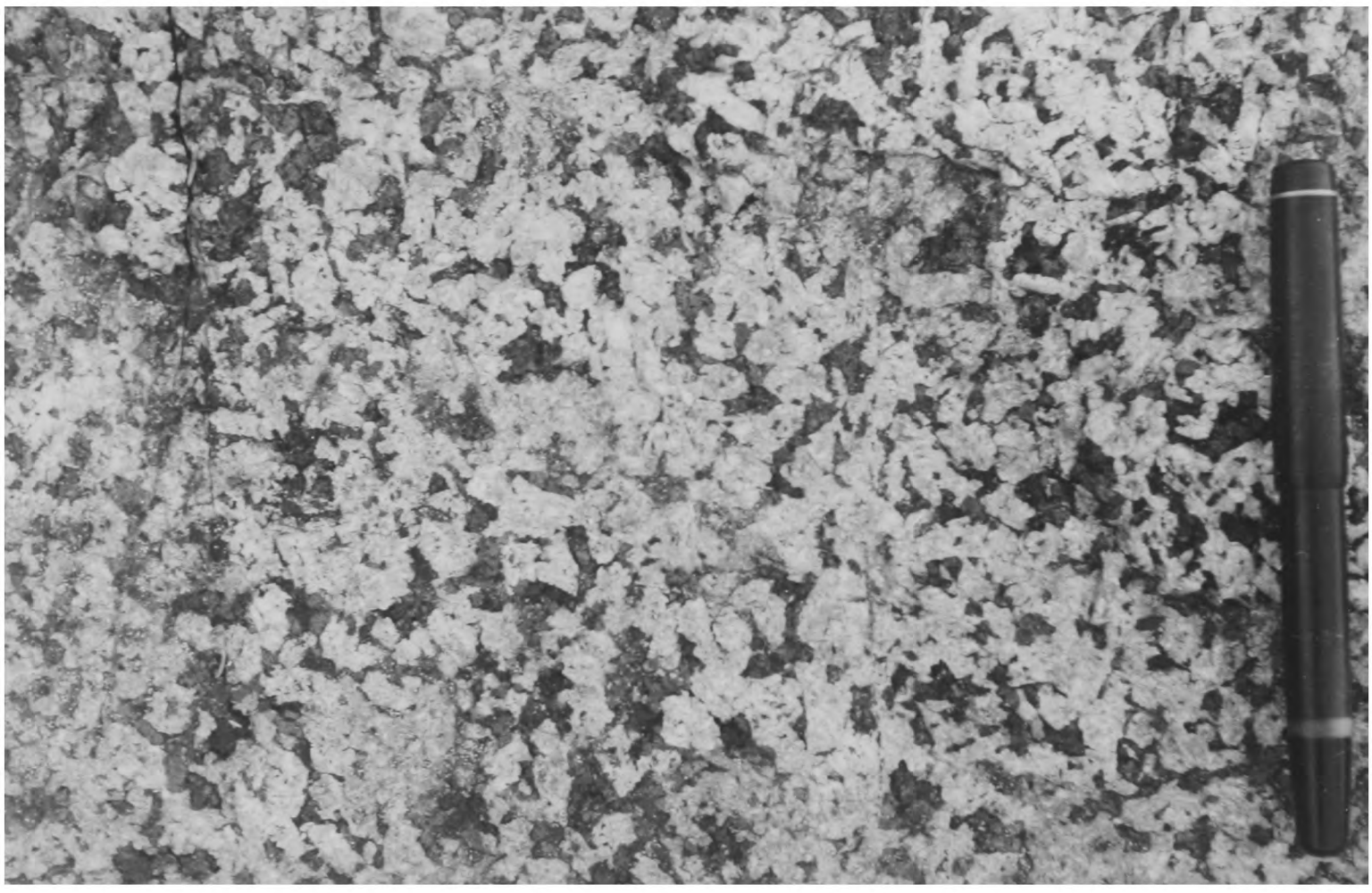


PLATE 3 - 6 Cumulus plagioclase texture of the Big Feldspar Gabbro. Shore east of island .

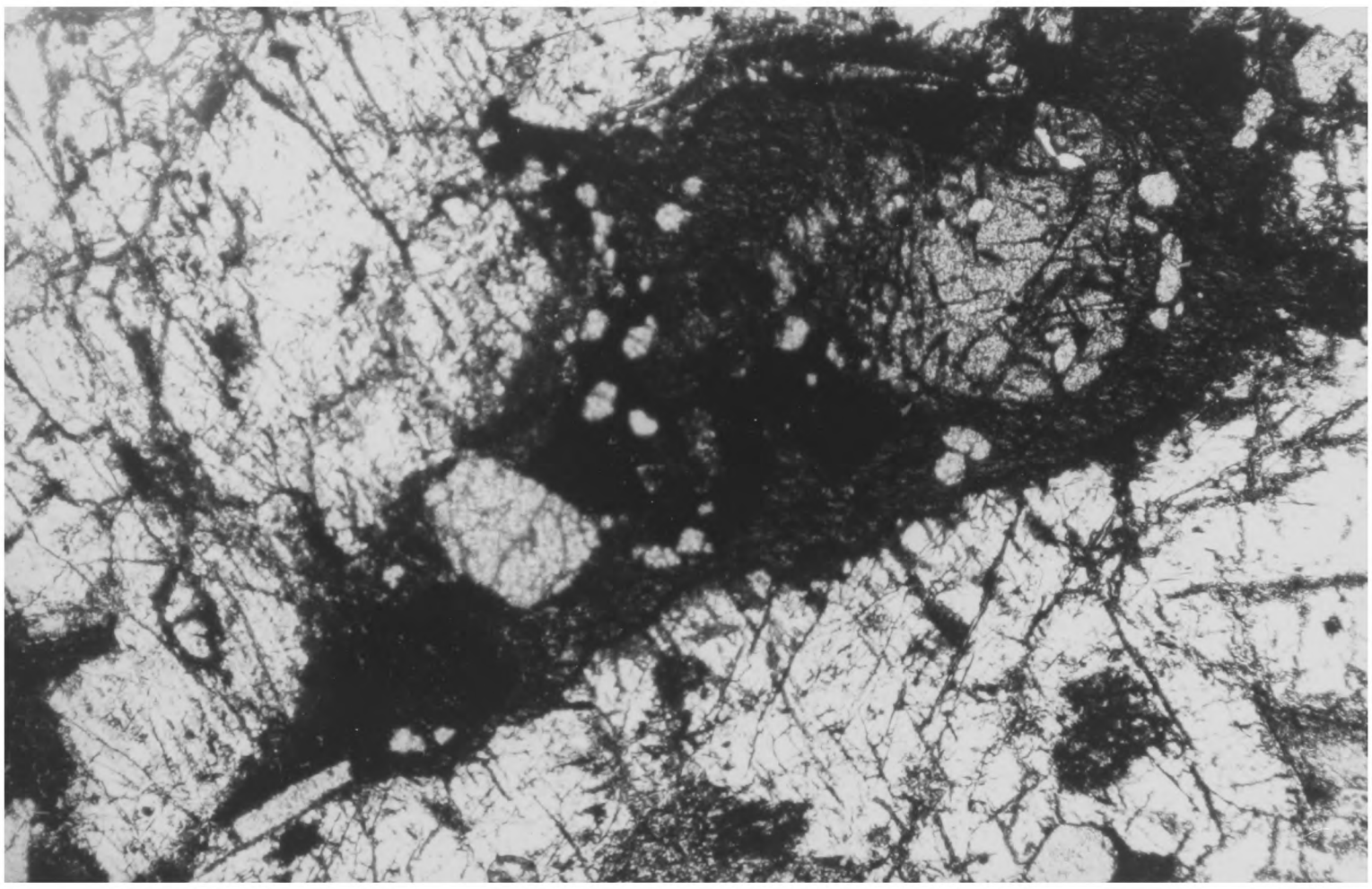


PLATE 3 - 7 Mafic aggregate in the Big Feldspar Gabbro. Central pyroxene together with cumulous apatite and oxide are enclosed within poikilitic barkevikite. Shore east of island . spec. 67293 x 4



PLATE 3 - 8 Lamination in the lower leucocratic gabbro. Shore east of island F.



PLATE 3 - 9 Mafic mineral banding in the lower L.L.C. The banding is formed through the winnowing of mafic minerals and there are no complementary feldspathic horizons. Shore exposure east of island F.

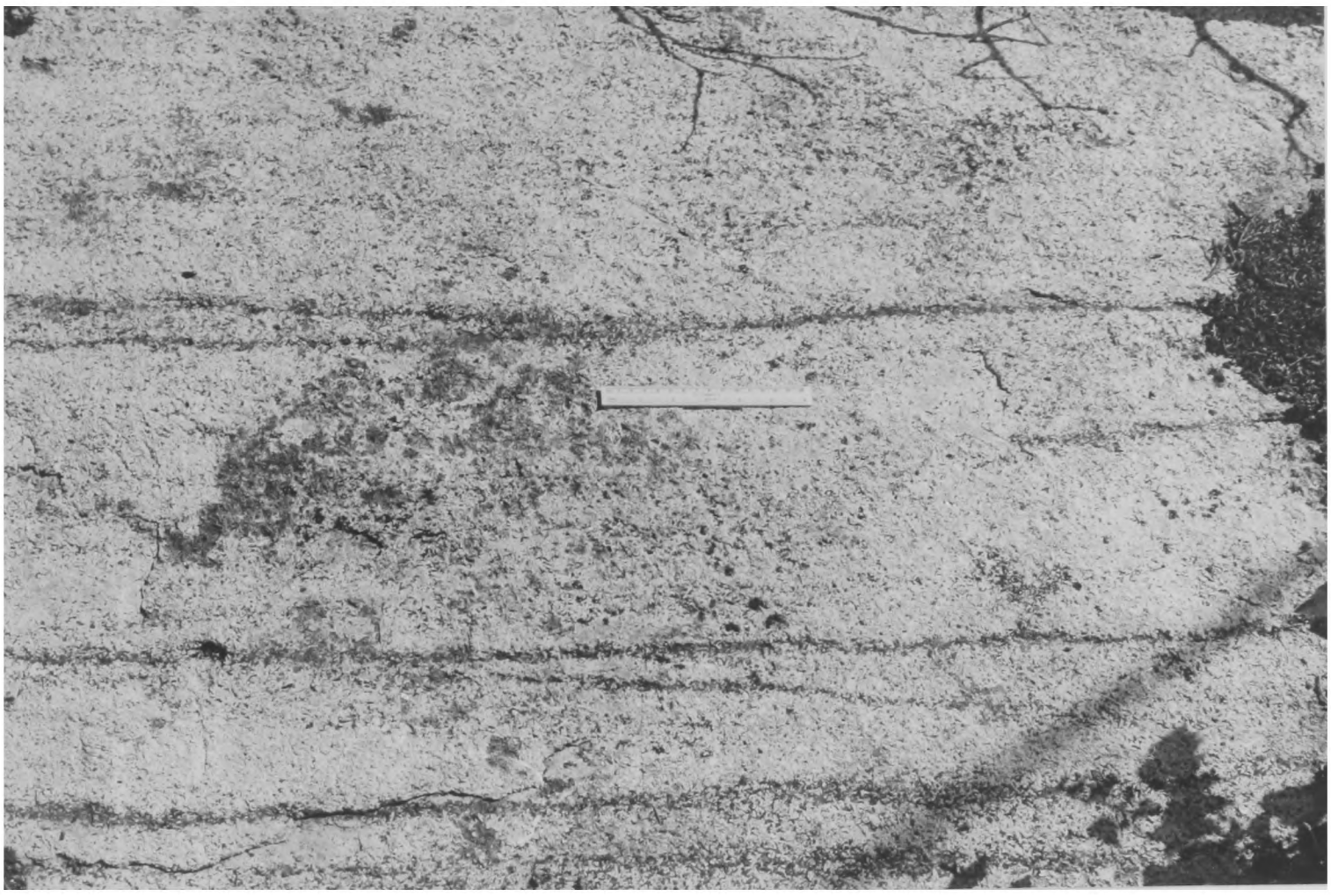


PLATE 3 - 10 Crossbedding of the mafic mineral bands. The intervening rock is laminated parallel to the banding. Detail of same exposure as pl. 3-9.



PLATE 3 - 11 Persistent rhythmic banding in the lower R.B.G. Roche moutonnee 200m S.W. of Arete Lake. Magnetite -pyroxenite intruding the fault A-A, forms the high ground in the background.

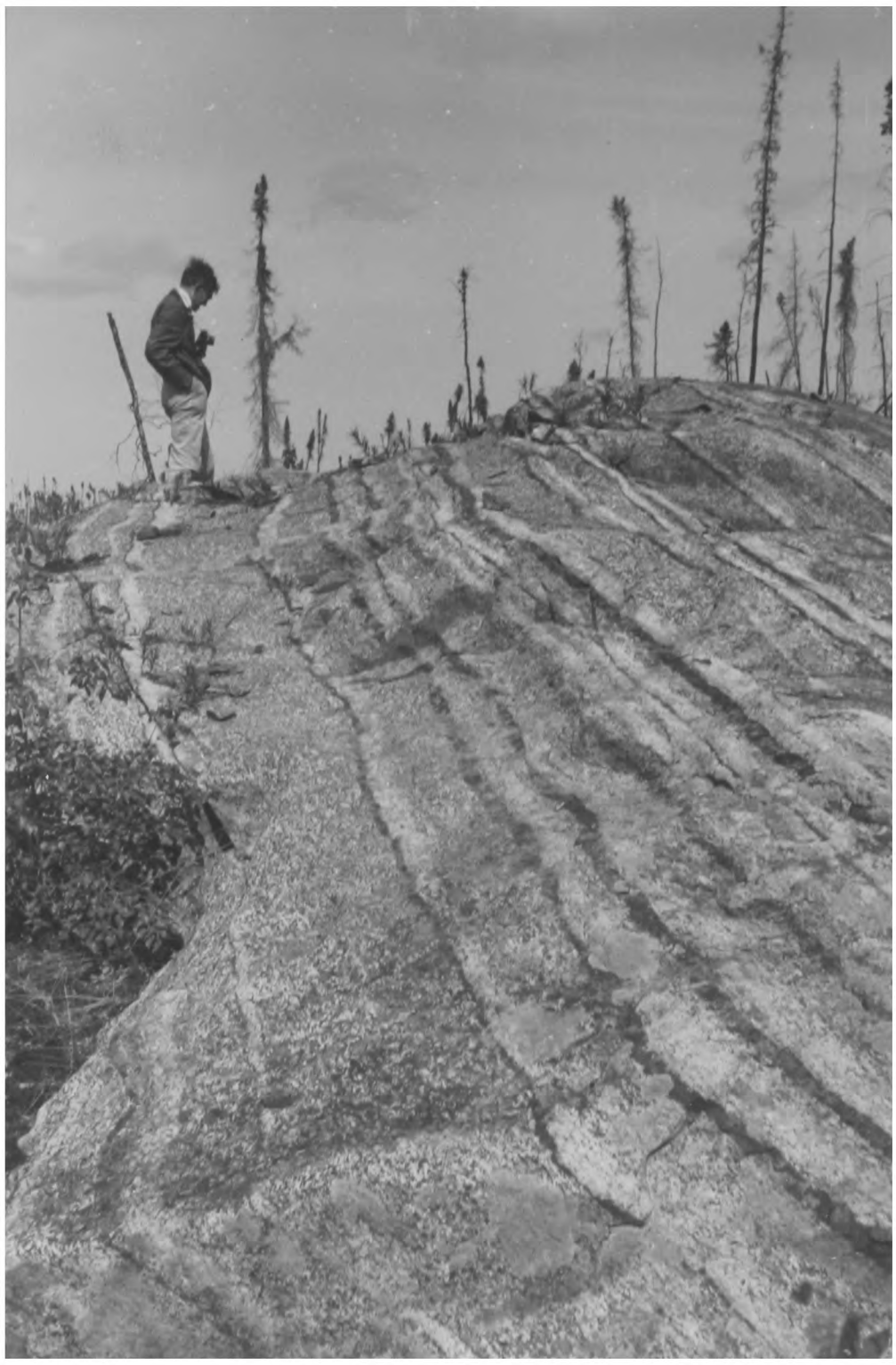


PLATE 3 - 12 Complementary magnetite-pyroxenite and anorthosite rhythmic units in the middle R.B.G. Each unit is separated by a variable thickness homogeneous mafic laminated gabbro. 100m S.W. of Arete Lake



PLATE 3 - 13 Impersistent trough banding in the middle R.B.G. The trough is only a few centimetres deep and approx. 3m across 100m S.W. of Arete Lake.

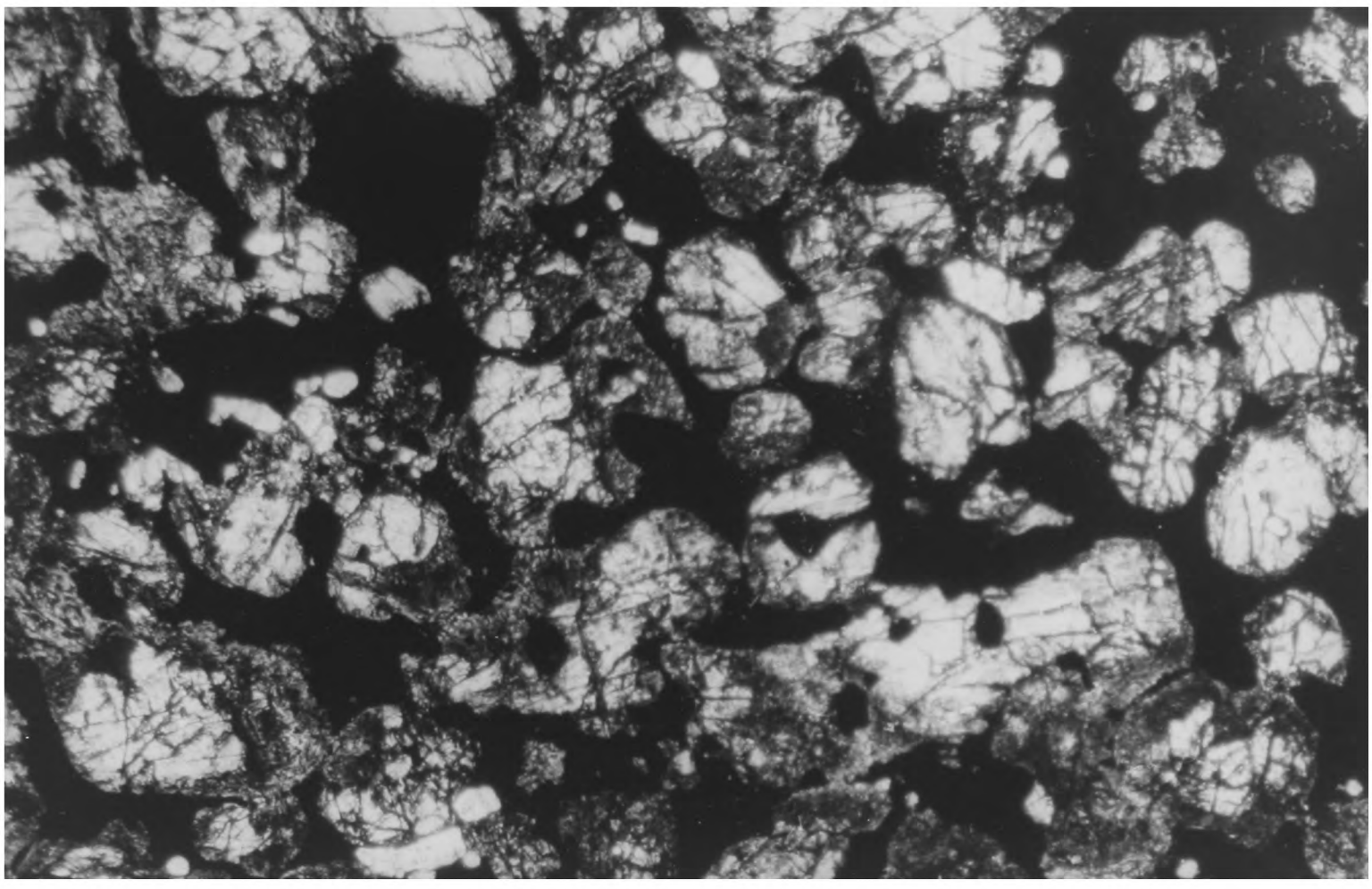


PLATE 3 - 14 [illegible]us magnetite - pyroxenite from the middle R.B.G. The cumulus minerals are pyroxene, magnetite, ilmenite and apatite. The oxides show extensive adcumulus growth. Spec. 67320A. x 6

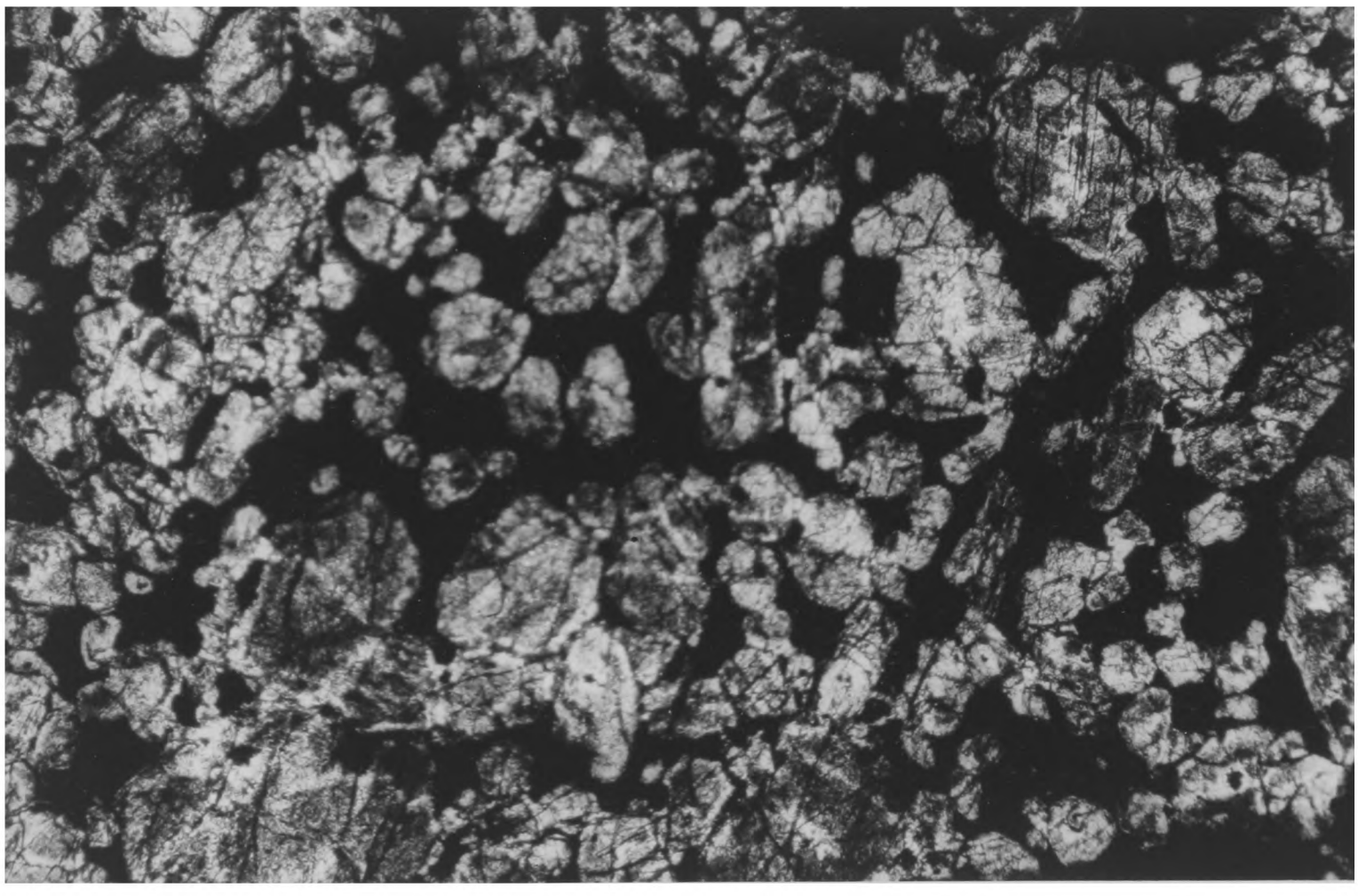


PLATE 3 - 14A For comparison, chilled magnetite - pyroxenite. Both pyroxene and magnetite are euhedral, but included oxide is rare and apatite is absent. Magnetite and ilmenite show interstitial [illegible]. Spec. 67259 x [illegible].

and relatively high Rb, Sr, Nb and Ba. The dominative composition contains low olivine and lacks nepheline and quartz except in altered varieties. In this it contrasts with the essexites of the Monteregian province, (Dresser and Denis 1944) of Massum, (Mathias 1956), Okonjeje (Simpson 1954), and with the syenogabbros of West Greenland (Watts 1966)

THE RELATIONSHIP OF THE UNITS.

As described above, the B.F.G. forms a non-cumulus border group to the layered gabbros. It is thought to have formed through crystallization on the magma chamber walls simultaneously with the formation of cumulate rocks on the floor. The increasing proportion of feldspar in the B.F.G is thought to represent a real change in the liquid composition towards a more feldspathic alkaline diorite or syenite through the formation of olivine, pyroxene, labradorite-andesine cumulates at greater depths within the pipe. The increasing alkalinity of the residual liquid is reflected in the increasing proportion of barkevikite, apatite and oligoclase in the inner B.F.G. The exposed layered rocks are orthocumulates modified by winnowing to produce rhythmic banded units, and represent only a small proportion, ~180m of the total thickness of cumulate rocks. The abrupt transition from L.L.G. to mafic gabbro (R.B.G.) is most readily explained by a new influx of magma similar to the B.F.G.

The intrusion of Kiglapait (Morse 1962) which possesses a similar alkali gabbro parent shows successive differentiates of diorite (and anorthosite), troctolite, melagabbro, ferrodiorite and larvikite. The upper differentiates show extreme enrichment in Fe-Ti oxides and show strong rhythmic banding. With the exception of the olivine rich nature of the Kiglapait gabbro the fractionation trend of this gabbro, if fully exposed, is thought to be similar. The final differentiates would then be quartz free ferrodiorite, and quartz free iron-rich syenite similar to syenites 1 and 3.

THE INTRUSIVE OLIVINE MAGNETITE PYROXENITES.

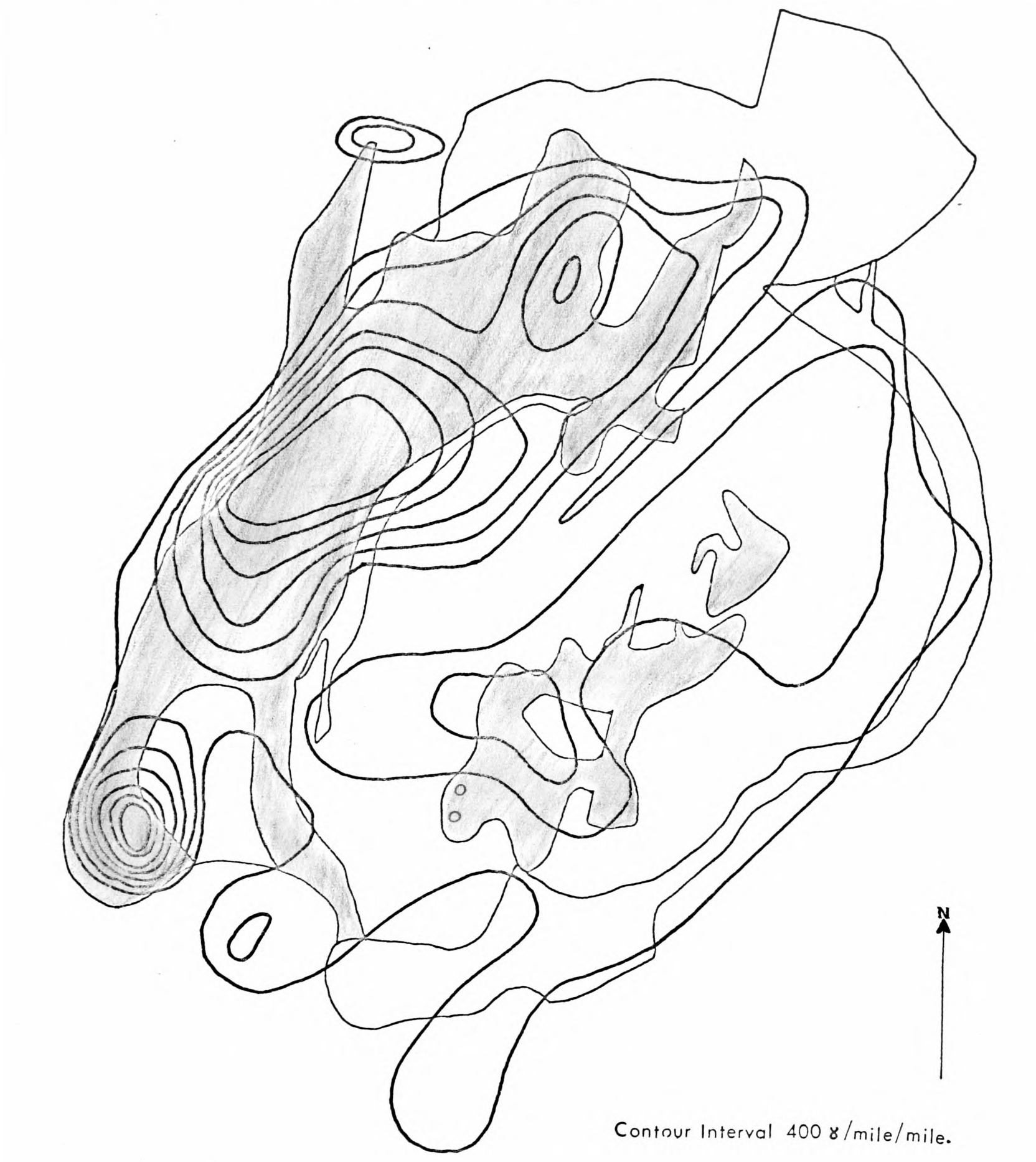
The intrusive pyroxenites occur in two areas which are delineated by the second derivative of the magnetic anomaly (Map 3-3). These are -

i) an arcuate mass around the western diorite margin
ii) numerous dykes and small masses within the central gabbro area.

The arcuate mass follows the same vertical fracture as the syenite ring dyke 3 but is confined to the segment west of the bisecting transcurrent fault A-A. As is shown on map 3-3, this fracture predates the transcurrent faulting and follows the diorite-granodiorite contact except around the northern sector which it truncates.

The former extent of this mass to the southwest of the exposed area may be followed in the field by the occurrence of pyroxenite xenoliths in the syenites and by the occurrence of a screen of pyroxenite and remobilized granodiorite between syenites 2 and 4. The eastern contact of the arc is exposed along most of its length on the eastern lake shore and on the offshore reefs.

MAP 3-3 SECOND DERIVATIVE OF THE AEROMAGNETIC ANOMALY CENTRE 1



The second derivative (curvature) has been calculated by the method of Vacquier et al (1952) using a $\frac{1}{4}$ mile grid spacing. The grid is based on the $\frac{1}{2}$ mile spacing of the flight lines in plate 2-1. Note how closely the anomaly follows the exposed olivine-magnetite-pyroxenites[Grey]

Associated dykes branching from the mass are rare.

The second derivative of the magnetic anomaly shows the steepest curvature along the north-west margin extending south to Ship island. This indicates a sharp vertical contact extending to a depth of greater than 300m with a high susceptibility contrast consistent with the granodiorite-pyroxenite contact exposed at the north-west margin of the anomaly.

The smaller pyroxenite masses are also outlined by a weak low curvature anomaly denying a larger mass at depth. They are confined to the area of the gabbro wedging out on approaching the gabbro margin. The dykes range from a few centimetres to 30m in width, and the larger ones from 50m to 1000m in length. Most are concentric about the same centre as the layered intrusions but being vertical crosscut the layering.

Much displacement, mostly vertical, occurs at the margins of the larger masses. Several of the dykes intrude pre-existing faults including the fault A-A. The field distribution suggests that much of this central area was intruded synchronous with, or after the displacement on A-A.

THE COMPOSITION OF THE PYROXENITES.

All the larger masses are olivine-magnetite-pyroxenites with an average composition of circa 19% olivine, 59% pyroxene, 22% magnetite + ilmenite. Towards the margin the grain size decreases whilst the oxide content rises such that the chills are composed of olivine-free magnetite-pyroxenite. Frequently the chilled rock is absent, and the masses are bordered by hybrid remobilized gabbros or diorites.

Most dykes are composed of fine-grained magnetite pyroxenites with 24-32% oxide. The broader dykes show an increased pyroxene content together with a small proportion of olivine. The chilled rocks and the dykes contain 0-5% euhedral olivine and pyroxene phenocrysts.

A single mass O-O is composed of olivine-plagioclase-pyroxenite with an original composition of circa 30% olivine, 40% pyroxene, 10% oxide, 20% plagioclase. No chills from this mass nor contacts with the other pyroxenites are exposed.

Within the area of the pyroxenites there are found 1-5cm. dykes of plagioclase pyroxenite with 5-10% olivine, pyroxene and oxide phenocrysts. The modal composition is ultramafic (<30% plag), and the chemical composition similar to that of the olivine-plagioclase pyroxenite, and the amphibolite member of the Alaskan type ultramafic intrusions.

REMOBILIZATION AT THE OUTER CONTACT.

For up to 30m from the granodiorite contact the country rock is remobilized. The partial melt contains coarse feldspar phenocrysts, mosaic patches of quartz, and rare rounded pyroxenite xenoliths in a flinty grey matrix. The remelted material shows a modal composition of circa 25% corroded biotite, 40% feldspar (with about equal proportions of plagioclase and potassic microperthite), 35% rounded quartz, 2% oxide, and several large zircons and coarse allanite. Locally the matrix becomes granophyric.

The composition of this melt, as a biotite rich quartz monzonite, is quite distinct from the diorite-syenite trend.

REMOBILIZATION OF THE GABBROS AND DIORITES.

The remobilization of partially crystalline material also occurs at the gabbro and diorite margins. In the gabbro lobate pillow-like margins form against the pyroxenite. Gabbro also backveins the dykes.

For up to 10m. from the contact diorite is hybridized to form a vertically laminated platey feldspar ferrodiorite. Locally a remobilized hybrid containing xenocrysts of pyroxene, olivine, and magnetite invades both the diorite and pyroxenite. The feldspars in the diorite are shattered and iron oxide exsolved at the pyroxene rims as small globules.

THE MINERALOGY.

In the magnetite-pyroxenites and olivine-magnetite-pyroxenites rounded subhedral grains of pyroxene and olivine are enclosed in an almost continuous network of magnetite and ilmenite. In reflected light both magnetite and ilmenite can be seen also to have subhedral cores. The grain diameters are typically in the ratio Ol:Px:oxide 10: 30: 4. Poikilitic oxides extend for up to five pyroxene grain diameters.

In the plagioclase bearing pyroxenite, plagioclase replaces the oxide as the poikilitic phase.

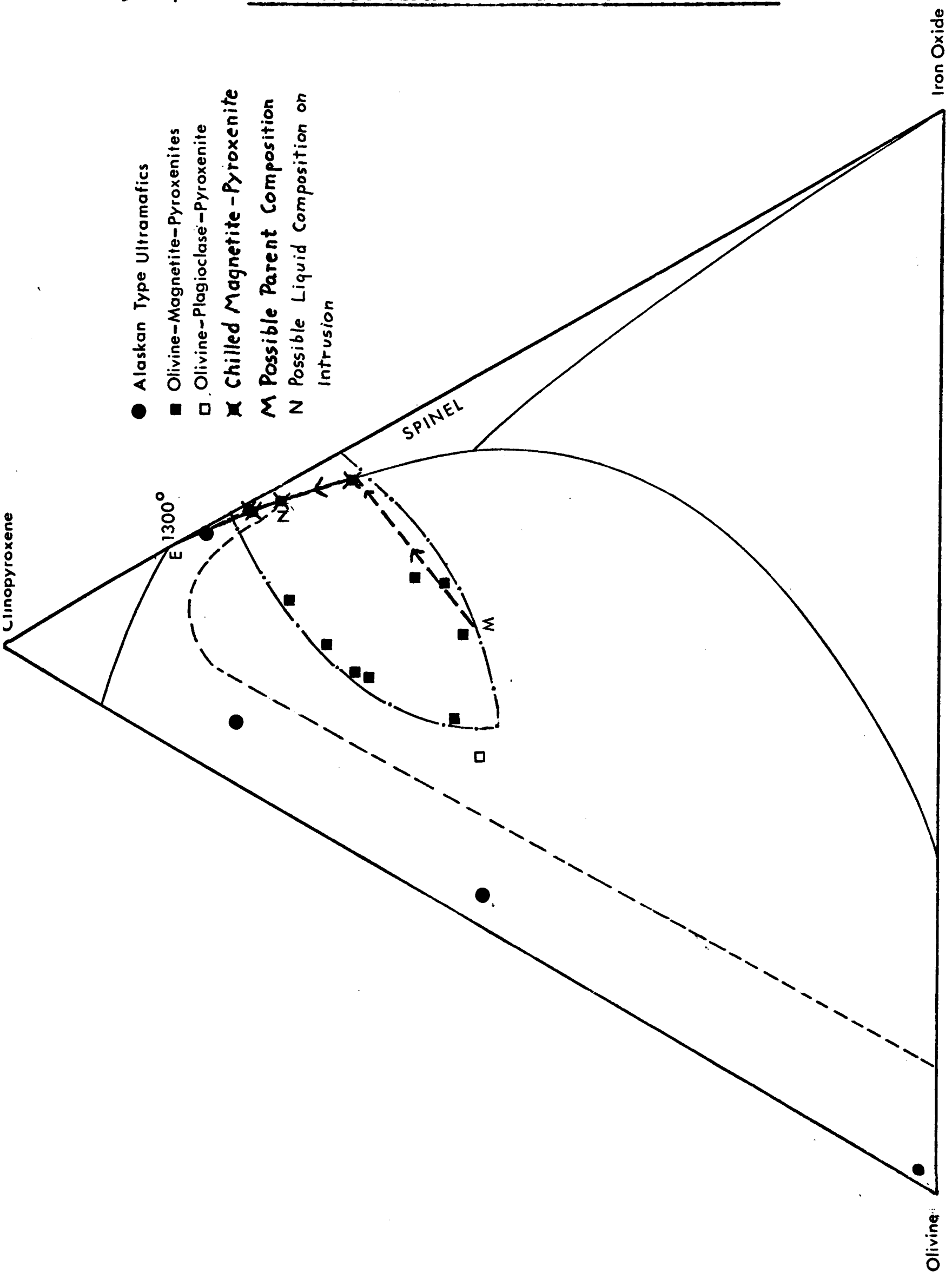
The sequence of crystallization appears to be olivine, olivine + oxide, olivine + oxide + pyroxene, oxide + pyroxene, oxide+ barkevikite + biotite ± apatite.

Within the broad arcuate mass elongate pyroxenes define a clear vertical lamination. In some cases a weak horizontal lineation is also shown. Both features are strongly developed in the magnetite-pyroxenite chilled dykes. Combined with the occurrence of marginal laminated remobilized diorite this is taken as evidence for the forceful upward movement of the partially crystalline magma.

The modal composition of the ultramafic rocks based on point counting (average 1,800 counts/slide) of a representative series is shown in Fig.3-4. For comparison the compositions of the Alaskan zoned ultramafic intrusions (Irvine 1963, Ruckmick and Noble 1959) are also shown, together with the field boundaries in the pseudoternary system, forsterite-diopside-iron oxide at 10^{-6} atm. PO_2(Presnall 1966). These pyroxenites are clearly richer in oxide than either the comparable Alaskan pyroxenites or the piercing point E. Most pyroxenites contain less than 5% other phases and thus lie genuinely within the diagram.

Two important points stand out. Firstly the magnetite-pyroxenites lie along the boundary between the olivine and the spinel fields, and secondly the composition field of all the pyroxenites is elongate parallel to a line joining the magnetite pyroxenite chill to the olivine apex.

FIG 3 - 4 MODAL COMPOSITION [illegible] IVE PYROXENITES



The modal analyses of the Alaskan zoned ultramafic intrusions dominantly fall within the dashed area. The average compositions of the Union Bay dunite, peridotite, olivine-pyroxenite, and magnetite-pyroxenite are given by the dots. The field boundaries in the system $MgSiO_4$-$CaMgSi_2O_6$,-FeO are those at 10^{-6} atm. oxygen fugacity recalculated[4] to modal compositions from Presnall (1966).

The first suggests that the magnetite-pyroxenites are derived by crystal fractionation, the second that the fractionated mineral is largely olivine. The sequence of crystallization is in accordance with this hypothesis.

The distribution of points on fig 3 -4 shows that there are real differences in composition in the different areas. These may be explained in terms of the fractionation, through crystal settling of the olivine and oxide phases, such that at any time the magma composition lies along a line joining the liquid composition on N-E to the olivine corner. Bhattacharji and Smith (1964), in scale experiments simulating magmatic flow in the Muskox feeder dyke, have demonstrated the concentration of olivine phenocrysts in the central zone, the concentration being favoured by a low viscosity and by high rates of flow.

In view of the extensive vertical lamination and the central concentration of olivine it is suggested that a similar fractionation occurred at Big-spruce lake. Comparable features have been observed and simulated in picritic dykes and sills such as those of Skye (Simkin 1967, Drever and Johnson 1967, Bhattacharji 1967). The parent magma is believed to be an olivine-magnetite-pyroxenite comparable to M.

DETAILED MINERALOGY.

Olivine: Fresh olivine is rare. It occurs as clear colourless grains crossed by irregular magnetite-rich fractures, enclosed in the oxide matrix. Most crystals show a $2v=85-87^{\circ}$, but micro-probe analysis shows a composition of Fo_{63-66}. The olivine in the plagioclase-pyroxenite is similar to that from the magnetite-pyroxenites.

Alteration within the ultramafic rocks is of two kinds; firstly a "static" alteration which involves no loss of crystal form, no disruption of the matrix and no shearing; secondly a "dynamic" alteration which succeeds the first, and is accompanied by extensive shearing.

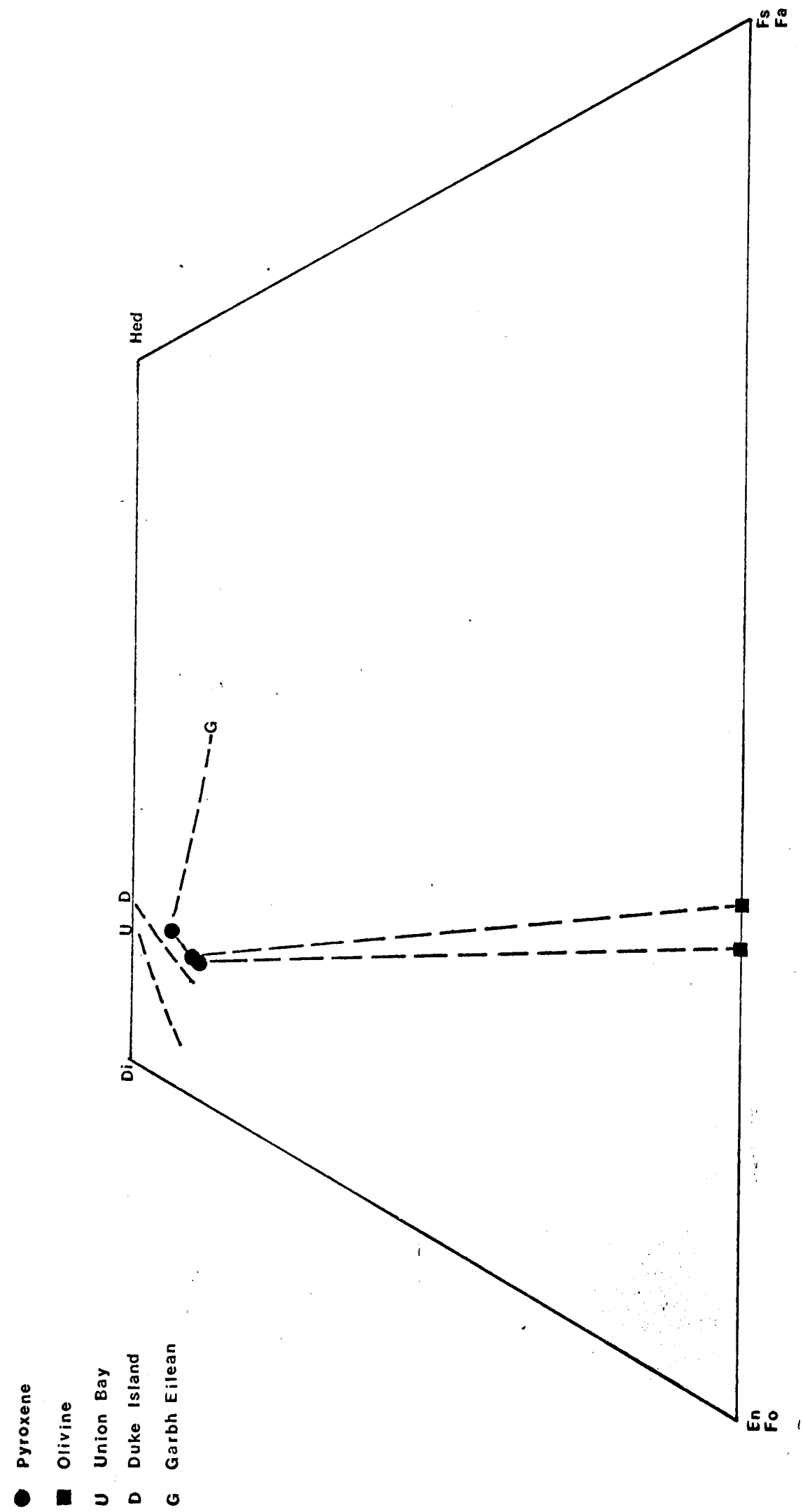
The static alteration of olivine, in the magnetite-pyroxenites, results in the formation of a colourless tremolite and talc. Generally talc forms a fibrous grid lining cracks. On shearing, olivine, tremolite and talc are replaced by blue green hornblende, chlorite, hematite, goethite, and dolomite.

In the plagioclase-pyroxenites, olivine-plagioclase contacts are rimmed with fibrous actinolite. Much of this olivine is replaced by pale yellow serpentine.

Pyroxene: The pyroxene occurs as subhedral elongate grains. It is pale pinky-brown with a weak pleochroism and $2v=50^{\circ}$. Most grains show a fine needle like exsolution of oxide which in a few cases defines a slight oscillatory iron enrichment towards the rim. Micro-probe analysis shows an almost constant composition of $Ca_{34.6}\ Mg_{55.8}\ Fe_{9.6}$ (the discordant result has excess CaMgFe in the analysis).

This composition is comparable to that of the pyroxenes of the Tulameen or Duke Island pyroxenites (Irvine 1967). It is somewhat less calcic

FIG 3 - 5 **ANALYSES OF COEXISTING PYROXENES AND OLIVINES FROM THE OLIVINE-METAGABBRO-PYROXENITES.**



For comparison the olivines from the Union Bay complex average $Fo_{73}Fa_{27}$ (Ruckmick and Noble, 1959).

TABLE 3 - 3. ANALYSES OF THE INTRUSIVE PYROXENITES.

	67259	68123	2784	67306	2779	67252	A	B	C
	Magnetite - Pyroxenites			Olivine-Magnetite Pyroxenite	Olivine-Plagioclase Pyroxenite	Amphibolite			
SiO_2	32.28	36.75	38.96	39.75	43.11	40.05	39.97	38.3	37.37
Al_2O_3	3.83	5.56	4.01	6.30	6.33	9.84	8.68	7.2	15.34
Fe_2O_3	10.19	7.77	-	6.86	6.88	8.85	8.63	13.3	9.48
FeO	19.44	14.95	27.54	15.15	10.62	14.31	7.99	9.7	7.64
MgO	11.99	11.08	10.03	11.16	17.54	6.37	10.32	11.7	13.00
CaO	9.73	12.48	10.60	10.16	10.68	10.14	15.18	16.7	11.80
Na_2O	0.57	0.32	0.48	1.39	1.07	1.98	1.19	0.9	1.74
K_2O	0.06	0.10	0.00	0.95	0.34	0.70	0.74	0.2	0.49
TiO_2	9.96	9.67	8.20	7.52	2.53	6.30	4.05	1.8	1.47
MnO	0.19	0.26	0.18	0.17	0.27	0.22	0.19	0.1	0.10
P_2O_5	0.00	0.07	0.00	0.10	0.03	0.40	0.10	-	0.00

A. Yamaskite, Yamaska, Monteregian Province Washington (1917)

B. Magnetite-hornblende-pyroxenite Duke Islands Complex. Taylor (1965)

C. Hornblende-clinopyroxenite Duke Islands Complex Irvine (1965).

TABLE 3 - 3. TRACE ELEMENTS.

	67259	68123	2784	67306	2779	67252	A	B	C	
Rb	< 2	< 2	< 2	31	-	16	-	-	-	
Ba	< 5	< 5	< 5	405	167	546	-	-	-	
Sr	59	95	66	298	273	744	-	-	-	
La	-	-	-	62	-	126	-	-	-	
Ce	-	-	-	96	-	105	-	-	-	
Y	-	16	-	-	-	-	-	-	-	
Zr	61	95	48	187	85	136	-	-	-	
Nb	4	20	< 2	19	< 2	27	-	-	-	

than that expected from an alkaline intrusion and is not enriched in soda.

The olivine-pyroxene tie-line shows a distinctive negative slope which may result from the much greater iron enrichment of the magma than in the Alaskan ultramafics or from a higher degree of differentiation with low PO_2.

Pyroxenes associated with steatized olivines show no alteration apart from narrow hornblende rims. Many marginal rocks, or sheared rocks, are wholly converted to hornblendite, with minor actinolite and chlorite.

Opaque Minerals. Titanian magnetite is two or three times as abundant as ilmenite and still more abundant in the chills. Both contain small angular cores with more intense exsolution. Magnetite shows a grid-like fine exsolution of ilmenite in addition to broad ilmenite exsolution blades. Magnetite and hematite lamellae in ilmenite are narrow and rare.

Droplets of sulphide dominantly pyrite, chalcopyrite and pyrrhotite are also rare.

Plagioclase. Large poikilitic plates in the olivine-plagioclase-pyroxenite, 5-6cm across, show albite twinning. The composition of An_{42-49} results from the reaction of the original plagioclase with olivine to form tremolite, at all the crystal interfaces.

Biotite and Barkevikite.

Biotite, which is confined to the coarser grained olivine rich rocks, forms plates 3-6cm across. It fills the interstices, but does not replace olivine, crystallizing, with barkevikite, from the interstitial liquid. It is strongly pleochroic with a very high absorption.

α = brown

$\beta = \gamma$ = almost opaque red-brown.

Barkevikite crystallizes as a primary phase in all coarse rocks, and replaces pyroxene particularly around included ilmenites, even within the chill.

Together amphibole and biotite constitute under 5% of any rock. They appear to represent the small residue of an alkaline trapped liquid.

Apatite. Apatite is most significant through its virtual absence. No slide contains more than a few grains, most none. This is in contrast to the 5-15% found in the jacupirangites or anorthosite type magnetite-ilmenite-pyroxenites, for instance of Magnet Cove or Jacupiranga; or of Allard Lake.

CHEMISTRY. Table 3-3 shows the composition of the type pyroxenites. The outstanding characteristics are the extreme enrichment in titanium, the high total iron content relative to magnesium, and the saturated nature shown by the normative ortho-pyroxene. In all these they differ from the comparable Alaskan varieties (although Tulameen B.C. contains ortho-pyroxene).

THE ORIGIN OF THE PYROXENITES.

The modal composition has been used to show that the olivine magnetite pyroxenites and magnetite pyroxenites may be derived by olivine fractionation from an ultramafic olivine-rich parent. Flow of the porphyritic magma up a narrow conduit is thought to have concentrated the olivine phenocrysts at the centre of each mass.

On intrusion olivine, oxide and possibly pyroxene were phenocryst phases and therefore on the liquidus. The liquid composition must therefore have lain along the olivine-spinel boundary in the natural system olivine-Fe/Ti oxide - diopside-silica. In view of the olivine poor nature of the magnetite-pyroxenite chill, this liquid probably lay close to the composition field of pyroxene in this system.

The synthetic system forsterite-diopside-iron oxide, represents a pseudo-ternary section through the system $CaO-MgO-FeO-Fe_2O_3-SiO_2$ (Presnall 1966). For purposes of discussion the field boundaries in this section have been drawn at an oxygen fugacity of $PO_2 = 10^{-6}$ atm and recalculated to modal percent.

The immediate parent composition cannot be calculated from the observed chill nor from the bulk composition of the arcuate mass, because of the known fractionation of the phenocrysts during emplacement, and because of differential crystal settling of olivine, magnetite, and pyroxene. If the parent composition is taken as M, on cooling olivine containing a small proportion of iron may crystallize, such that the liquid may follow a curved path close to that shown to the olivine-spinel boundary. At this point magnetite and olivine may crystallize together, and the liquid may follow the field boundary towards N. This composition is believed to be similar to that of the liquid fraction of the magma, which may now carry 19% phenocrysts (by volume); 12% olivine, and 7% oxide. Further crystallization will allow the liquid to reach E, where pyroxene will join the other crystallizing phases, olivine may be resorbed, and the liquid passes out of the system towards the field of silica. (these boundaries represent the projection of the true boundaries in the larger system on to the Fo-Di-Fe oxide section).

The scatter of the modal analyses is real, and represents a regional variation in the composition of the pyroxenite bodies. Such a variation may have been produced through the fractionation of the oxides, relative to olivine.

THE ASSOCIATED METASOMATISM.

Around these pyroxenites, as around the Alaskan and Ural pyroxenites, there is developed a broad zone of saussuritized gabbros. The gabbro is intensely shattered. The feldspars are clouded with sericite. The pyroxenes are largely altered to blue-green hornblende and epidote. Between the feldspar and pyroxene or oxide, is developed a zone of fibrous biotite. These changes reflect the introduction into, the surrounding gabbros, of very abundant water. Presnall (1966) has drawn attention to the possibility that these escaping volatiles may

a) buffer the PO_2 during the pyroxenite crystallization, and
b) lower the liquidus temperature.

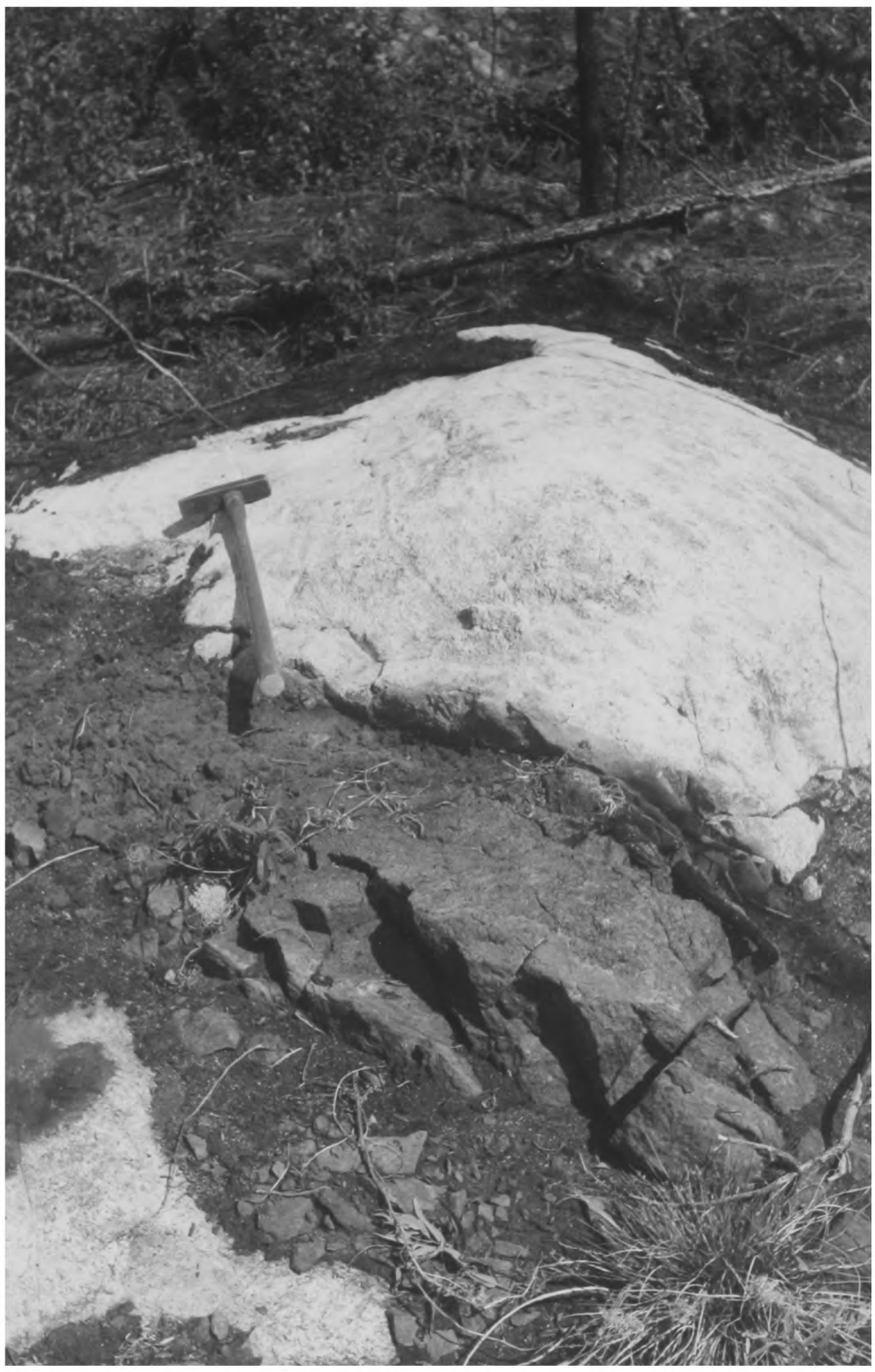


PLATE 3 - 15 Magnetite - pyroxenite dyke crosscutting the banding in the L.L.G. 300m W.S.W. of Arete Lake.

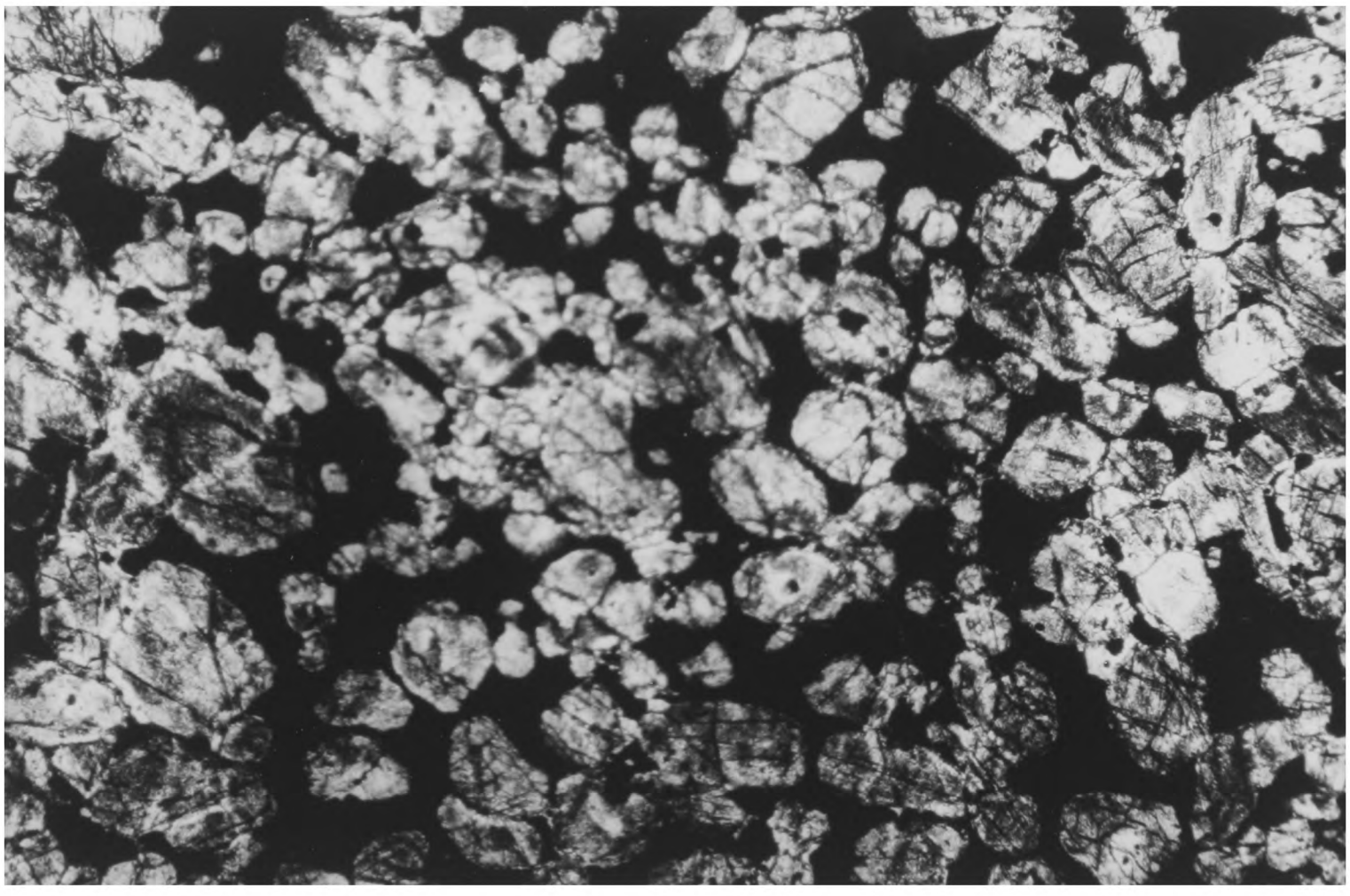


PLATE 3 - 16 Texture of the chilled magnetite pyroxenite. Margin of a 4m. dyke, S.W. corner of island E. spec 67259 x 4.



PLATE 3 - 17 Detail of the chilled margin to an olivine-magnetite-pyroxenite dyke, crosscutting the mineral banding in the lower R.B.G. The coarse near-margin rock contains streaks of a gabbro-pyroxenite hybrid.

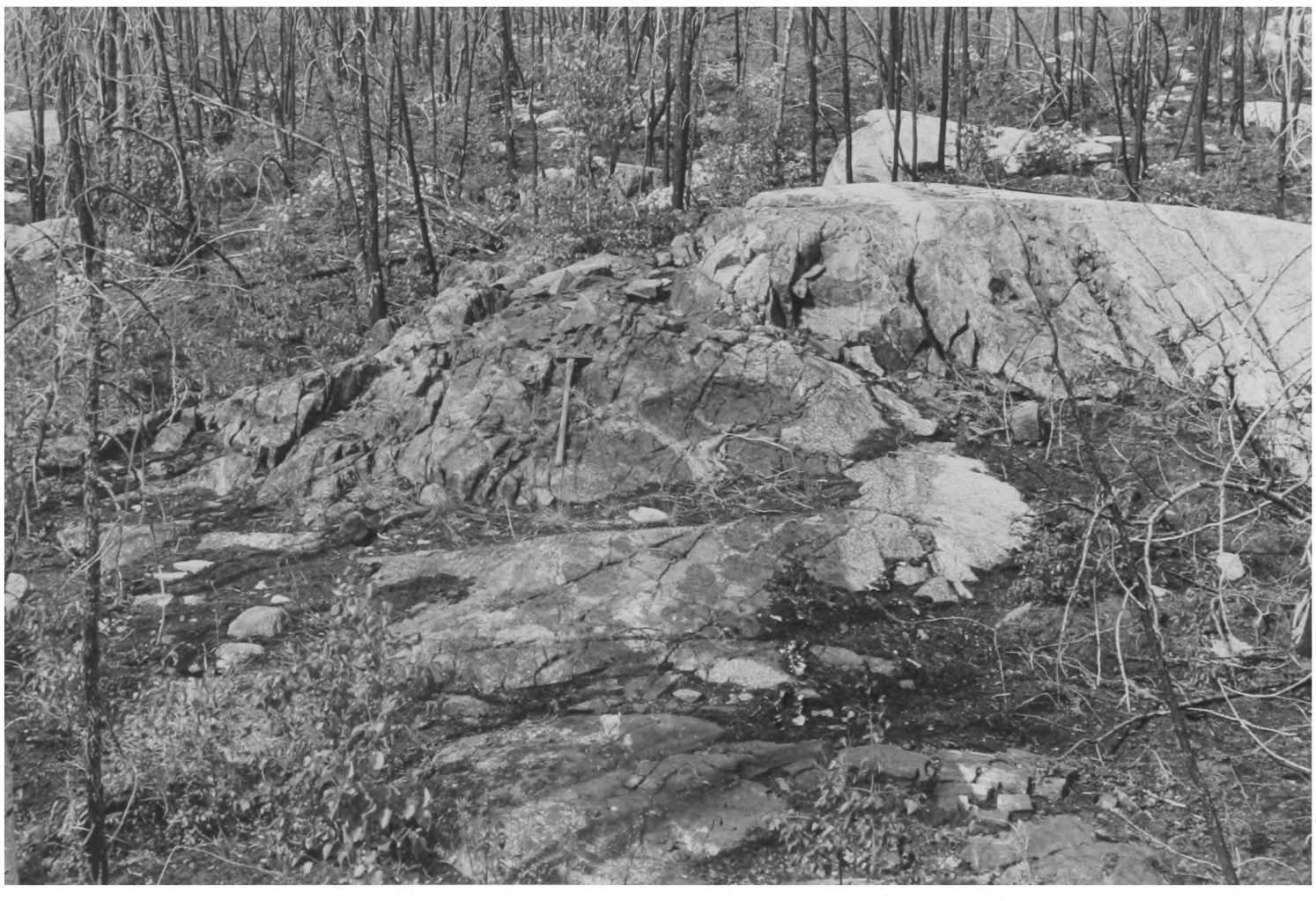


PLATE 3 - 18 Hybridization and remobilization at the margin of a 30m olivine-magnetite-pyroxenite dyke in the lower L.L.G. Backveining of the mafic hybrid has produced a pillow-structure for 2-3m from the contact.

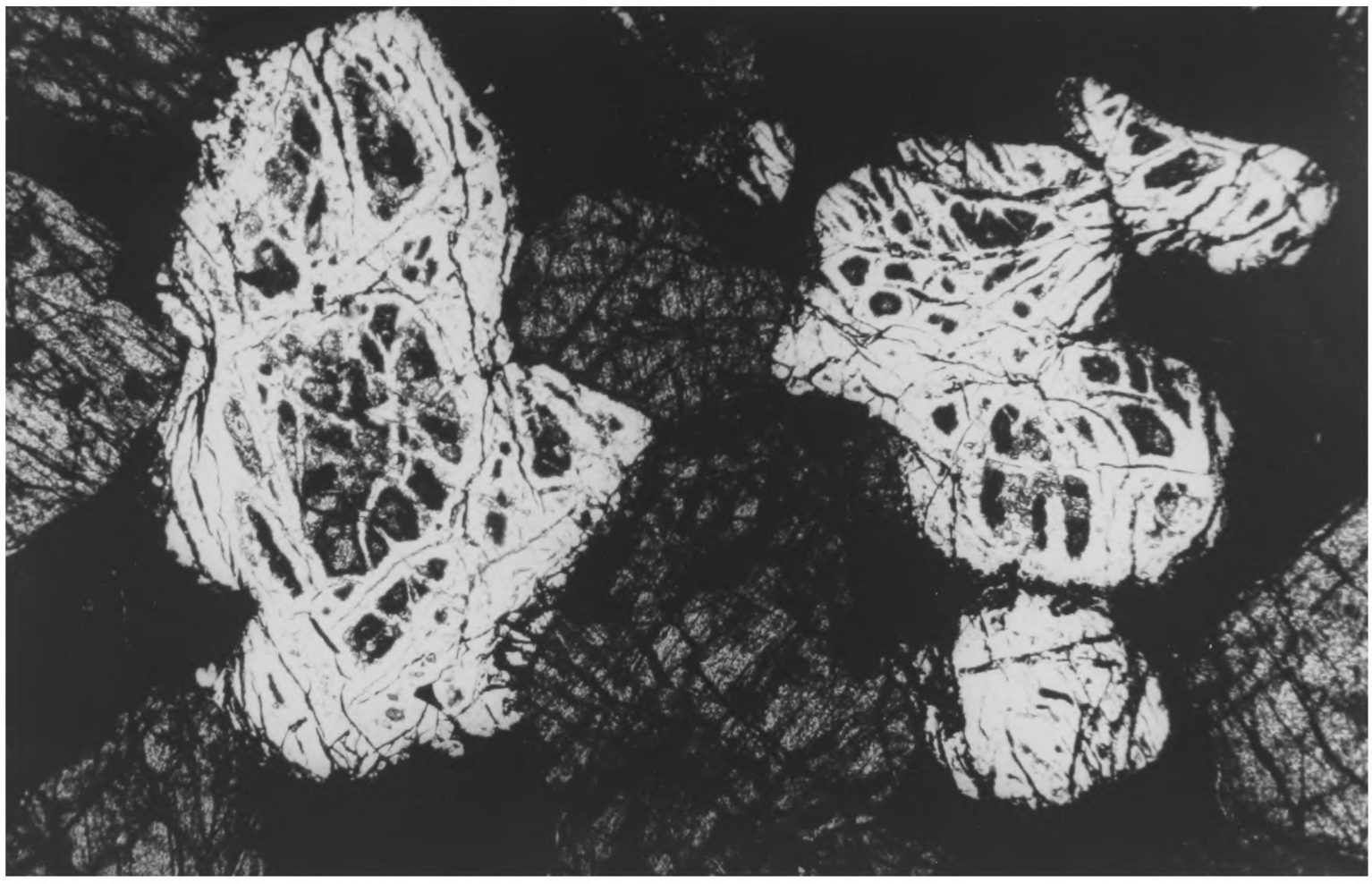


PLATE 3 - 19 Texture of the olivine-magnetite-pyroxenite. Tremolite and talc are replacing olivine along the fractures. Coarse olivine-magnetite-pyroxenite from the centre of the outer arcuate mass. East side of island C. spec. 67169. x 5.



PLATE 3 - 20 Oscillatory zoned pyroxene in olivine-magnetite-pyroxenite, showing the overgrowths of interstitial barkevikite. The large pyroxene grain, (upper right of centre) shows zoning outlined by iron oxide exsolution. Note the subhedral form of pyroxene, olivine and enclosed oxide in slides 3 - 18 to 3 - 20. N.E. end of the arcuate mass 500m W. of Beaver Lake. spec BSCL 29, x 6.



PLATE 3 - 21 The crete of Arete L . Magnetite-pyroxenite dyke intruding the transcurrent fault A-A. The dyke is bordered to the west (facing) by the lower L.L.G. and to the east by the upper R.B.G., or uplifted B.F.G. The dyke is 3-6m wide.



PLATE 2 - 22 Magnetite-pyroxenite dykes and amphibolite dykes displaced along shears complementary to the fault A-A. The shear zones are intruded elsewhere by the plagioclase porphyry dykes 350m S.E. of Arete Lake.

Mn/Mg than these rocks and hence may still be derived from an aluminous parent.

All these rocks show similar enrichment in Ti and total iron which is characteristic of centre 1 and centre 2. A derivation by successive fusion of mantle material as suggested by Taylor (1967) is therefore unlikely, for the second (pyroxenite) fraction should be depleted in Ti and Fe in addition to the alkalies and alumina.

Both Irvine and Taylor (1967) agree that magnetite-hornblende-pyroxenite provides a possible parent for the pyroxenites. The association with anorthosites in other types of complex suggests that plagioclase fractionation may be important in their derivation. Fractionation of hornblende in view of the abundance of water, may have been of greater importance producing deep-seated hornblendites. Both would deplete the alkali-basalt (composition) parent in Ca, alkalies and Al.

The alkali gabbro, which is of intermediate composition may then be derived through the fractionation of olivine, pyroxene and Ca-plagioclase from the same parent. If the gabbro and pyroxenite differentiated within the same pipe, but at different levels, as suggested for the diorite then the observed distribution may be explained.

CHAPTER IV. THE SYENITES OF CENTRE 2.

Pre-syenite metasomatism: The intrusive pyroxenites, which terminated the main igneous activity of centre 1, are separated from the syenites of centre 2, by a phase of faulting, and metasomatism. During this period there took place a 360m sinistral displacement on the fault A-A, the development of closely spaced complementary shear planes in approximately N-W and N-E directions, and the growth of epidote, blue-green hornblende, biotite, and sericite in the diorites and gabbros. Into these shear planes, and often displaced by them, were intruded a varied series of volatile rich feldspar porphyry dykes. These have undergone autometasomatism with the formation of epidote, biotite, fluorite, calcite, and secondary albite after alkali feldspar.

Pre-syenite faulting: Faulting, regional fracture, metasomatism and dyke intrusion are related in a single episode. The fault A-A is sharply bounded, occupying a 0.3 - 1m gully, dead straight, across all the units of centre 1. It is intruded by carbonated biotite-peridotites (which may belong to centre 5), and crosscut by late feldspar porphyry dykes, and the ring syenite 3. The shearing in the ultramafics postdates the cooling, and the formation from olivine, of tremolite, and serpentine (circa 550°C, 400°C max. data from Winkler 1967),

Pre-syenite Porphyry Dykes: The porphyry dykes in this sequence are

1. olivine-pyroxene porphyries (~ mafic gabbro).
2. plagioclase-pyroxene porphyry(~ big feldspar gabbro)
3. plagioclase porphyry (~ trachy-andesite)
4. rhomb anorthoclase porphyry (~ mugearite)
5. biotite-peridotite (~ alnoite)

Many of the dykes near the south margin of the intrusion are multiple dykes, with a host rock margin of plagioclase porphyry, and internal units of olivine-magnetite-pyroxenite, or one of the other porphyries. The absence of chilling, and the hybridization between these porphyries proves the co-existance of all these magmas and hence of elements of the sodic saturated (plagioclase porphyry), sodic undersaturated (rhomb porphyry) and potassic (biotite-peridotite) magma series.

Other porphyry Dykes: Similar, but more highly differentiated, porphyry dykes, were intruded during, and after, the intrusion of the syenites of centre 2, and before the intrusion of the foyaites of centre 3. These porphyries form a petrographic and geochemical series which bridges the gaps between the major intrusive basic, syenitic and undersaturated members of the complex. For convenience therefore they are described together after the end of this chapter and not in their intrusive sequence. The remaining members are : -

1. Comendite (post syenite 3)
2. Rhomb porphyries (mostly trachytes)(various ages)
3. Nepheline-sanidine porphyry (phonolite) (post syenite 4 pre-foyaite).

THE SYENITES:

General . Centre 2 is formed by at least four petrographically distinct intrusions of syenite. The syenites have been numbered 1-4 in order of intrusion. But with the exception of syenite 4, which contains xenoliths of rhomb porphyry and comendite, this sequence is based on their assumed geometry when extrapolated beyond the field exposures. The geochemical sequence based on SiO_2, $\frac{K}{Na+K}$ $\frac{Fe}{Fe+Mg}$ and Ba/K is 1, 3, 2, 4. This sequence accords with the observation that the quartz free syenites 1 and 3 occur in the area of centre 1, rimming the diorite, whilst the quartz syenites occur in the new geographical area of centre 2, lying to the south-west. Syenites 2 and 3 have an almost perfect ring dyke form, with chilled outer, and inner contacts, near constant width, and 200 and 300° preserved curvature respectively. Syenite 4 probably has this form but the central area is submerged. The form of syenite 1 is unknown but it is possibly a small plug.

From the northern margin of the foyaite to island G, there occur in the syenite, N-S veinlets of quartz rich leucocratic syenite. These appear to intrude closely spaced tension gashes parallel to the east coast lineament, and circa 100m either side of it. Petrographically these veinlets are the most alkaline and siliceous of the coarse grained intrusive syenites.

The petrography of all the syenites is similar. They are composed of platey (syenite 1) or rhombic alkali feldspar, in a mafic matrix of amphibole, (biotite), perthite, oxide, apatite, quartz and zircon. The rhombic feldspar contains rare cores of plagioclase, but is predominantly clear anorthoclase with a perthite rim. The amphibole surrounds cores of altered pyroxene, and rare (?) olivine, and is reddish brown or brownish green. Near its rims it is typically rich in magnetite and apatite. The groundmass is generally much finer grained than the 1-3mm euhedral feldspars, and is filling the angular interstices. The matrix feldspar is generally a ropy textured mesoperthite. In quartz syenites it is commonly in a granophyric or myrmekitic intergrowth with quartz.

SYENITE 1.

Syenite 1 is a medium grained, light pink weathering, rock composed of 1 cm feldspar tablets, in an interstitial matrix of amphibole and oxide. The feldspar is a clear anorthoclase without twinning, which usually has recrystallized to two or three crystals per original plate. Exsolution to perthite is rare, and even at the rims the proportion of the two phases indicates a soda-rich composition. The amphibole is a brown, strongly pleochroic ferrohastingsite, with rare cores of blue-green hornblende pseudomorphing euhedral pyroxene. Towards the rim of the amphibole, is abundant euhedral included titanian magnetite, ilmenite and apatite. There is no quartz and very little zircon in contrast to the other syenites.

The syenite outcrops only on island G. On the east side of the island there is a N-S zone of fine-grained syenite suggesting a contact only a few metres offshore. On the southwest coast, there is a zone of 1-15m olivine-magnetite-pyroxenite xenoliths. The magnetic intensity and curvature contour maps, show that pyroxenite lies to the northeast and southwest. The syenite, therefore, can extend only to the northwest and is probably in the form of a small plug (250 - 300m) centred on the island.

SYENITE 2.

Syenite 2 is a coarse-grained pink or brick red syenite found around the rim of centre 2. It is composed of 1.5 - 3cm feldspar rhombs, in a fine-grained matrix of amphibole, quartz (5 - 15%) and mesoperthite.

The feldspar is strongly zoned, with small cores of sericitized plagioclase (An_{26}) and narrow rims of mesoperthite. The majority of the crystals are composed of untwinned sodic perthite. Most are oscillatory zoned, with narrow concentric bands of mesoperthite and included amphibole. The matrix feldspar is a granular, ropy textured, mesoperthite of grain-size circa 1 - 2 mm.

The amphibole is pleochroic from brown to deep-olive green, and weakly zoned with a greener rim. It includes 0.5 - 1% pseudomorphs after pyroxene, and calcite + magnetite pseudomorphs after fayalitic olivine (?). Biotite, which replaces amphibole in the chill, forms

small hexagonal pale yellow plates.

Magnetite, ilmenite, minor apatite and zircon are included near the rims of the pyroxene. The coarse zircon (1mm) and paucity of apatite are characteristic features ofthis syenite.

Quartz and mesoperthite, with minor amphibole, apatite and zircon are the final minerals to crystallize. Variations in the proportion of this matrix are the main cause of the differences in composition within the syenite.

Syenite 2 outcrops as a long strip on the eastern margin of centre 2 (1,600m x 180 - 300m), and as two lunate masses on the western and northwest margin (1,200m x 300m and 200 x 250m). Between these outcrops and to the south it is crosscut by syenite 4. In both the western and eastern areas, it is separated from syenite 4 by a narrow (0-50m) screen of country rock, and hence exposes both external and internal chills. The exposed outcrop is sufficient to define an elliptical ring dyke form elongate east-west with major axes of 3,900m and ~2,700 m and a width of 200 - 300m. The enclosed central block of country rock, as preserved in the screens, is predominantly granodiorite, but includes diorite and pyroxenite in the north-east.

SYENITE 3.

Syenite 3 is a white or pink weathering quartz free syenite, outcropping as a narrow ring around the margin of the diorite. It is distinguished from syenites 2 and 4 by the absence of quartz, and from syenite 1 by the large feldspars and the abundance of zircon and of primary sphene.

The feldspars are thick, bluntly terminated 1.3 - 3cm tablets, of anorthoclase with anhedral overgrowths of sodic perthite. They contain rare cores of sericitized plagioclase and concentric zones of amphibole inclusions. Most specimens have recrystallised feldspars, now represented by sodic plagioclase and minor microcline.

The amphibole occurs as large interstitial aggregates of crystals poikilitic to magnetite, ilmenite and apatite in similar proportions to syenite 1. It is zoned with a reddish tinged brown core and brownish green rim, and is strongly pleochroic. Pseudomorphs after pyroxene are common in coarse-grained syenite (4-6% in 25% mafic minerals) and there are rare pseudomorphs after olivine.

Biotite, reddish brown, or with inclusions of granular rutile, is found as anhedral poikilitic crystals in the amphibole aggregates.

Zircon and sphene occur as 1-1.5mm euhedra at the margins of the amphibole crystals.

The syenite is exposed as an almost continuous narrow ring around the outer margin of the diorite. On the east and southeast side, the syenite is chilled, against granodiorite, and cuts of narrow screens of chilled diorite. On the west side it follows the contact between the diorite and pyroxenite, and is chilled against pyroxenite. The chill is fine-grained, and lacks the feldspar euhedra of the chilled quartz syenites.

The internal contact is coarse, and gradational against the diorite. On the north side there is a narrow gap across which the ring fault cannot be traced and at the edge of which both horns wedge out. However, on the south side the syenité crosses the transcurrent fault A-A with fracturing but without displacement. Stoping from the fault-face has thickened the syenite in this area. A short segment on the south-west is submerged and is probably crosscut by syenite 4.

The syenite, therefore, forms an elliptical ring dyke, following pre-existing arcuate fractures, elongate north-east to southwest with major axes of 3,180m and 1,680m and an average width of 75-150m.

The chemical and mineralogical composition of the quartz free syenites is relatively constant, since they lack the variation in the ratio of phenocryst to matrix phases, present in the quartz syenites. The chilled syenite 3 however shows a curious example of alkali exchange in contact with the pyroxenite as shown below.

	Na + K	Na	K
Coarse syenite 68031	5.97	3.90	1.97
Coarse syenite 67327	6.03	4.18	1.85
Chilled syenite 68092	6.03	5.85	0.18
Chilled syenite 68250	6.04	5.93	0.11

The mafic minerals within the chilled syenite show no greater degree of alteration than within the coarse syenite, and mosaic recrystallization of the feldspar occurs within both. This very high degree of alkali exchange between syenite and country rock (pyroxenite), demonstrates that the syenites cannot be regarded as having crystallized within a closed system, at least within the possibly still hot northern complex, and probably explains the scatter of the many of the syenites on the Qtz-Ne-Ks, and CaO-Na_2O-K_2O diagrams (figs 5-1 and 8-1).

SYENITE 4.

Syenite 4 is a coarse, mafic, quartz syenite, similar to syenite 2. Unchilled specimens are composed of 30-40% 2-3cm elongate rhombic feldspars, in a matrix of amphibole, mesoperthite, oxide, apatite, quartz and zircon. The core and rim structure of the feldspar is easily apparent in the field. The central core is composed of clear sodic anorthoclase, and marginal rims are ropy textured mesoperthite. The transition is sharp but gradational with approximately 4/5ths of the crystal length being anorthoclase. These cores are invariably euhedral with acute apices. The rims are continuous into the medium grained matrix. Subhedral green-brown amphibole is the predominant mafic mineral together with sepia biotite within the chill. The crystals are subhedral, and enclosing corroded pseudomorphs after pyroxene, occur in the angular re-entrants between the phenocrysts. Apatite, oxide (magnetite≈ilmenite), and zircon are concentrated near the amphibole margins as in syenite 1.

The interstitial liquid filling the remaining sub-angular patches has crystallized as granophyric intergrowths of quartz, and mesoperthite,

TABLE 4 - 1. ANALYSES OF SYENITES 1 AND 3.

	68360	A	68031	67327	68092[x]	67250[x]	B	C
SiO_2	57.10	57.80	59.97	62.60	63.54	63.07	58.07	57.75
Al_2O_3	17.03	18.82	17.27	16.89	15.96	16.11	16.01	17.50
Fe_2O_3	2.94	1.60	2.44	1.62	2.38	-	1.23	2.92
FeO	5.06	3.50	3.39	3.19	3.29	5.05	7.28	2.94
MgO	1.43	1.48	1.35	1.17	1.56	1.93	0.76	1.70
CaO	5.04	3.72	3.95	3.12	3.19	3.46	4.06	3.86
Na_2O	6.26	6.48	5.67	6.14	8.67[x]	8.80[x]	5.70	5.08
K_2O	2.82	3.97	4.36	4.13	0.42[x]	0.29[x]	4.20	3.51
TiO_2	1.67	1.15	1.18	1.05	0.75	0.73	1.18	1.53
MnO	0.12	0.14	0.08	-	0.09	0.08	0.17	0.19
P_2O_5	0.36	0.55	0.23	0.03	0.16	0.12	0.37	1.05

A. Larvikite Oslo province Brogger (1933).

B. Syenite Gardar province Watts (1966, 34).

C. "Ekerite" Yamaska, Monteregian Province (Dresser and Denis 1944).

TABLE 4 - 1. TRACE ELEMENTS.

	68360	A	68031	67327	63092[x]	67250[x]	B	C
Rb	53	-	-	30	-	-	-	-
Ba	4,300	1,700	-	2,680	-	-	-	-
Sr	1,020	1,300	-	1,030	-	-	-	-
La	-	-	-	-	-	-	-	-
Ce	-	-	-	-	-	-	-	-
Y	15	-	-	17	-	-	-	-
Zr	213	-	-	149	-	-	-	-
Nb	54	-	-	18	-	-	-	-
	S_1		S_3	S_3	S_3CHILL	S_3CHILL		

[x]ALKALI EXCHANGE

TABLE 4 - 2. ANALYSES OF SYENITE 2 AND 4.

	68276	S10	68318E	68318D	A	67103	67106	67198	68318C	67199	68314	2790	B	C
SiO_2	61.56	66.53	65.11	67.04	65.43	61.95	62.42	63.37	64.70	67.20	62.88	55.69	61.17	63.89
Al_2O_3	15.70	14.41	15.22	15.63	16.96	15.79	14.72	14.67	15.83	14.35	16.40	17.57	16.10	16.58
Fe_2O_3	-	2.28	-	-	1.55	-	3.12	1.86	1.59	2.95	-	3.86	2.00	2.00
FeO	6.38	2.52	4.43	2.21	1.53	5.30	5.04	4.38	2.40	2.60	4.89	6.42	4.37	2.28
MgO	1.53	1.06	1.50	0.70	0.22	1.23	1.18	0.78	0.54	0.41	0.93	2.39	0.66	0.67
CaO	3.15	1.59	2.69	2.66	1.36	3.41	2.71	2.31	2.79	1.39	2.70	2.88	2.69	1.23
Na_2O	5.52	5.16	5.13	4.22	5.95	6.49	4.60	5.23	5.47	5.01	5.95	4.71	5.40	5.82
K_2O	4.47	5.47	4.69	6.26	5.36	4.19	5.20	5.70	5.84	5.61	4.68	5.88	5.60	5.42
TiO_2	1.04	0.69	0.56	0.67	0.16	1.06	0.65	0.62	0.59	0.44	0.74	0.53	1.04	0.58
MnO	0.10	0.10	0.08	0.04	0.40	0.08	0.18	-	0.09	-	-	0.18	0.16	0.19
P_2O_5	0.24	0.00	0.23	0.13	0.02	0.19	0.09	-	0.14	-	0.02	-	0.34	0.46

A. Nordmarkite, Shefford, Monteregian Province, Dresser and Denis (1944).

B. Syenite Nunarssuit, Gardar Province, Watts (1966, 28).

C. Avge. 8 Nordmarkites, Oslo Province, Brogger (1933).

TABLE 4 - 2. TRACE ELEMENTS.

	68276	S_{10}	68318E	68318D	A	67103	67106	67198	68318C	67199	68314	2790	B	C
Rb	78	-	117	147	-	-	133	102	-	113	60	278	-	-
Ba	-	-	1,090	-	-	-	553	-	-	-	-	1,300	-	100
Sr	545	-	272	479	-	459	199	358	-	89	767	936	-	-
La	-	-	-	-	-	-	169	-	-	-	-	-	-	-
Ce	-	-	-	-	-	-	225	-	-	-	-	-	-	-
Y	-	-	55	-	-	-	47	-	-	-	-	-	-	-
Zr	154	-	572	-	-	691	848	-	-	443	274	279	- -	600
Nb	51	-	47	-	-	82	82	-	-	65	57	46	-	-
	S_2	S_2	S_2 CHILL	S_2		S_4	S_4 CHILL	S_4	S_4	S_4 CHILL	S_4	S_4		

TABLE 4 - 3. ANALYSES OF PERALKALINE SYENITE DYKES.

	67267	67148	A	68152	R 38	B	C
SiO_2	67.19	68.64	68.49	65.92	68.64	73.68	70.62
Al_2O_3	15.18	14.92	14.46	12.81	12.49	11.05	11.47
Fe_2O_3	1.45	-	2.31	-	4.48	3.93	5.74
FeO	1.65	1.97	1.77	5.72	1.38	1.45	1.30
MgO	0.70	0.40	0.31	0.76	0.33	0.00	0.28
CaO	1.68	1.92	0.26	4.43	2.45	0.48	0.54
Na_2O	5.68	5.53	5.41	4.77	4.90	5.20	5.37
K_2O	5.87	5.82	5.14	4.48	4.69	4.05	4.17
TiO_2	0.56	0.38	0.50	0.63	0.53	0.57	0.23
MnO	-	0.05	0.32	0.12	0.06	tr	0.44
P_2O_5	-	0.03	0.02	0.01	0.00	0.00	0.02

SYENITES COMENDITES

A. Avge. 6 Nordmarkite-ekerites Oslo Province Brogger (1933)

B. Comendite Ilimaussaq Gardar Province Watts (11)

C. Avge 5 Ekerites Oslo Province Brogger (1933).

TABLE 4 - 3. TRACE ELEMENTS.

	67267	67148	A	68152	R 38	B	C
Rb	74	74	-	-	76	-	-
Ba	-	-	200	-	108	-	-
Sr	257	72	-	-	105	-	-
La	-	-	-	-	203	-	-
Ce	-	-	-	-	232	-	-
Y	-	-	-	-	101	-	-
Zr	236	452	-	-	1,100	2.400	-
Nb	62	52	-	-	75	-	-
	SYENITES				COMENDITES		

together with minor green amphibole.

The chilled margins of the intrusion, being depleted in the phenocrysts, are relatively more leucocratic and more alkaline than the coarser facies.

Syenite 4 occupies the entire central exposed area of centre 2, with the exception of Seagull island which is composed of intensely sheared sericite-K feldspar rock. The magnetic curvature anomaly map, indicates a weak positive anomaly overlying the exposed mafic syenite. The rocks within the central submerged area are therefore less magnetic than the marginal syenite and may be composed of granodiorite. Lord (1942) described sheared granitic rocks along the line of the Snare fault in this area. It is presumed, therefore, that the syenite is a ring dyke, without its central roof, and with contacts a few tens of metres offshore. The leucocratic syenite veinlets suggest that the East-coast lineament fracture zone, which had already displaced the pyroxenites on the north lake shore, and would subsequently act as a conduit for alkali metasomatizing fluids in the foyaite, was active at this time. The eastern internal margin is therefore mapped in along this line.

THE CHEMISTRY.

The chemical composition of 18 analysed syenites, and the two analysed comendites, is listed in Tables 4-1, 4-2, 4-3.

Geochemical trends within the series are partly obscured by the large range in composition found in both the quartz syenites, as a result of the variation in the phenocryst to matrix ratio. If the extreme phenocryst rich rocks 2790 and 68276 are ignored there is a progressive increase in silica, total alkalies, Zr, Nb and Y, in the sequence S_1, S_3, S_2, S_4, syenite veins, comendite, and a decrease in alumina, calcium, phosphorus, Ba and Sr. The decrease in alumina combined with the increase in alkalies results in successive syenites becoming more nearly peralkaline.

Rock No.	Al	Na+K	$\frac{Na+K}{Al}$	
68360	7.19	5.64	0.78	S_1
68031	7.23	5.87	0.81	S_3
67327	7.00	6.03	0.86	S_3
68276	6.58	5.82	0.88	S_2
67103	6.57	6.32	0.96	S_4
68318	6.56	6.35	0.97	S_4
67199	5.95	5.93	1.00	S_4
67267	6.24	6.45	1.03	Veins
67148	6.12	6.31	1.03	Veins
67R38	5.17	5.44	1.05	Com.

The phenocryst poor chills (67199) are more peralkaline than coarse facies. This trend is also found in both the saturated and undersaturated porphyry dykes.

There is little variation in the Mg/Mn, or Fe/ Fe+Mg and with the exception of S_1, only a slight increase in the ratio K/Na.

Differentiation. The mineralogical changes found in the syenites are the continuous reaction series plagioclase (An_{26}), "anorthoclase" (up to Or_{33} from 67103), mesoperthite (up to Or_{38} from 67148, 67327), and the discontinuous reaction series, pyroxene, and olivine to hornblende, and the abrupt appearance of quartz. The coarse feldspar phenocrysts suggest that fractionation of feldspar must have occurred.

The geochemical trends seen in the least altered phenocryst poor syenites are illustrated in figs 5-1 (porphyries and chills), 8-1 and 8-2. Because most of the syenites contain abundant, but variable quantities of, phenocrysts, most plot to the CaO, and MgO + FeO rich side of these trend lines. With the exception of S_1, which is distinctly more calcic, and S_3 which is slightly more calcic, the main differentiation trend seen is an increase in the proportion of quartz and a slight increase in orthoclase relative to albite, as is shown in fig 5-1. This trend is indistinguishable from the projected path of the thermal valley in the non-peralkaline system $NaAlSi_3O_8$-$KAlSi_3O_8$ - SiO_2- H_2O (1Kb) given in Carmichael and Mackenzie (1963). The comendites (68152) and peralkaline syenite veins lie along the same trend. The syenites, since they lie in the thermal valley, have almost certainly been derived from a liquid itself within the thermal valley, and lie along a path of ideal feldspar fractionation.

Carmichael and Mackenzie also point out, that in a natural calcium bearing system the separation of calcium bearing feldspar from a parent trachyte (syenite) may lead to a peralkaline residuum. This is precisely what is seen to occur within these syenites, through the separation of the phenocrysts.

Relationship to Centre 1. The presence of pyroxene, olivine, and plagioclase amongst the earliest formed phenocrysts indicates a possibly more basic parent. Indeed mineralogically the quartz syenites closely resemble the chilled matrix of the diorite.

The geochemical trends of the syenite (figs 8-1 and 8-2) may be followed back in a smooth curve through the chilled diorite and gabbro, both of which contain less normative quartz, and through the saturated basic porphyries. This gradation is supported by the continuous increase in Zr and Nb and $\frac{Fe}{Fe+Mg}$ along the trend, and the rapid increase followed by the abrupt but progressive decrease of Ba accompanying the first appearance of alkali feldspar. It is apparent from the phenocrysts within the chills, and from the trends illustrated in Figs 5-1 8-1 and 8-2 that the course of differentation was controlled by the fractionation of plagioclase, rather than by the fractionation individually of olivine, pyroxene or magnetite. That is to say the trends show a major decrease in $\frac{Ca}{Na+K+Ca}$, and in $\frac{Fe+Mg}{Fe+Mg+Na+K}$, and in $\frac{Na}{K+Na}$, with only a marginal decrease in $\frac{Mg}{Fe+Mg}$ or $\frac{Mg}{Mn}$.

The chilled diorite (67336) contains no normative quartz (wet chemical and X.R.F analyses agree on this), yet it contains circa 8% modal

primary amphibole, and 4-5% modal quartz. Throughout the diorites the proportion of amphibole shows a close relationship to the proportion of quartz. Separation and settling of primary amphibole, therefore, provides a possible mechanism by which the quartz free syenite magma of S_1 could give rise to the quartz bearing magma of S_2 and S_4. Even a small displacement towards the silica field would allow feldspar fractionation to continue the trend towards a quartz rich peralkaline residuum.

Relationship to Centre 2. Both the southern, and northern foyaites, are chilled against syenite 4. The complex, therefore, falls in Tilley's (1957) Group B - complexes starting with granite but closing with nepheline syenite.

At Kangerdluassuq (Kempe 1967) a transition from quartz syenite to foyaite has been recognised, and a similar transition has been postulated by Barth for the Oslo province (Turner and Verhoogen 1960). Although thermal saddles in the system $KAlSiO_4$ - $NaAlSiO_4$ - SiO_2 and in Na_2O - Al_2O_3 - Fe_2O_3 - SiO_2 prevent the transition through fractionation of the simple end members, the entry of Fe^{3+} into feldspar in place of magnetite (Bailey and Schairer 1966) provides a possible explanation.

The silica enrichment trend described above indicates that this process is inapplicable here. Additionally the porphyry dyke swarms (Fig 5-2) trend indicate that the undersaturated trend persists at least as basic as the Bigfeldspar gabbro.

The divergent saturated and undersaturated trends then resemble those of the gabbro - quartz syenite - foyaite complexes of Okonjeje (Simpson 1954) and Werner Bjerge (Bearth 1959.)



PLATE 4 - 1 Spalling of the diorite at the ring syenite S_3 contact. The dark dyke rock is a barkevikite lamprophyre associated with the plagioclase porphyry multiple dykes. Southern contact.

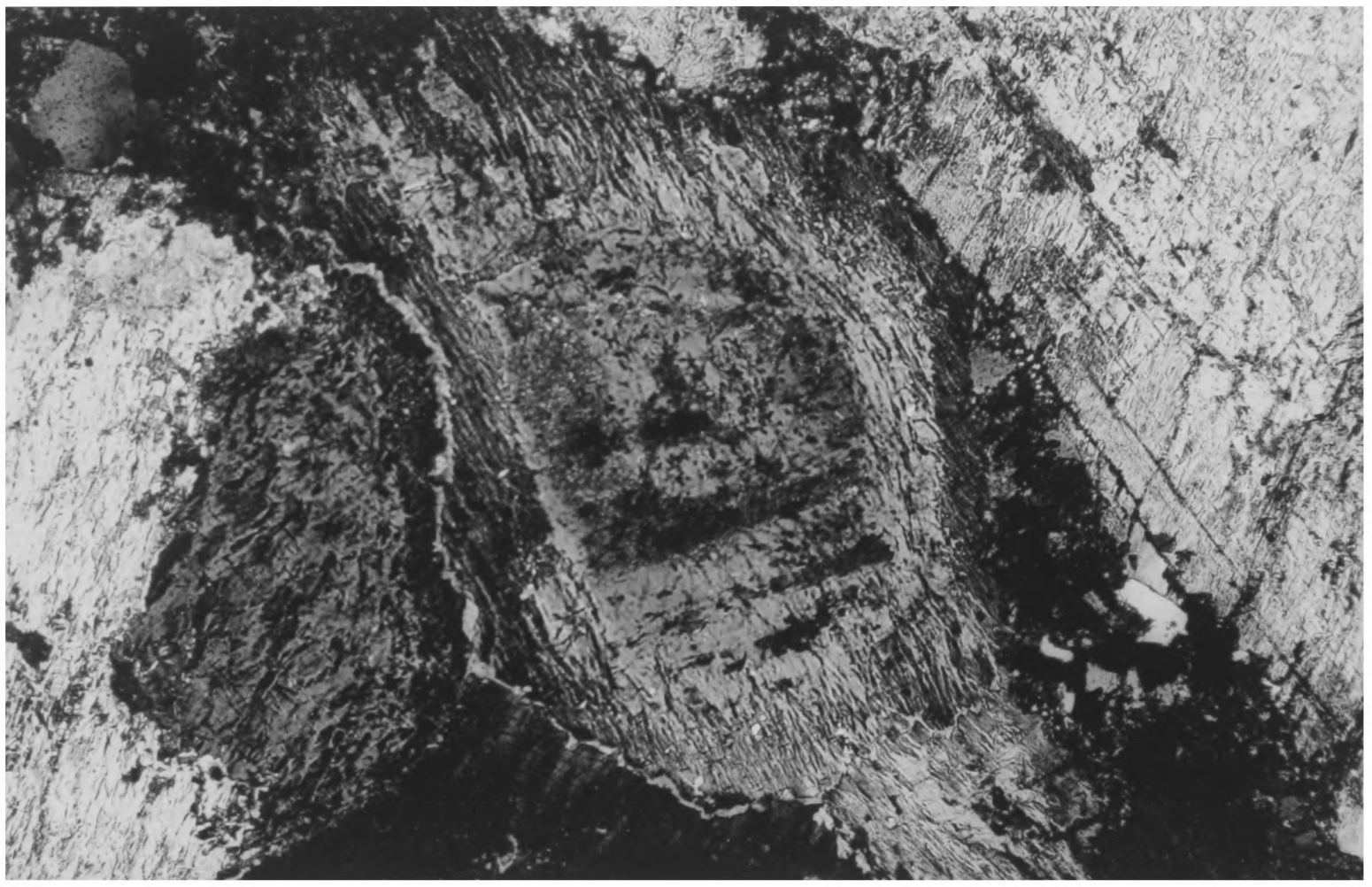


PLATE 4 - 2 Zoning of rhombic feldspar in the mafic quartz syenite S_4. The rim shows the typical ropey exsolution of the interstitial mesoperthite.

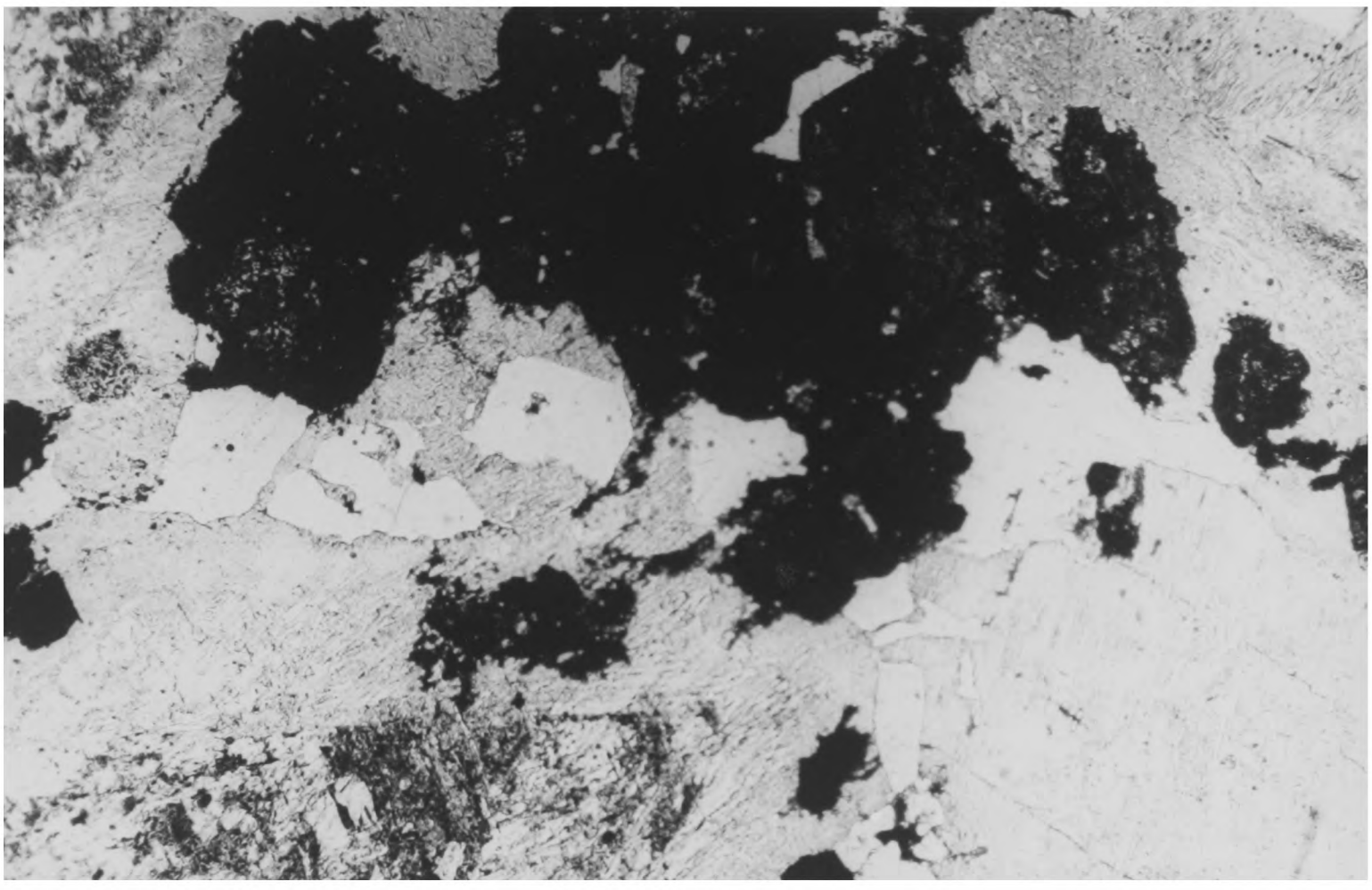


PLATE 4 - 3 Interstitial quartz and amphibole in the quartz syenite S_2 Much of the amphibole (dark grey to black) surrounds pseudomorphed pyroxene cores. The quartz is intergrown with mesoperthite, overgrowths on rhombic anorthoclase.

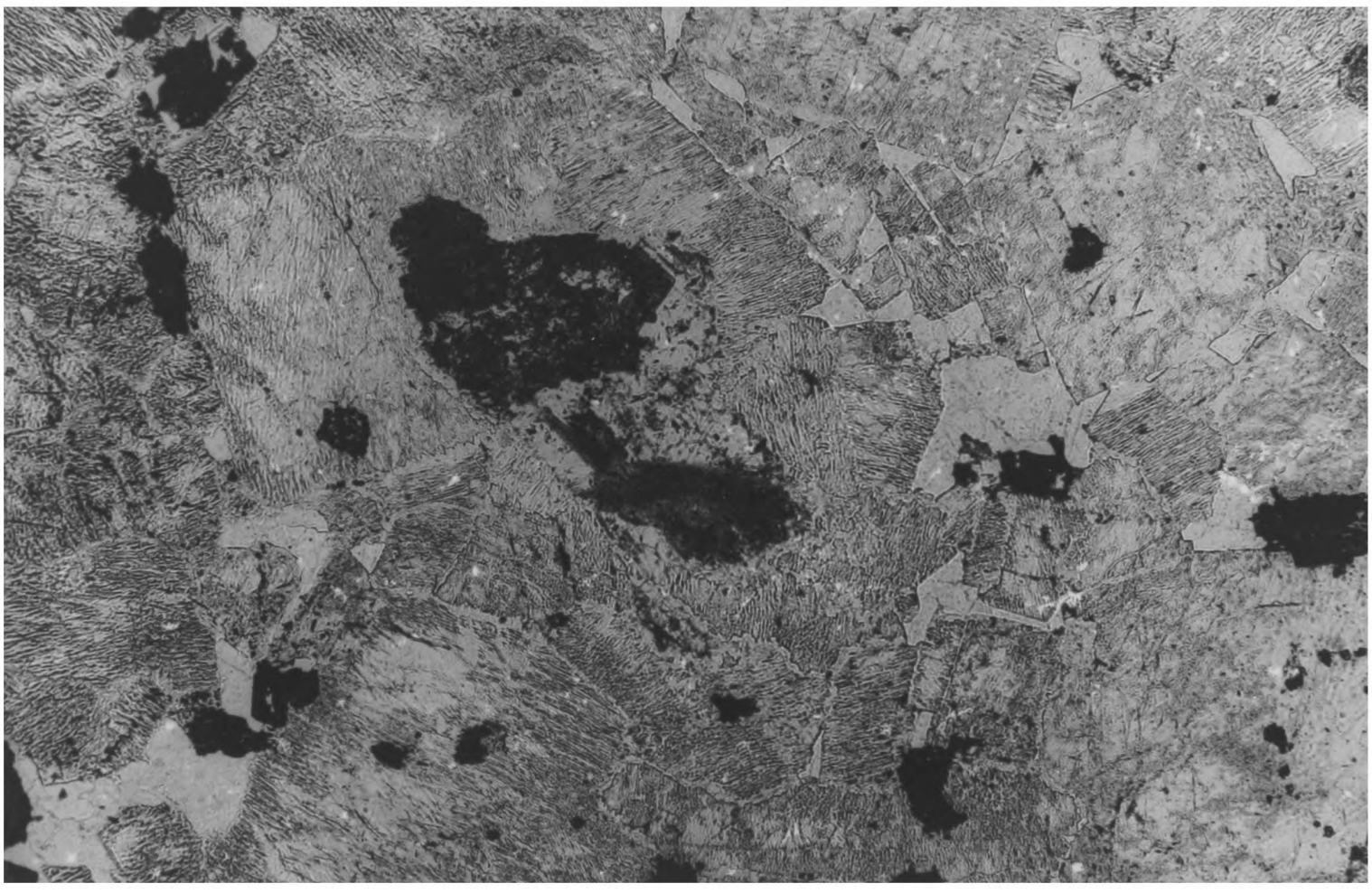


PLATE 4 - 4 Perthite texture in the peralkaline syenite dykes. Dyke filling a series of en echelon fractures parallel to the East coast lineament, in S_1, island G. spec 67267, x 4.

CHAPTER V. CENTRE 3 ALKALINE UNDERSATURATED ROCKS.

It was one of the aims at the start of research into the complex to discover possible links between the saturated and undersaturated members of the complex. Unfortunately, the reports of a transition between quartz syenite and foyaite were unfounded. The foyaites show a sharp chilled contact with syenite 4 on the East coast, and there are no coarse grained intermediates between the two series. However, it is probable that the porphyry dykes intruded between the termination of centre 1 activity and the start of centre 3 bridge this gap.

Porphyry Dykes. The porphyry dykes can be divided in the field into three series.

a) The prismatic feldspar - plagioclase porphyries.
b) The rhombic feldspar - anorthoclase porphyries
c) The platy feldspar - sanidine cryptoperthite porphyries

Typically all the porphyries contain phenocrysts of feldspar, pyroxene, magnetite and often apatite. Nepheline is present in the most alkaline, nepheline - sanidine porphyries, and olivine in the most basic, ultramafic porphyries. The comendites, and all the anorthoclase and sanidine porphyries, are exceedingly rich in volatiles, and highly oxidized. Nepheline, and often porphyritic feldspar, is altered to coarse white mica; aegirine broken down to magnetite; ilmenite to sphene; and magnetite to hematite. Fluorite is abundant in the altered minerals. The alteration results from primary volatiles since it occurs regardless of chilling, or of the rock type intruded, in unsheared, narrow dykes.

Plagioclase porphyries. Ultramafic porphyries.

The most basic, ultramafic porphyries, are thin veins of pyroxene-olivine-magnetite porphyry crosscutting the Big feldspar gabbro, and magnetite pyroxenites. The matrix is composed of microliths of albitic plagioclase (30%) pyroxene (20%), magnetite (20%) and minor biotite and apatite. Pyroxene in the matrix is replaced by green hornblende. The olivine phenocrysts are altered to tremolite and surrounded by broad coronas of hornblende and biotite. The mineralogy and composition are similar to the olivine-plagioclase-magnetite-pyroxenite. Slightly more alkaline dykes of this type intrude the multiple dykes of plagioclase porphyry-rhomb porphyry and syenite, demonstrating the co-existence (and mixing) of the ultramafic, basic and alkaline magmas.

Gabbro Porphyries. The Bigfeldspar porphyry dykes are found crosscutting the gabbro layered series, in the magnetite pyroxenites, and intruding the multiple dykes. Their composition and mineralogy are similar to the chilled Bigfeldspar gabbro (67293) and are similar to the proposed parent magma.

Syenite Porphyries. The plagioclase porphyry (Sensustricto) is a common dyke type in centre 1, but very rare outside it. It is similar in composition to the most basic of the syenites (Syenite 1) and contains about one half of a percent of normative quartz. The feldspar phenocrysts are very strongly zoned from oligoclase cores (circa An_{25}) through

clear feldspar to narrow perthite rims. A few of the phenocrysts have a rhombic section. Pyroxene phenocrysts often included in an outer zone of the feldspar, are altered to and rimmed by, amphibole. The matrix is composed of primary greeny-brown hornblende, apatite, magnetite, perthite, and minor quartz. There are a very few calcite-magnetite pseudomorphs after fayalite included in the pyroxene. The porphyry clearly belongs in the syenite series between syenites 1 and 4,

Comendite Porphyries. The comendites are a rare dyke type crosscutting the multiple dykes, and syenite 2 and 3, but included as xenoliths in syenite 4. They contain normative acmite and are rich in magnetite, hematite, aegirine and quartz. The feldspar is almost entirely re-crystalized, into secondary aggregates of albite. Pale green to yellow aegirine is generally replaced by magnetite. The primary mineralogy shows anorthoclase perthite phenocrysts, and rare acicular aegirine, in a matrix of aegirine, perthite, and quartz.

A few dykes corresponding in mineralogy to quartz free diorite are also present.

Anorthoclase and Sanidine Porphyries. The undersaturated porphyries form a single series, with an abrupt transition from rhombic anorthoclase, to platy sanidine cryptoperthite, on the appearance of phenocrystic nepheline.

All contain feldspar, pyroxene, magnetite and apatite phenocrysts. With the exception of a single coarse grained dyke of nepheline-sanidine porphyry, the pyroxene is always altered to hornblende, biotite, epidote, or calcite. With the same exception, nepheline phenocrysts are always altered to sericite.

The majority of the dykes are microcrystalline with a trachytic texture of feldspar microliths, The proportion of mafic minerals decreases progressively along the series.

Rhomb-feldspar Pyroxene Porphyries. The most basic porphyry contains 2-6 cm fat rhombs of anorthoclase, and microphenocrysts (1-4mm) of pyroxene, oxide, and apatite, in a mafic matrix containing 30-50% of hornblende, biotite, and epidote pseudomorphs after pyroxene, and magnetite. The texture, with the exception of the feldspar rhombs is similar to that of the basic plagioclase porphyries, but the composition is more alkaline, and includes 1% normative nepheline. The anorthoclase when fresh is clear, and contains rare sericitized plagioclase cores. The matrix feldspar is an albitic plagioclase.

Rhomb-feldspar Nepheline Porphyries. Similar more leucocratic porphyries, with more potassic phenocrysts, and with perthite in the matrix, are common as narrow chilled dykes crosscutting the rocks of centre 1 and 2. Xenoliths of this type are found in syenite 4.

The dykes contain thin acute rhombic feldspar phenocrysts, in a leucocratic trachytic matrix containing abundant minute sericite pseudomorphs after nepheline. The form of the stubby euhedral pyroxene, magnetite

FIG 5 - 1 NORMATIVE TRENDS FOR THE SATURATED AND UNDERSATURATED PORPHYRY DYKE SERIES.

Fig 5-1

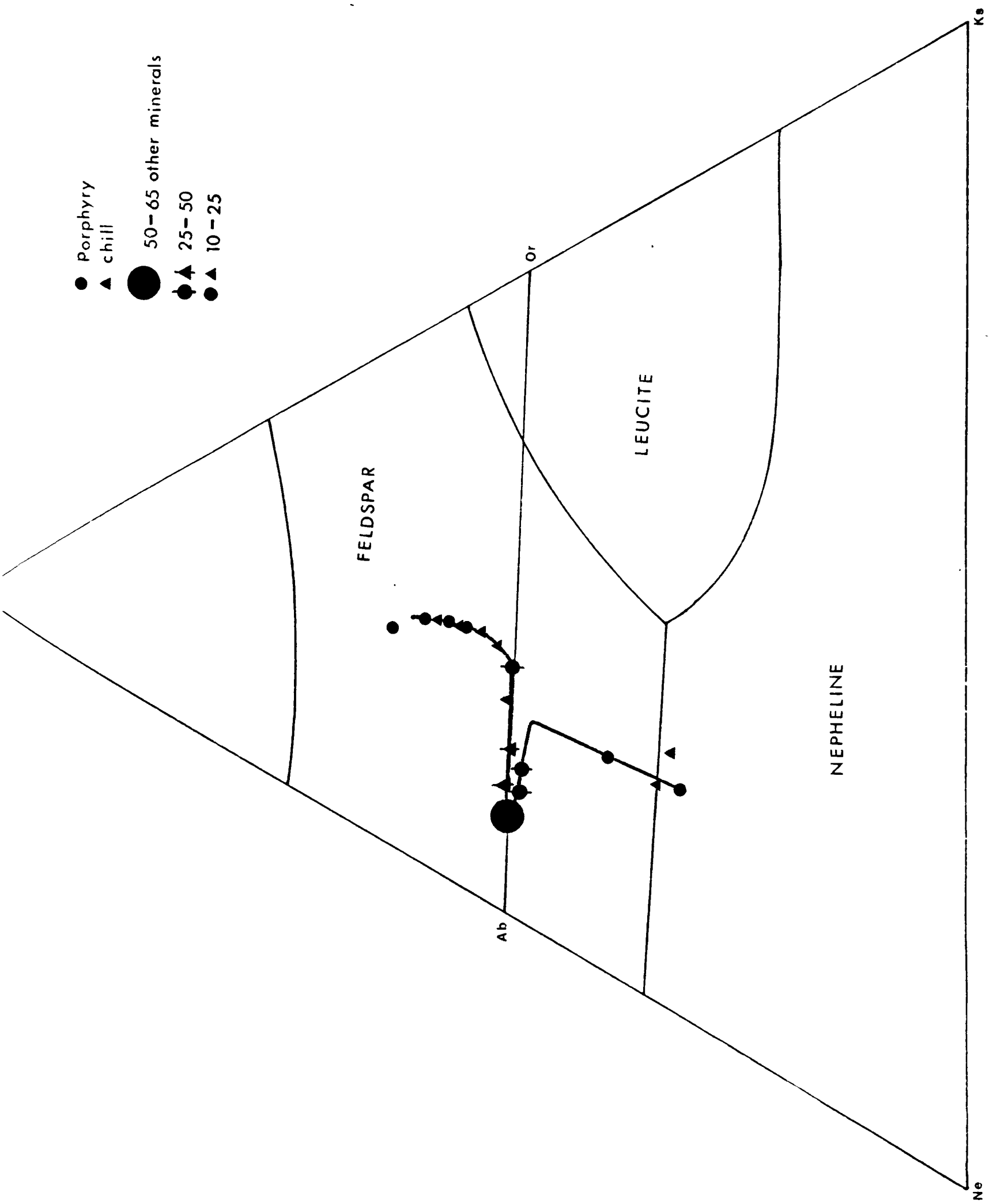


TABLE 5 - 1. PORPHYRY DYKE ANALYSES.

	OLIVINE - PYROXENE PORPHYRY	CHILLED GABBRO.	CHILLED DIORITE	CHILLED SYENITE 1.	PLAGIOCLASE PORPHYRY	SYENITE VEIN	COMENDITE	COMENDITE	RHOMB FELDSPAR-PYROXENE PORPHYRY	RHOMB FELDSPAR-PYROXENE PORPHYRY	RHOMB PORPHYRY	RHOMB FELDSPAR-NEPHELINE PORPHYRY	NEPHELINE-SANIDINE PORPHYRY	CHILLED FOYAITE 2.	CHILLED FOYAITE 1.
ROCK NUMBER	68252	67293	67336	68360	68177	67148	68152	67R38	68168	68159	68264	68278	2835	67374	68051
SiO_2	40.75	46.92	54.81	57.10	57.01	68.64	65.79	68.64	50.88	52.49	57.98	57.54	55.49	57.71	53.65
Al_2O_3	10.02	16.50	14.86	17.03	15.84	14.92	12.78	12.49	15.16	15.87	15.57	19.59	22.14	21.52	19.95
Fe_2O_3	8.90	4.22	3.36	2.94	3.08	-	-	4.48	-	-	-	-	3.30	0.62	5.54
FeO	14.56	8.60	6.87	5.06	6.19	1.97	5.72	1.38	11.69	11.09	8.97	5.90	0.99	2.13	1.97
MgO	6.49	5.74	3.77	1.43	2.01	0.40	0.75	0.33	4.31	3.95	1.56	1.75	1.04	0.02	0.48
CaO	10.32	9.79	6.18	5.04	4.64	1.92	4.42	2.45	6.02	6.32	4.65	3.27	1.69	1.69	3.92
Na_2O	2.02	2.99	4.79	6.26	4.89	5.53	4.76	4.90	4.76	5.73	6.97	6.03	10.11	9.92	9.08
K_2O	0.72	1.16	2.61	2.82	4.15	5.82	4.47	4.69	3.57	1.31	2.42	4.57	5.05	5.69	4.58
TiO_2	6.41	3.46	2.04	1.67	1.50	0.38	0.62	0.53	2.74	2.23	1.10	1.02	0.45	0.54	0.53
MnO	0.23	0.14	0.19	0.12	0.14	0.05	0.12	0.06	0.14	0.10	0.16	0.12	0.12	0.06	0.20
P_2O_5	0.41	0.32	0.38	0.36	0.36	0.03	0.01	0.00	0.38	0.57	0.28	0.21	0.05	0.01	0.02

TABLE 5 - 1. TRACE ELEMENTS.

	OLIVINE-PYROXENE PORPHYRY	CHILLED GABBRO.	CHILLED DIORITE	CHILLED SYENITE 1.	PLAGIOCLASE PORPHYRY	SYENITE VEIN.	COMENDITE	COMENDITE	RHOMB FELDSPAR-PYROXENE PORPHYRY	RHOMB FELDSPAR-PYROXENE PORPHYRY	RHOMB PORPHYRY.	RHOMB FELDSPAR-NEPHELINE PORPHYRY	NEPHELINE-SANIDINE PORPHYRY	CHILLED FOYAITE 2.	CHILLED FOYAITE 1.
ROCK NUMBER	68252	67293	67336	68360	68177	67148	68152	67R38	68168	68159	68264	68278	2835	67374	68051
Rb	16	20	73	53	49	74	-	76	-	-	-	-	123	94	163
Ba	550	593	1,050	4,300	2,020	-	-	108	-	-	-	-	672	1,000	1,690
K	0.34	0.55	1.21	1.29	1.91	-	-	2.10	-	-	-	-	2.24	2.53	2.08
Sr	744	1,870	962	1,020	1,160	187	-	105	-	-	-	-	1,700	1,060	1,340
La	126	-	-	-	-	-	-	203	-	-	-	-	272	-	-
Ce	105	-	-	-	-	-	-	232	-	-	-	-	380	-	-
Y.	-	14	-	15	-	-	-	101	-	-	-	-	120	7	32
Zr	136	87	217	213	188	452	-	1,200	-	-	-	-	667	179	858
Nb	27	20	30	54	58	52	-	75	-	-	-	-	139	28	144

and enclosed apatite microphenocrysts is unchanged. Fluorite is common in the altered minerals.

Nepheline-Sanidine Porphyries. The nepheline-sanidine porphyries, are the most abundant porphyry dyke type occurring through centre 1 and 2, and up to at least five miles from the complex. They are light grey and microcrystalline with 5-30% of phenocrysts, of thin platy cryptoperthite and sericite pseudomorphs after hexagonal nepheline. The ratio of nepheline to feldspar phenocrysts ranges from zero to forty percent.

The feldspar in the nepheline poor varieties consists of potassic cryptoperthite (Or_{80} 1 specimen) rimming sericitized plagioclase cores. In the nepheline rich varieties it is a potassic cryptoperthite, often inverted to microcline.

The nepheline is in the form of oscillatory zoned hexagonal tablets, as in the foyaites. Fresh nepheline has the composition Ne_{73}(1 specimen).

The pyroxene, magnetite, and apatite retain the same form and abundance, as in the rhomb-feldspar-nepheline porphyries, in the nepheline-poor nepheline-sanidine porphyries. But, as the proportion of nepheline phenocrysts increases, magnetite, and apatite decrease, and pyroxene assumes the acicular form of aegirine.

The only non-metasomatised dyke found, which lies along the north side of the south-west arm of the lake,is composed of 20-30% nepheline, and feldspar phenocrysts in a matrix of mesoperthite, nepheline, aegirine, and magnetite. At an early stage the matrix has been partially replaced by analcite, sodalite and sericite, after nepheline, magnetite, and albite after aegirine, sphene and hematite after magnetite, and late crystallizing fluorite and apatite. The feldspar phenocrysts have reacted with the liquid to form a perthosite indistinguishable, in thin section, from the matrix. The richness of the residual liquid in H_2O, F and Cl (but not in CO_2 since there is little cancrinite), is amply illustrated by these reactions.

Chemistry. The compositions of the porphyries are similar to those of the coarse-grained rocks where equivalent coarse-grained rocks are present. Thus the plagioclase porphyry is similar to syenite 1, the basic porphyries to the gabbro and pyroxenite, and the nepheline-sanidine porphyry to the chilled southern foyaite. The end member porphyries - the comendite and nepheline-sanidine porphyry - however are relatively enriched in volatiles (as indicated by the mineralogy) and the trace elements Nb, Y, La and Ce, and are depleted in Ba.

Conclusions. The significance of the porphyries is that they occupy gaps in the evolution history of the saturated and undersaturated series, the filling of which allows probable differentiation trends to be seen. These are illustrated in figs 5-1, 8-1, and 8-2. The basic porphyries demonstrate that the divergence between the saturated and undersaturated series began at an early stage from a possibly gabbroic but not a



PLATE 5 - 1 Multiple porphyry dyke, associated with pre-syenite faulting. From base to top, plagioclase porphyry (intermediate), olivine-pyroxene porphyry (ultrabasic) syenite, plagioclase porphyry (basic) in marginal diorite, 600m S.E. of Arete Lake, spec Locality 68168, 68264.

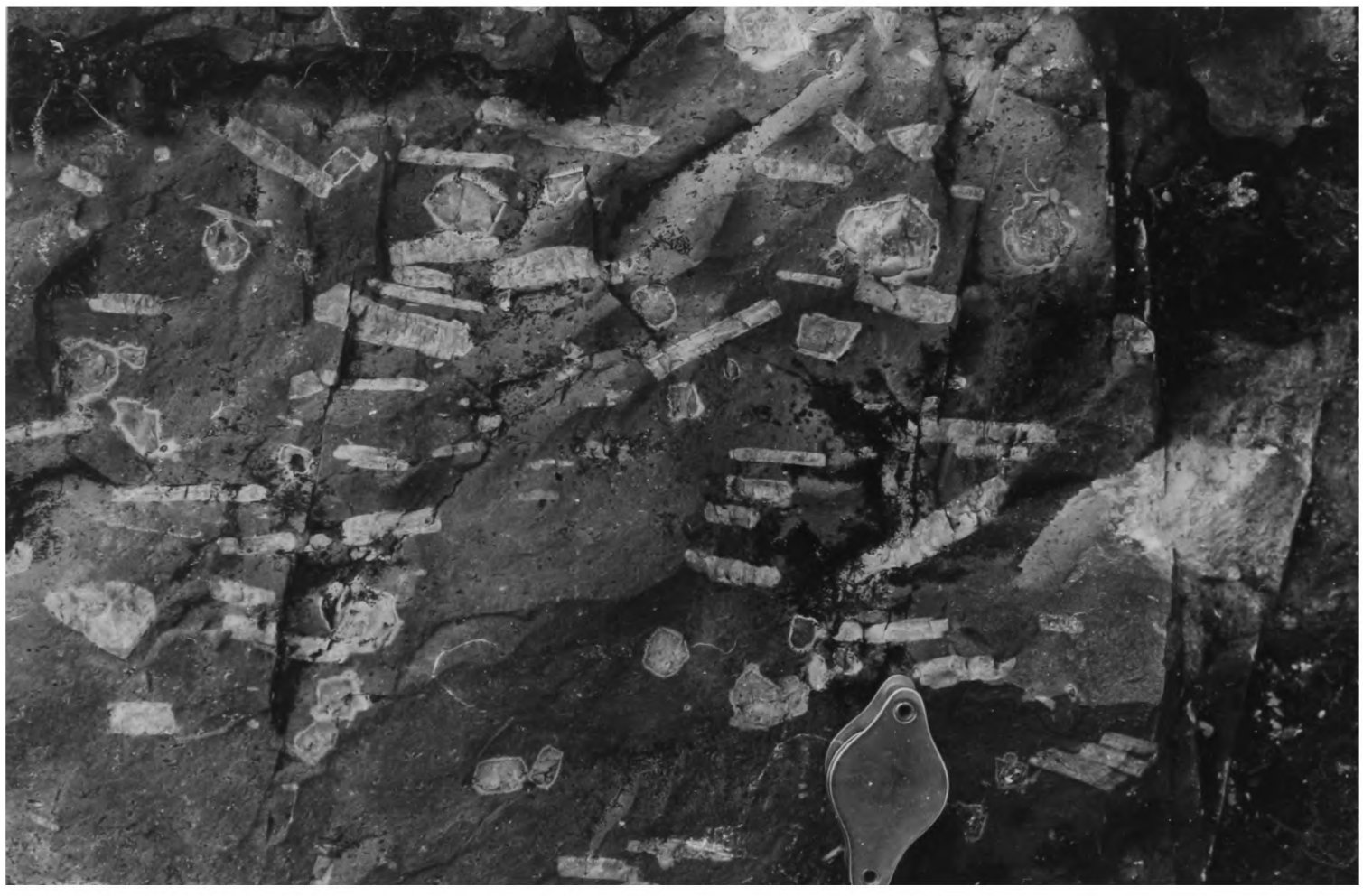


PLATE 5 - 2 Sanidine and nepheline phenocrysts in a nepheline - sanidine porphyry dyke. The plate shows the oscillatory zoning in nepheline (now pseudomorphed by sericite and fluorite), bleached, oxidized reaction rims, the euhedral form, and the flow foliation typical of these dykes. Centre 1 area.

trachytic parent. Both trends followed similar courses of crystallization to produce trachytes which contain circa 0.5% and 2% normative quartz and normative nepheline respectively. The opposing trends then follow almost straight paths in the normative projection Qtz-Ne-Ks close to, but not identical with, the thermal troughs in the experimental, peralkaline (4.5% ns + 4.5% ac) SiO_2 - Ne - Ks system at 1kb H_2O which would be expected had ideal fractionation in the natural system of the feldspars occurred. Both series produced final differentiates that were peralkaline, leucocratic and rich in volatiles and in the R.E. elements. The nepheline sanidine porphyry additionally lies within the low temperature sink, slightly displaced towards the nepheline rich side of the nepheline-feldspar field boundary (Carmichael and MacKenzie 1963, Hamilton and MacKenzie 1965).

The phenocryst phases support the importance of the fractionation of plagioclase and of alkali feldspar and to a much lesser extent of pyroxene, magnetite and apatite, in the derivation of the peralkaline members of the sequence.

The evolution of both sequences took place in parallel such that the trachytic members and the peralkaline members (comendite and acute rhomb feldspar porphyries) existed, and were intruded simultaneously.

THE NEPHELINE SYENITES.

GENERAL. The southern portion of Bigspruce lake is underlain by nepheline syenite. It outcrops on all the enclosed islands south of Seagull island, and on most of the peninsulars projecting into the lake, particularly the broad nose which separates the southern, from the south western, arm of the lake. The majority of the syenite exposed, is foyaite, which, as was recognised by Lambert (1964), occurs as two distinct masses.

Northern Foyaite. The northern foyaite is medium grained, and generally richer in aegirine than the southern one. It outcrops on Bigspruce and Littlespruce islands, and on a series of partially submerged reefs just offshore of the coast, northwest, west and south of Bigspruce island. Blocks of southern foyaite occur in the dykes associated with the northern foyaite fenite.

Southern Foyaite. The southern foyaite is coarse grained or pegmatitic, with feldspars measuring 2-4cm. It occurs on all the islands except Bigspruce, Littlespruce and island R, with its outer contact lying close to the lake shore in most cases. Over 80% of this intrusion lies underwater, but it is generally better exposed than the northern foyaite, by virtue of its long unsheared coastal section.

Fenite Zones. Both intrusions are surrounded by concentric zones of fenite, which enable the submerged contacts to be extrapolated with some certainty. The southern foyaite is rimmed by 5-90m of leucocratic syenite fenite, and 50-100m of microgranite. The northern foyaite contact with granodiorite is not exposed, but it is surrounded by a broad zone of aegirine-syenite fenite developing along the margins of sinuous radial arfvedsonite-syenite veinlets, and in the shattered granodiorite.

Mineralogy. The rocks of both intrusions are almost entirely made up of nepheline, cryptoperthite and aegirine, in varying amounts, with only trace quantities of sphene, apatite, magnetite, fluorite, calcite and allanite. Secondary alteration of the nepheline at the margins of crystals is common, with the formation of cancrinite + analcite + sodalite. Exsolution of cryptoperthite to microcline and albite is also common, and there maybe some primary albite in the interstitial matrix. With more extreme alteration, aegirine has broken down to biotite and magnetite, and minor andradite and vesuvianite..

Chilled Margins. Both intrusions show chilled contacts consisting of a 1-5m zone of laminated syenite, passing into fine grained leucocratic foyaite. This syenite is composed of thin plates of feldspar (2x2x0.1 cm) and thick tablets of nepheline (0.3 x 0.3 x 0.2cm) in a fine grained matrix of cryptoperthite, nepheline, aegirine and magnetite. The modal composition in the southern foyaite is circa

Nepheline + cancrinite	34%
Cryptoperthite	59%
Aegirine + biotite	6.8%
Magnetite	0.2%

The northern foyaite shows a similar nepheline to feldspar ratio, but contains about 15% aegirine. Similar chill zones occur as internal contacts (plate 5-3) near the margin of the intrusion, on the peninsular south of Bigspruce island, and on the north-west margin of Bigspruce island suggesting that both intrusions were emplaced by several pulses of identical magma. These contacts are all vertical.

SUBDIVISION OF THE FOYAITES.

Although both intrusions consist predominantly of foyaite, there is extensive variation in the mineral proportions, such that a single exposure might be termed pulaskite, foyaite, ijolite or urtite on the basis of the predominance of particular minerals.

Each intrusion shows a crude zonation of the predominant rock type, with, relative to the chill, feldspathic rocks towards the margin and nephelinitic rocks towards the centre. The greatest area in each body is occupied by rock more enriched in nepheline than the chill, the commonest exposed foyaites in each intrusion containing

	N. Foyaite	S.Foyaite
Nepheline	43 - 47%	50 - 60%
Cryptoperthite	43 - 45%	30 - 40%
Aegirine	9 - 14%	3 - 10%

(modal analyses based on point counting, and on stained acetate peels).

The feldspathic foyaites towards the intrusion margins contain respectively -

	N. Foyaite	S. Foyaite
Nepheline	20-25%	25-30%
Cryptoperthite	60-65%	55-60%
Aegirine	10-15%	10-20%

The southern foyaite additionally contains horizons of urtite with the mineral proportions shown below, and of a fine-grained white pulaskite.

	Urtite	Pulaskite
Nepheline	75 - 85%	1-5%
Cryptoperthite	15 - 20%	90 - 95%
Aegirine	1 - 5%	1 - 5%

The northern foyaite also contains horizons of urtite exposed on the shore lines of Bigspruce island but these are now represented by cancrinite rock. It contains several horizons, of nepheline - aegirine rock with the mineral proportions of an ijolite, but the texture of the foyaite

	Nepheline - aegirine rock
Nepheline	60 - 70%
Cryptoperthite	Trace
Aegirine	30 - 40%

The mineral proportions within each rock type are relatively constant. The contacts between the types are narrow, gradational, and usually close to horizontal.

Intrusive form. The foyaites are both interpreted as undersaturated layered intrusions, on the evidence of the cumulus mineral textures, the crudely concentric zonation of the rock types, and the low angle of most internal contacts.

Field relations between rock units. A radial section into the southern foyaite along the southern, or the western margin shows that there are three types of relationship between the units.

a) There is a continuous concentric gradation from the chill, through feldspathic foyaite to nepheline foyaite.

b) There are short exposed lengths of repetitive layering with the feldspathic units towards the base and nepheline rich units at the top.

c) There are large, and small, angular, and rounded xenoliths of one rock type, within another.

Because the contact between the units is sub-horizontal single rock types, for instance the nepheline-aegirine rock on reefs west of Bigspruce island, cover extensive low lying areas. It has not been possible to map individual units, or groups of units.

Mineral textures: Most of the foyaites are composed of large plates of feldspar (2-4cm and 1 - 1.5cm in S and N.foyaite), and thick tablets of nepheline (1-2cm and 0.5cm) arranged in an open but continuous framework within which nepheline, feldspar, and aegirine in approximately the chill proportions have crystallized. Towards the margin of the southern foyaite, and through out the northern foyaite, this matrix is fine-grained, and so the distinction between cumulus coarse feldspar and nepheline, and the

interstitial matrix is readily apparent. In the coarse southern foyaite, particularly in the nepheline rich varieties, the matrix minerals are coarse and poikilitic.

These rock types, therefore, resemble orthocumulates in the terminology of Wager et al (1960). Nepheline, and feldspar are the cumulus phases; nepheline, aegirine, and feldspar are in the matrix formed from the trapped interstitial pore liquid.

The concentric zonation is a consequence of the relatively more rapid settling of feldspar than of nepheline due to its greater density and size. The preponderance of nepheline rich rocks is a consequence of the low angle of dip of the internal units, the settling towards the base of the feldspar with saucer shaped crystal-liquid surfaces, and the relatively high level in the intrusion of the present exposure.

This zonation is comparable to that described by Wager (1965) in the Kangerdlussuaq intrusion in which are found concentric saucers of quartz syenite, pulaskite, pulaskitic foyaite, and foyaite with the feldspathic rocks towards the margin, and a disproportionately large surface area of exposed nepheline rich rock.

The urtites contain more nepheline (75 - 85%), than may reasonably be explained by crystal accumulation. They show hexagonal nepheline cores (~ 60%) with broad poikilitic overgrowths, separated by minor poikilitic feldspar, aegirine and analcite. The rocks therefore resemble mesocumulates, with some adcumulus growth of nepheline.

The nepheline-aegirine rocks are composed of euhedral nepheline, in a granular to poikilitic matrix of aegirine, and scattered plates of feldspar. The rock is interpreted as an adcumulate, with cumulus nepheline and possibly aegirine, and adcumulus aegirine.

There are no cumulus aegirine rocks.

The pulaskite is composed of fine-grained mesoperthite platelets with minor patches of nepheline, albite, fluorite, biotite and magnetite. It is found at the base of certain repetitive units on island L, and as xenoliths in the foyaites. It is clearly not a feldspar cumulate since it is fine-grained. Possibly it might be a remobilized liquid fenite. Possibly, however, it results from the eutectic nature of the primary magma, and crystallised from the magma in consequence of a shift of the eutectic towards the nepheline side of the field.

Evidence of layering. The exposure of foyaite on land is intermittent, and deeply weathered. The main evidence for layering therefore comes from the 1-3m ice polished fringe above the water line.

With the exception of the laminated vertical chill, preferential orientation of the minerals is weak, or absent. In view of the extreme platey form of the feldspar this must indicate the absence of regular convecting currents. Where a weak preferred orientation can be seen it is close to horizontal. The contact between feldspathic and urtititic units is also subhorizontal. These rhythmic units are 3m or more

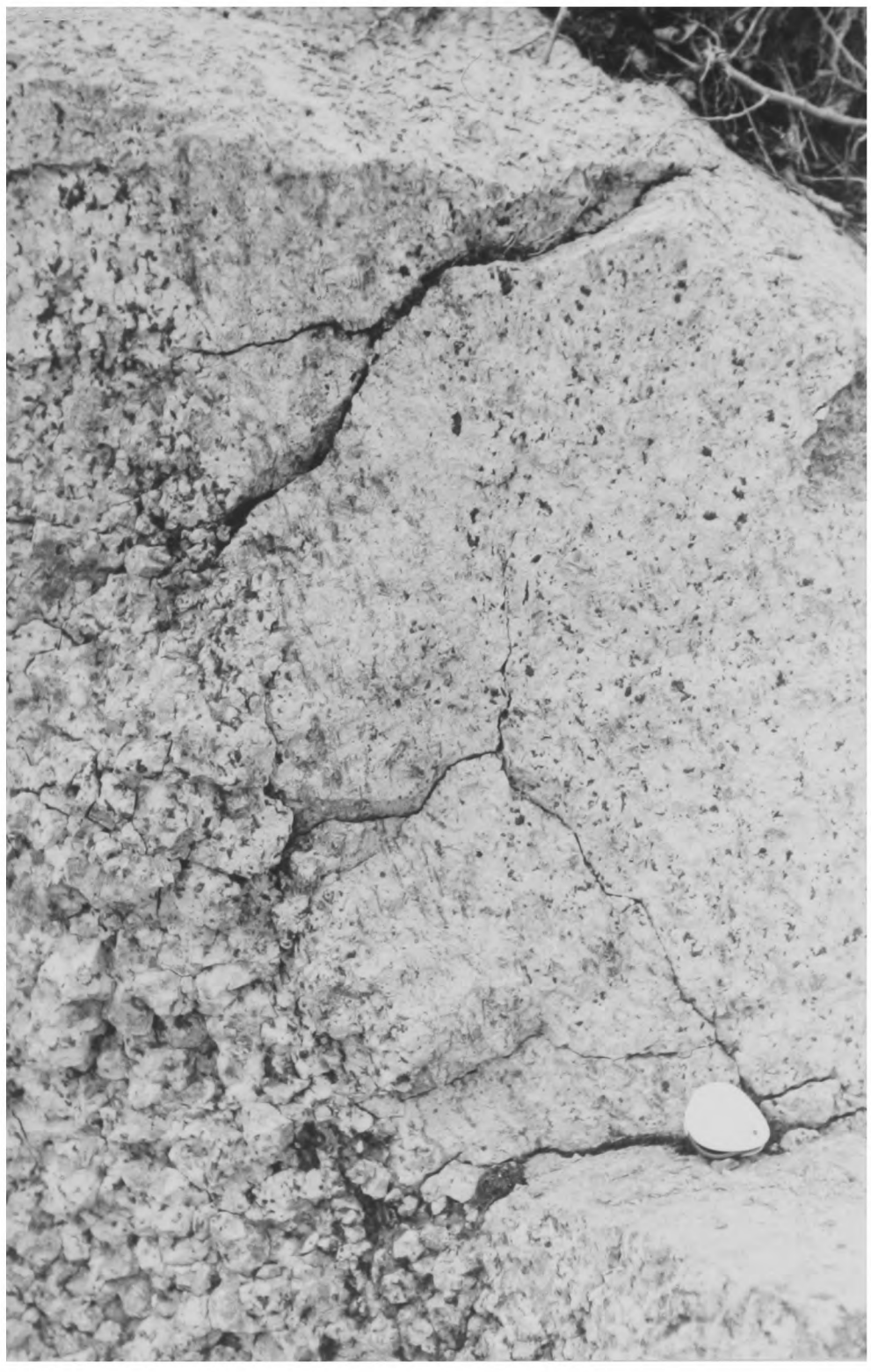


PLATE 5 - 3 Vertical lamination outlined by sanidine phenocrysts in chilled southern foyaite. The chill contains both nepheline and sanidine phenocrysts and is transitional into feldspathic foyaite on the right. Internal contact Fall-in peninsulor. Spec. Locality 67130.



PLATE 5 - 4 Foyaite - urtite transition in the southern foyaite. The urtite lacks the microcline plates of the foyaite but contains interstitial microcline in the matrix. Subhorizontal contact. island L.



PLATE 5 -5 Feldspathic foyaite - pulaskite contact in the Southern foyaite. N.E. margin of island L.

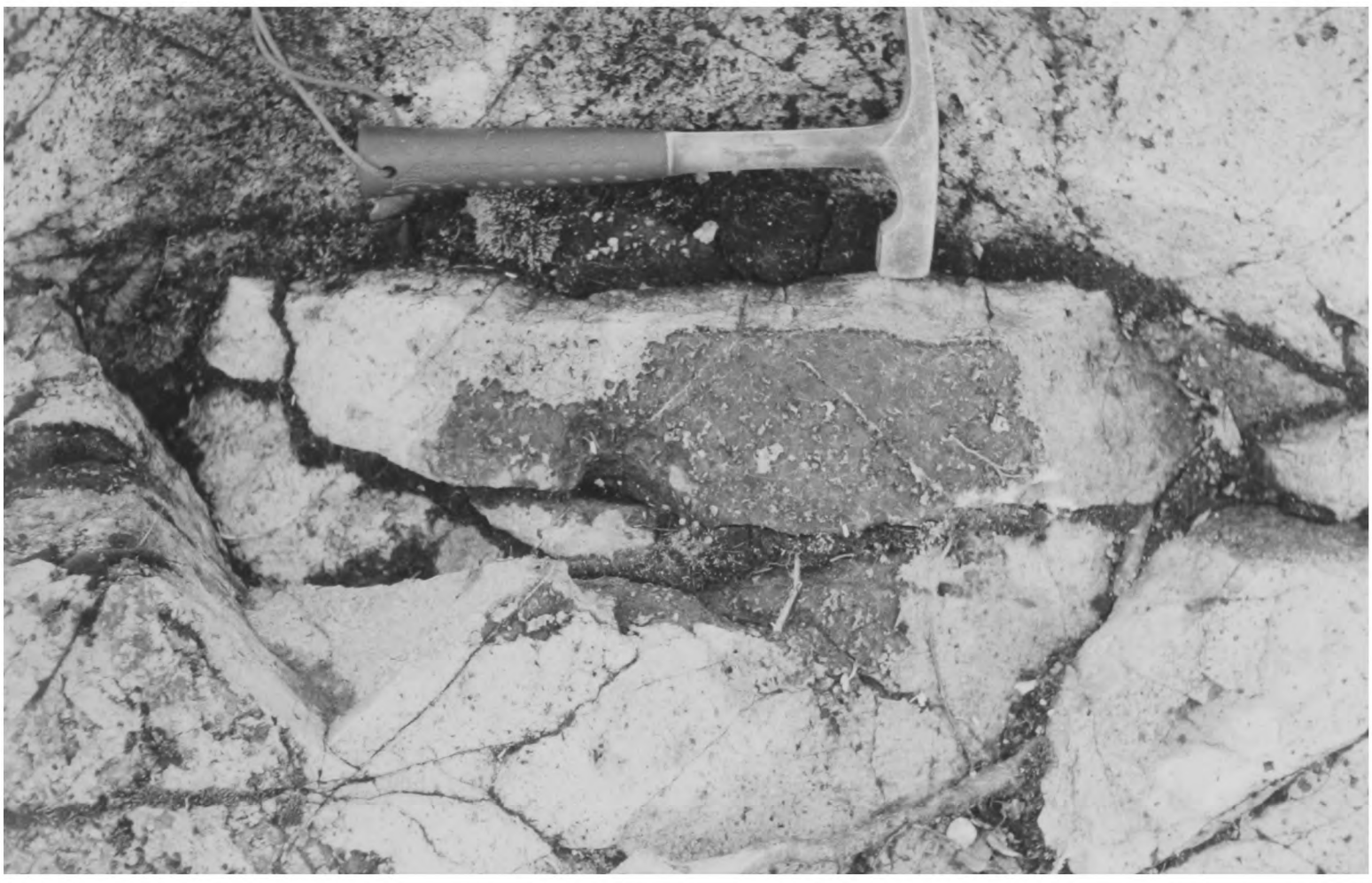


PLATE 5 - 6 Angular urtite xenolith in pulaskite. Xenoliths of pulaskite are also found in the foyaite. Southern foyaite N.E. shore of island L.

thick. The sharp basal unit is feldspathic, and the transition to urtite gradational. This, the coexistence of feldspar and nepheline in the chill, the concentration of feldspathic foyaites around the rim and the textures provide evidence of crystal settling.

Nepheline. Nepheline in the foyaites, occurs as thick, emerald green hexagonal tablets. Typically it is of two generations; large cumulus tablets with a weak horizontal preferred orientation, and small euhedral crystals in the matrix. Slight adcumulus overgrowths occur in some rocks particularly in the urtites. Intercumulus analcite in a small proportion of slides shows that nepheline could be replaced by a hydrous phase in the final stages of crystallization. Cumulus nepheline ranges from circa 10 - 20 - 60% of the rock in the sequence chill - feldspathic foyaite - urtite.

Coarse crystals, in hand specimen, show oscillatory zoning, with thin pale green bands in the dark green host. In thin section these light bands are seen to be formed by densely packed aegirine microliths. This zoning, visible in all sections of nepheline is variably developed, and is strongest in the intrusive ijolites. Bailey and Schairer (1966) have demonstrated a region of solid solution between nepheline and acmite in the iron rich sodic synthetic system Na_2O - Al_2O_3-Fe_2O_3-SiO_2, with up 40% $Na_2O.\ Fe_2O_3.4SiO_2$ in solid solution with the nepheline - Na_2O-Al_2O_3-$2SiO_2$.

Staining according to the method of Shand (1939) -2 minutes etch with syrupy phosphoric acid, 1 minute's staining with 0.25% methelyne blue, slide covered WET - demonstrates a second, parallel form, of oscillatory zoning, expressed as narrow unstained bands, in the now blue-stained host. Shand, from experiments using analysed nephelines from phonolites, has demonstrated that these light bands represent zones of excess silica in the nepheline structure. Although acmite exsolution (?) typically occurs near the centre of the crystals, and fine scale oscillatory zoning near the rims, those zones containing weak concentrations of acmite often take only a pale stain, and zones of intense acmite exsolution often pass laterally into unstained zones without exsolution. It is concluded that the crystals are oscillatory zoned with respect to both acmite and albite with, generally, the iron rich zones in the core (and in iron rich rocks) and albitic zones towards the rim.

Zoning with respect to acmite is present in all the foyaites, but zoning with respect to silica is visible only in the northern foyaites, and in the chill of the southern foyaite. This suggested that the coarse nephelines in the southern foyaite have been rehomogenized following acmite exsolution from iron nepheline. X-ray photographs of nepheline from the chill, coarse foyaite, nepheline-sacidine porphyry, and ijolite yielded composition of Ne_{69}, Ne_{72}, Ne_{73}, Ne_{72} and 73 respectively. Different zones from a crystal showing strong acmite exsolution in the coarse foyaite yielded constant values of Ne_{72}. Tilley (1954) has shown that rocks containing primary, or exsolved, microcline and albite

tend to have nepheline compositions falling within the Morozewicz-Buerger convergence field (Ne_{73-75}), whilst those containing primary feldspar in the sanidine-anorthoclase series tend to contain nephelines whose composition is dependent on the rock composition. The primary feldspar of the foyaites, and tinguaites is a platy cryptoperthite with a composition of circa Or_{66}, which has largely exsolved to coarse perthite, or discrete areas of microcline and albite. It is concluded that the primary nepheline composition was at least as potassic as Ne_{69}, and that subsolidus equilibration has generally taken place to produce nephelines within the low temperature stability field.

Feldspar: The feldspar in the foyaites and tinguaites is of two generations. In the dykes, and in the chill it is found as 1-4cm thin white plates of cryptoperthite, and as 1-4mm microliths in the matrix. The phenocrysts therefore, demonstrate that nepheline and feldspar were both on the liquidus prior to intrusion. In the coarse foyaites feldspar is also of two generations, occurring as 2-4cm (S.Foy) or 1-2cm (N.Foy) thick plates, which are cumulus crystals, and as anhedral interstitial, or poikilitic crystals in the matrix. The transition from feldspathic to nepheline foyaite is predominantly a decrease in the proportion of euhedral (cumulus) feldspar. This proportion in the southern foyaite follows the trend 15-25-5-0% in the sequence chill-feldspar foyaite - nepheline foyaite-urtite. The initial increase is taken to indicate two factors, first is the slight fractionation through crystal settling of feldspar relative to nepheline, and second the absence of feldspar as an early crystallizing phase in the nepheline foyaite and urtite stages of crystallization. The northern foyaite shows a similar but less extreme pattern in which feldspar is always present as a euhedral coarse phase, but in which some nepheline-feldspar fractionation must have occurred.

The composition of the primary feldspar is taken as Or_{65-66}. X-ray determinations of the composition of large phenocrysts from the tinguaites, chill*south*-foyaite, and coarse foyaite gave values of Or_{66}, Or_{65} and Or_{73}. respectively. Most crystals show undulose extinction owing to the irregular development of perthite, and the growth of discrete areas of twinned microcline and albite. The tie line linking the feldspar to the nepheline primary phase composition, is consistently more potassic than the normative composition of the analysed rocks would have indicated. This is taken as evidence for the existence of primary albite, analcite, or cancrinite within the matrix, or the reaction between the crystalline phases and a residual, sodic, volatile-rich, liquid. Primary analcite is present in the least altered tinguaites.

Aegirine: With the exception of the tinguaites, and the possible exception of the nepheline-aegirine rocks in the northern foyaite, aegirine is not a cumulus phase. It is pleochroic from yellow green to emerald green, unzoned, and typically granular. In coarse foyaites both aegirine and feldspar are poikilitic.

Magnetite: Primary magnetite is found enclosed in aegirine only within the chills.

Allanite: Small brown strongly pleochroic crystals of allanite occur within the foyaite matrix. Typically they are strongly zoned, sometimes with a metamict core, and are surrounded by a pleochroic halo if near biotite.

Analcite: Cancrinite and Sodalite: Analcite is a primary phase in the tinguaites where it occurs as polyhedra and poikilitic crystals in the matrix. Rarely in the nepheline foyaites and urtites, analcite is found enclosing euhedral nepheline and may be primary.

Nepheline is typically slightly altered to gieseckite along cracks. This alteration precedes the rimming of most crystals by a narrow zone of cancrinite. In contact with calcite, flame-like crystals of cancrinite have grown into the nepheline. Granular aggregates of cancrinite rimming nepheline, typically, contain a small proportion of granular analcite and sodalite.

Sodalite is found as secondary veinlets near the northeast and southern boundary of the complex. It is deep blue and translucent and has been used as a gemstone.

Calcite and fluorite: Calcite and fluorite together have been found filling the angular interstices between nepheline and feldspar in two chilled rocks. In altered rocks both react with nepheline to form cancrinite.

Ijolites: The northern foyaite of Bigspruce island is intruded by four small masses of fine-grained dark green ijolite. Each mass contains abundant angular blocks of porphyritic ijolite with up to 15% nepheline phenocrysts in an ijolitic matrix. Each is surrounded by a broad zone of cancrinitized foyaite breccia. The contact between the foyaite, and the ijolite breccia is gradational.

The ijolite matrix is composed of granular 0.1-0.3mm nepheline and aegirine in the constant ratio of 6:4, together with minor secondary biotite, andradite, and cancrinite. The nepheline is rich in exsolved acmite. The aegirine is deep green and slightly zoned.

The phenocrysts of nepheline (1 - 1.5cm) are euhedral and rich in acmite, and include small cores with silica zoning similar to those of the northern foyaite. A few phenocrysts are fractured and veined by ijolite.

Most hand specimens include 5 - 10% of partially resorbed platey feldspar xenocrysts possibly derived from the foyaite. These have reacted with the liquid to form cloudy albite, and are partially replaced by nepheline and aegirine in similar porportions to the matrix.

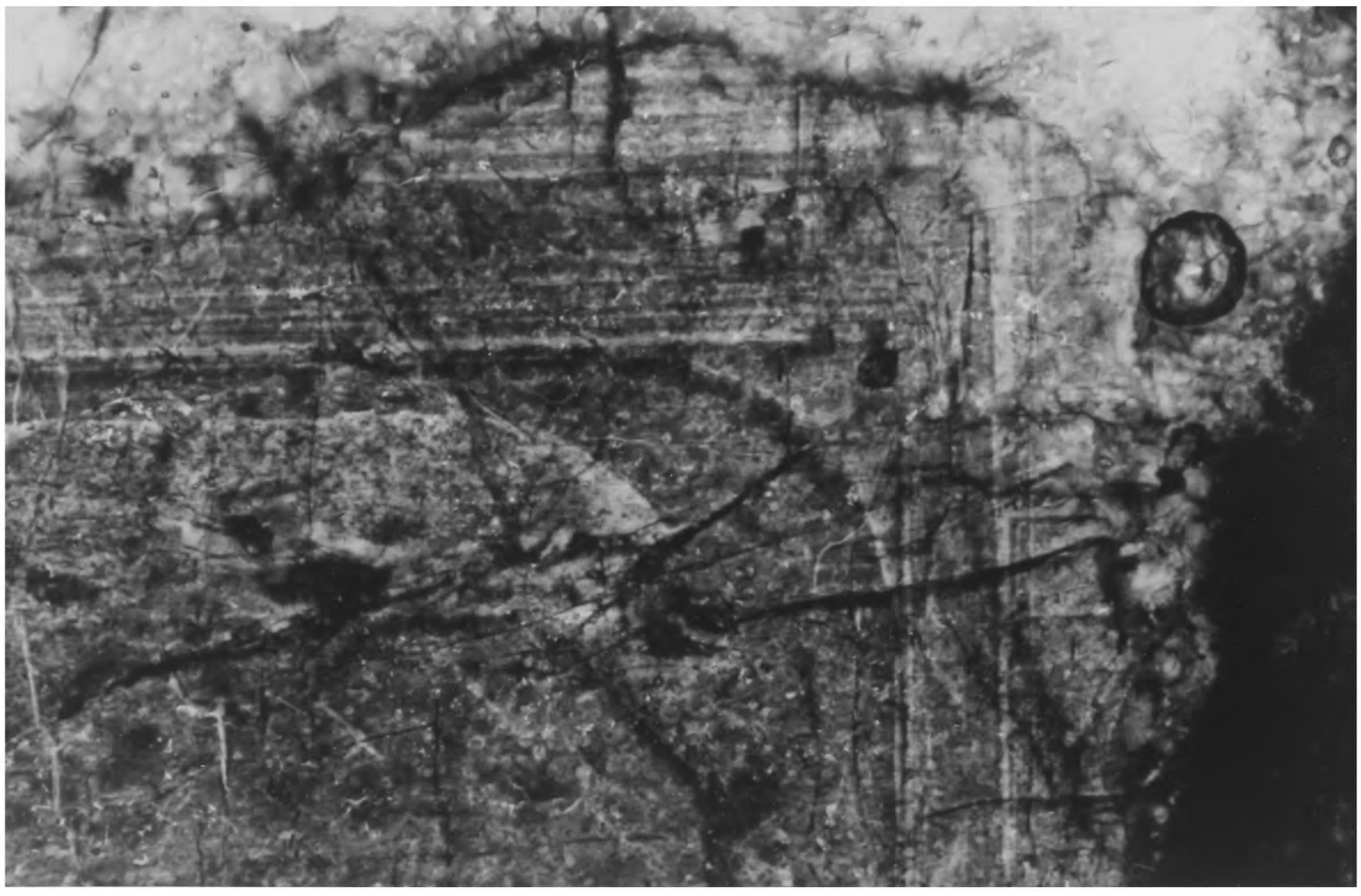


PLATE 5 - 7 Detail of fine-scale silica zoning in stained nepheline. The lighter unstained bands are relatively enriched in silica. Northern foyaite, N.E. side of Bigspruce island. Spec. 68295, x 50

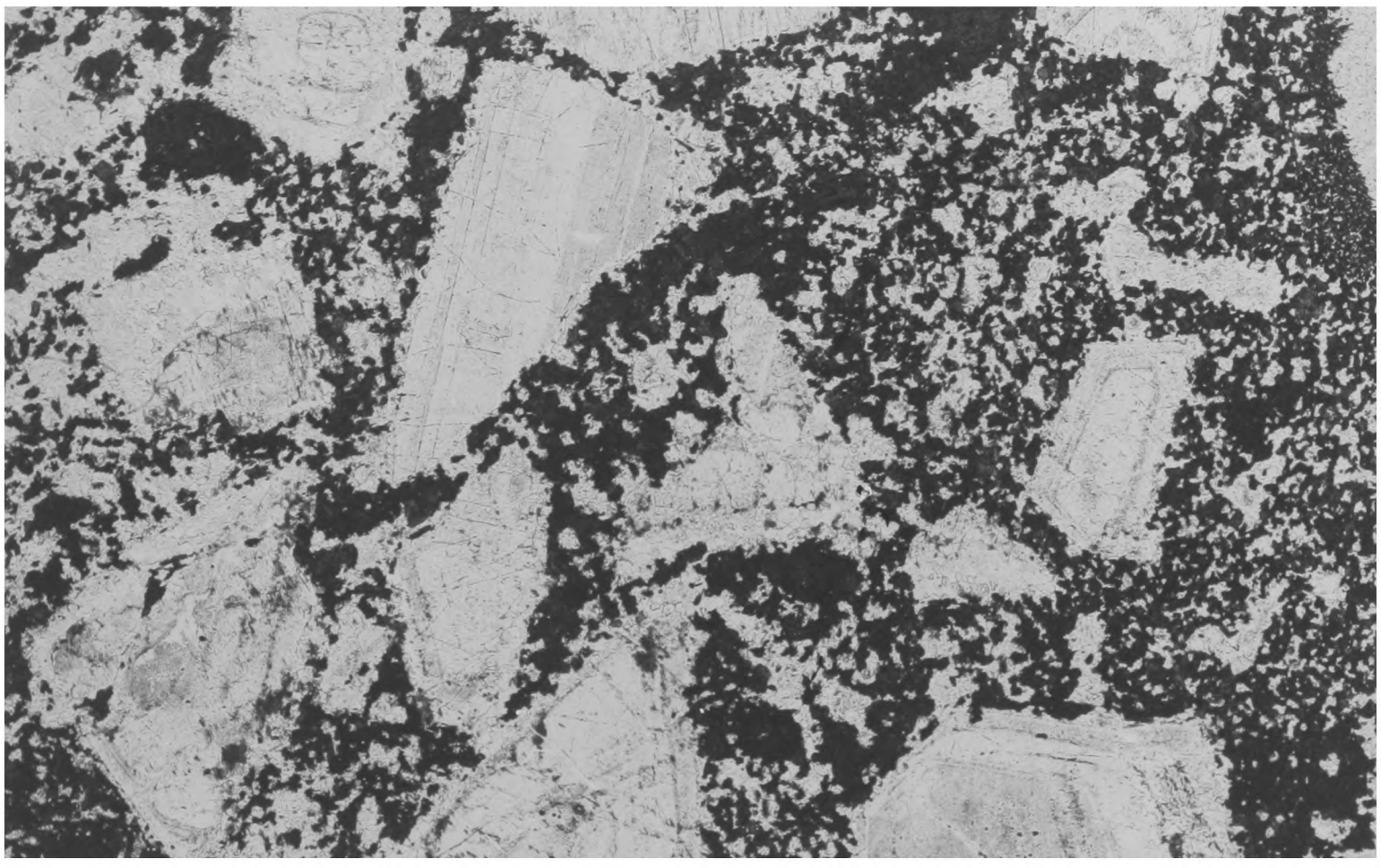


PLATE 5 - 8 Fractured nepheline xenocrysts in ijolite. The cores of many of these crystals showed silica oscillatory zoning on staining but the visible zoning is produced by the exsolution of acmite needles. The matrix is composed of granular aegirine and nepheline. S.E. pensinsular Bigspruce island, ijolite breccia, spec. 67283. x 6

TABLE 5 - 2. ANALYSES OF THE NORTHERN FOYAITES AND SOUTHERN FOYAITES.

	68051	68352	68357	68351	68295	67116	A	67374	2814	67130	2810	67003	68335	2821	B	C	D
SiO_2	55.65	51.38	51.12	51.04	50.84	40.48	55.90	57.71	56.09	53.57	52.74	51.35	50.10	48.62	53.76	55.65	54.83
Al_2O_3	19.95	20.93	22.89	22.73	23.56	17.75	19.75	21.52	20.34	20.24	20.94	24.42	25.28	25.58	21.64	19.79	22.63
Fe_2O_3	5.54	-	-	3.93	3.41	-	1.00	-	3.49	3.37	5.37	-	-	3.05	1.09	4.98	1.56
FeO	1.97	5.76	5.28	1.66	1.77	17.69	2.05	2.75	3.60	3.05	2.91	3.09	3.47	1.51	3.60	3.03	3.45
Mgo	0.48	0.65	0.26	0.31	0.16	2.84	0.59	0.02	0.39	0.23	0.17	0.12	0.17	0.12	1.22	0.52	tr
CaO	3.92	4.31	3.05	3.03	2.82	5.84	3.10	1.69	2.31	3.44	1.27	2.32	2.70	2.62	1.61	1.40	1.94
Na_2O	9.08	10.57	10.87	11.10	11.26	8.06	7.25	9.92	6.20	10.05	8.22	11.48	11.92	12.71	8.63	7.60	10.63
K_2O	4.58	5.19	5.34	5.25	5.26	3.60	5.61	5.69	6.65	5.05	6.79	6.30	5.84	4.72	5.69	5.27	4.16
TiO_2	0.53	0.39	0.39	0.40	0.39	1.17	0.70	0.54	0.69	0.56	1.40	0.36	0.43	0.57	0.94	0.15	0.31
MnO	0.20	0.25	0.19	0.19	0.16	0.60	0.10	0.06	0.21	0.24	0.16	0.08	0.08	0.12	0.07	0.15	tr
P_2O_5	0.02	0.05	0.09	0.06	0.10	0.61	0.01	0.01	-	-	-	0.01	0.02	0.15	0.04	0.22	-

A. Nepheline syenite Mt Royal Monteregian province Dresser and Denis (1944)
B. Average of 3 Nepheline syenites Gremyakha Vyrmes complex
C. Nepheline syenite Gronnedal Ika, Gardar province Watts (1966 55)
D. Nepheline syenite Ditro Streckeisen (1954)

TABLE 5 - 2. TRACE ELEMENTS.

	68051	68352	68357	68351	68295	67116	A	67374	2814	67130	2810	67003	68335	2821	B	C	D
Rb	163	-	95	100	95	-	-	94	-	-	-	-	175	166	-	-	-
Ba	1,690	-	3,300	2,810	2,510	-	-	1,000	-	-	-	-	1,810	1310	-	-	-
Sr	1,340	-	1,700	1,760	1,380	-	-	1,060	963	-	-	-	1,010	1440	-	-	-
La	-	-	-	-	121	-	-	-	-	-	-	-	-	96	-	-	-
Ce	-	-	-	-	28	-	-	-	-	-	-	-	-	172	-	-	-
Y	32	-	12	21	-	-	-	7	-	-	-	-	-	25	-	-	-
Zr	858	-	442	516	511	-	-	179	294	-	-	-	215	359	-	-	-
Nb	144	-	57	55	58	-	-	28	55	-	-	-	48	90	-	-	-
	CHILL					Ne-Aeg Rock		CHILL									

NORTHERN FOYAITE SOUTHERN FOYAITE

TABLE 5 - 3. ANALYSES OF TINGUAITES AND IJOLITES.

	67186	2822	67348	67007	2729		2700	67234	68283	A	B	C
SiO_2	56.00	55.41	55.11	54.99	52.92		42.62	44.68	44.85	45.28	45.49	37.59
Al_2O_3	20.16	18.68	19.44	19.44	15.81		17.74	19.68	21.31	20.51	11.99	16.36
Fe_2O_3	-	5.22	-	2.45	9.79		4.13	-	-	4.71	7.08	4.17
Fe O	5.33	0.88	6.12	2.70	3.70		5.57	11.96	9.89	4.40	6.46	3.95
Mg O	0.12	0.60	0.17	0.19	0.29		1.13	1.26	1.14	1.92	3.82	2.91
CaO	3.06	3.57	3.42	4.24	2.49		7.99	6.95	6.56	6.46	12.32	21.95
Na_2O	8.44	7.75	8.81	8.08	7.41		12.51	11.71	12.48	11.11	5.45	5.80
K_2O	5.82	7.20	5.80	6.44	5.58		1.47	2.17	2.23	3.46	1.35	2.57
TiO_2	0.54	0.66	0.52	1.30	1.09		0.18	0.33	0.33	0.79	0.41	2.43
MnO	0.19	-	0.19	0.12	0.44		0.34	0.54	0.51	0.16	0.35	0.12
P_2O_5	0.00	-	0.00	0.00	-		0.15	0.03	0.08	0.47	0.16	2.13

A. Avge ijolite Gremyakha Vyrmes massif Gerosimoskiy (1967)

B. Ijolite Budeda
C. Ijolite Napak
} King (1965).

TABLE 5 - 3: TRACE ELEMENTS.

	67186	2822	67348	67007	2729		2700	67234	68283	A	B	C
Rb	143	-	169	198	-		-	9	68	-	-	-
Ba	2,010	-	-	4.360	-		-	-	252	-	-	-
Sr	367	1,170	1,640	2,950	1,150		2,110	528	1,020	-	-	-
La	-	-	-	107	-		-	-	99	-	-	-
Ce	-	-	-	84	-		-	-	180	-	-	-
Y	5	-	-	17	88		-	-	27	- -	-	-
Zr	444	405	314	460	1,450		935	1,400	825	-	-	-
Nb	17	43	12	104	178		14	25	164	-	-	-

Modal mineral proportions show -

	67279	67165	2700
Nepheline	32.9	30.2	5.7
Cancrinite	24.1	23.3	54.6
Analcite	0.1	0.7	5.1
Feldspar	6.4	3.9	-
Aegirine	26.1	39.6	25.2
Biotite	5.6	1.0	4.7
Andradite	4.8	-	4.5
Apatite	Tr	0.1	0.1
Calcite	-	1.2	

Tinguaites: The tinguaite dyke swarm runs N8°W through the western portion of both foyaites, and across the ijolite. The dykes lack sharp chills, commonly bifurcate and enclose rounded blocks of foyaite. They are dark green fine-grained rocks containing phenocrysts of cryptoperthite and nepheline. Typically, they contain vuggy patches of macroscopic aegirine and golden sphene. The phenocrysts of nepheline, or feldspar may be locally concentrated in a single dyke to form nepheline, or feldspar tinguaites but mineral proportions in the matrix are constant. It is composed of cryptoperthite, nepheline, aegirine, primary polyhedral analcite, and sphene with the modal proportions of (including phenocrysts) -

	2822	67007
Nepheline	23.7	26.2
Cryptoperthite	41.6	46.4
Cancrinite	5.0	0.3
Analcite	-	3.3
Aegirine	27.3	20.5
Sphene	2.4	3.3
Apatite	Tr	Tr
Fluorite	Tr	Tr

The aegirine is deep green with slight colour zoning. The feldspar phenocrysts are carlsbad twins typically with $(0\bar{2}1, 02\bar{1})$ double Baveno twins.

The chemical composition of the tinguaites is illustrated in table 5-3.

Chemistry of the Alkaline Rocks. The analyses of the nepheline-sanidine porphyry, northern foyaite and southern foyaite are given in table 5-2. Considering the chill composition, there is a close similarity between the three. All show relatively high silica 53.5 - 57.7, low calcium and magnesium, low TiO_2, very low P_2O_5 and high Ba and Sr. The abundance of Zr is related to the abundance of the mafic minerals and in particular of sphene. All these rocks are peralkaline, with, typically, high $\frac{Fe^{3+}}{Fe^{2+}+Fe^{3+}}$.

The major element geochemistry is comparable to the foyaite of Ditro, of the Gronnedal-Ika complex (Gardar province) or of the Gremyaka Vyrmes massif (Kola peninsular).

The ijolites are soda rich and relatively calcium and magnesium poor. CaO, MgO and TiO_2 are notably lower than in ijolites from Napak or Budeda where they are associated with carbonatites. They are similar to ijolites from the peralkaline Gremyaka Vyrmes massif. The trace element concentrations are similar to those of the foyaites.

Agpaitic versus Miascitic Syenites. Sorenson (1960) and Heinrich (1966) amongst others have discussed the significance, or lack of it, of the distinction between agpaitic and miascitic nepheline syenites. The distinction is essentially a mineralogical one dividing those syenites containing aegirine and soda amphibole from those containing diopside, augite, biotite, or hornblende, as the primary mafic mineral. The geochemical distinction has come to be drawn at $\frac{Na + K}{Al} = 1.2$ or $\frac{Na_2O + K_2O}{Al_2O_3} = 1$.

Other geochemical characteristics of agpaites are :

1. Abundant Fe: $Fe^{3+} \geqslant Fe^{2+}$, lack of oxide
2. Low Mg, and Ca
3. Abundant Zr and Cl mainly in eudialyte and sodalite
4. Abundant volatiles; F, Cl and H_2O as opposed to H_2O and CO_2.
5. The early crystallization of feldspar, nepheline and sodalite.

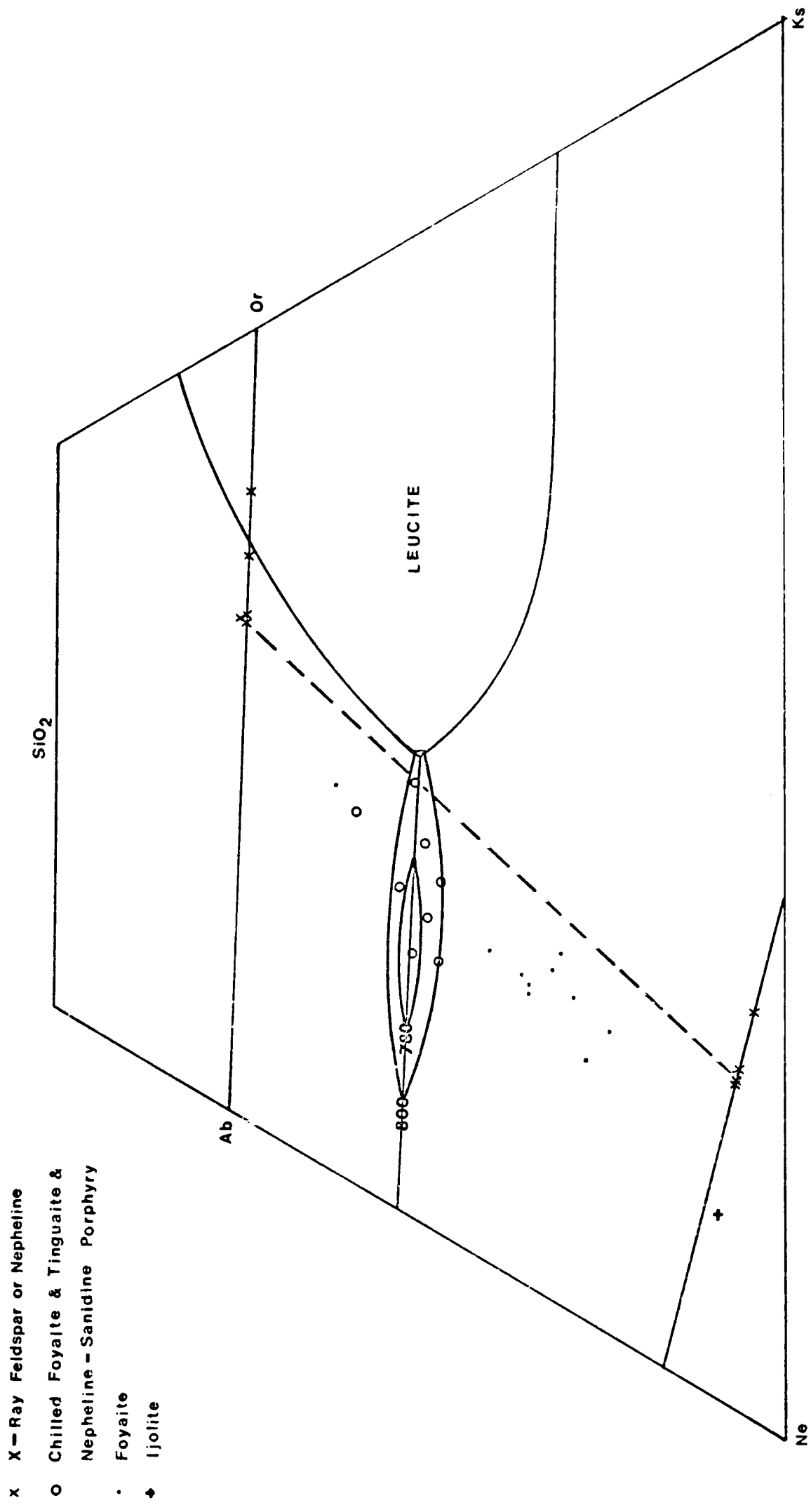
With the exception of the $\frac{Na + K}{Al}$ ratio these characteristics are all common also to the peralkaline (nepheline) syenites.

The agpaites, it is claimed, are commonly associated with saturated syenites, for instance in the Oslo province, Gardar province and Damaraland province, whereas the miascites are commonly associated with carbonatites which rarely contain a saturated sequence, for instance at Napak, Oka, Alno and Fen.

However, a great number of exceptions to this rule are known. Thus carbonatite occurs within the layered foyaite of the Gronnedal Ika; carbonate rich rocks occur near the type agpaite of Ilimaussaq; peralkaline, and agpaitic rocks (nepheline-syenites and phonolites) occur at the carbonatite centres of Napak, Toror and Budeda, and in the Chilwa province (Garson 1965, King 1965). Many well known nepheline syenites free of carbonatite, and rich in aegirine, for instance the Pilansberg, Khibina, Lovozero and Mariupole contain foyaites and ijolites which are peralkaline, but not agpaitic (Sorenson 1960), and indeed the same applies to the majority of rocks in the Oslo province, the Gardar province, and the Damaraland province. It should also be pointed out that although those rocks most closely associated with carbonatites-ijolites, nephelinites, melilite nephelinites, ankaratrites, and melteigites, in the high level African provinces are miascitic they typically have $\frac{Na + K}{Al} < 1$ (King 1965, Garson 1965).

The foyaites, tinguaites, and ijolites of Bigspruce Lake are peralkaline (1.00 - 1.19) but they are not agpaitic. They contain high Fe^{3+}: Fe^{2+}, low Ca, Mg and Ti, and high Sr and Ba but they do not contain complex zirconium silicates, nor notably high Zr or Cl.

FIG 5 - 2 NORMATIVE COMPOSITIONS OF THE FOYAITES, TINGUAIITES AND IJOLITES.



The field boundaries in the system $NaAlSiO_4$-$KAlSiO_4$-SiO_2-H_2O at 1Kb total pressure are taken from Hamilton & Mackenzie (1965). The analyses of the co-existing feldspars and nephelines have been determined by x-ray diffraction.

	Zr	Cl
2835	667	2000
2821	359	2400
2810	-	5500
2729	1450	3500
2700	935	4300

Relationship to Carbonatites. They are intruded by carbonatites, and the sovite centre of Bigspruce island lies near the centre of the northern foyaite, and the ijolites.

The association is, however, petrologically fortuitous, although the foyaites probably provided a convenient conduit for the rise of the parent magma. The gas escape vents, which rim the carbonatite centre, rim the quartz syenites also. The carbonatites contain blocks of high potassic rocks, biotite-peridotites, and pyroxenites, but not of ijolite or foyaite. The high potassic rocks contain veinlets and vesicles of calcite and apatite; the centre 3 rocks do not. The high potassic rocks are rich in biotite, augite, and apatite and have more similar Ca, Mg, P, Rb, Ba and R.E. concentrations. The K/Rb ratio of the carbonatites and high potassic rocks are similar (60 - 220, Avge 150-160), and significantly lower than those of the foyaites, and ijolites (270-500, Avge 450). The high potassic rocks are alkaline but miascitic, with $\frac{Na + K}{Al.} \approx 0.6$.

Where carbonatites invade the foyaites, biotite and magnetite are introduced, and the rocks become less peralkaline.

The very different geochemistry particularly the difference in the Na: K ratio (1.2:1 and 3:1 respectively) make it unlikely that the peralkaline rocks and high potassic rocks are closely related (see also figs.8-1 and 8 - 2).

In view of the close association between peralkaline rocks, and trachytes or syenites, (Bailey and Schairer 1966, Carmichael and Mackenzie 1965) and the general lack of such an association for the alkaline undersaturated rocks, it is concluded that the presence or absence of peralkaline rocks is of much more significance than the presence or absence of agpaites. This distinction will then serve the purpose of separating those syenites which may have been derived by fractional crystallization of trachytic magmas, from those which have not been so derived.

For example King (1965) singles out the phonolites and trachytes of the eastern Uganda province as lying along a divergent trend from the more abundant ankaratrites nephelinites and urtites. The former are peralkaline but not agpaitic and contain low Ca, Mg; the latter are not. The melteigites, and nephelinites are most closely associated with the carbonatites.

Relationship of foyaites to centres 1 and 2. The normative composition of the analysed nepheline syenites are plotted on the Qtz-Ne-Ks triangle in Fig 5-1, and 5 - 2. The normative composition of the chilled foyaites, of the nepheline-sanidine porphyry, and the majority of tinguaites fall

close to the nepheline - feldspar field boundary, within the low temperature thermal trough in the 1kb H_2O synthetic system (Hamilton and Mackenzie 1965). The mean of these analyses is slightly displaced towards the nepheline side of the boundary. The unchilled cumulus rocks lie close to tie lines linking the chill to the initial nepheline or feldspar composition. It is concluded that the chills crystallized from liquids on or very close to the feldspar-nepheline eutectic in the slightly peralkaline natural system, and that the unchilled rocks represent nepheline or feldspar cumulates. Since the chilled liquids all lie close to a eutectic it is logical to derive these liquids either by partial fusion, or by the fractional crystallization of a liquid itself within a related thermal trough. Hamilton and Mackenzie have demonstrated the existence of a thermal trough in the water saturated 1kb system running from close to the orthoclase-albite tie line to the minimum, on the nepheline-feldspar field boundary. Within this trough lie the majority of analysed syenites, phonolites, and trachytes. Because of the thermal saddle separating the saturated from the undersaturated field along the albite-orthoclase tie line, the system provides no indication of how quartz syenites could give rise to the nepheline-sanidine porphyry or vice-versa.

Fig.5-1 illustrates the analysed composition of the porphyry dykes. These undersaturated porphyries belong to a single series in which the feldspar is the primary phenocryst phase and shows a continuous reaction series from plagioclase, through sodic anorthoclase, to mesoperthite. When the rock has the composition of a trachyte, nepheline is first found in the matrix. Nepheline, as a phenocryst phase, appears only when the rock has the composition of the nepheline-sanidine porphyry, which as is shown in fig 5-1 is at the nepheline-feldspar phase boundary. The phenocryst phases demonstrate that the fractionation in the natural system is controlled dominantly by the feldspar, and to a lesser extent by pyroxene, magnetite and apatite. The derived fractionation curve, linking the analyses, but based on the observed mineralogy, lies close to the ideal feldspar fractionation curves given by Hamilton and Mackenzie for the mafic free system at 1kb H_2O.

It is concluded that the nepheline-sanidine porphyry arose by feldspar fractionation from an alkali gabbroic parent. The close similarity between the foyaites, and this porphyry suggest that the foyaites arose in the same manner; the more basic pulaskites, and essexites which would lie along this fractionation trend being unexposed and at greater depth. This trend is thus similar to that proposed for Okonjeje and for several oceanic islands such as Kerguelen (Edwards 1938, in Turner and Verhoogen 1960). Such a trend precludes any close connection between the foyaites and quartz syenites or diorites, but the trends converge towards the composition of the olivine bearing big feldspar gabbro (see also figs 8-1 and 8-2).

It is concluded that through the separation of either pyroxene or amphibole a magma similar or more basic than this, might give rise to both series.

Origin of the Ijolites. The field evidence demonstrates the existence of an intrusive ijolite magma occupying breccia pipes. The fine grain size and near uniform composition indicate that this magma was similar in composition to the exposed rocks, with the exception of the loss of Na_2O, CO_2 and H_2O to form cancrinite (and andradite) in the brecciated foyaite margins. The composition of the nepheline, and aegirine is similar to that in the foyaite. The rocks are rich in Na, and poor in Ca, Mg, Ti and P_2O_5, in distinction from the diopsidic nephelinites, melanephelinites, ijolites and melteigites of many of the East African volcanoes, and of the carbonatite complexes such as Oka and Napak.

The resorbed xenocrysts demonstrate that microcline, and albite were not stable phases in the magma. Bailey and Schairer (1966) have shown that "for a particular range of undersaturated compositions (viz. mariupolite and iron rich syenite) sodic ijolite apparently constitutes a low temperature residuum, analagous to the granitic residuum of oversaturated rocks. Furthermore, similar bulk compositions containing potential sodium silicate.....may have a still lower final eutectic (than the 908°C of the anhydrous system Na_2O-Al_2O_3-Fe_2O_3-SiO_2) to which the univarient path ac + ne + ab + liquid proceeds from the (synthetic feldspar bearing) ijolite point". They suggest that there are three possible modes of origin. The calcic ijolites, they suggest, may be derived either by the fractionation of highly undersaturated cafemic magmas, such as melilite basalt, or by the reaction between carbonatite and phonolite-trachyte magmas. The sodic ijolites, they suggest, may be derived by the palingenesis of iron rich peralkaline syenites. They cite Alno as an example.

An alternative mechanism applicable to the observed transition into the northern foyaite is consistent with the association with the carbonatite and with the resorption of the feldspar.

Koster van Groos (1966) has investigated the effects of Na_2CO_3 on selected joins in the system Na_2O - CaO - Al_2O_3 - SiO_2 - H_2O. Amongst other points he has noted -

1. "The addition of Na_2CO_3 in conjunction with H_2O reduces the stability of albite: Cancrinite is formed instead."
2. "The composition of the vapour in the joins investigated is probably enriched in sodium silicates."
3. "Liquids persist to low temperatures, perhaps they are continuous with a water rich vapour phase."
4. In the join Ab_{80} An_{20} - Na_2CO_3 + H_2O (10%) noselite and cancrinite and wollastonite) have a high temperature stability field over almost the entire join in place of feldspar.
5. In the join Ab-Na_2CO_3 in the presence of water albite breaks down according to the reaction $NaAlSi_3O_8 + Na_2CO_3 \rightarrow NaAlSiO_4 + Na_2Si_2O_5 + CO_2$.

It is suggested that the ijolite has formed from the northern foyaite following the metasomatism, loss of feldspar, and palingenesis in the presence of H_2O and CO_2, and potential sodium silicate. The excess sodium silicate has been lost, in the vapour phase to the surrounding cancrinitized rocks. The ijolite "magma" is still essentially 'in situ' in the breccia rents. The source of the volatiles is the proto-sovite-centre of Bigspruce island and is probably a large mass of biotite-peridotite, or biotite-pyroxenite crystallizing at depth, beneath the present centre. The formation of the ijolites is separated, by intrusion of the tinguaites, from the intrusion of the sovite pegmatites.

THE LAYERING IN THE FOYAITES.

Wager and Brown (1968) list four nepheline syenite layered intrusions,, Lovozero, Ilimaussaq, Gronnedal-Ika and Kangerdluassuq. All are peralkaline, and Ilimaussaq is agpaitic. In each, the early crystallizing minerals are feldspar, and feldspathoids. Ilimaussaq, Gronnedal-Ika and Lovozero show trachytic textures and rhythmic banding suggestive of strong convecting currents. In Kangerdluassuq the banding is gradational, and strongly developed preferred orientation is absent. In each intrusion the feldspathic rocks are found towards the base of each rhythmic group, and towards the base and margin of the intrusion.

In the Bigspruce lake foyaites slight preferential settling of feldspar relative to nepheline in the absence of convective currents may explain the observed zonation. The reason for the absence of convective currents may lie in the relatively small size of the intrusions, the eutectic nature of the liquid, the small temperature difference between the solidus, and liquidus, and the small density difference between the liquid, and the crystallizing phases.

The eutectic nature of the magma ensures that slight changes in the physical conditions of the magma, for instance PH_2O, which may change the eutectic composition, may cause the liquid to lie within the feldspar, or nepheline phase field, and hence produce nepheline rich, or feldspar rich cumulates.

A further consequence of the eutectic is that the trapped interstitial liquid may crystallize soon after the settling of the cumulates, almost isothermally. Hence the layers may consolidate rapidly, and angular xenoliths of urtite or pulaskite, rather than crystal density currents may transport material to the floor from the chambers roof or walls. Such xenoliths are abundant in the foyaites of Ilimaussaq and Gronnedal Ika where they are also explained as foundered remnants from the roof or walls.

Nature and formation of the fenites.

The name fenite was originated by Brogger to describe the syenitic rocks (circa 70 - 90% feldspar) formed through the metasomatism of granitic country rocks around an alkaline, or carbonatite complex. The process of metasomatism he described as fenitization. The sequence of metasomatic change seen in granitic rocks around most such complexes is similar.

Thus at Alno Eckermann (1948) described -

1. The thermodynamic shattering of the microstructure of the country rock; granulation of quartz: perthitization of the feldspars (thermal shock zone).
2. The loss of quartz, growth of aegirine, and hydration of the feldspars (quartz syenite fenite zone).
3. The formation of soda orthoclase (syenite fenite zone).
4. The growth of nepheline within the clouded feldspars, the growth of diopside, and melanite, liquifaction of the leucocratic components; formation of a cafemic "rest fenite", and a leucocratic intrusive "rheomorphic fenite". (zone of nephelinization).

The initial stages, 1-3, are those most commonly found. Nephelinization is rarely seen in situ.

The mineralogical changes observed in many fenites are (Smith 1956, McKie, in Tuttle and Gittins 1966, Heinrich 1966).

1. The recrystallization of quartz to a micromosaic; the exsolution of feldspar to perthite; the coating of joint planes with aegirine (Chilwa), blue or green hornblende (Chishanya), or red-russet biotite (Sekulu, Bukusu or Sekululu).
2. The growth within quartz of needles of aegirine, or soda-amphibole; the formation of veinlets of albite or soda-orthoclase; the resorbtion or replacement of biotite; the crystallization of coarse apatite, sphene, zircon or titanomagnetite.
3. The growth of aegirine or amphibole as rims to quartz, themselves bordered by small new crystals of albite, soda orthoclase or microcline; the resorption of most quartz, and its replacement by feldspar.
4. Loss of the remaining quartz; the replacement of riebeckite-arfvedsonite by aegirine; the complete recrystallization of feldspar to orthoclase (Spitzkop and Chilwa high K fenites), orthoclase plus albite (Chishanya), or soda orthoclase (Fen and Alno).

The material balance has been estimated for several complexes. In general there is an addition of Na+K, and Al to form feldspar, and an increase in Fe^{3+}/Fe^{2+} to form riebeckite or aegirine. Silica is universally removed (or there is a presumed doming with increasing volume- Eckermann 1948). In many cases Fe, Ca, Ti, P, CO_2 and H_2O increase within the fenites.

Fenitization is characteristic of carbonatite bearing complexes, although it is often related to the earlier silicate rocks. Fenites also occur around volatile rich carbonatite free complexes as at Norra Karr, Libby (biotite-pyroxenite + foyaite) Montana, and Seal Lake, Labrador. The width of the fenite zones is highly variable. At Fen they range from 100 - 400m; at Alno up to 2000m.

Bigspruce Lake Fenites: At Bigspruce lake fenites are found around the northern foyaite, southern foyaite, biotite-pyroxenites, and carbonatites.

Around the carbonatite dykes alteration is confined to the shattering of

the country rock, the introduction of calcite or dolomite, and of apatite, the clouding of feldspars and the occasional formation of sericite.

Associated with the carbonatites are several elliptical gas escape vents. Within each there is recrystallization wholly, or partially around the fractures, to microgranite, and the formation, bordering the fractures, of perthite (Thermal shock zone of Eckermann). The central area shows a 3 - 5% increase in silica.

The remaining fenites show a zonation of the fenite, and sequence of recrystallization similar to that described above. Each fenite differs in its details. Each is formed from coarse phenocrystic two feldspar, 2 mica, apatite and zircon bearing granodiorite, and terminates in a leucocratic aegirine - perthite - syenite.

Southern Foyaite Fenite: The southern foyaite is surrounded by two fenite zones; an outer zone of microgranite; and an inner zone of aegirine-syenite. There is no zone of amphibole syenite. The contact between the aegirine syenite and microgranite is sharp.

The microgranite is gradational into the country rock at 50-150m. The mineralogical changes observed are -

1. loss of all muscovite.
2. sericitization of plagioclase, partial resorption of the phenocrysts.
3. formation of perthite from microcline, plus plagioclase inclusions, in the phenocryst phase.
4. growth ofsmall perthite crystals rimming plagioclase.
5. recrystallization of quartz to a micromosaic.
6. colour change in the biotite from sepia to russet brown. The development of numerous intense pleochroic haloes around ? allanite and zircon.
7. development of minor idiomorphic titanomagnetite, ilmenite, and zircon in some rocks.

In a few areas the granodiorite is crosscut by quartz veinlets, and much biotite has been introduced along fracture planes.

The aegirine syenite is composed of yellow or pale pink perthite (85-95%) of variable but usually medium grain size (0.5 - 1.5cm) enclosing biotite, amphibole epidote and magnetite pseudomorphs after aegirine, and minor primary magnetite and ilmenite. Some rocks contain up to 0.5% quartz and minor calcite and pyrite. A few sericitized relics of plagioclase are preserved. Basic dykes continue, altered, into the fenite.

The internal contact is also sharp, against reddened, laminated foyaite.

Northern Foyaite Fenite: The northern foyaite fenite is sporadically exposed west and south of Bigspruce island but is nowhere in contact with the foyaite itself. There is no zone of microgranite. Instead the outermost granodiorite, at 50-70m is shattered by arfvedsonite or biotite (or both) coated fractures, adding up to 20% extra mafic minerals to the bulk rock. There are three metasomatic zones. The outermost is the zone of shattering, the next a zone of arfvedsonite-perthite-



PLATE 5 - 9 Texture of the unaltered granodiorite. Muscovite is intergrown with biotite. Plagioclase and microcline are present in approximately equal proportion; Both occur as phenocrysts. By the Snare rapids dam. spec. 2836, x 4.

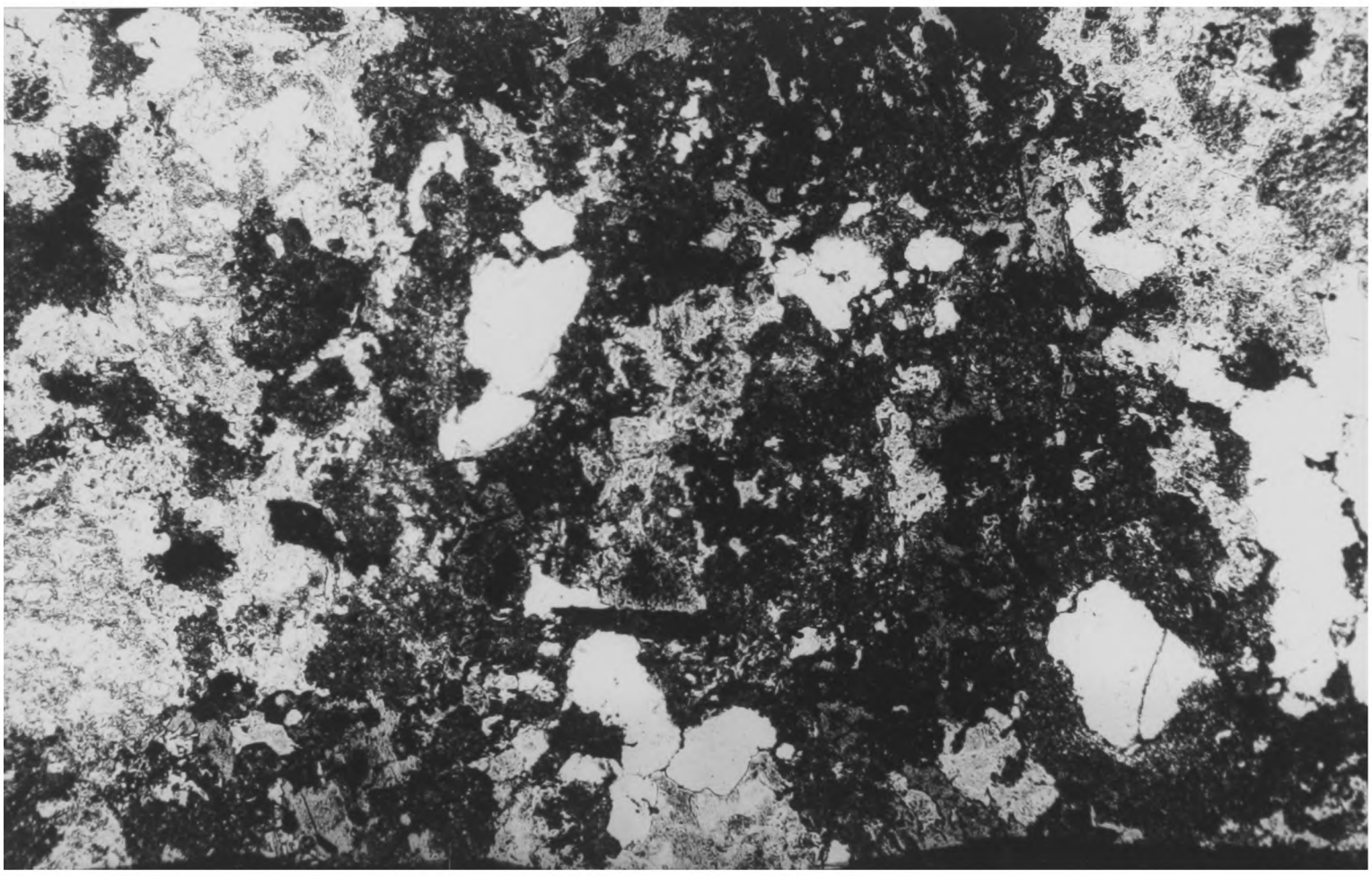


PLATE 5-10 Biotite coated fracture in the outer fenite zone of the Southern foyaite. The microcrystalline aggregates of biotite are rich in pleochroic haloes. The feldspars are sericitized and albitized. Quartz is becoming globular. 50m West of foyaite chill, Fallin peninsulor, Spec. 67005, x4

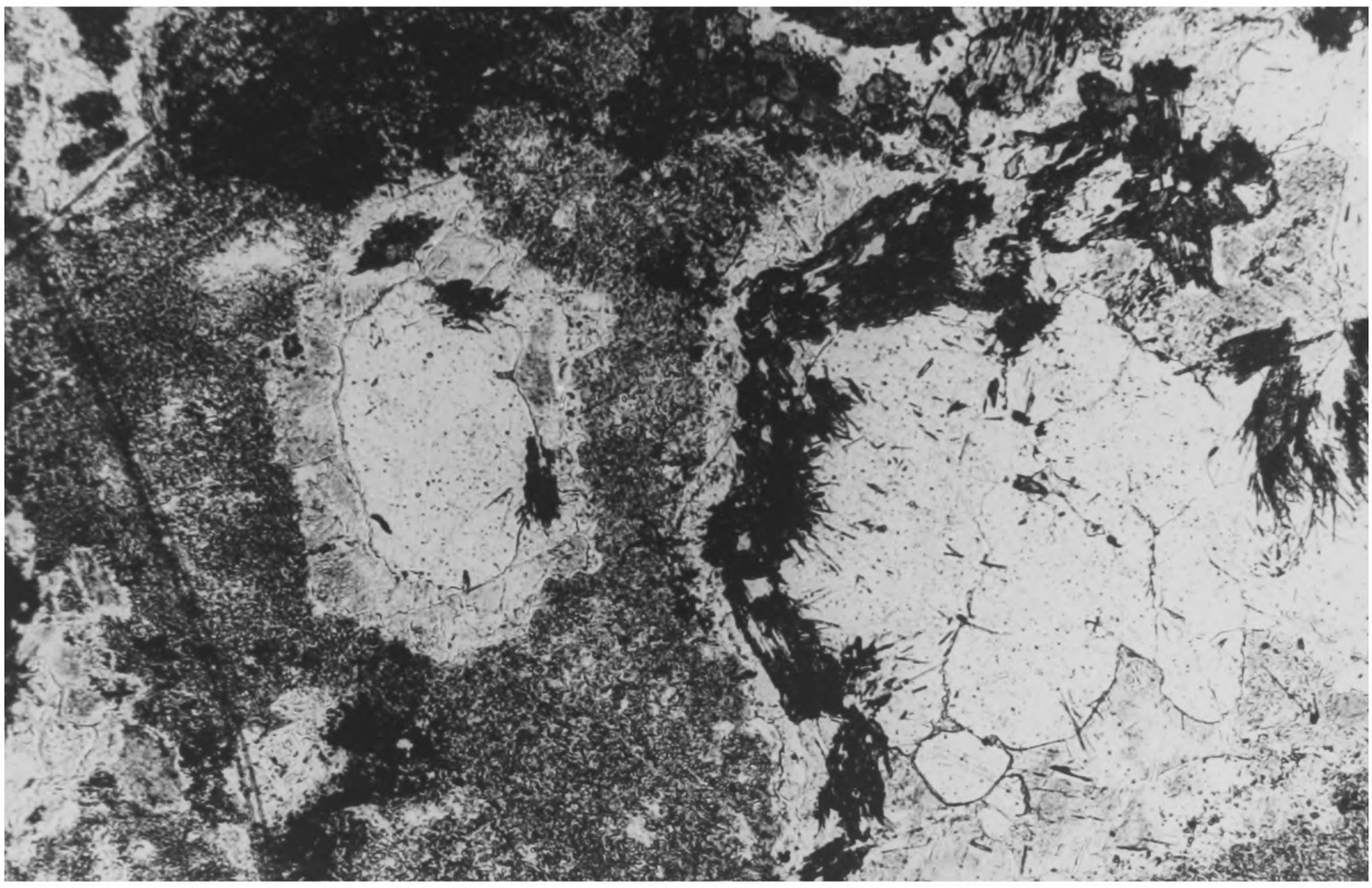


PLATE 5 - 11 Albite and arfvedsonite reaction rims to partially resorbed quartz, outer arfvedsonite fenite zone. The grey stippled texture is sericitized microcline. Affvedsonite needles grow into the quartz c. 40m S. of N. foyaite chill. Spec. 2705, x 5

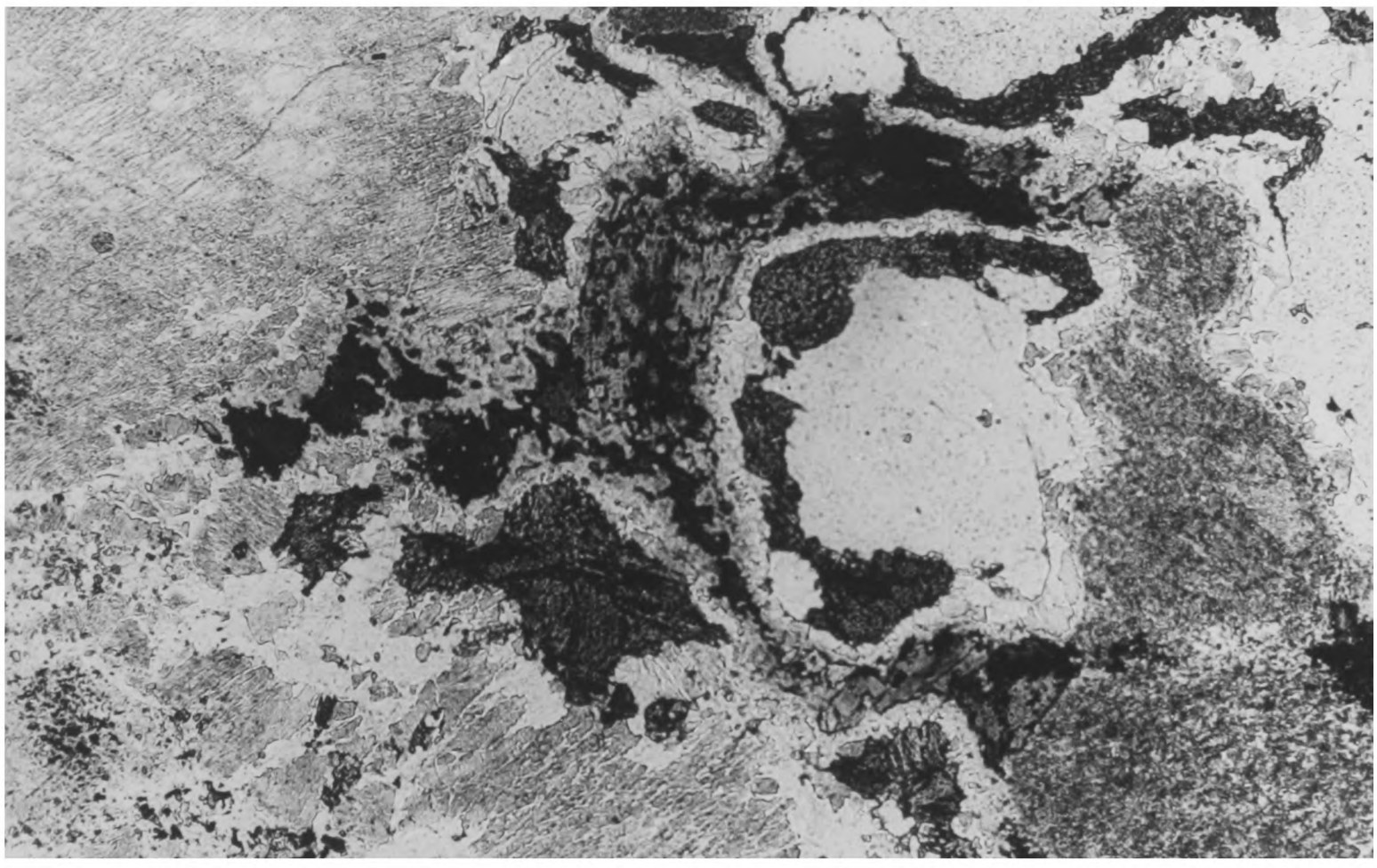


PLATE 5 - 12 Perthite replacement of plagioclase, inner arfvedsonite fenite zone. Biotite is stable here and rich in pleochrioc haloes. Much of the quartz is resorbed, and the arfvedsonite is consolidated. c. 30m S. of N. foyaite chill. Spec 2704, x 6.

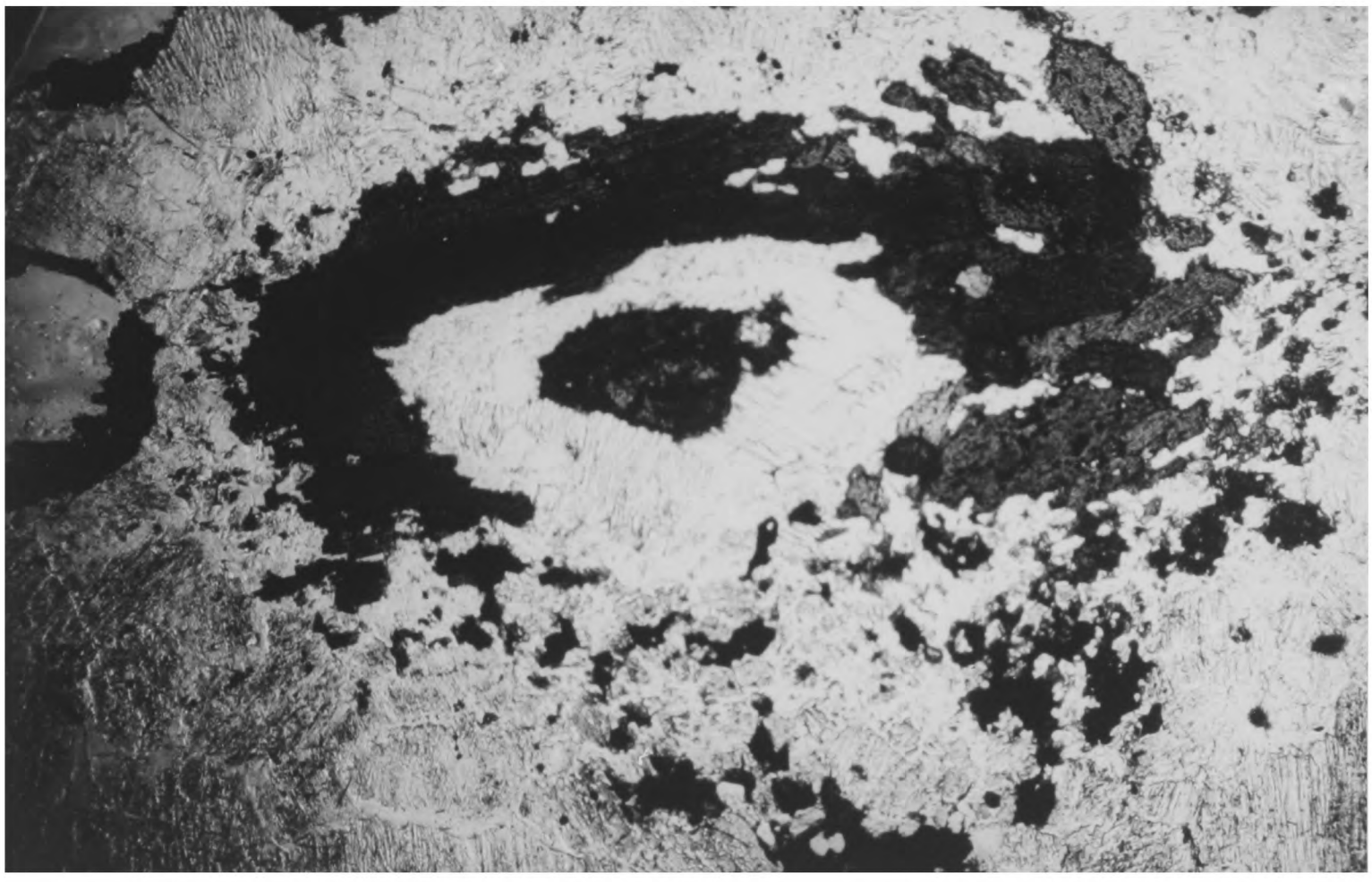


PLATE 5 - 13 Pseudomorph of a quartz patch in the aegirine syenite fenite. The original quartz is replaced by mesoperthite, with a central aegirine crystal. The outer rim is formed of intensely pleochroic biotite rich in zircon and magnetite. Granular albite, and magnetite, preserve the form of the original albite rim. 2m from syenite veins (plate 5 - 18) N. foyaite fenite. spec. 68037, x 20.

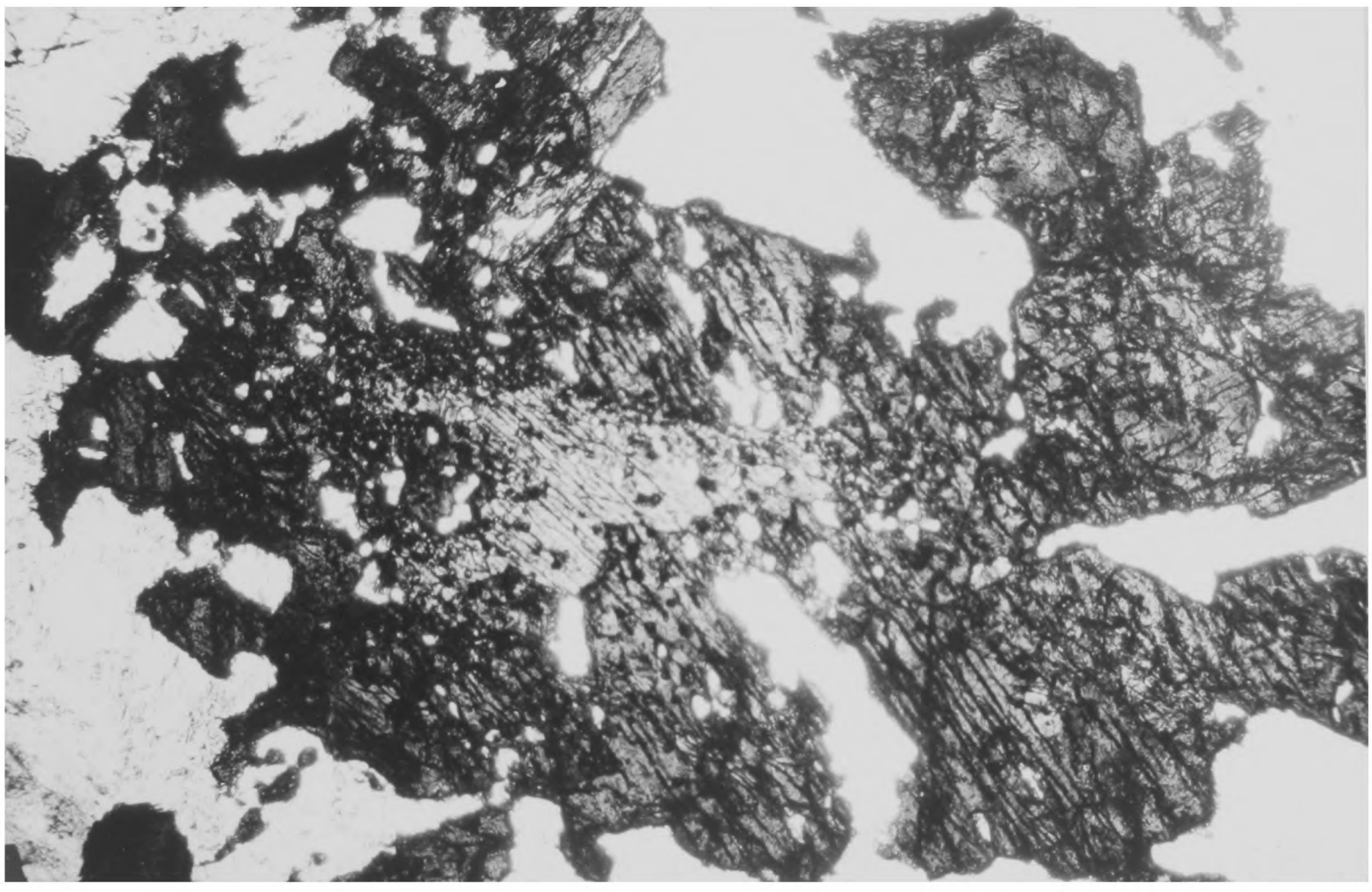


PLATE 5 - 14 Aegirine (dark) replacing arfvedsonite, aegirine syenite fenite. The matrix is mesoperthite. Spec. 68037, x 20.



PLATE 5-15 Mesoperthite replacing sericitized feldspar in the biotite-pyroxenite fenite; aegirine syenite zone. The calcite patch on the right is rimmed by microcline and albite. Crossed Nicols. Spec. 68216, x 6.

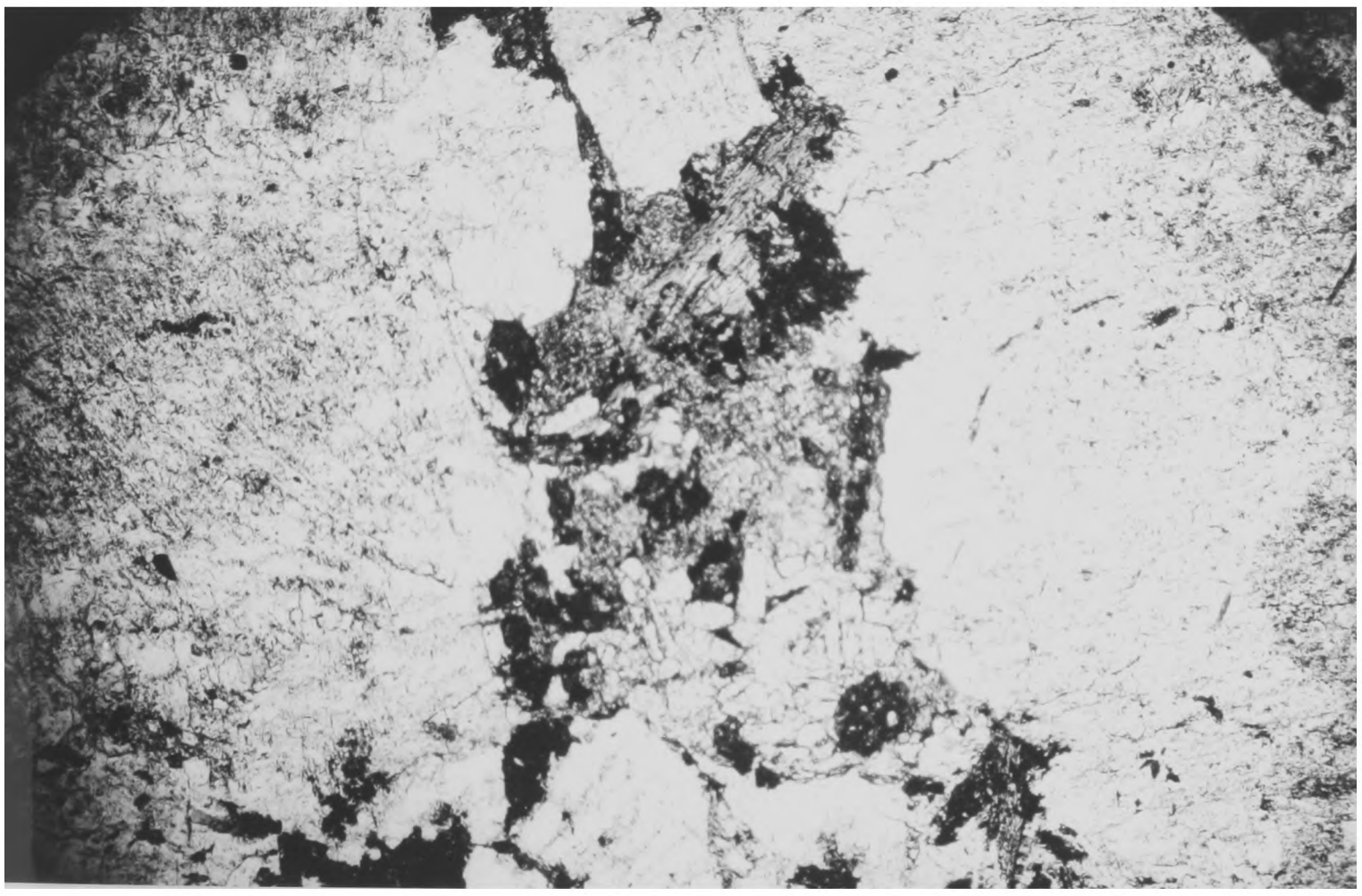


PLATE 5-16 Crystal settling of apatite in a layered calcite vesicle in the biotite-pyroxenite fenite; aegirine syenite zone. Stubby crystals of apatite (white) fill the base of the lens. Aegirine (black) and arfvedsonite (grey laths) are scattered around the margin. Spec. from borehole. x. 20.

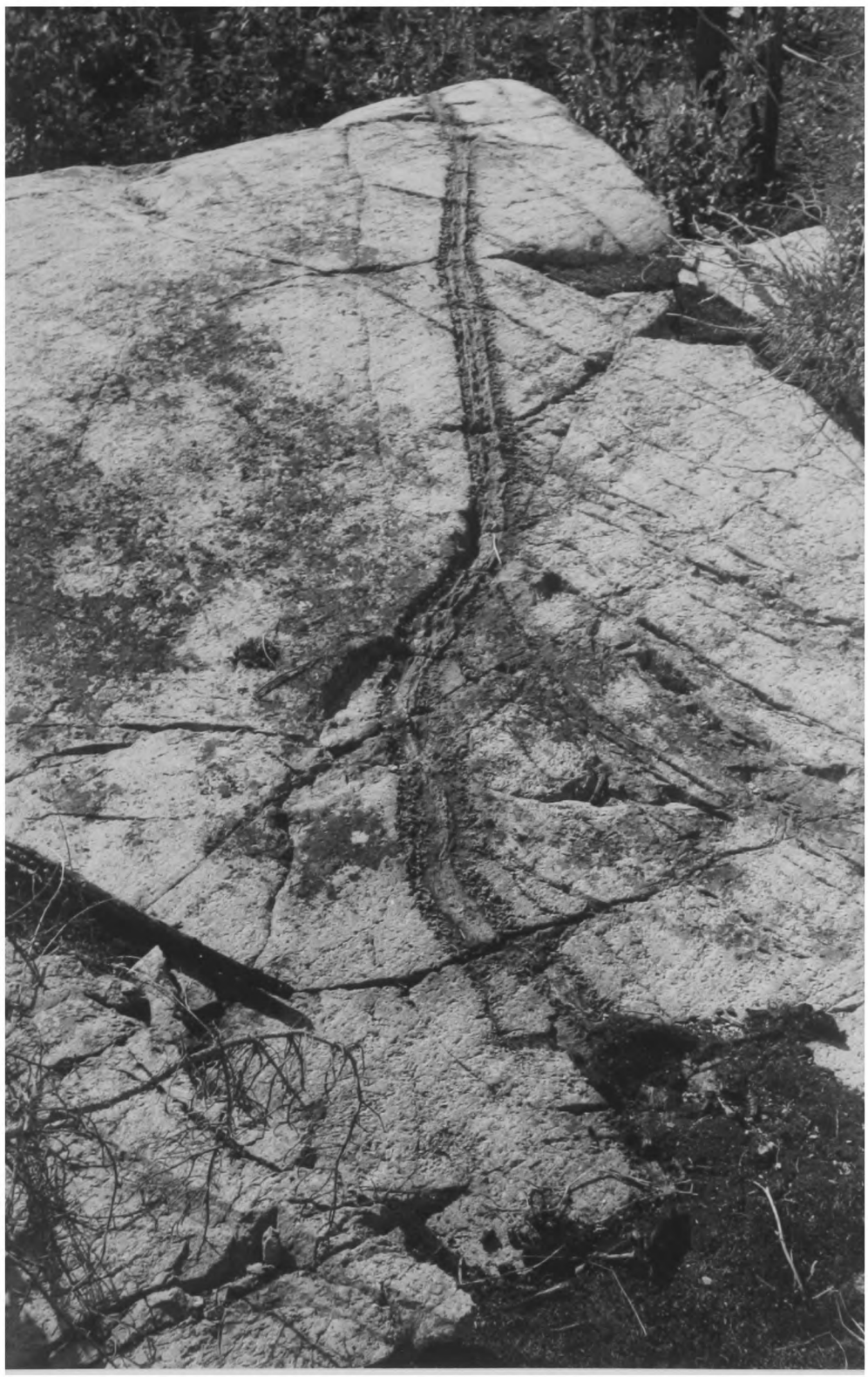


PLATE 5 - 17 Fenite bordered fracture in granodiorite. The central portion is occupied by a quartz-sericite vein; the margins are arfvedsonite-syenite fenite. S. side of Moose island.centre 4.

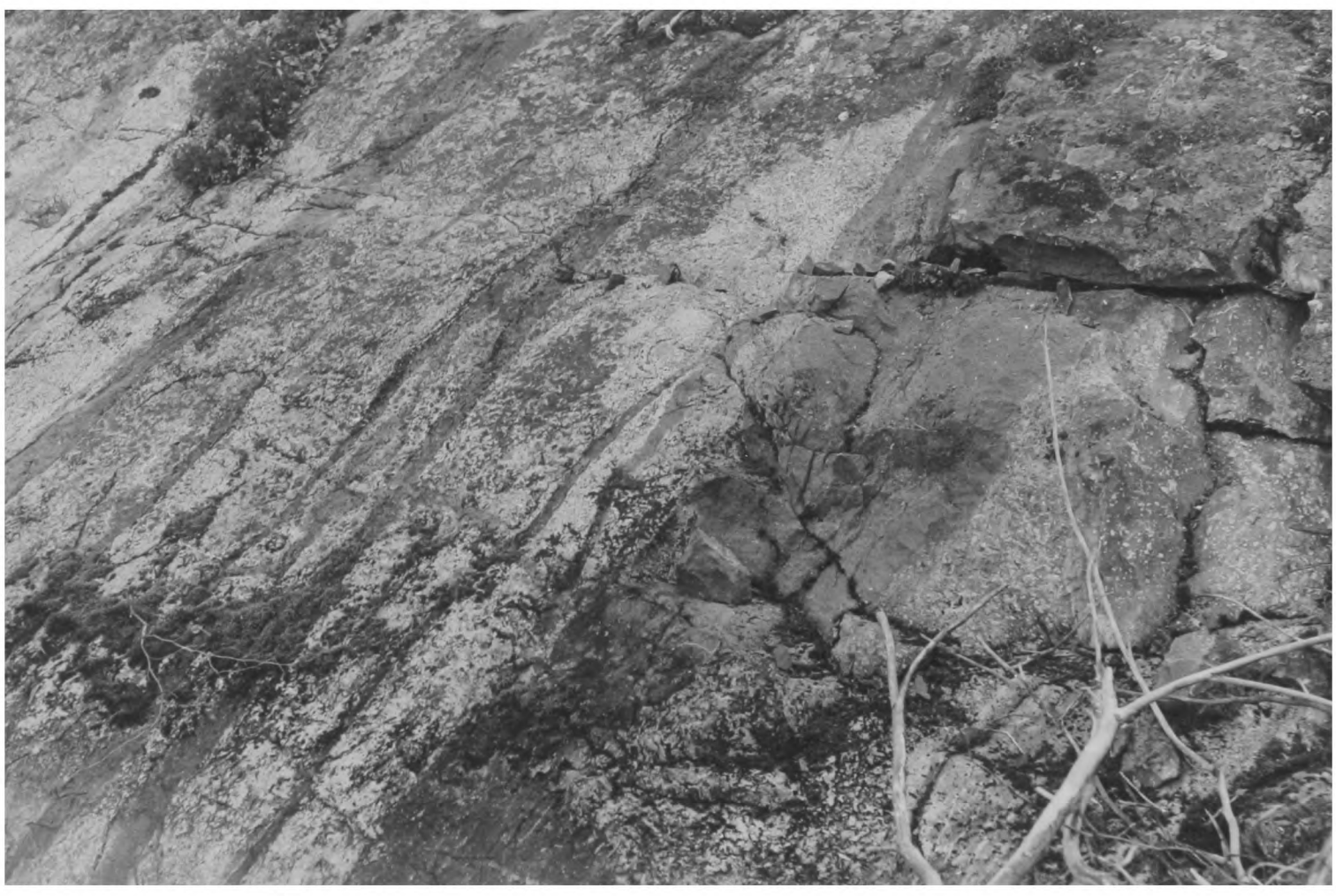


PLATE 5 - 18 Fenite bordered veinlets in the Northern foyaite fenite. The veins are of arfvedsonite-sphene-syenite. The borders grade from aegirine-syenite fenite to arfvedsonite syenite fenite and into biotite veined shattered granodiorite (shock zone fenite) Spec. locality 68037,68043

granite, the most intense, a zone of aegirine syenite. The inner two are closely associated with sinuous radial mafic arfvedsonite-sphene-perthite veinlets. The mineralogical changes observed are -

1. The introduction of red-russet biotite and blue-green hornblende (now chlorite) also some allanite, sphene and small idiomorphic magnetite, and ilmenite.
2. The clouding of plagioclase; the growth of perthite rims; the resorption of microcline; the corrosion of biotite, exsolution of rutite and oxide; the corrosion of quartz with the formation of needles of arfvedsonite and rimming perthite or albite; the introduction of zircon.
3. With increasing perthite replacement of plagioclase and quartz the growth of thick arfvedsonite-riebeckite rims to quartz mosaics, within the perthite rim.
4. The complete loss of quartz, complete replacement of plagioclase by perthite; deep green aegirine, rims, and replaces, lavender-grey to deep blue amphibole; biotite is again stable, and is deep red. The original form of the amphibole rims, and sericitized cores is preserved.

Biotite Pyroxenite Fenite: Each biotite-pyroxenite pipe is surrounded by 10-15m of quartz poor syenite fenite, sharply bounded against reddened microgranite. The contact between the two fenites is marked by vertical, radioactive, hematite coated joints. The biotite pyroxenite is transitional into the syenite fenite through a narrow zone of apatite rich, zeolite-microcline-aegirine shonkinite. These zones, and the mineralogical changes may be summarised as -

1. Microgranite fenite: "Thermal shock" zone of Alno. Quartz is recrystallized to a fine mosaic; crystals show undulose extinction. Muscovite disappears; biotite forms small flakes. Plagioclase and microcline are lightly sericitized.
2. Hematite-amphibole syenite fenite: "Zone of hydration" of Alno. Quartz is reduced to 1-5% of the rock. Both feldspars are extensively hydrated to sericite, and stained brick red by hematite; potash feldspar remains as perthitized phenocrysts; plagioclase, and quartz are replaced by granular albite, and microcline. Biotite, and quartz are replaced by aggregates of fibrous bluey-green pale soda amphibole, hematite and minor calcite, apatite, and magnetite. This zone is crosscut by vertical radio-active shears.
3. Amphibole-syenite fenite. Quartz is now very rare ($\sim$ 1%). Potash feldspar is replaced by perthite beginning to grow at the expense of albite and microcline; many crystals are continuously zoned from K-rich cores to Na rich rims (circa Or_{80}-Or_{50} opt estimate). The amphibole is consolidated to subhedral laths showing slight colour zoning with deeper margins; the anomalous interference colours are lurid ranging from royal purple, through prussian blue, to bright grey. Calcite occurs as white rhombs, and as 1mm - 6mm vesicles showing the settling of apatite with layers of (i) apatite + magnetite + hematite (base).

(ii) calcite.

FIG 5 - 3 **NORMATIVE COMPOSITIONS OF THE FOYAITE FENITES IN COMPARISON TO THE COMPOSITIONS OF THE GRANODIORITE AND CHILLED FOYAITE.**

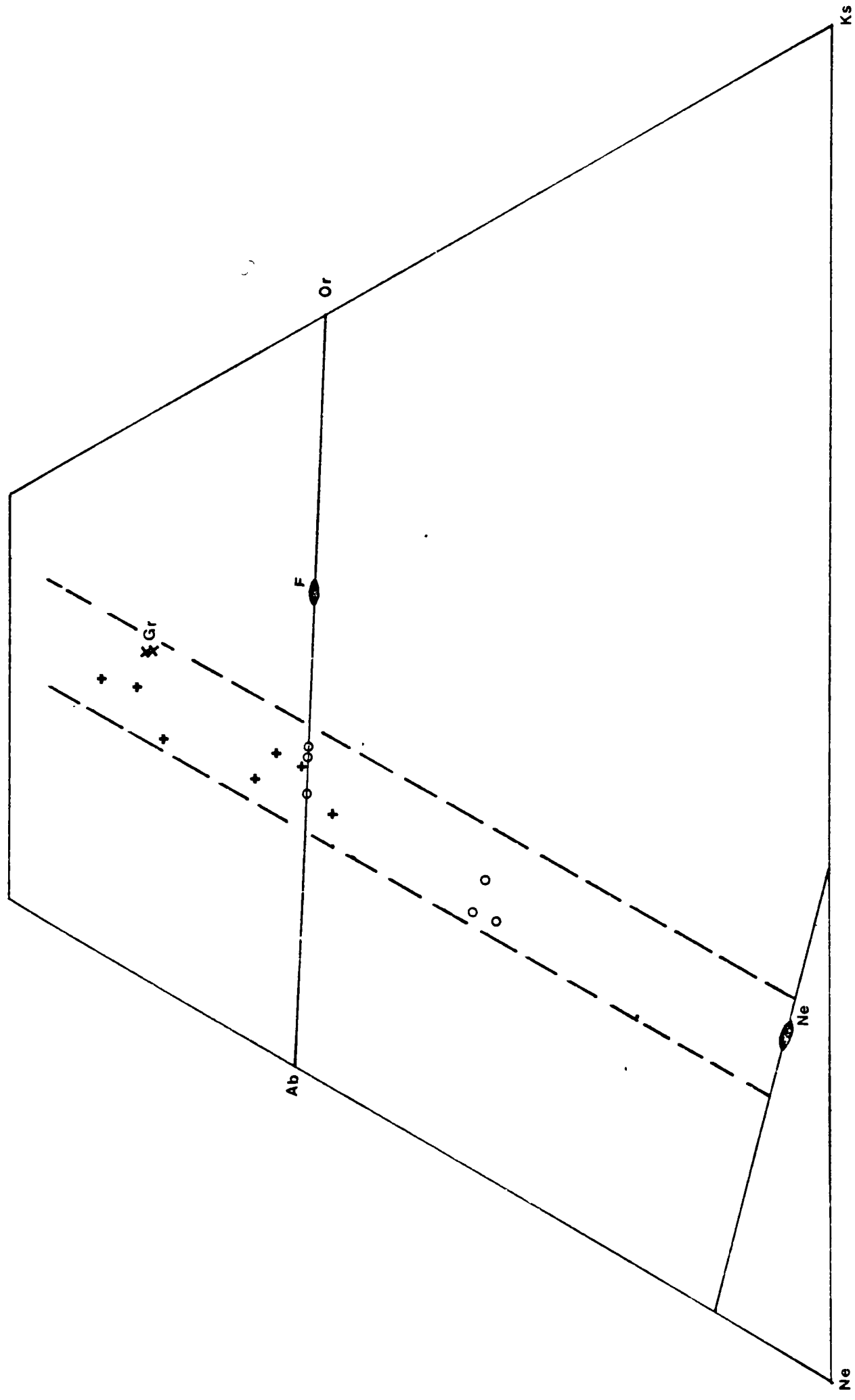


TABLE 5 - 4. ANALYSES OF THE GRANODIORITES AND FENITES.

	2741	2742	2836	2833	2713	2826	67219	68043	68037	2800	67194	67195	67196	67134
SiO_2	69.49	69.52	69.75	68.44	73.73	72.39	75.66	70.74	61.77	63.21	63.59	63.83	64.35	61.98
Al_2O_3	14.79	14.09	14.41	14.97	12.83	13.16	13.74	13.30	16.24	15.97	16.62	17.21	17.14	17.05
Fe_2O_3	0.83	-	-	0.86	0.57	0.76	-	0.09	2.35	-	1.29	0.90	1.17	2.15
FeO	2.00	3.15	3.75	2.62	0.95	1.00	0.96	2.41	2.80	3.50	1.80	1.32	1.77	2.50
MgO	1.56	1.59	1.46	1.27	1.01	0.65	0.49	0.85	1.22	1.61	0.99	1.06	0.66	0.40
CaO	1.66	0.68	1.36	2.14	1.49	1.62	0.40	2.54	3.39	1.66	3.20	2.23	0.81	2.53
Na_2O	3.12	4.60	3.10	3.12	3.45	3.59	c.4.5	4.74	6.56	4.68	6.20	5.18	5.57	5.63
K_2O	5.98	5.14	5.57	5.86	5.39	6.25	3.42	4.69	4.83	8.17	5.61	7.64	7.88	6.91
TiO_2	0.44	0.47	0.41	0.60	0.41	0.37	0.31	0.46	0.52	0.40	0.36	0.34	0.43	0.63
MnO	0.08	0.08	0.03	0.07	0.04	0.04	0.07	0.05	0.19	0.08	0.05	0.07	0.10	0.13
P_2O_5	-	-	-	-	0.06	0.07	-	0.04	0.05	-	0.02	0.10	0.07	0.07
	(GRANODIORITES)				(MICROGRANITES)			RIEB. FENITE	AEG. FENITE	(SYENITE FENITES)				REMOB-ILIZED FENITE.

TABLE 5 - 4. TRACE ELEMENTS.

	2741	2742	2836	2833	2713	2826	67219	68043	68037	2800	67194	67195	67196	67134.
Rb	-	129	138	177	-	174	-	-	162	-	113	-	-	160
Ba	-	-	385	1,410	-	372	156	1,560	1,730	-	367	-	-	1,910
Sr	-	148	135	211	-	160	-	-	906	-	255	-	-	955
La	-	-	-	-	-	-	-	-	-	-	-	-	-	-
Ce	-	-	-	-	-	-	-	-	-	-	-	-	-	-
Y	-	25	21	22	-	25	-	17	45	-	62	-	-	25
Zr	-	168	159	218	-	189	-	237	769	-	214	-	-	530
Nb	11	11	11	11	-	18	-	19	85	-	144	-	54	77
	GRANODIORITES					MICROGRANITES		RIEB. FENITE	AEG. FENITE		SYENITE FENITES			REMOB-ILIZED FENITE

Such vesicles contain abundant pale aegirine replacing amphibole. Thereafter aegirine replaces amphibole becoming progressively deeper in colour.

4. Aegirine syenite. "Aegirine-syenite zone" of Alno. Soda amphibole is replaced by aegirine. Perthite replaces albite and microcline, and the zoned perthites; both perthites retain sericitized cores. Oxides become rare.

5. Inner aegirine syenite zone: "Start of nephelinization" of Alno. The proportion of mafic dark green aegirine increases up to circa 25-30%. The sericitized cores of the perthites show vermicular intergrowths of pink fibrous unidentified zeolite and alkali feldspar.

This latter zone is probably transitional into the marginal shonkinite containing dark aegirine and abundant apatite and sphene in poikilitic plates of microcline perthite, and polyhedral hematite stained zeolite.

The biotite pyroxenite contains veinlets of aegirine syenite identical to the zeolite free aegirine-syenite-fenite. These veinlets pass into pyroxenite with the appearance of cores of augite, the appearance of biotite, and the decrease to zero of feldspar. Veinlets of calcite showing an identical apatite bearing aegirine-augite-shonkinite margin also occur.

Composition of the Fenites: Table 5-4 gives the analysed compositions of the granodiorites, northern foyaite fenite, and southern foyaite fenite. Relative to the unaltered granite the microgranite is enriched in silica, and depleted in alumina. The syenite fenites, and quartz-syenite fenites are depleted in SiO_2, and enriched in Al_2O_3, FeO, Na_2O, and Nb. Sr and Zr, and Y show an irregular often large increase related to the calcite zircon, and apatite content. P_2O_5, Rb and Ba are not significantly altered. The innermost syenite fenites (2800, 67195A and 67196) are greatly enriched in K_2O and depleted in Ba. This feature is also noted in the high potassic most intense fenites of Spitzkop, and many other carbonatite intrusions show orthoclase fenites (e.g. Chilwa, Oldonyo Dili).

Composition of the Fenitizing Agent: The chemical changes found in these fenites, as in those described from most other complexes, are dominated by the removal of silica, and the addition of feldspar. The reaction and replacement takes place at the feldspar-quartz crystal boundaries; The metasomatising phase must therefore percolate along rock fractures, and along the crystal boundaries, depositing feldspar and dissolving silica. Von Eckermann (1948) notes the addition of CO_2, F, H_2O and CaO within his outer fenite zone which is similar to the outer pyroxenite fenite zone. Possible relics of such a phase are preserved in the calcite-apatite-amphibole-magnetite-hematite vesicles which by their layering must represent a distinct low temperature carbonatite fluid.

Van Groos (1966) has shown that a CO_2-H_2O vapour may dissolve an appreciable proportion of sodium silicates, and that the solubility of albite in a water rich vapour phase is significantly increased by the presence of NaF. At pressures as low as 3.5Kb albite and sodium fluoride can form a liquid which is continuously soluble with a water rich vapour.

McKie (in Tuttle and Gittins 1965) has concluded that the provision of large volumes of metasomatizing solutions is the property of the volatile rich fraction of a magma, and is hence particularly associated with residual magmas such as peralkaline syenites, and carbonatites. These magmas are known to be enriched in H_2O, F, Cl, CO_2 as these volatiles are enriched in pantellerites, comendites, phonolites, and carbonatites.

An estimate of the composition of the silicate fraction of the fenitizing solution may be gained from the postulated derivation of biotite pyroxenite, from shonkinite. To form the biotite pyroxenite now found in the pipes 38% by weight (w.r.t. the shonkinite) of material with the composition of

SiO_2	65%
Al_2O_3	16 - 19%
K_2O	7%
Na_2O	6%
TiO_2	2%

must be extracted.

This material if added to the granodiorite, and the appropriate volume of SiO_2 removed (? to the siliceous microgranite) would yield circa 3 times the pipe volume of syenite fenite (loss of 21% norm Qtz). A recent drill hole through the central pipe and fenite, gives radii from the centre of 15m and 32m respectively, in fair agreement with the above estimate.

Although no estimate of the composition of the solutions leaving the foyaite can be obtained, the restriction of the fenite normative Qtz-Ne-Ks compositions, fig 5-2, to a narrow band linking the granodiorite, to the foyaite liquid composition, suggests that the Na : K ratio of the fenitizing solution was similar to that of the foyaite magma. The composition of the feldspar in the syenite fenite is circa Or_{31-37} (3 specimens).

Saether (1958) has deduced a temperature of circa 700°C for the intrusive syenite fenites of Fen, on the basis of the presence of homogenous soda-orthoclase. This is in agreement with experimental and predicted phase relations in the Ab-Or-H_2O synthetic and natural systems, and at variance with von Eckermann's estimate of 300°C for similar fenites at Alno. At Bigspruce lake the soda orthoclase also suggests temperatures of the order of 700°C throughout the perthite bearing fenite, falling towards the margin where albite and microcline are found and aegirine is replaced by riebeckite.

In the aegirine fenites Aeg. + Mgt. + Quartz are stable co-existing phases; in the amphibole fenites Rieb. + Hem. $\pm$ Mgt + Quartz are stable phases. For a PO_2 close to the magnetite-hematite buffer the stability of aegirine indicates a temperature in excess of 500°C at 1kb fluid pressure (Clarke 1966, p.356) at lower PO_2's and in the presence of a magnesium bearing amphibole the lower stability limit rises - to circa 625°C at 1kb fluid pressure on the Mgt.- Qtz.- Fa. buffer. The stability field of this amphibole barely overlaps the field of mesoperthite.

It is concluded that -

i) The fenites surrounding the northern foyaite and biotite pyroxenite are similar. The southern foyaite fenites lack a zone of riebeckite.

ii) The temperature within the aegirine-perthite fenite lies at least as high as 650°C probably in the range 650 - 750°C.

iii) The silicate fraction of the fenitizing solution approximates to that of feldspar with a Na : K ratio similar to the intruding magma.

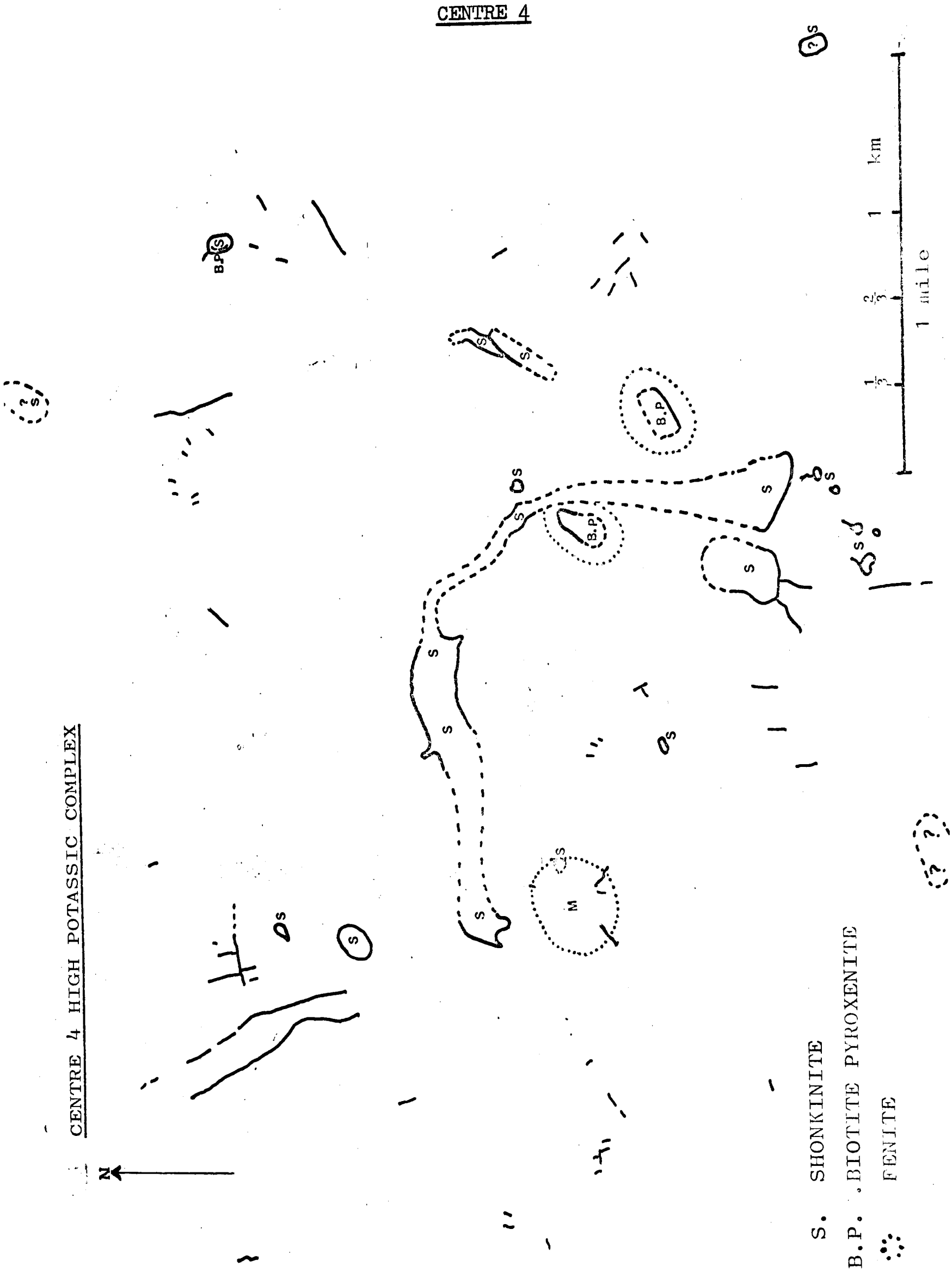
iv) The replacement reactions occur at the quartz-feldspar boundaries. These reactions involve the alkali exchange between fluid and crystal phases, the introduction of feldspar, and the removal of quartz.

v) The removed quartz now occurs in the silicified microgranite.

vi) The volatile fraction carrying the silicate phase was an acqueous fluid rich in CO_2, and F.

vii) The PO_2 of this fluid was buffered at close to the magnetite-hematite buffer at the amphibole syenite-aegirine syenite transition.

MAP 6 - 1 DISTRIBUTION OF THE ROCK TYPES IN THE HIGH POTASSIC CENTRE 4



The majority of the dykes mapped are either minette or shonkinite; a very few in the central area are of pseudo-leucite porphyry. The mapping of dykes is very incomplete and is the result of relatively few traverses.

THE HIGH POTASSIC ROCKS.

GENERAL. The high potassic rocks of Bigspruce lake form a relatively compact group distinct from the sodic rocks of centres 1, 2 and 3. All are dark dense mafic rocks with a high proportion of phenocrysts of augite, biotite and olivine in a matrix rich in biotite. The rock types are -

1. Shonkinites
2. Minettes
3. Biotite-pyroxenites
4. Pseudo-leucite porphyries
5. Biotite-peridotites
6. Augite-kersantites

All except the pseudo-leucite porphyry are found within the area of centres 1 - 2, particularly associated with the gas-escape vents of centre 5 and the Bigspruce island pegmatite centre. The greatest concentration of high potassic rocks however is found within the area of an 800γ aeromagnetic anomaly situated five miles south-east of the southern foyaite.

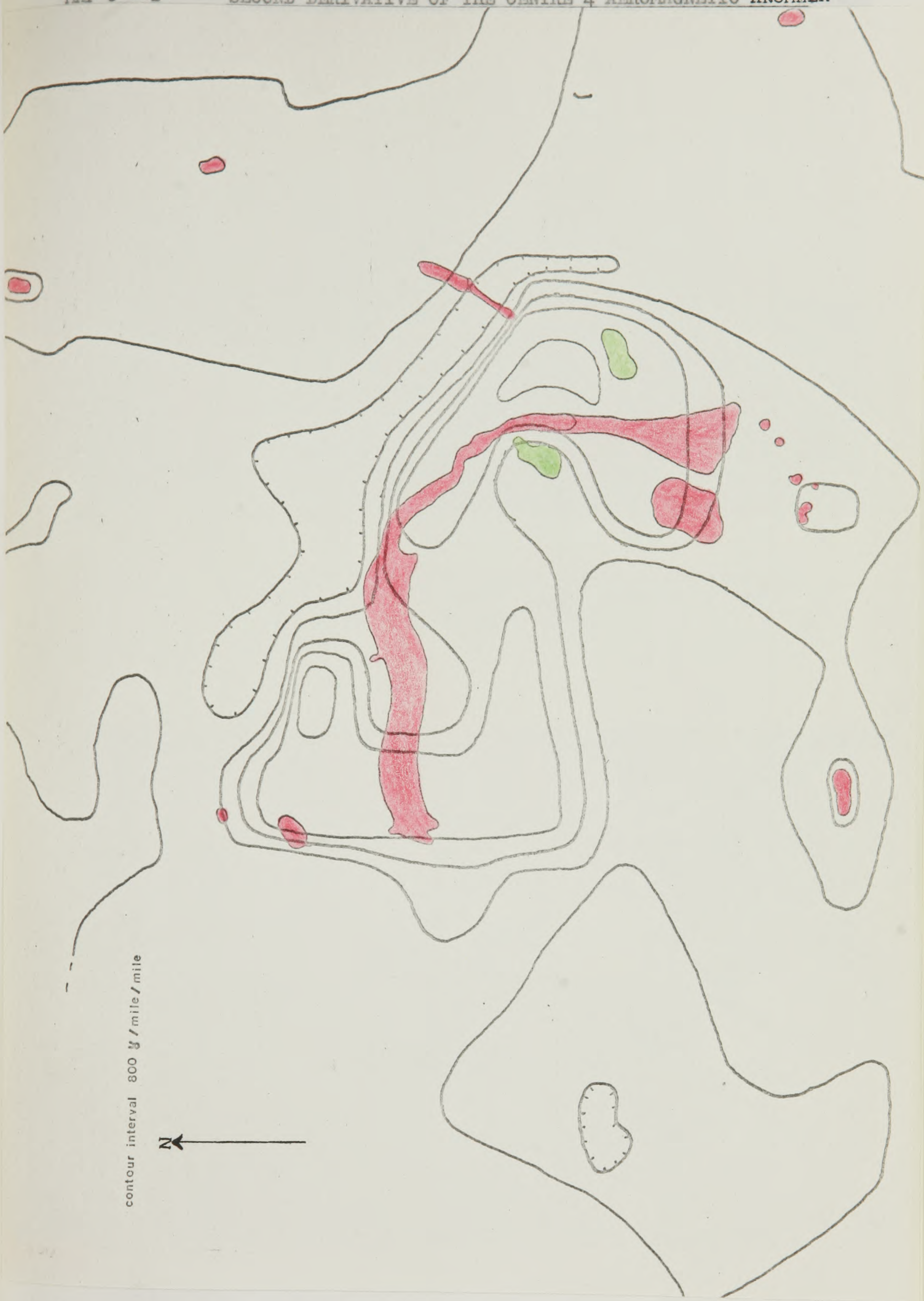
This anomaly was noted by Giant Yellowknife mines, and the rocks mapped by L. Burgess. His report indicated the occurrence of biotite-rich basaltic rocks as pipes and dykes and associated with reddened granitic rocks. The outer limit of dyke intrusion was estimated as corresponding to the 60,300γ contour.

Subsequent mapping has modified the outlines of a few of the bodies and located others but the map of this centre is essentially based on the reconnaissance survey.

MOOSE ISLAND CENTRE. The intrusive rocks of this centre comprise only a small proportion, less than 5% of the area of the magnetic anomaly. They consist of a central zone of shonkinite, and biotite-pyroxenite, and a broader marginal belt containing narrow dykes of minette and shonkinite. The patchy distribution mapped, of these dykes, reflects an incomplete survey, not their true distribution.

Magnetic Anomaly Pattern. Unfortunately, the intrusions are too small, and too closely spaced to be resolved individually on the aeromagnetic intensity map ($\frac{1}{2}$ mile flight-line interval), or its second derivative. The anomalies do however indicate the location of outlying vents, the extent of reddening and minette dyke intrusion, and a central, high intensity, area. Because of its relatively higher content of Fe-Ti oxides, this central area, corresponds approximately to the distribution of the shonkinite. The closely spaced curvature contours along the north and east margins (Map 6-2) indicate sharp, steep contacts extending to depth, consistent with the observed outcrop, and the extrapolated arcuate dyke linking the shonkinite bodies. Depth estimates derived from the measured spacing of the intensity and curvature contours, using the graphs and model forms of Vacquier et al (1952) suggest that the anomaly may be produced by the exposed surface rocks, rather than by a larger single mass at greater depth. Estimates based on the spacing along the north and east margin indicate depths beneath the

MAP 6 - 2 SECOND DERIVATIVE OF THE CENTRE 4 AEROMAGNETIC ANOMALY



The curvature has been calculated using the method of Vacquier et al (1952) using a $\frac{1}{4}$ mile grid spacing based on the $\frac{1}{2}$ mile spaced flight lines shown in plate 2-1. The anomaly is consistent with the mapped and inferred distribution of shonkinite both in form and intensity.

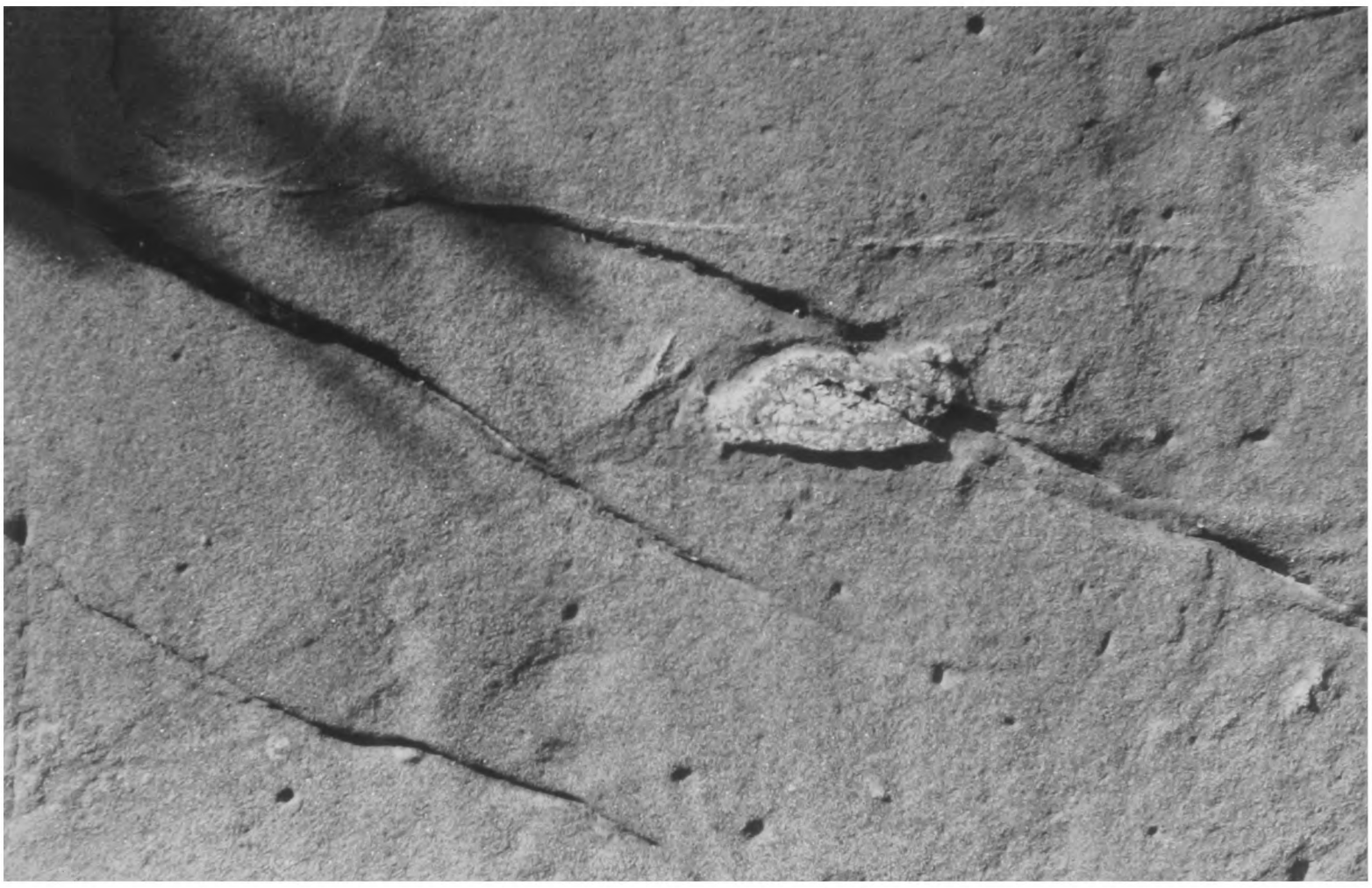


PLATE 6 - 1 Biotitic reaction rim around a granodiorite xenolith in the chilled shonkinite. W. termination of the arcuate dyke spec. Locality 68021, x ¼

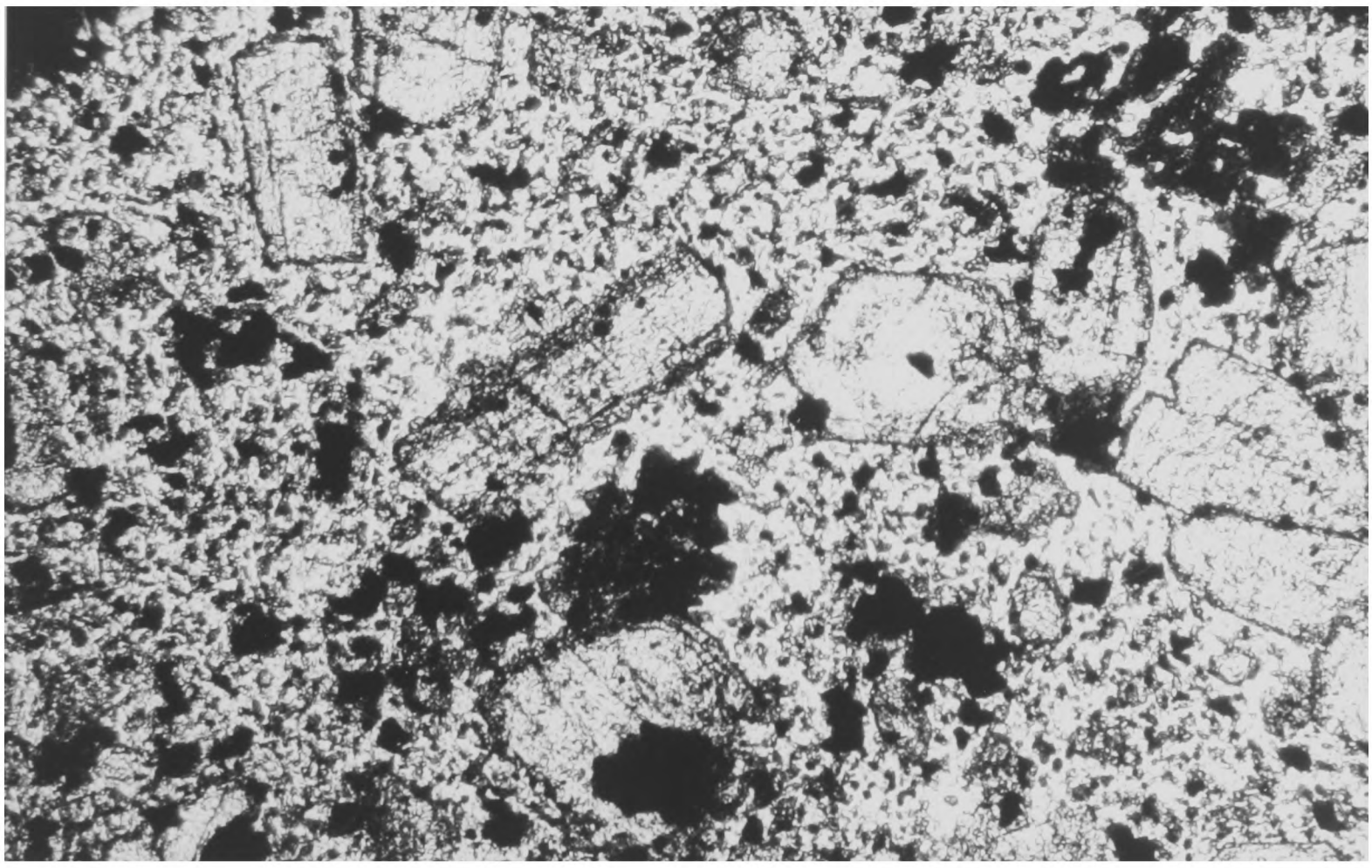


PLATE 6 - 2 Pyroxene and magnetite phenocrysts in chilled shonkinite. The euhedral oxide is rimmed by pyroxene; skeletal aggregates of biotite (lower centre) have begun to form; there is no olivine. The groundmass is cryptoperthite, pyroxene and biotite. Spec. 68021, x 32.



PLATE 6 - 3 Sub - angular xenoliths of chilled shonkinite in coarse shonkinite, near the margin a breccia pipe. The matrix is hybridized with the granodiorite xenoliths and contains quartz. S. side, Moose island complex. Spec. locality, 68093.

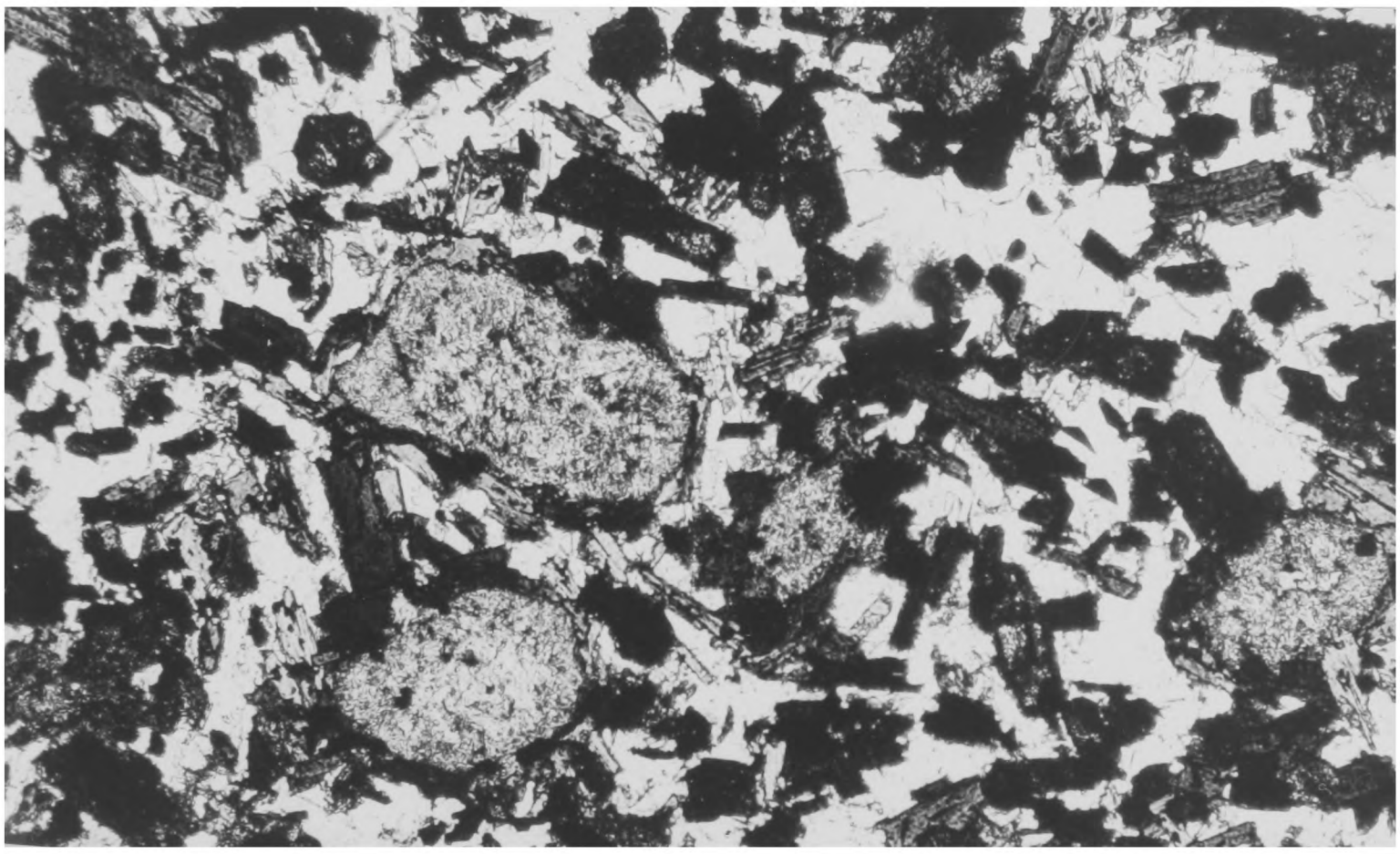


PLATE 6 - 4 Olivine phenocrysts with biotite reaction rims, in the matrix of the breccia pipe. Spec. 68399, x 6.



PLATE 6 - 5 Coarse shonkinite with pegmatitic biotite - pyroxenite schlieren. Lichen covered outcrop exposed by blasting. Arcuate dyke, spec. locality 68010

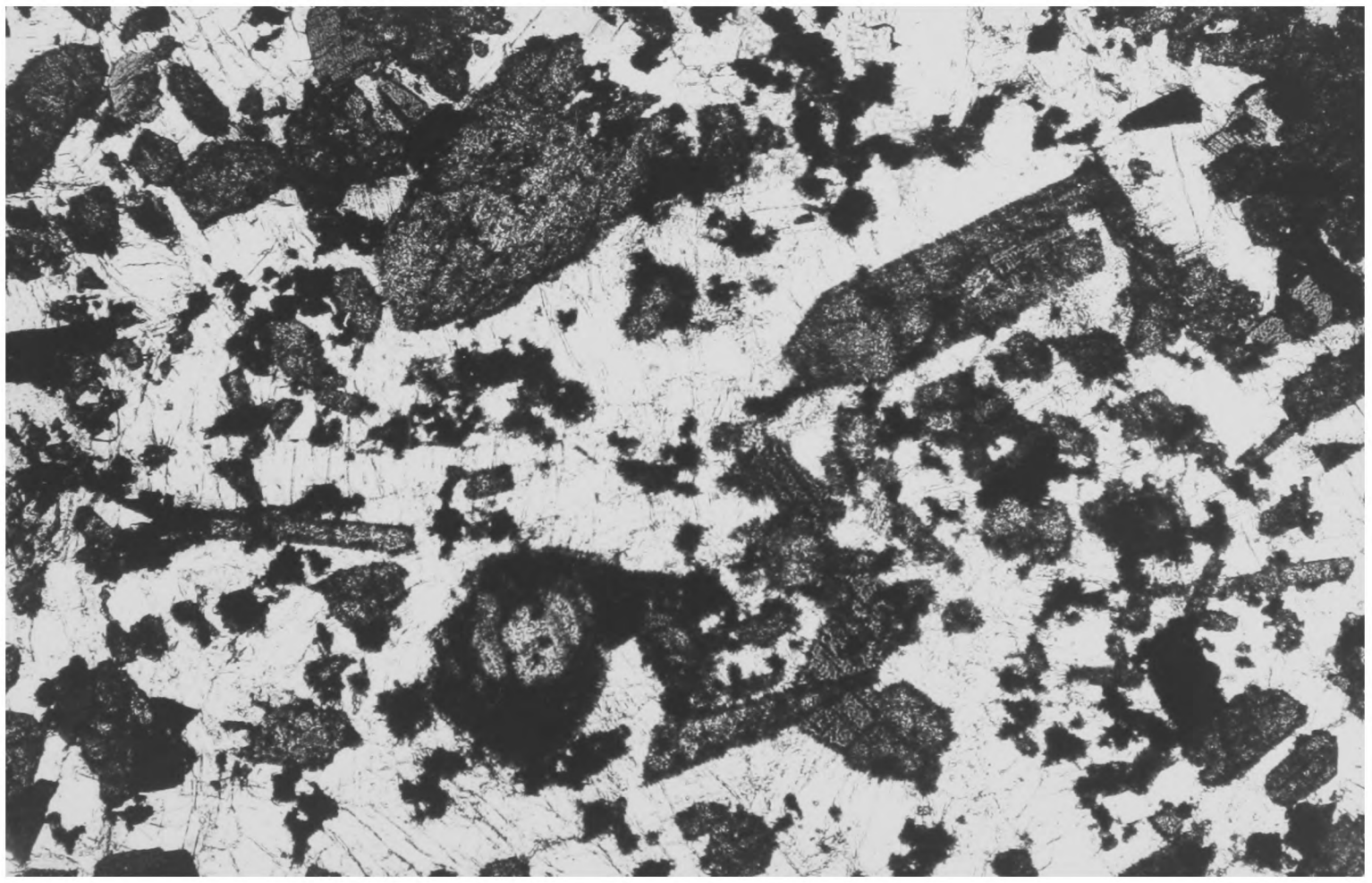


PLATE 6 - 6 Pyroxene and olivine (low centre) in coarse shonkinite. Near S. termination of the arcuate dyke. Spec. 68394 x 4

flight path of 900 - 1,400 ft (1000 ft average flight height).

Shonkinite: Shonkinite is the dominant rock rype of centre 4. It is composed of phenocrysts of augite, with or without olivine and biotite, in a matrix of felted microliths of cryptoperthite, biotite, magnetite, with minor apatite and alkali amphibole. Feldspar constitutes 30 -45% of the rock.

It occurs as narrow 0.3 - 2m dykes associated with minette, as 10m - 100 m dykes in the central zone (most which may be linked to form a single 3km, 90° arcuate dyke), and as 10-12 small 10-100m pipes peripheral to the central high of the anomaly.

The type shonkinite is that found in the broad dykes. These show chilled dark grey "basaltic" margins against the granodiorite, with little contact alteration. The pyroxenes are commonly lineated horizontally, parallel to the margins, and in coarser rocks there may be a vertical foliation resulting from poikilitic biotite.

Towards the centre, the pyroxene grain-size increases from 1mm to 2-4mm, the rock becomes more leucocratic with glistening, translucent laths of enclosing feldspar; there is an increase in the proportion of biotite, a decrease of oxide and the appearance, first of nuclei, then of phenocrysts of olivine.

Within the coarse-grained facies there are irregular thin pegmatitic schlieren of biotite-pyroxenite.

The two largest pipes are essentially similar but lack chilled margins; instead, showing a 0-6m hybrid zone consisting of angular blocks of biotitic shonkinite in a matrix of hybrid biotite-amphibole diorite. A similar hybrid is, locally, found around the arcuate dyke.

Locally the shonkinite becomes pegmatitic with 2-3 cm biotite and feldspar plates in equal proportions riddled with enclosed lineated 2-4mm elongate augites.

The smaller vents show a tendency to be brecciated, but this feature is visible only on favourable, e.g. exfoliated, surfaces, since the breccia is composed of well-rounded 10-20cm fragments of shonkinite in a shonkinite matrix. Such rocks are enriched in altered olivine (10-12%), show exsolved pink feldspar, amphibolized pyroxene, and included quartz, and are generally rich in sulphides, dominantly pyrite.

The shonkinite pipes typically lie at the terminations of narrow shonkinite or minette dykes. This relationship is similar to that described from the petrographically similar Navajo-Hopi vents (Williams 1936) but differs from the crosscutting relationship of the dykes to the vents, of the Scottish kentallenites (Bowes and Wright 1962, 1967).

The largest and best exposed pipe (Map 6-3) is surrounded by a radiating fracture pattern of joints and quartz-sericite veins (L.Burgess pers comm.) in the granodiorite, indicating fracture and perhaps doming preceding pipe intrusion

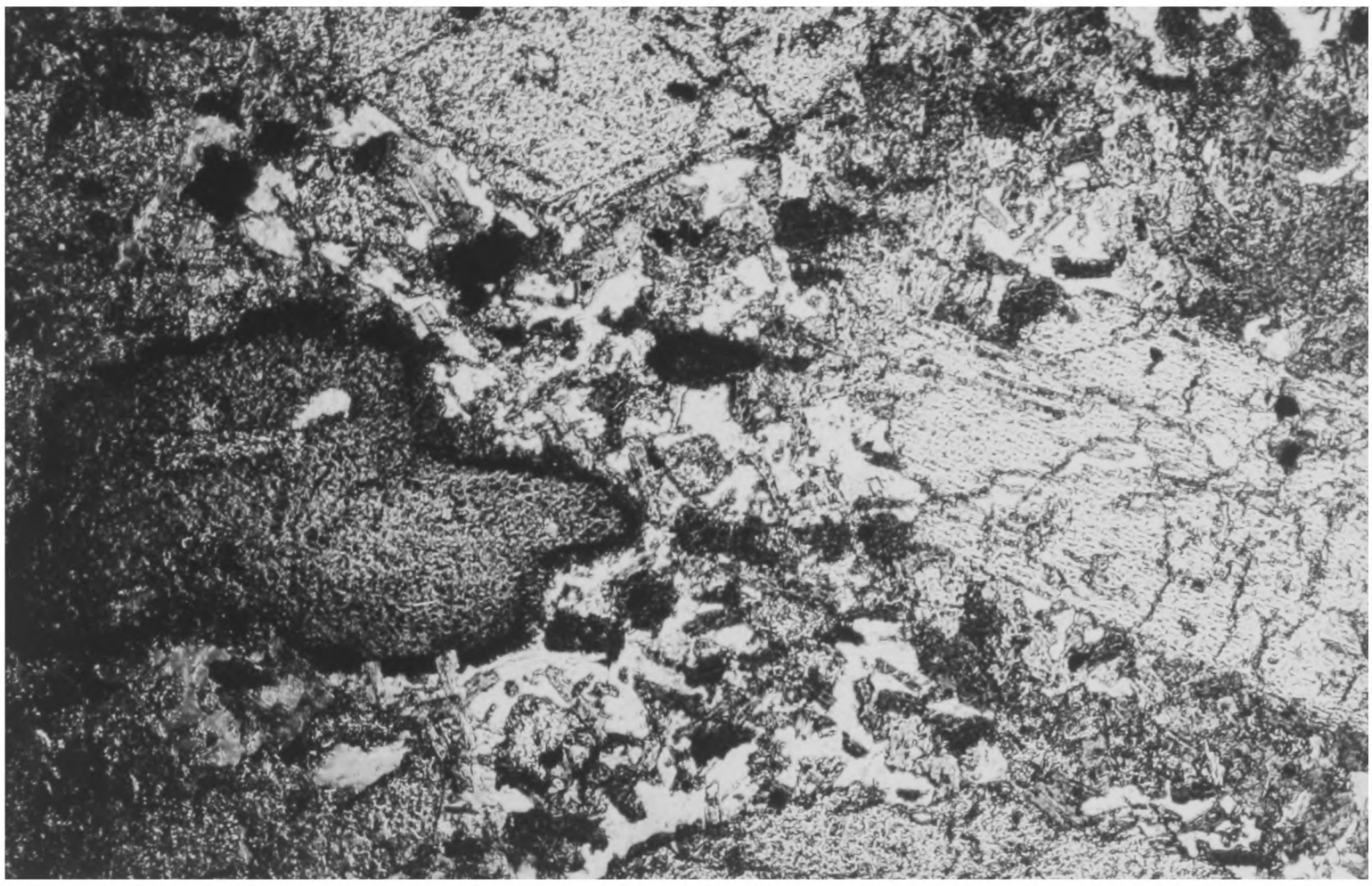


PLATE 6 - 7 Pyroxene and biotite phenocrysts in minette. The matrix contains pale green pyroxene, biotite and cryptoperthite. There is a complete absence of olivine or magnetite. Spec. 68401 x 25.



PLATE 6 - 8 Zoned biotite phenocryst in the minette. Spec. 68401 x 25.

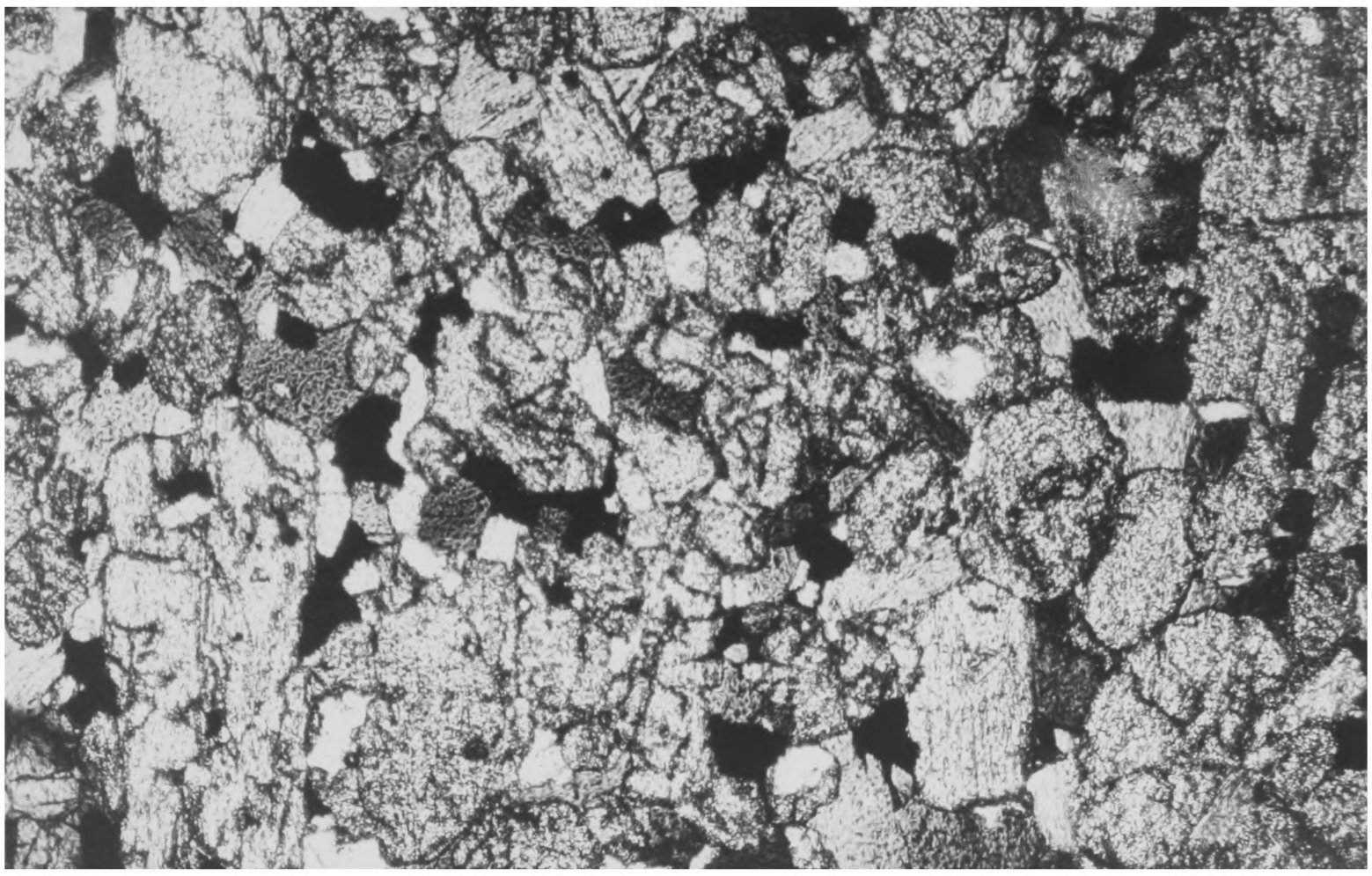


PLATE 6 - 9 The mineral texture of the biotite - pyroxenite subhedral pyroxenes are separated by late biotite, apatite and titanomagnetite. From the S. biotite pyroxenite pipe spec. 68395 c, x 25.

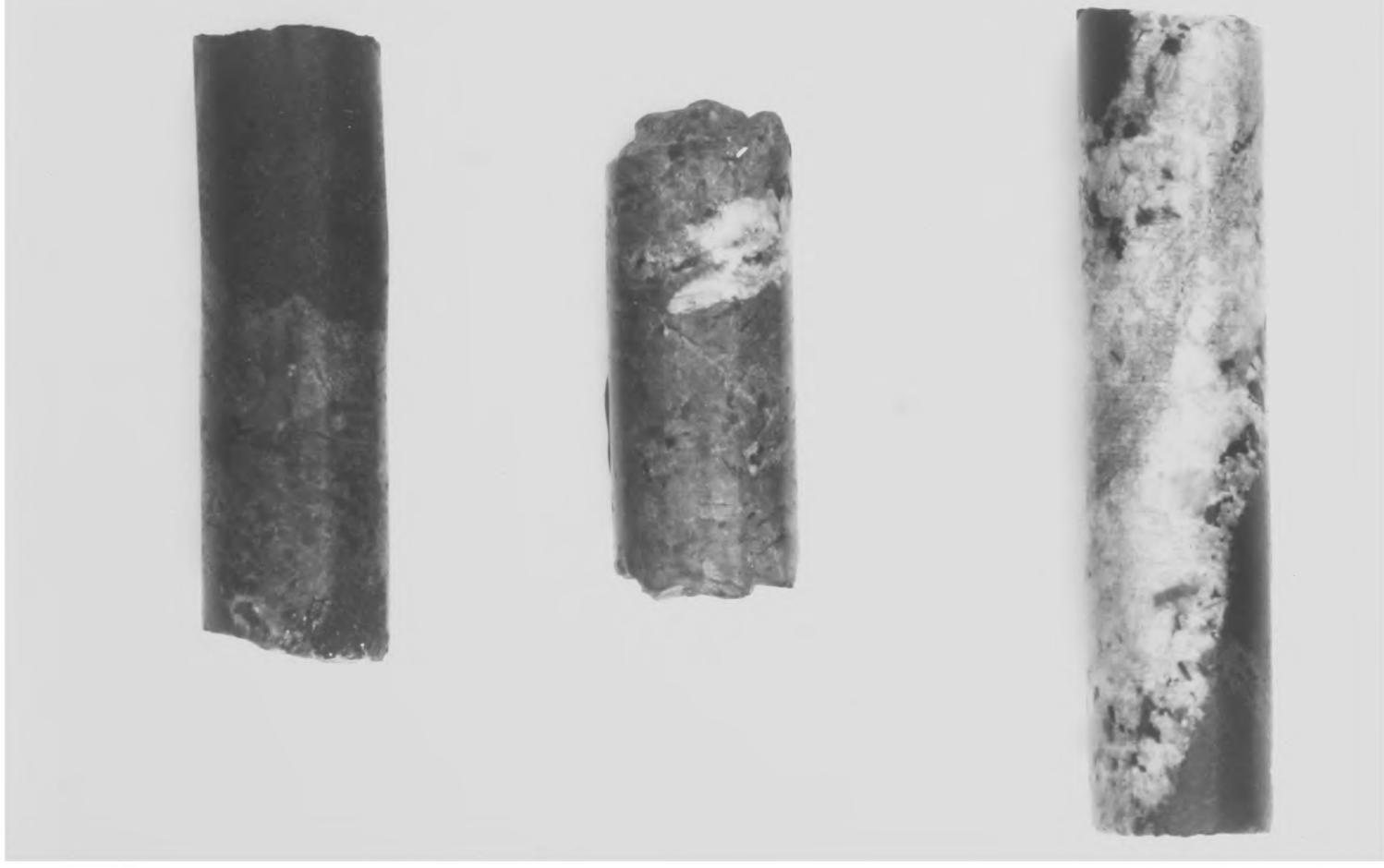


PLATE 6 - 10 Drill core sections from the biotite - pyroxenite. A syenite vein in pyroxenite B. Calcite rhombs in the aegirine - syenite fenite. C. Aegirine - sovite vein in pyroxenite. The sovite and the aegirine - syenite vein, are transitional into pyroxenite through a zone of shonkinite. Central biotite pyroxenite pipe. x 1

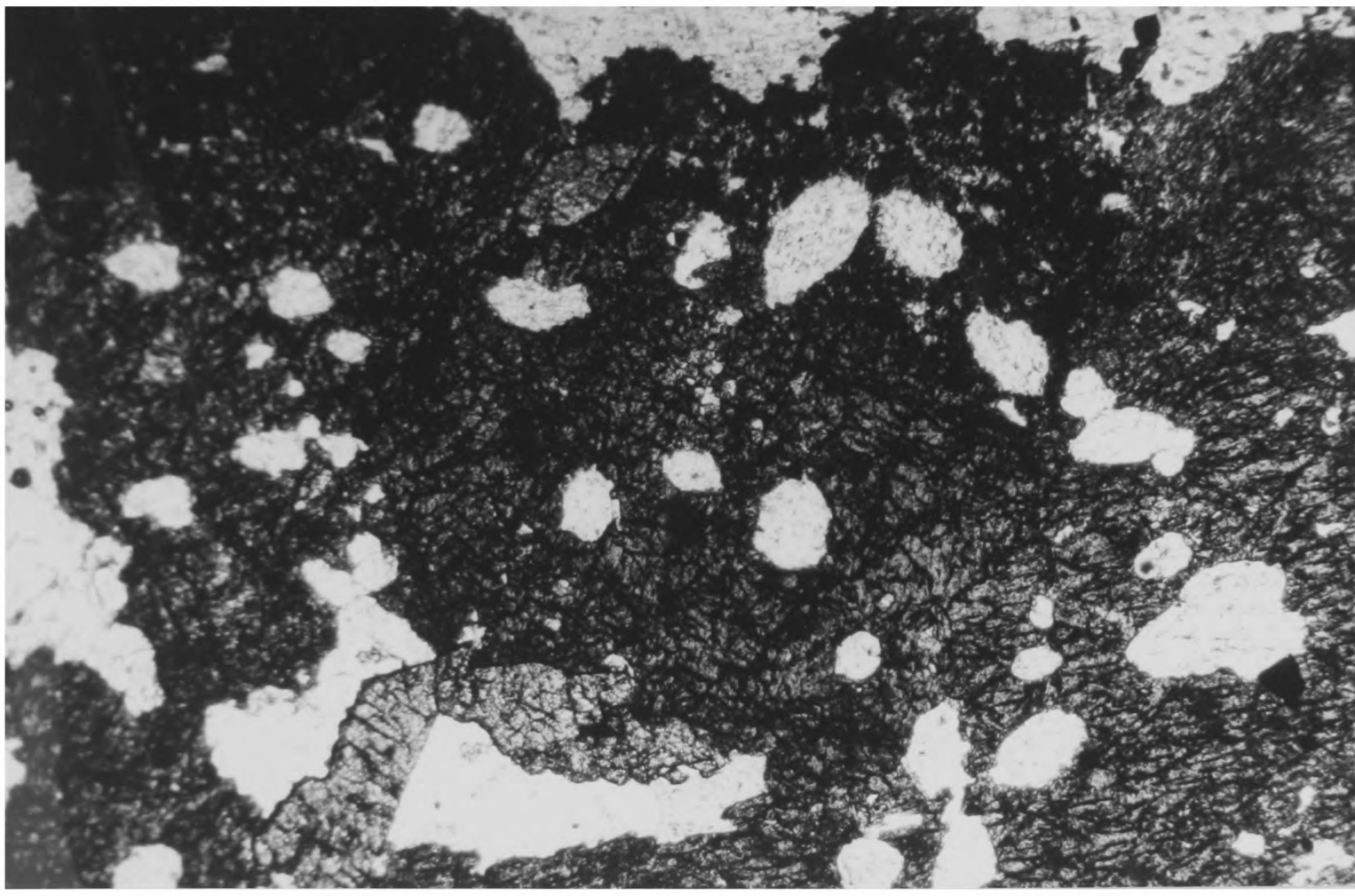


PLATE 6 - 11 Calcite rhombs in aegirine from the aegirine sovite vein. The aegirine also encloses sections of sphene. The matrix is calcite. From drill core, x 20.

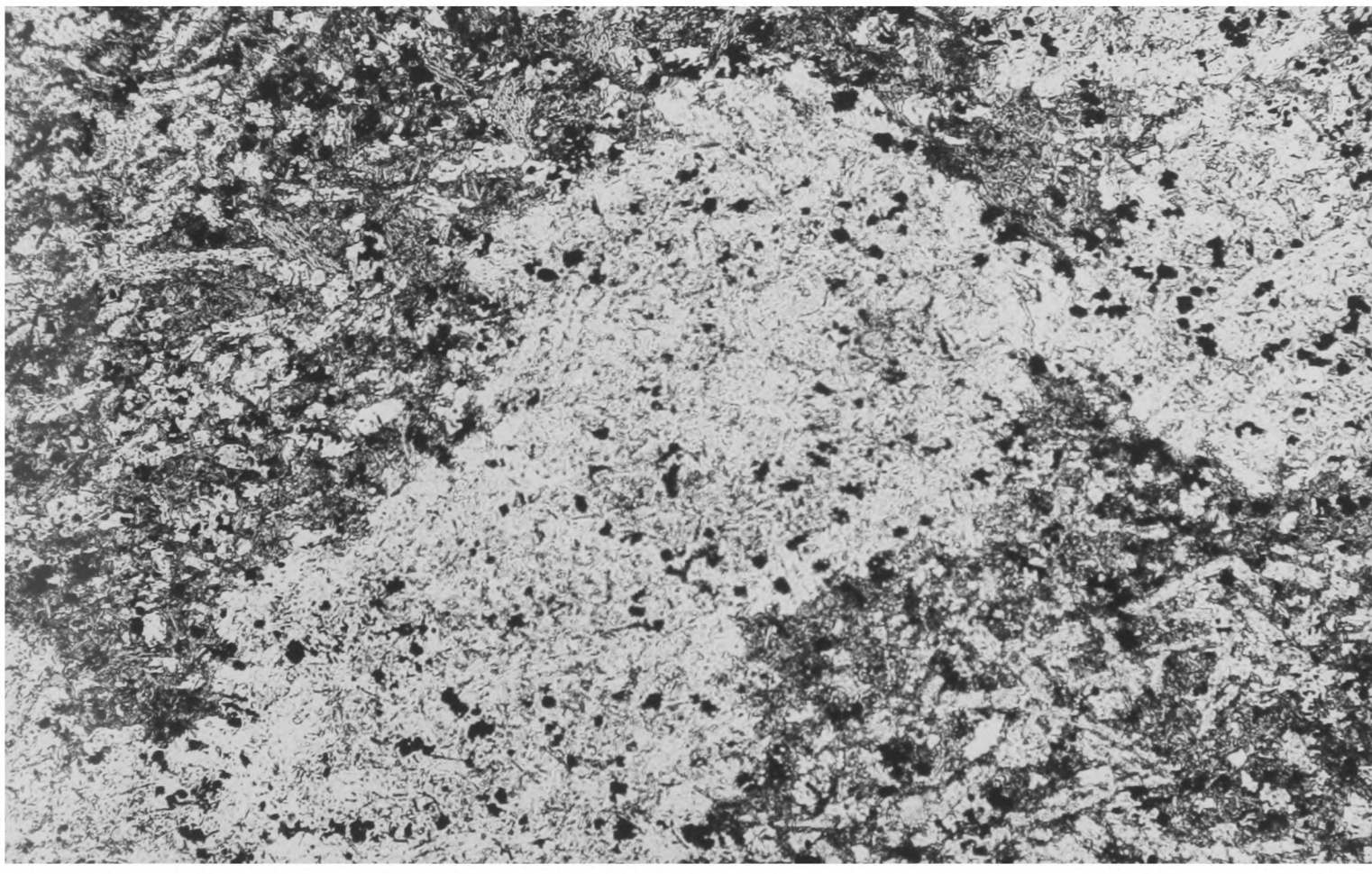
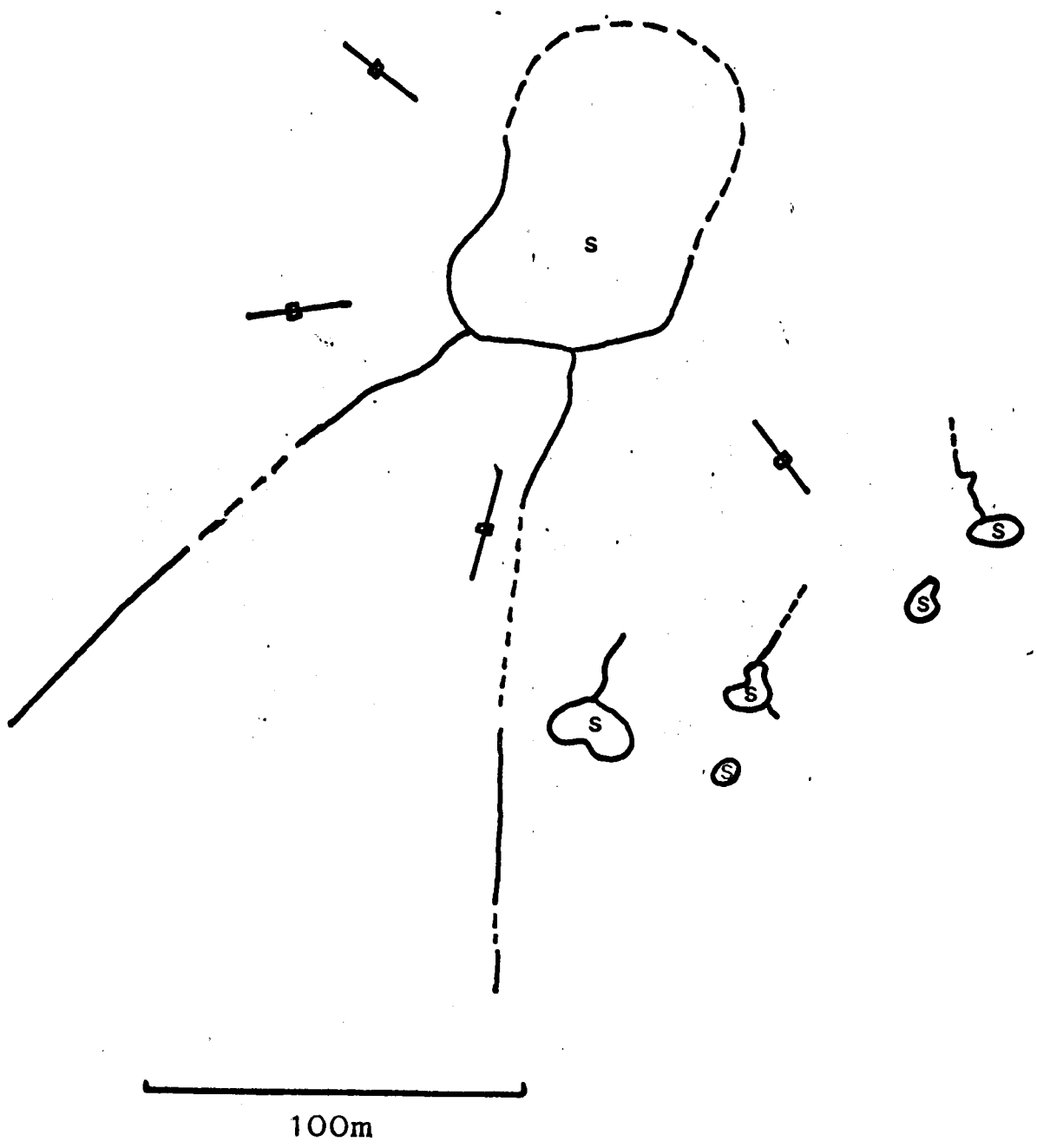


PLATE 6 - 12 Pseudoleucite phenocrysts in a porphyry dyke. The pseudomorphs are composed of microcline and albite with minor tremolite and magnetite. The groundmass is composed of albite and biotite with minor tremolite, magnetite and quartz. Shore S.E. of Moose island. spec. 68388 x 4.

MAP 6 - 3 RADIAL JOINT SYSTEM, AND KIMBERLITE DYKES AROUND THE SHONKINITE PIPES



In the shonkinite series, particularly in the pipes and narrow dykes, there is a reciprocal variation between the proportion of olivine and biotite phenocrysts; and between the abundance of magnetite and biotite in the matrix. With the loss of olivine and decrease in magnetite and cryptoperthite, the shonkinite passes into minette. The main difference between shonkinite and minette is therefore one of volatile content and may be considered in terms of the reactions

olivine + liquid = biotite + orthoclase + pyroxene (Luth 1966)

magnetite + sanidine + water = annite + (O)

Minette: Dykes of minette are common throughout the area, but are dominant in the peripheral regions. The minette is composed of phenocrysts of both hexagonal biotite (0.5 - 1cm), and elongate augite (2-4mm), in a glistening, black, biotitic, matrix, containing 10-35% cryptoperthite, albite, or zeolite, and minor oxide, apatite, calcite and sphene. Often the rock shows a lamination due to vertical platy biotite and horizontally lineated pyroxene. Where the rock has been sheared abundant cubes of pyrite and abundant calcite or dolomite have developed.

In peripheral regions, the dykes appear to occupy a system of radial and tangential fractures around the central zone (e.g. north-west segment), but little mapping has been done in these areas. The relationship of minette dykes to the pipes of shonkinite has already been described. In addition to these, there are areas, for instance at M (Map 6-1), in which squiggly thin minette dykes such as are associated with the pipes, are intruded radially into elliptical areas of reddened, recrystallized granodiorite. These dykes, wedge out into sinuous veinlets of quartz and sericite, bordered by fenitized granodiorite (plate5-17).

This suggests a sequence of pipe formation of

1. doming and radiating fracture of granodiorite
2. escape of volatiles, reddening and heating of granodiorite, formation of quartz-sericite veinlets by escaping solutions, intrusion of volatile-rich minette
3. explosive escape of volatiles, intrusion of shonkinite in a gas-streaming column, rounding of shonkinite fragments,
4. at greater depth or following 3 the intrusion of shonkinite magma crystallizing under relatively low volatile pressure, formation of hybrid with hot granodiorite.

This sequence is essentially similar to that postulated for the kentallenite vents (Bowes and Wright 1967).

Biotite Pyroxenite. The biotite pyroxenites are dark dense rocks intruded as elliptical pipes into fenitized granodiorite. They consist of 50-60% closely packed subhedral to euhedral pyroxene laths, in a matrix of slightly poikilitic biotite (30-35%) and apatite (4-8%). There are rare biotite phenocrysts. Minor interstitial magnetite, alkali hornblende, sphene, quartz, cryptoperthite and calcite occur in most slides. In coarse varieties there appears to be a reaction relationship with biotite corroding augite, and pyroxene developing acmitic rims. Commonly the pyroxene is lineated horizontally parallel to the pipe contacts.

In some specimens, apatite, which normally occurs as small stubby crystals between the pyroxenes, is aggregated around the margins of hollow, or calcite, or zeolite filled, vugs, 5-10mm across. In these cases the apatite is blood red, and the pyroxene a deep green aegirine.

Towards the margin the biotite pyroxenite is crosscut by narrow lenticles or veins of syenite composed of mesoperthite laths with slight ropy textured exsolution, and minor colourless acmitic aegirine. Apatite and titaniferous magnetite occur in patches (~ 1%) in this syenite and calcite fills angular cavities between the feldspar grains. Calcite also occurs as 5-10cm veinlets in the margins of the pipes. These narrow white carbonatites are rimmed with colourless apatite segregations and separated from the biotite pyroxenite by a narrow band of aegirine shonkinite. The zonation of the "pegmatites", the presence of aegirine in the carbonatite, the lack of reaction between the calcite and feldspar and the calcite in the host rock suggest that both syenite and carbonatite are primary segregations of the biotite pyroxenite.

The field relationships of the two biotite pyroxenites are illustrated in Map 6-1. The pipes measure circa 50m x 30m and are surrounded by 10-15m of syenite fenite, against which they are chilled. This fenite is similar to the syenite segregations within the pipes but the mesoperthites contain sericitized cores of relict plagioclase and there is a gradation outwards from acmite to arfvedsonite then riebeckite as the dominant mafic mineral. Many of the calcite patches are rimmed with amphibole, albite, microcline or quartz. Some show a consistent vertical zonation apparently due to primary crystal settling of apatite

1. Arfvedsonite + calcite
2. Calcite + acmite
3. Apatite + magnetite + acmite.

Up to 5% interstitial quartz and minor relict biotite occur in these fenites.

The contact with the microgranite is sharp, with generally a shear zone at, or close to, the margin. These shear zones are hydrated with the breakdown of the mafic minerals to hematite rich, dolomite-amphibole aggregates, exsolution of feldspar and marked radioactivity.

THE MINERALOGY.

The comparative modes of the shonkinite, minette and biotite pyroxenite are shown in Table 6-2. From these it may be seen that there is a consistent increase in biotite and pyroxene from shonkinite to biotite-pyroxenite with a decreasing content of oxide and feldspar. Zeolite is confined to the minettes and biotite pyroxenites, olivine to the shonkinites.

The shonkinite pipe (68399) contains an unusually high proportion of mafic minerals and is gradational through loss of feldspar and replacement of olivine by cummingtonite into a type of biotite pyroxenite.

Although nepheline normative as a result of the high biotite content the biotite pyroxenites contain a small proportion of quartz.

a) PYROXENE.

Pyroxene is present in most of the rocks in two generations with the phenocrysts generally arranged with a horizontal lineation parallel to the margins. The phenocrysts form euhedral prisms, typically 2-4mm long, with strong zoning from colourless cores to purple titaniferous rims. The contact between the two zones is abrupt with sometimes included olivine, biotite or exsolved oxide at the interface. In the minettes the outer zone and contact are marked by minute elongate fluid inclusions parallel to the crystal margins. These are also rarely present in the outer zones of the shonkinite pyroxenes. They are taken as evidence for a free vapour (fluid) phase distinct from the silicate liquid.

The contents of the inclusions have not been resolved; they appear simply to be hollow and translucent, and may be analogous to the liquid CO_2 inclusions found by Roedder (1965) in phenocrysts from basalts.

In certain minettes, and in the biotite-pyroxenites, the titaniferous zone is rimmed by an irregular narrow margin of pale grey-green weakly pleochroic hedenbergitic pyroxene which also occurs as granules in the matrix.

Within the late-stage syenite veins in the biotite-pyroxenite and within calcite veins titanaugite is zoned to aegirine and primary euhedral deep green aegirine is also present.

b) OLIVINE.

Olivine forms 3-4% of the coarse shonkinites rising to 10% in the shonkinite vents. It is invariably altered to colourless tremolitic amphibole or pale yellow serpentine Although absent from the chill, the grain-size rises rapidly to that of the pyroxene phenocrysts in coarser rocks. Its inclusion as small grains between the core and rim of the pyroxenes shows that olivine began to crystallize only after intrusion. Olivine is rimmed in all cases by biotite, arranged tangentially around the crystal margin. Locally it is also rimmed, inside the biotite, by pale green hedenbergitic pyroxene.

Olivine is typically absent from the minettes and biotite pyroxenites where its place is taken by biotite.

c) BIOTITE.

Biotite is commonly of two generations. Phenocrysts occur in some shonkinites, in minettes, and in biotite-pyroxenites. The phenocrysts are hexagonal plates (5 -10mm) with abrupt colour zoning from pale yellow centres to deep brown rims with a red-brown pleochroism. Where rutile is exsolved it is concentrated at the rims, and the biotite is a deep green. These titaniferous rims to pyroxene and biotite correspond, in the sequence of crystallization, to the loss of ilmenite and magnetite from the crystallizing phases. Verhoogen (1962) has indicated that Ti will enter the silicate phases when SiO_2 is low, the temperature high and

when the partial pressure of oxygen is relatively high. At lower temperatures and higher PO_2, Ti will tend to enter magnetite and sphene. This situation is found in the final stages of the biotite-pyroxenite crystallization, when biotite is rimmed by oxide, and pink strongly pleochroic sphene appears as interstitial crystals.

The matrix biotite is interstitial to pyroxene and sometimes poikilitic. It is pleochroic from pale-yellow to deep red-brown; is similar to the phenocryst rims and shows well-developed crystal faces against cryptoperthite. Biotite forms parallel growths around the rims of olivine and oxide.

d) FELDSPAR.

The shonkinite feldspar consists of clear carlsbad twinned microliths of cryptoperthite. The x-ray powder patterns ($\bar{2}01$) indicate a composition of Or_{48-52}. Pure pale-yellow concentrates of the cryptoperthite, when homogenized at 1060°C prior to x-ray work, turned brick red, in contrast to all other feldspars from the complex which were bleached. This exsolution of hematite suggests a very high iron content in solid solution.

Up to 18% iron orthoclase in solid solution with soda-poor sanidine has been described from the orendites of Wyoming, and jumillite of Murcia Spain, by Carmichael (1967). High Fe_2O_3 has also been described from Palabora by Shand (1931).

Similar cryptoperthite is found in the minettes and biotite-pyroxenites.

e) ZEOLITE.

Primary clear zeolite occurs in the minette groundmass where it forms fine radiating sheafs of crystals.

In the biotite-pyroxenite's aegirine-sphene-cryptoperthite-zeolite pegmatite sericitized polygonal zeolite occurs, both poikilitically or in rounded vesicles.

f) THE OPAQUE MINERALS.

Titaniferous magnetite, with a lattice pattern of ilmenite exsolution, is 3-4 times as abundant as primary ilmenite. The oxides are most abundant in the shonkinite chill (15%), rimmed with biotite in coarse shonkinite, and virtually absent from biotitic minettes and biotite-pyroxenites.

The sulphides, dominantly pyrite, chalcopyrite, pyrrhotite, occur abundantly in amphibolitized shonkinite breccia, and in sheared minette.

g) APATITE.

Apatite occurs in the groundmass of all types, increasing with mafic mineral content in the series shonkinite-minette-biotite pyroxenite. In the biotite-pyroxenite 4-10% apatite occurs interstitial to pyroxene with biotite, sphene and magnetite.

h) AMPHIBOLE.

The primary amphibole is a ferrohastingsite. It is pleochroic from

α pale sepia

β opaque deep brown

γ deep olive green

forms 0.5 - 2% of most slides, and is interstitial to pyroxene which it presumably replaces as a late stage, low temperature, volatile rich phase

i) SPHENE.

In the biotite-pyroxenites irregular granules of sphene occur interstitial to pyroxene. The sphene is markedly pleochroic from pale pink to brown possibly due to Fe_2O_3 and rare earth enrichment (Deer, Howie and Zussman 1963). Sphene also occurs as subhedral late crystals associated with zeolite, calcite and secondary amphibole in the minettes and breccia shonkinites.

j) OTHER MINERALS.

Quartz is present as a primary phase, associated with late amphibole in the biotite-pyroxenite. In the breccia or chilled shonkinites, 0.5 - 1% quartz probably results from slight assimilation of granite. The exsolution of feldspar to albite and microcline with the loss of iron orthoclase as magnetite, may also liberate free silica in these hydrated rocks (Bailey and Schairer 1964).

Calcite occurs interstitially in fresh minettes together with zeolite, fluorite, biotite and apatite. Zircon is present in a few minettes but is very rare, and possibly derived through assimilation of the granodiorite.

OTHER HIGH POTASSIC ROCKS.

Pseudo-Leucite Porphyry.

On the shore north of the largest shonkinite vent are intruded several subparallel dykes of a light grey rock with abundant polygonal 0.5cm pale phenocrysts. The dykes range from 0.5 - 10m in width with from 10-45% phenocrysts.

In thin section the phenocrysts show a typically rounded or six-sided cross-section, and are composed of a single crystal of potash feldspar, often calsbad twinned, riddled with lath-like albitic feldspar, and containing also small crystallites of pale green amphibole and oxide. The matrix consists of laths of albitic plagioclase (40%), pale biotite (40%) pale grey green amphibole (5%), granular quartz ($\ll$5%), magnetite and fluorite.

In view of the quartz in the matrix it is suggested that the phenocrysts represent primary leucite, or potash analcite (Fudali 1957), which crystallized in the orthoclase-quartz composition field, and which subsequently reacted with the liquid to form the present assemblage.

Biotite-Peridotites.

The biotite peridotites are closely associated with the carbonatites within the area of centres 1-3. Most known dykes occur either in the granodiorite or intruded into centre 1. Most are extensively carbonated.

The chilled margins are composed of 5-10% augite and olivine phenocrysts in a matrix of microscopic magnetite, biotite, pale green amphibole and calcite. The most conspicuous feature is 1-5% (0.1 - 0.4mm) rounded calcite vesicles in the matrix. These consist of 2-3 crystals of calcite and are rimmed by slightly coarser biotite.

TABLE 6 - 1. ANALYSES OF THE HIGH POTASSIC ROCKS.

	68021 CHEM.	68021 XRF	68396A	68396C	68394	68093	68399	68401	68020	68017	68395	68165	68159	68160	68162	68163	A	B	C	D
SiO_2	50.41	51.59	50.19	48.17	51.44	52.40	51.47	45.11	43.26	42.01.	41.13	39.18	42.26	42.01	47.14	46.32	51.80	41.10	48.98	40.53
Al_2O_3	13.43	13.44	12.12	11.38	12.52	10.84	10.60	9.56	7.43	6.88	4.63	8.19	7.59	6.19	12.45	14.80	11.10	12.50	12.29	6.80
Fe_2O_3	4.43	4.75	-	6.27	3.72	4.95	5.14	6.73	6.52	6.93	10.29	8.07	7.51	-	5.74	-	3.55	4.01	2.88	6.05
FeO	8.28	8.06	16.52	7.79	7.89	6.12	6.39	8.99	10.90	11.63	8.66	14.31	10.45	19.54	9.43	11.13	3.42	9.30	5.77	8.11
MgO	4.17	4.00	5.91	7.60	7.09	8.12	11.22	11.36	10.99	11.00	12.73	8.45	13.00	13.51	8.18	10.71	8.15	10.02	9.19	10.98
CaO	8.09	7.47	8.90	8.48	7.02	8.34	6.98	10.19	12.07	12.63	15.15	12.87	13.65	15.60	8.86	8.64	7.95	10.60	9.65	17.25
Na_2O	3.18	3.25	2.18	2.46	2.78	2.45	2.53	1.50	1.29	1.08	0.59	1.08	0.48	0.59	2.58	2.68	2.25	2.94	2.22	1.25
K_2O	4.29	3.72	1.06	3.55	4.30	3.95	3.04	3.30	2.79	2.95	1.56	2.11	1.32	0.62	3.99	4.16	5.97	2.26	4.96	1.27
TiO_2	2.48	2.65	1.69	3.05	2.24	1.59	1.58	2.21	1.42	2.85	2.42	4.29	2.70	2.49	1.06	0.52	1.80	3.70	1.44	1.71
MnO	0.20	0.24	0.21	0.17	0.13	0.15	0.13	0.20	0.20	0.25	0.23	0.26	0.21	0.18	0.16	0.24	tr	0.18	0.08	4.47
P_2O_5	0.75	0.74	0.19	0.96	0.74	0.68	0.74	0.63	1.72	1.62	2.26	0.40	0.38	0.25	0.08	0.05	0.95	1.24	0.98	0.15

68021: Chilled shonkinite, Moose Island centre.
68396A. Chilled (hybrid ?) shonkinite Moose island centre.
68396B. Coarse shonkinite, Moose island centre.
68394: Coarse shonkinite, Moose island centre.
68093: Breccia shonkinite from pipe Moose island centre.
68399: Breccia shonkinite from pipe Moose island centre.

A: Minette dyke, S.of Shiprock Navajo area) Williams (1936)
B: Limburgite, Roundtop Hopi Buttes)
C: Shonkinite, Yogo Peak, Montana. Hillebrand (1895)
D: Potash Ankaratrite, Nyamunuku. Holmes & Harwood (1932).

68401: Minette dyke Moose island centre.
68020: Biotite-pyroxenite Moose island centre pipe.
68017: Biotite-pyroxenite Moose island centre pipe.
68395: Biotite-pyroxenite, Moose island centre from 68399 pipe.
68165: Chilled Biotite-peridotite centre 1.
68159: Coarse Biotite-peridotite centre 1.
68160: Coarse Biotite-peridotite centre 1.
68162: Augite-kersantite dyke swarm Bigspruce island.
68163: Augite-kersantite dyke swarm Bigspruce island.

TABLE 6 - 1. TRACE ELEMENTS.

	68021 CHEM	68021 XRF	68396A	68396C	68394	68093	68399	68401	68020	68017	68395	68165	68159	68160	68162	68163	
Rb		200	30	133	212	-	153	173	173	199	225	48	35	20	235	48	
Ba		1,700	340	2,350	2,650	-	1,740	2,280	3,090	3,470	2,590	1,090	581	273	4,570	150	
K		1.76	0.50	1.70	2.02	-	1.41	1.58	1.36	1.47	0.77	1.03	0.64	0.30	1.88	1.93	
Sr.		899	216	1,530	1,380	-	1,170	1,290	1,070	1,330	377	408	460	227	484	181	
La.		88	-	169	-	-	93	275	173	155	139	150	72	-	-	-	
Ce		372	-	203	-	-	159	138	283	377	342	140	10	-	-	-	
Y		27	32	27	30	-	26	29	39	34	<2	25	-	13	35	-	
Zr		229	175	162	320	286	199	253	165	187	123	242	163	138	100	46	
Nb		16	7	23	29	22	19	33	24	20	3	40	21	27	8	<2	

TABLE 6 - 2. MODES OF THE HIGH POTASSIC ROCKS.

	68399	68021	68004	68010	68394	68010B	68401	68213
Serpentine (ol)	8.6	-	2.1	0.6	2.5	-	-	-
Biotite	35.5	10.8	15.3	15.9	17.8	29.9	35.9	33.0
Pyroxene	18.7	47.2	33.4	34.1	28.8	43.6	47.9	55.6
Magnetite	1.5	14.8	8.9	6.2	5.5	4.6	1.2	3.4
Feldspar	24.8	27.0	38.0	42.0	44.0	20.4	10.0	0.1
Zeolite	-	-	-	-	-	-	5.2	0.4
Apatite	0.7	0.2	1.2	1.3	0.9	1.6	0.2	4.3
Sphene	1.3	-	-	-	-	-	T	1.3
Quartz	1.8	-	-	-	-	-	-	0.2
Green Amphibole	6.8	T	T	T	0.5	T	T	T
Calcite	-	-	-	-	-	-	-	0.6

68399. Shonkinite from N.W. pipe
68021. Chilled shonkinite from shonkinite arc.
68004. Chilled shonkinite from shonkinite arc.
68010. Coarse shonkinite from S. end of shonkinite arc.
68010 (2) Biotite-pyroxenite schlieren from 68010.
68394. Coarse shonkinite from centre of shonkinite arc.
68401. Minette dyke from centre of shonkinite arc.
68213. Biotite-pyroxenite from centre of Camp island pipe.

The central portion of the dyke is coarse grained, consisting of euhedral but touching, 3-5mm crystals of pyroxene and olivine, surrounded by alkali-amphibole and oxide in a matrix, filling the angular interstices, of calcite, biotite, apatite, fluorite and bastnasite. Secondary tremolite and calcite replace olivine; green hornblende and blue-green hornblende marginally replace pyroxene; sphene replaces oxide; and abundant blue-green amphibole and epidote have developed in the amphibole-oxide primary surround to the phenocrysts.

The "carbonatite" matrix in these rocks is clearly primary but occupies only 2-5% of the volume. Phenocryst-silicate matrix, replacement reactions lead to the formation of replacive carbonatites, explosion breccias and intrusive carbonatites on the one hand, and to alkali-amphibole amphibolite lamprophyres with no carbonate on the other.

Lamprophyres.

A second group of lamprophyres, forms a dyke swarm crosscutting centre 3, consisting of circa 10% plagioclase laths enclosed by poikilitic plates of clinopyroxene, in a fine matrix of biotite and epidote. Vesuvianite extensively replaces plagioclase. Rounded and elongate biotite filled pseudomorphs suggest the original presence of olivine and a possible relationship to the biotite peridotites.

Minette, shonkinite and biotite-carbonatite dykes are also present in the area of Bigspruce lake (Chap.7.)

CHEMICAL COMPOSITION:

The analyses of high potassic rocks from Bigspruce lake are given in Table 6-1. In common with other rocks of their kind they show relatively high Mg, K, Ti, P, S, Ba, Rb, Zr, Rare earths and Y. Similar enrichment is found in the lavas of southwest Uganda (Holmes and Harwood 1937) (Higazy 1954), the dykes and pipes of the Navajo district (Williams 1936) the lavas of Leucite Hills, West Kimberly and Murcia (Carmichael 1957), the Devon lavas (Knill 1968) and the majority of Kimberlites (Dawson 1962).

With the exception of 68396a, which is a marginal rock showing signs of hybridization, all show $K_2O > Na_2O$ and $Al_2O_3 > (K_2O + Na_2O)$ as found by Higazy (1954) for the S.W.Uganda lavas, and Williams for the Navajo rocks (1936). Also in common with these rocks they show relatively high total iron and $Fe^{2+}/ Fe^{2+}+Fe^{3+}$. This is in contrast to the highly oxidized, iron deficient Leucite Hills rocks, and typical Kimberlites. This enrichment of iron relative to magnesium is a consistent feature throughout all rocks of Bigspruce lake, and therefore appears to be a fundamental feature of the source rocks from which they were derived.

Shaw (1968) has reviewed the nature of K/Rb fractionation trends in igneous rocks, illustrating a general decrease during extreme fractionation, particularly in alkaline rocks, a pronounced mineral effect with biotite possessing lower ratios than pyroxene, or hornblende, and regional differences assumed to represent mantle or lower crystal inhomogeneities, possibly due to repetitive zone melting. The high potassic rocks of Bigspruce Lake show markedly lower ratios (Avge 158)

than the sodic rocks (Avge 300-600), or typical tholeiitic or alkaline basalts (230-500), (Gunn 1965) (Shaw 1968). There is a slight decrease from shonkinite to biotite-pyroxenite. Estimated ratios from the biotite carbonatites are similar (120-160).

Differentiation of High K Rocks.

The mineralogy and chemistry of the high potassic rocks indicate the close similarity between all the types, modified by chemical reactions to produce volatile rich phases, and the removal of the residual liquids either through crystal settling and intrusion, or through(?)vapour transport into the fenites

Luth (1967) has studied the vapour saturated phase relations in the system $KAlSiO_4 - Mg_2SiO_4 - SiO_2 - H_2O$ which may be taken as an analogue of the natural system olivine-biotite-diopside-leucite-orthoclase-quartz. The synthetic system differs in three important ways from the natural one. First it cannot take into account the important oxidation reactions involving biotite, olivine and oxide. Second, in the natural system there will be considerable progressive change in the composition of the vapour phase (dominantly H_2O, and CO_2), which will affect the nature and composition of the crystallizing phases. Third, there will be only a limited reaction relationship between olivine and clino-pyroxene so that olivine + clino-pyroxene + orthoclase may coexist at low vapour pressure.

The course of crystallization may be considered in three stages -

a) Crystallization in the non-vapour-saturated, lower level magma chamber. Olivine, pyroxene, magnetite, leucite stable phenocryst phases.
b) Crystallization in the high level, saturated position of intrusion. Olivine, biotite, pyroxene (and ? magnetite) stable phenocryst phases.
c) Crystallization, with the simultaneous escape of volatiles, either at low vapour pressure in the breccia pipes, or at higher vapour pressure within the fenites with significant loss of alkalis, alumina and silica.

The inferred phase relations on the saturation surface are illustrated in Luth 1967. At low vapour pressures ($\sim$ 500 bars) olivine, pyroxene, leucite and orthoclase occur on the liquidus related by the reaction points

1. Leucite + Liquid = Orthoclase + Forsterite + Vapour

2. Forsterite + Liquid = Orthoclase + Enstatite + Vapour

At high vapour pressures a field of biotite appears separating the fields of olivine from those of leucite and orthoclase. The reaction points then become

3. Fo + Lc + V = Phlogopite + L.
4. Fo + L + V = Ph + En
5. Lc + L = Or + Ph + V

Reactions 1, 2 and 5 may persist in the non-vapour-saturated portion of the system; reactions 3 and 4, however, will be replaced by the reactions,

6. Fo + Lc + L = Ph + Or
7. Fo + L = En + Or + Ph.

The most important influence of the free vapour (Luth 1967) phase, therefore, is to inhibit the formation of leucite or orthoclase until practically the entire complement of mafic minerals has been crystallized.

The presence of fluid vesicles in the pyroxenes shows that a free vapour phase was present only during the post-intrusion crystallization stage of the minette and biotite-pyroxenite, and possibly in the very late stages of crystallization of the shonkinite. Shonkinite crystallization, and pseudoleucite-porphyry crystallization may be considered in terms of reactions 1, 2, 5, 6 and 7.

If the initial magma is assumed to have a composition similar to the olivine shonkinite 68394 then the liquid in the saturated or unsaturated (low vapour pressure) system falls in the olivine field possibly close to the olivine-diopside-biotite reaction point.

At low vapour pressures, with olivine fractionation, leucite can become a primary crystallizing phase, the liquid changing composition along the field boundary to reaction point 6 when olivine will tend to be resorbed. The petrography shows that olivine resorbtion is shielded by the formation of biotite. The liquid may then crystallize both leucite and phlogopite up to reaction point 5 at which point leucite will react with the liquid to form feldspar. If sufficient olivine fractionation has taken place, the liquid may traverse the field of orthoclase, on the orthoclase-biotite boundary, to the minimum Or + Bi + Qtz. This sequence is consistent with that found in the pseudo-leucite porphyry.

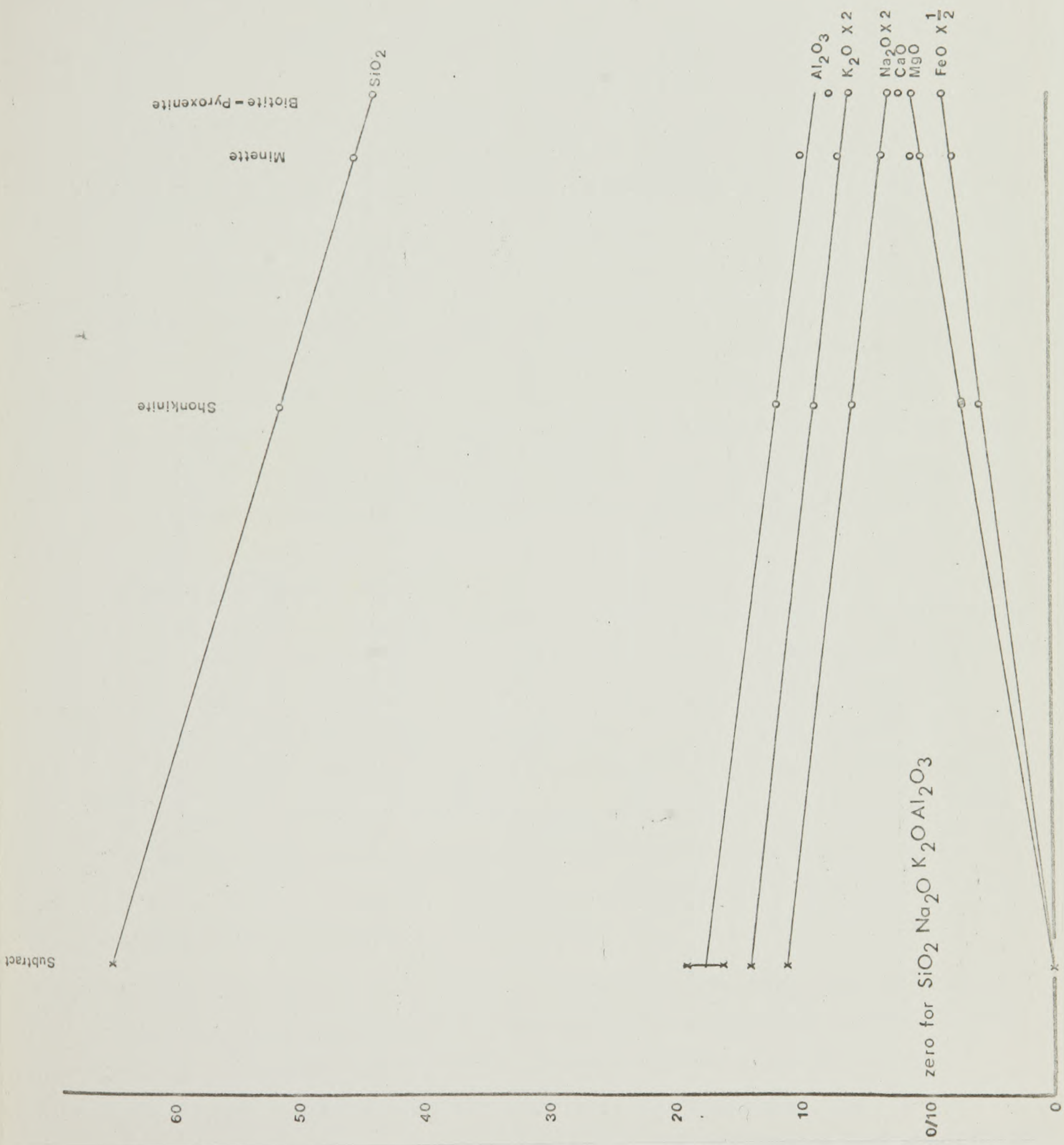
At high vapour pressures, although still in the absence of a free vapour phase, biotite will crystallize following olivine, and olivine may be resorbed according to reaction 7 in line with the observed mantling of olivine by pyroxene and biotite, and the mineralogy of the shonkinite.

The presence of a free vapour phase in the minette and biotite-pyroxenite, by substituting reaction 4 for reaction 7, may prevent the early crystallization of feldspar. The liquid may change composition, through settling out of biotite and pyroxene, towards the field of quartz, becoming progressively enriched in water, reactive volatiles, orthoclase and kalsilite. The presence of fenitized granodiorite and syenite fenite around the margins of the minette and biotite pyroxenite, suggests that the crystallizing system cannot be regarded as closed with respect to alkalis or volatiles.

Fig 6-1 demonstrates the nature of the chemical variation between representative shonkinite, minette and biotite-pyroxenite, plotted so that the silica decrease is linear. All other elements with the exception of P can be seen to follow a similar linear variation. The composition of the material which must be removed for the formation of the minette or biotite-pyroxenite can therefore be calculated. The material is found to have the composition of the cryptoperthite found within the shonkinite viz. SiO_2 ~65%, Al_2O_3 ~16 - 19%, K_2O ~7%, Na_2O ~6% together with circa 2% TiO_2.

The biotite-pyroxenite is relatively enriched in Fe^{3+} and in P_2O_5 (in apatite)

FIG 6 - 1 SUBTRACTION DIAGRAM TO ILLUSTRATE THE COMPOSITION OF THE MATERIAL REMOVED IN THE FORMATION OF THE BIOTITE -PYROXENITE FROM SHONKINITE



The diagram has been constructed on the basis of a linear silica variation using the analysed rocks 68017,68401,68394. The composition of the material removed is approximately that of the feldspar which must have been added to the granodiorite to form the surrounding fenite.

A similar, and independent estimate bay be derived through comparison of the fenites to the surround granodiorites (see chapter V).

The volume of "normative" alkali feldspar needed to be subtracted from the shonkinites to form the biotite-pyroxenites is equivalent to the volume of feldspar which must be added to the granodiorites to produce the fenites (see chapter V - fenites). These volumes are very large. Circa 38% of the shonkinite volume must be removed to produce the biotite-pyroxenite.

Van Groos (1966) has demonstrated that in the system albite-NaF -H_2O "The solubility of albite in a water-rich vapour phase is increased significantly in the presence of NaF. It is possible that this provides a mechanism for transport of silicates at low temperatures". The effect of NaF on the solubility of water in an albite melt is also very large, a melt saturated in NaF and H_2O containing at 1Kb pressure about 60% albite, 10% sodium fluoride and 30% water. The biotite-pyroxenite contains 4-8% fluor-apatite. The biotite is possibly also rich in fluorine as found by Gittins for many carbonatites. The fenite is rich in hydrated feldspar. It is possible therefore that the required volume of feldspar may have been carried in a fluor-rich aqueous fluid phase, particularly if the exposed biotite-pyroxenite lies high in a pipe up which volatiles could be concentrated.

OTHER BIOTITE PYROXENITES.

A stock of biotite-pyroxenite has been described from Libby Montana by Larsen and Pardee (1929). The average rock is composed of circa 70% pale green pyroxene, 10% apatite, 10-20% biotite and minor sphene, magnetite and microcline-microperthite. The biotite proportion is highly variable from 0-100%. A few areas contain up to 15% microperthite. The rocks have undergone very extensive hydration. The rocks are very rich in fluorine. Associated with the pyroxenite is a smaller body of perthite syenite containing up to 10% muscovite pseudomorphs after nepheline.

At Palabora (Shand 1931, Heinrich 1966) central cores of carbonatite (calcite-dolomite-magnetite rock) and phoscorite (apatite-magnetite-olivine-phlogopite-peridotite) intrude a large body of biotite-pyroxenite. The pyroxenite is rimmed by shonkinite (35% microcline 61% diopside), and by syenite fenite. The pyroxenite and shonkinite are intensely hydrated to form vermiculite rock. The phoscorite shows vertical mineral banding.

Holmes and Harwood (1932, 1937) Holmes (1950), and Higazy (1954) have described olivine-biotite-pyroxenite xenoliths (O.B.P. series, dominantly biotite-pyroxenite) from the ultrabasic high potassic rocks of south west Uganda and adjoining areas, and from Villa Senni in Italy. The xenoliths consist of clino-pyroxene, olivine, poikilitic biotite and abundant apatite together with minor sphene and melanite. They are thus similar to those of Libby, and of Bigspruce lake. Holmes and Harwood (1932) proposed that the biotite-pyroxenites were produced from a

mica-peridotite magma following the crystallization of olivine. The mica-peridotite, they derived from a peridotite magma through the crystallization, in the lower crust, of eclogite. Through a depth-pressure-time control of the proportion of eclogite and olivine settling from the primary magma, they derived the melilite basalts, olivine leucitites,and leucitites. The associated basalt-trachybasalt-trachyte series they derived through the differentiation of an independent alkali basalt magma.

Subsequently, to explain the partially resorbed xenoliths of granite, and the characteristic trace element assemblage (Holmes and Harwood 1937) they proposed an origin through the metasomatism of basement granitic rocks by a highly "energised" stream of "emanations". These emanations led to the formation of peridotite, biotite-pyroxenite, and katungite. Further assimilation led to the formation of the wide variety of lavas.

Holmes (1950) suggested a primary carbonatite magma in place of the emanations. The carbonatite contributed Ca, Mg, Fe, Ti, P, Sr, La, Y and V, whilst the assimilated sialic rocks contributed Si, Al, K, Rb and Ba. The O.B.P. formed as crystal cumulates through the reaction

Sial + Carbonatite = O.B.P. + Proto katungite

Biotite-pyroxenite xenoliths also are found in the nephelinites and carbonated rocks of oldoingo Lengai, and in the minette breccias of the Navajo region (Williams 1936). Williams suggested that the minettes might be derived from a biotite-pyroxenite magma itself derived from a primary peridotite magma.

These examples demonstrate the close field association between mica-peridotite, biotite-pyroxenite, shonkinite (or minette), and carbonatite, and also between this high potassic series and monchiquites (Navajo area), nephelinites, or melilite basalts.

POSSIBLE MODES OF ORIGIN FOR THE HIGH POTASSIC ROCKS.

Turner and Verhoogen (1960) and Bell and Powell (1969) have reviewed theories for the origin of high potassic rocks. These theories must explain.

a) The general features of high potassic rocks viz:

- Low SiO_2
- High total alkalies, K> Na
- High TiO_2
- Relatively high concentrations of Ca,Mg,Ba and Sr characteristic of basic rocks
- Relatively high concentrations of K, Rb, Sr, Nb, La, Ce,Y,H_2O, CO_2, F, generally characteristic of highly differentiated rocks

b) The particular features of Bigspruce Lake viz:

The occurrence of derivative carbonatites

The low $Sr^{87/86}$ of these carbonatites (0.702)

The association with alkali basic, and syenitic rocks

The common feature of high total iron relative to magnesium of both series.

1. Assimilation.

Bowen 1928 suggested that the settling of early crystallizing biotite or hornblende could enrich a basic magma in normative feldspathoids following partial fusion. To produce high potassic rocks partial fusion of biotite with a high K: Na ratio would be required. Unfortunately, there is no evidence that biotite is an early crystallizing phase in the sodic alkaline magma. Alternatively biotite might have been assimilated from mica schists within the Yellowknife series. However, in this case the $Sr^{87/86}$ of the high potassic rocks and carbonatites should have been raised far above the primitive value of 0.702.

Williams (1936) and Larsen (1940) noting the partially resorbed feldspars in granite xenoliths proposed the assimilation of sialic material by monchiquitic, or olivine-basaltic magma. Once again the $Sr^{87/86}$ ratio should have been raised. In addition the Rb, Ba and Nb concentrations in the potassic rocks are greater than in either starting material.

Holmes (1950) proposed the blending of carbonatite magma with sialic material. However, in most high potassic provinces the volume of carbonatite is insignificant.

2. Zone melting.

Harris (1957) suggested that a natural analogue of zone melting, within the mantle, might provide a mechanism for the concentration of K, Ba, Rb, Nb, R.E. which could not readily be accommodated in the structure of olivine, pyroxene, garnet or spinel. If hornblende (Oxburgh 1964), and/or biotite (Yoder 1968, Griffin and Murphy 1969) were present in the mantle, and preferentially incorporated in the rising column of magma then Sr, H_2O, F might be concentrated also. Roedder (1965) has demonstrated the abundance of liquid CO_2 inclusions in minerals from deep seated nodules. Zone melting should concentrate these inclusions also, greatly enriching the magma in CO_2. Zone melting, followed by more large scale melting in the mantle provides a possible explanation for the association of high potassic, with alkaline basic magmas.

3. Fractionation.

O'Hara and Yoder (1967) have demonstrated that fractionation of sodic eclogite from a hypersthene normative picrite magma may give rise to a residual liquid characterised by high Cr,Sr, Ni, Co and Mg and with high concentrations of Sr, Ba, Rb, K, Na, Ti and P plus high K/Na ratios. Eclogite nodules together with harzburgites and lherzolites are in fact found in the Navajo, West Uganda and some kimberlite rocks. Fractionation of the same magma at intermediate pressures, followed by further fractionation at low pressures could give rise to the alkali basalt magma (O'Hara and Yoder 1967). The high potassic residual liquid has "the geochemical characteristics of the groundmass kimberlite or of the potassic mafic lovas". Fractionation of olivine (Wade and Prider 1940) may then give rise to the volatile rich feldspathic rocks.

Bigspruce lake provides no evidence as to whether zone refining (Harris 1957), or fractional crystallization of eclogite (Holmes and Harwood 1932, O'Hara and Yoder 1967) should be preferred. However there seems strong reason to doubt whether assimilation on a large scale has played a part in the generation of the high potassic series.

CHAPTER VII. CARBONATITE CENTRE 5.

GENERAL. When the Bigspruce Lake complex was first described by Lord (1942) mention was made of "a small body of white crystalline banded limestone of probably Snare age on the northwest shore of Bigspruce Lake about ½ mile south of the point where Snare River enters the lake. The action of the intrusive rocks on the limestone has resulted in the formation of abundant purple fluorite."

This body has not been found and must now be submerged, but its description tallies with a narrow rare-earth, fluorite-rich, sovite dyke, inshore of this location. Other small carbonatite bodies are scattered throughout the complex, and in particular around its margins.

At the time at which Lord was writing very few carbonatites had been recognised as being igneous and intrusive (Alno, Fen, Chilwa island, Kaiserstuhl and Laacher see), and even in these cases the carbonate was commonly believed to be of metasedimentary origin (Brogger 1921, Daly 1933). Bigspruce Lake forms rather a poor case for any theory of alkali magma generation by contamination with carbonate rocks, since the nearest limest one is at least 15 miles away, and the complex is intruded into the granodiorites on which these were laid down. An origin for the carbonatites as remobilized limestones is unlikely for the same reason. In contrast, the Bigspruce lake rocks appear to show several stages in the generation of carbonatites from high potassic silicic rocks.

These stages may be represented as -

i) volatile enriched ultramafic biotite-peridotite, and minette or biotite-pyroxenite dykes

ii) Carbonated biotite-peridotite and minette i.e. mineralogical biotite-carbonatite with the texture of the parent rock fully preserved.

iii) Breccia pipes of mafic silico-carbonatite (20-50% carbonate).

iv) Intrusive chilled mafic carbonatite, with primary carbonate mineral textures.

v) Intrusive leucocratic carbonatite derived by differentiation of iv.

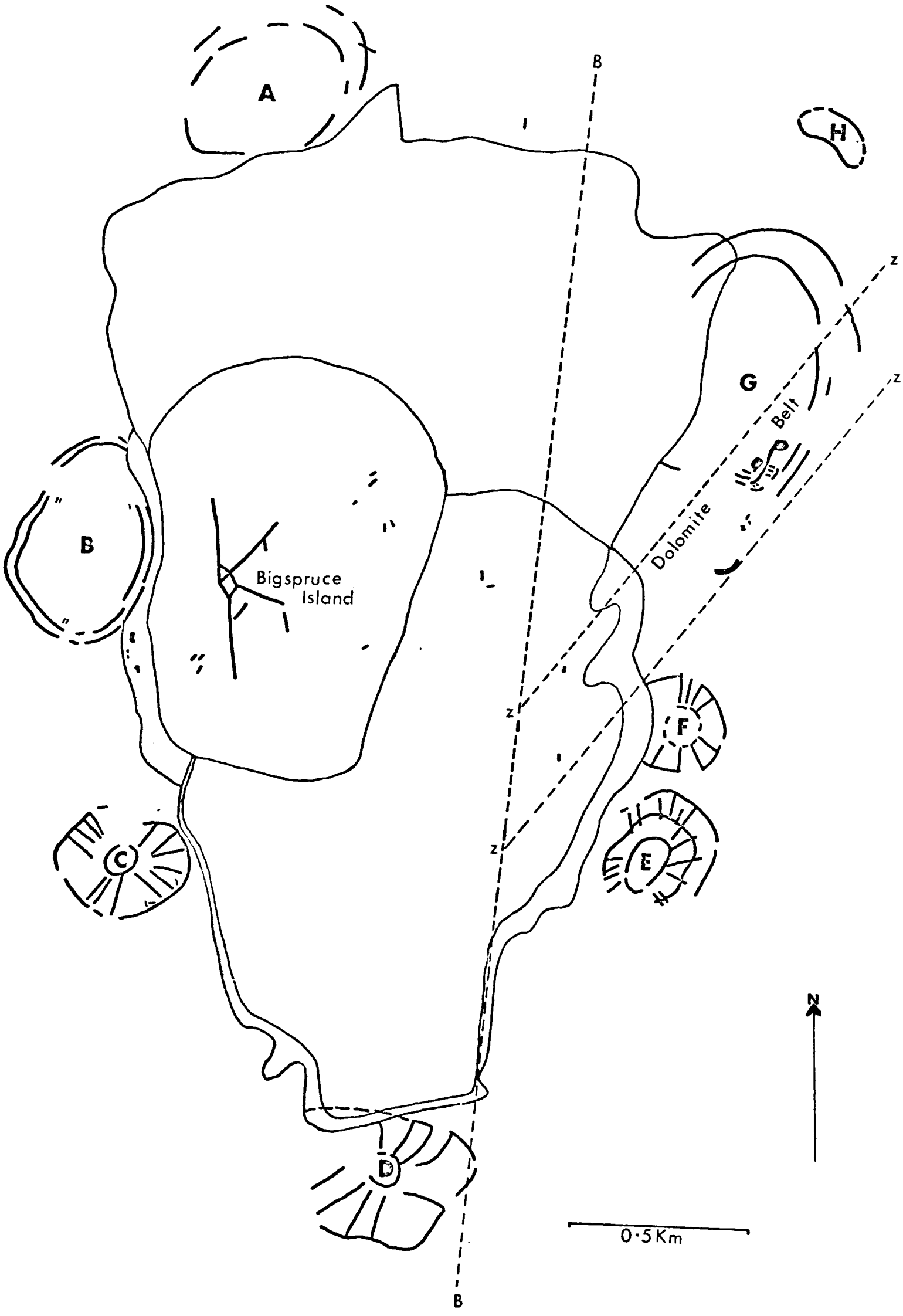
vi) Large fenitized gas escape vents.

LOCATION AND CARBONATITE ROCK TYPES.

The distribution of these features is illustrated in Map 7-1. The gas escape vents form a belt around the margin of centres 2 and 3, and form the major expression of centre 5. They each consist 1-3 outer rings of inwardly dipping, reddened, cone fractures, surrounding a central depression, with a well developed crosscutting radial fracture pattern. They are intruded by radial and tangential dykes of shonkinite, minette, "diabase", and carbonatite, but the volume of intrusive rock is insignificant in comparison to the size of the fracture pattern.

The carbonatites fall into two series distinguised by their carbonate mineralogy. The dolomite-ankerite carbonatites are associated with carbonated biotite peridotites (Fig 7-1). They occur in a 600m belt, Z-Z, running from the eastern side of the lake's east-coast linear, to the north-east side of gas vent G. This is along the line of a linear

MAP 7-1 PHOTOGEOLOGY OF CENTRE 5



The heavy lines are linear or curvilinear muskegs discordant to the fracture pattern in the basement. The short lines and small masses are carbonatites. -G are cone-fracture rimmed gas-escape vents. H is pipe of breccia. The fracture pattern over Bigspruce island overlies carbonatite pegmatite. Note how the dolomites are confined to a narrow fault bound zone west of -B. The zone Z-Z on B-B is intensely metasomatiz .

(? pre-intrusion fault) visible on the aerial photographs, illustrating a close connection between the structure and carbonatite intrusion

The majority of ankerite-dolomite dykes are arranged in a radial and cone-sheet pattern around the ankeritic silico-carbonatite breccia pipe, and show a sequence of increasing carbonate content of the rock, and decreasing iron content of the carbonate away from this centre.

The calcite carbonatites are mineralogically gradational into carbonated minette. They occur only to the west of the East-coast linear, and are focused on the prominent radial fracture pattern of Bigspruce island (plate 7-1). This fracture pattern is associated with numerous magnetite veinlets and is overlain by a strong magnetic anomaly. (750γ). There is no central breccia pipe, but the central area shows widespread aegirine-biotite-magnetite metasomatism, and each deep muskeg is occupied by an aegirine-biotite-magnetite-calcite pegmatite,

The relationship of the calcitic carbonatites to the silicate rock types is shown on the west shore opposite Bigspruce island where carbonated minette passes directly into a biotite-sovite breccia pipe crosscut by sovites.

Associated metasomatism. In general the alteration at the intrusive carbonatite dyke margins is slight. It is confined to reddening of the contacts in granodiorite, or the mechanical shattering of quartz and feldspar. In the foyaites or fenites alteration is usually insignificant.

The majority of the associated metasomatism appears to have been produced prior to magmatic carbonatite, or carbonatite breccia intrusion, as noted by Heinrich (p.291 1966) to be typical of alkali-carbonatite complexes.

In the complex two areas have undergone intense iron and alkali metasomatism. The area of the Bigspruce island carbonatite centre shows the introduction of aegirine, biotite and magnetite and the removal of orthoclase and nepheline. The resulting malignites are intruded by the carbonatite pegmatites. The other area is at the intersection of the dolomite belt with the East coast linear, on its East side, where a 1,300 x 150m zone of aegirine-sphene, and riebeckite-hematite, metasomatised foyaite averages circa 25% introduced mafic minerals. This introduction, or redistribution of mafic minerals, is seemingly controlled by volatile metasomatism. In both cases there is evidence for overlapping, successive, and concentric zones of chlorine, water and fluorine and carbonate alteration of which F and H_2O are the most important. Scapolite and sodalite sericite and fluorite, and cancrinite and calcite, are the diagnostic leucocratic minerals.

Gas escape vents. The fracture patterns associated with the vents are readily apparent on stereoscopic pairs of the aerial photographs (plate 7-13). On the ground most cone fractures are steeply dipping (60-85°), with their reddened microgranite margins, showing the development of salmon pink mesoperthite.

Rarely there is developed a concentric foliation, defined by platy feldspar (vent B); or a regional brecciation (vent D); or an arcuate satellite

breccia (Pipe vent G). The fragments are rounded, and mixed from several lateral or vertical horizons, in a fine matrix, rich in rounded quartz, sericite and clouded feldspar.

The dykes are narrow, sheared, and hydrated, shonkinites, minettes, diabase (vents A,B,C,D) or biotite peridotite (vent G), with minor carbonatite, and have a radial and tangential orientation in the vents. Commonly their margins are metasomatised. Quartz-chlorite-sericite veinlets also occur.

Analysis of the granodiorite and of the recrystallized microgranite at the fracture margins, in a series of 9 specimens across vent G, showed a slight increase in silica in the area within the arcuate ring cone fractures (+ 3 to 5%), and a slight increase in K, and Rb/Sr ratio, across the microgranite fractures.

The paucity of intrusive rocks, the large scale (0.5 to 1.3km) of the features, the occurrence of the hydrated breccias, introduced silica and silica-sericite veins, all support an origin by explosive fracturing and gas-streaming. The inward dip of the cone fractures, the radial pattern, and the central depression, define a small focus comparable in size to the shonkinite breccia pipes of centre 4. The depth of this focus however is unknown.

Kesler and Heath (1968), Hori (1964) and Faust (1949) have considered the effect of heat transport by volatiles, concluding that by virtue of their high mobility, and heat capacity significantly greater than that of a molten magma, transfer of heat by volatiles (CO_2 and H_2O) is both more effective and far more rapid than transfer of heat by conduction. The formation of mesoperthite (circa Or_{50}) in the immediate neighbourhood of the fractures implies localized heating to at least 600°C (Tuttle and Bowen 1958). Provided conduction is insignificant, this may approximate to the temperature of the flowing gas. Allowing for adiabatic expansion, heating of the wall rock, and wall rock reaction (e.g. leaching of silica or feldspar), the source temperature must be significantly higher than this,

The close association with minette, shonkinite and biotite pyroxenite, suggest that this source is a high potassic magma, which, as has already been shown, (chapter VI) is highly enriched in volatiles. The implication is that where these volatiles were able to escape at a high temperature, due to the formation of fenites, drilling of pipes or formation of gas explosion vents, a silicate rock could crystallize and be preserved. Where these volatiles were unable to escape, crystal-liquid-vapour reactions were able to take place, with falling temperature, and carbonated silicate dykes or equivalent secondary carbonatite magmas, were able to form. The gas-vents are the first stage, i.e. they result from explosive fracturing and quiescent escape of volatiles without significant carbonatite formation.

THE CARBONATITES.

The second stage in carbonatite formation is represented by the dolomitic and calcitic breccia pipes. Both occur in the peripheral areas of a gas-



PLATE 7 - 2 Southern margin of the dolomitic breccia pipe, looking south-west over Bigspruce Lake. The foliation of the microgranite fenite is parallel to the contact. Spec. locality 68110.



PLATE 7 - 3 Outer cone fracture of gas-escape vent B (see also plate 7 - 1). The scale is given by the figure on the right.

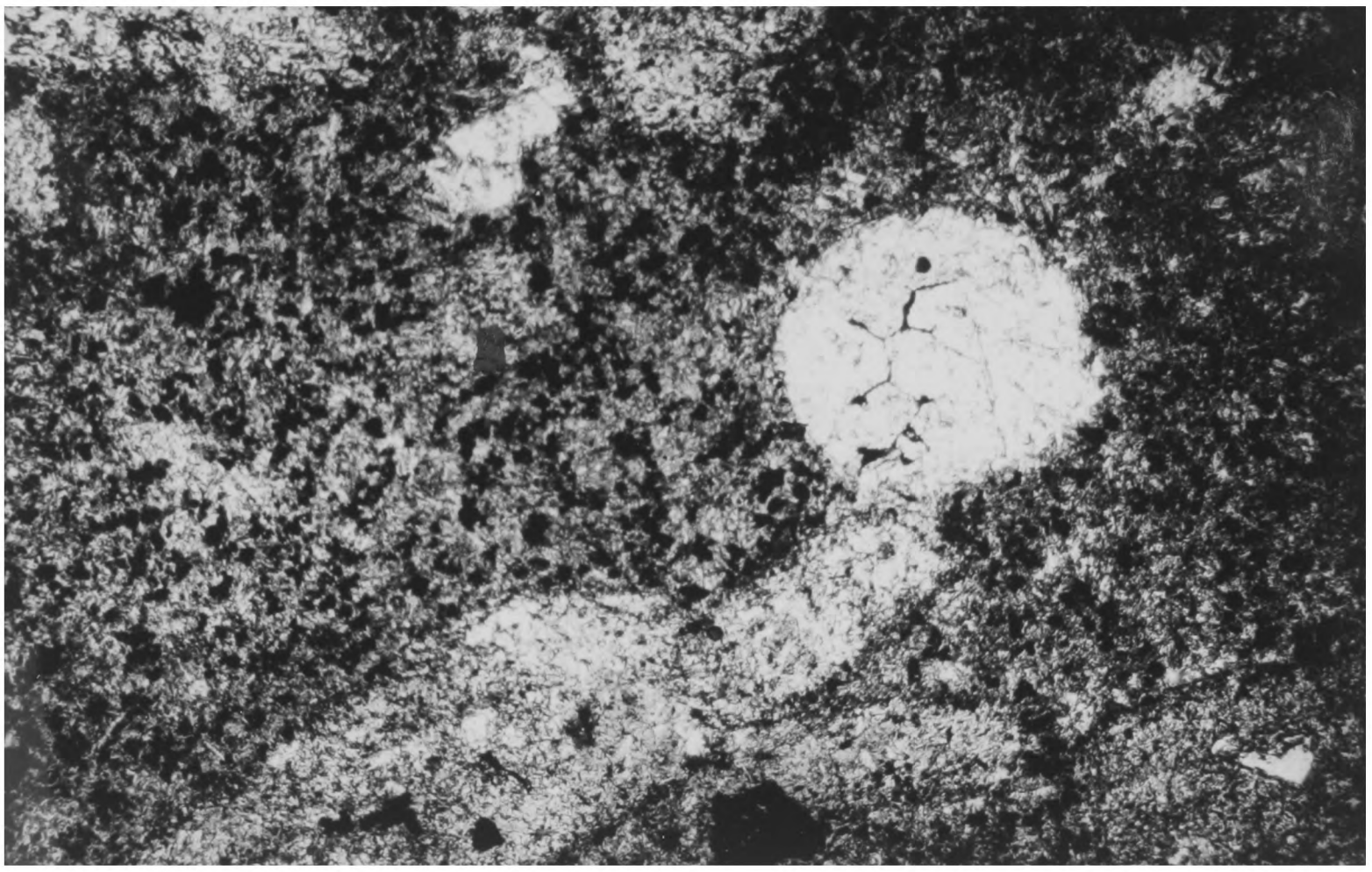


PLATE 7 - 4 **Calcite vesicle in chilled biotite perdotite. The phenocrysts are tremolite pseudomorphs after pyroxene. The matrix is submicroscopic biotite, tremolite, magnetite and calcite. 1m dyke 600m E.S.E. Arete Lake. Spec. 68165 x 20.**

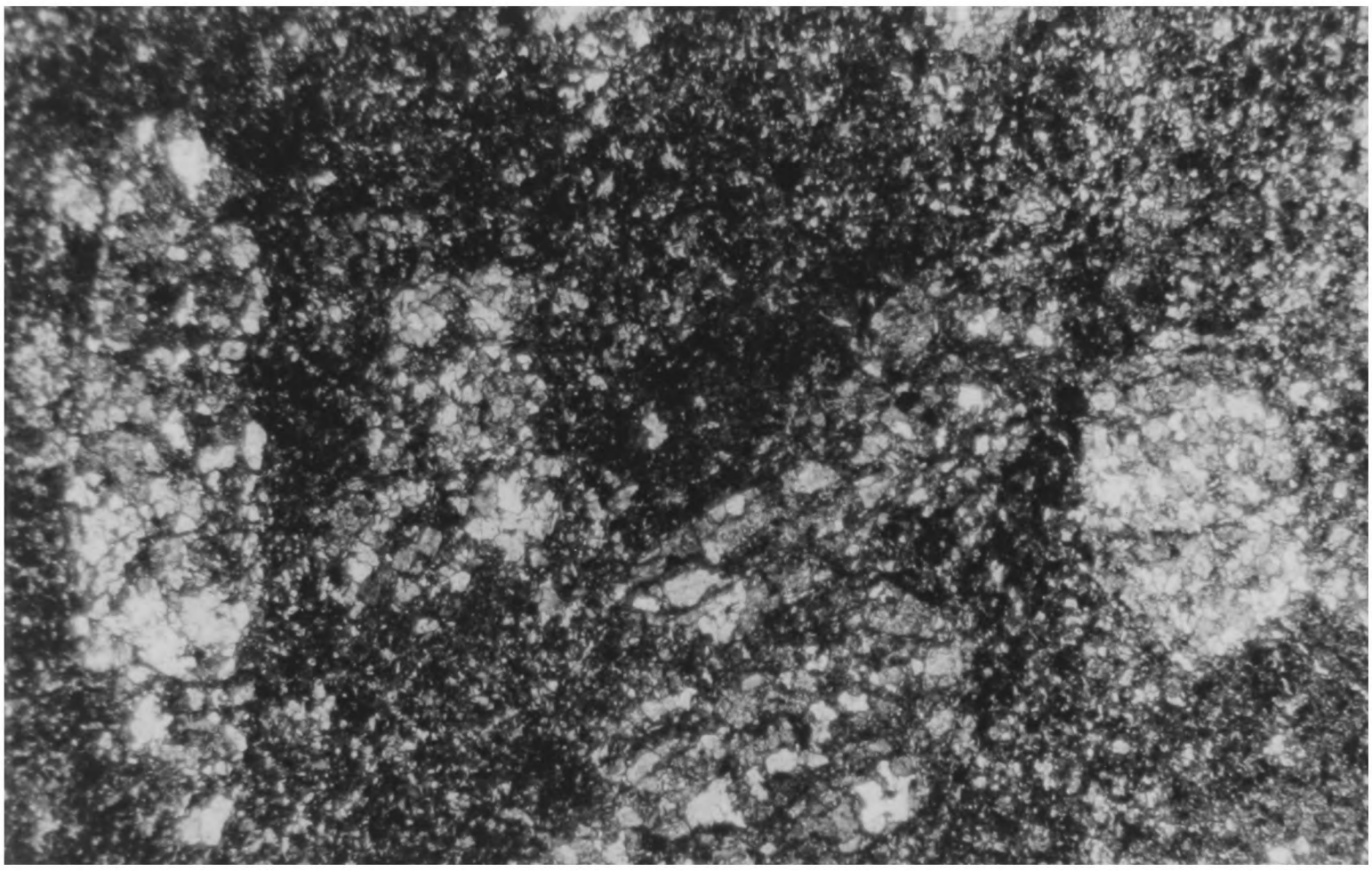


PLATE 7 - 5 **Carbonated biotite peridotite. Ferroan calcite, biotite and fluorite pseudomorph olivine and pyroxene, and the chilled matrix. 40cm dyke 200m S.S.E. of the dolomitic breccia pipe. Spec. 68115, x 6.**

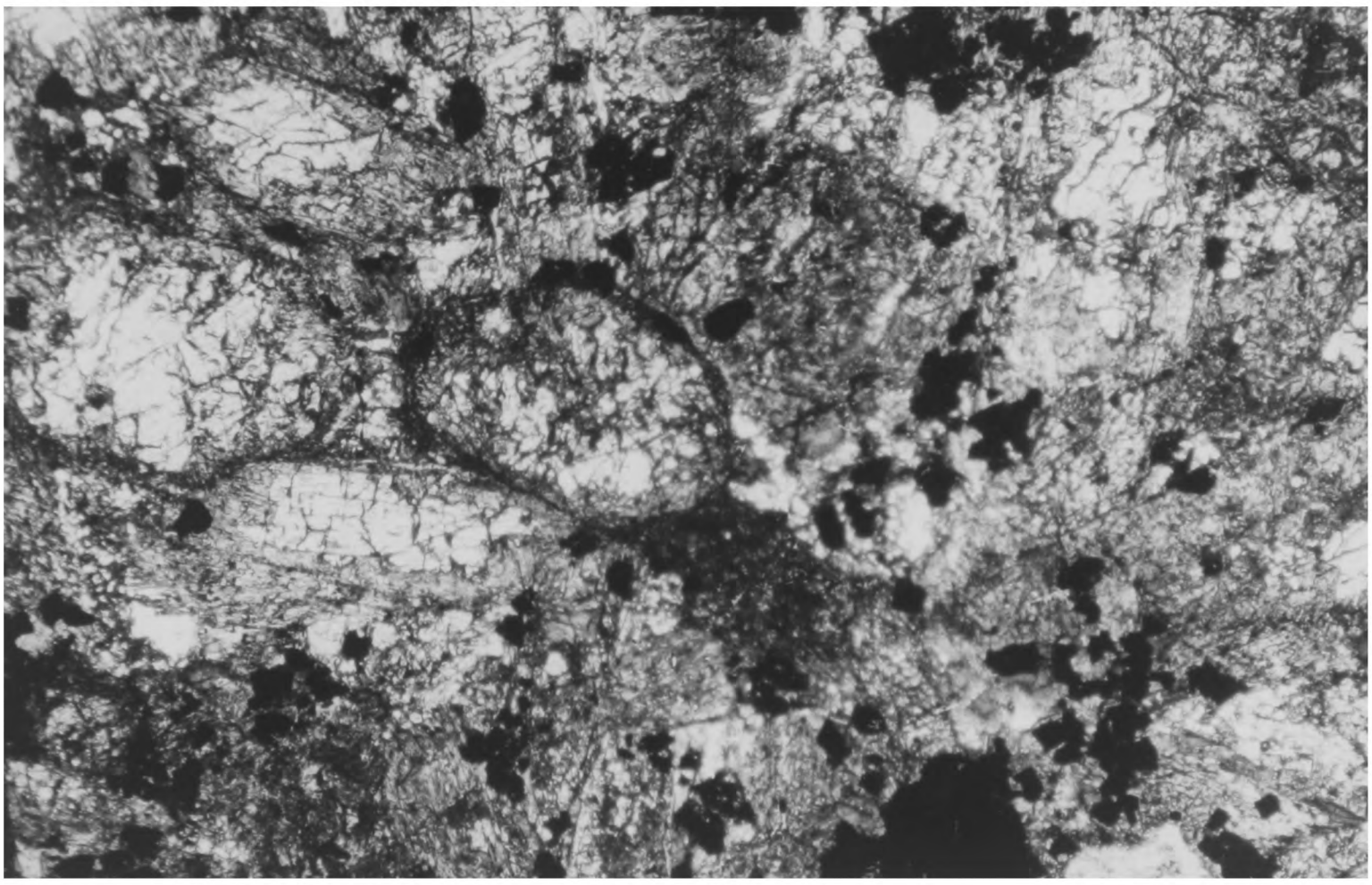


PLATE 7 - 6 Interstitial calcite (white) in coarse biotite-peridotite. The phenocrysts are olivine (left centre) and pyroxene; the matrix is biotite, magnetite, calcite and tremolite. 2m dyke in plagioclase porphyry. 400m E.S.E. Arete Lake. Spec 68160, x 4.

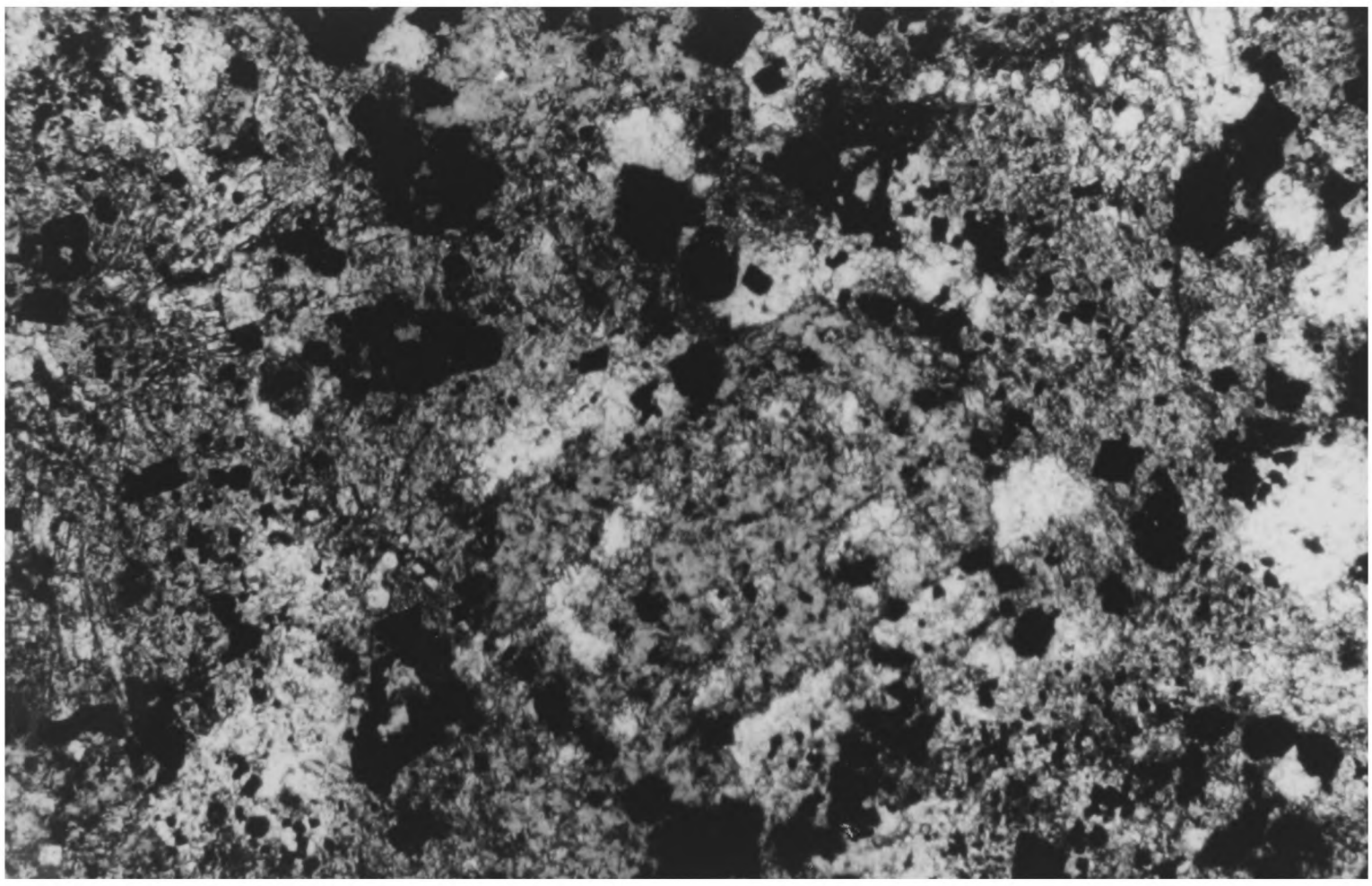


PLATE 7 - 7 Serpentine pseudomorph after biotite in the dolomitic breccia pipe. Quartz (white), dolomite (rough grey), magnetite (black) Spec. 68036 x 32.

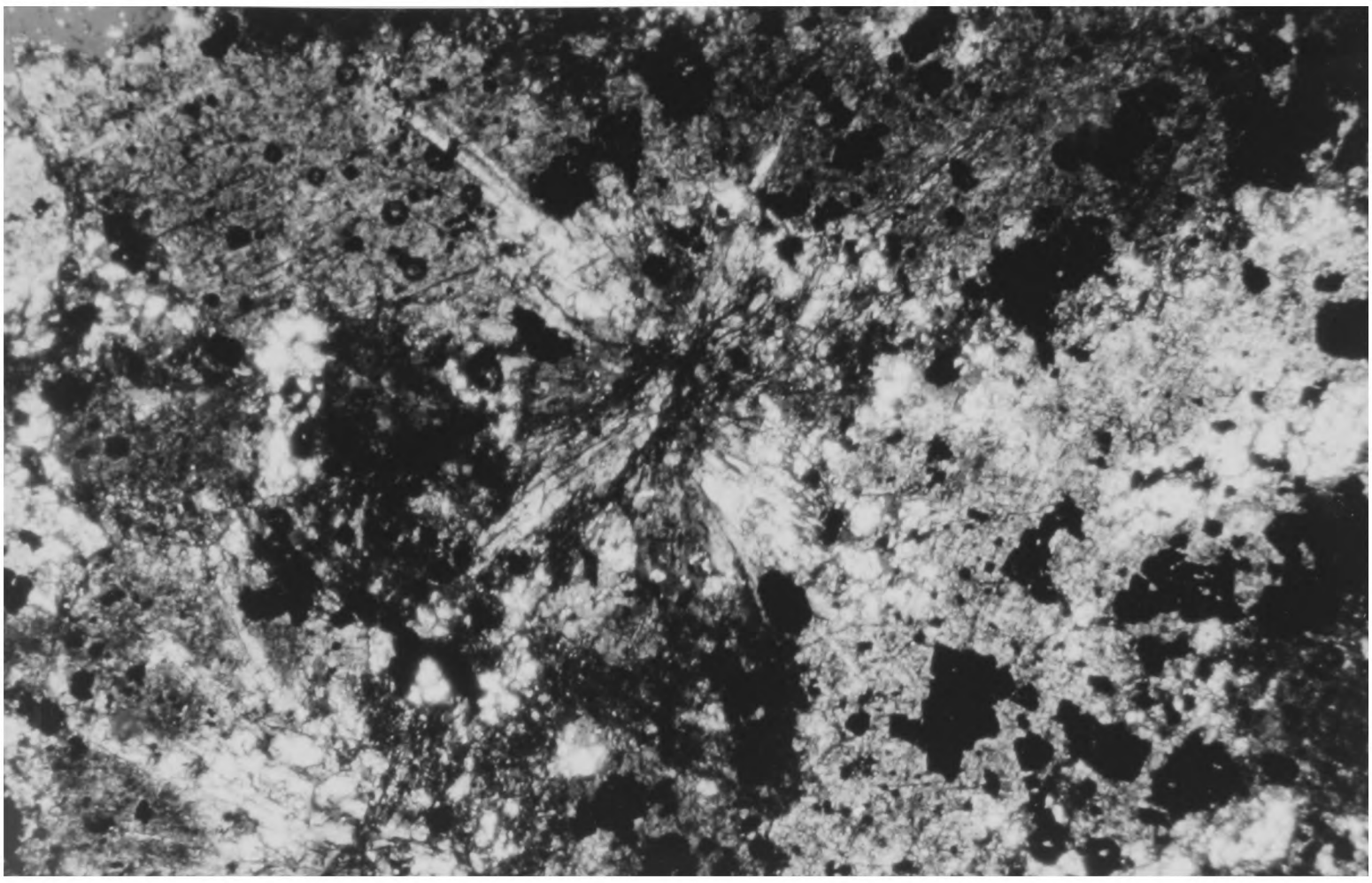


PLATE 7 - 8 Stellate apatite in the dolomite breccia similar to those from synthetic carbonatite quenched melts. ? Pyroxene pseudomorph on the right. Spec. 68036 x 32

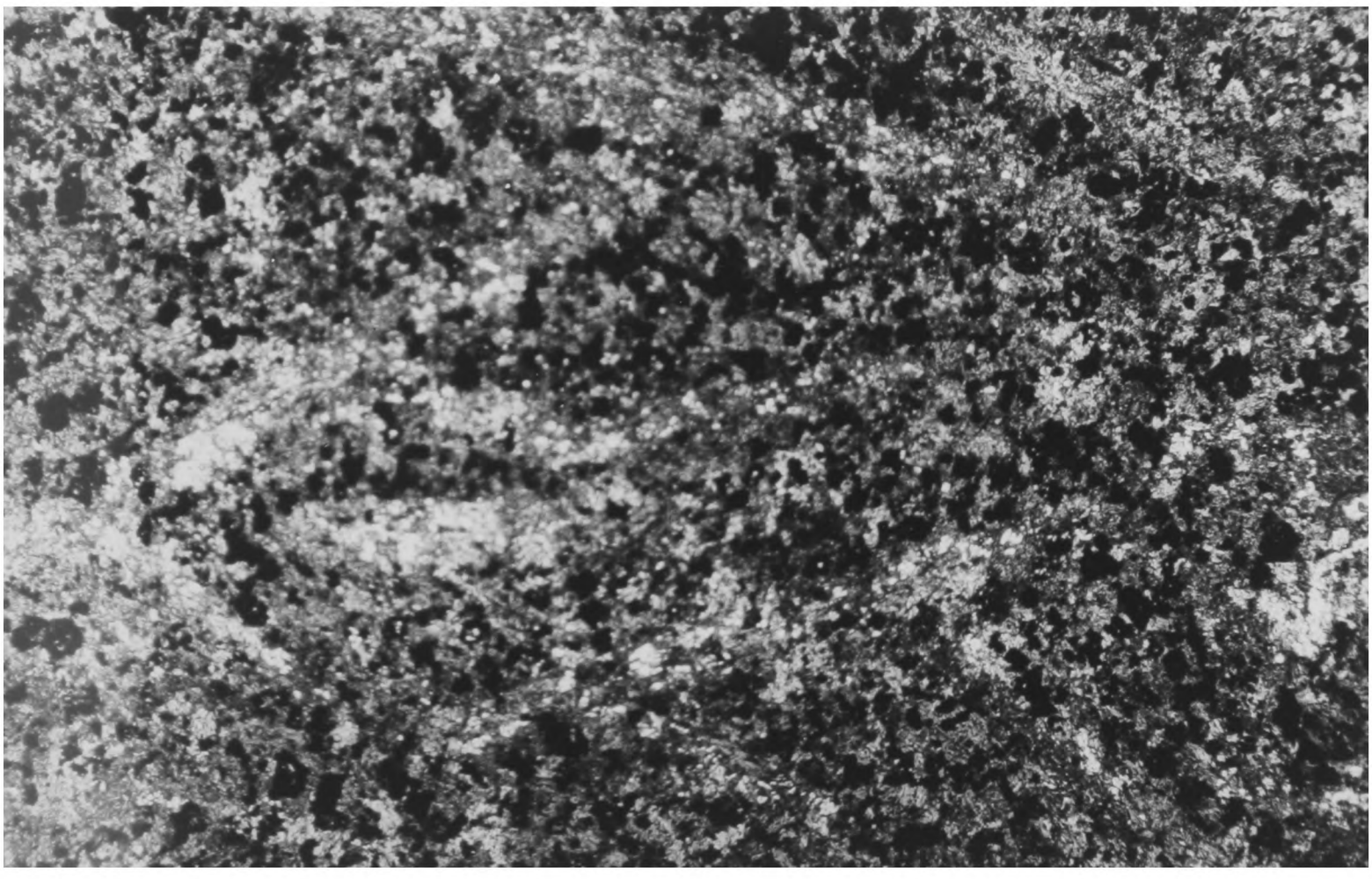


PLATE 7 - 9 Dolomite-plate phenocrysts in chilled magnetite dolomite rock. The plates have partially recrystallized. 4cm dyke 50m from the pipe. Spec.68097, x 4.

escape vent. Both are associated with intrusive carbonatite dykes, and with carbonated high potassic rocks. The sequence of these is -

1. formation of gas-escape vents
2 intrusion of volatile rich biotite-minette or biotite-peridotite. Carbonation in situ
3. intrusion of breccia pipe of silico-carbonatite
4. intrusion of sovite or rauhaugite.

THE DOLOMITIC PIPE. The dolomitic breccia pipe forms a rounded knoll by virtue of its sheath of fenite. It is composed of brown weathering, iron rich, siliceous dolomite, with a deeply pitted surface, rich in all sizes of rounded and angular granodiorite xenoliths. The carbonatite itself is brecciated, and consists of serpentine pseudomorphs after biotite, and rectangular sections of iron rich dolomite, in a matrix of quartz, magnetite, ilmenite, apatite and dolomite.

Point counting suggests an average composition of

Ferroan dolomite	52%
Serpentine	22%
Magnetite + Ilmenite	12%
Quartz	10%
Apatite	4%
Pyrite, feldspar fluorite	Trace %

Serpentine, and more rarely quartz, form thin platy hexagonal pseudomorphs, clearly after biotite. The oxides are equally divided between titanian magnetite and ilmenite, rarely in 2-8cm xenocrysts, and commonly as hollow sections of cubes or octahedra rimming dolomite, as though exsolved through the decomposition of ankerite.

$$6\ Ca(MgFe)(CO_3)_2 + (O) \rightarrow Fe_3O_4 + 3CaMg(CO_3)_2 + 3CaCO_3 + 3CO_2.$$

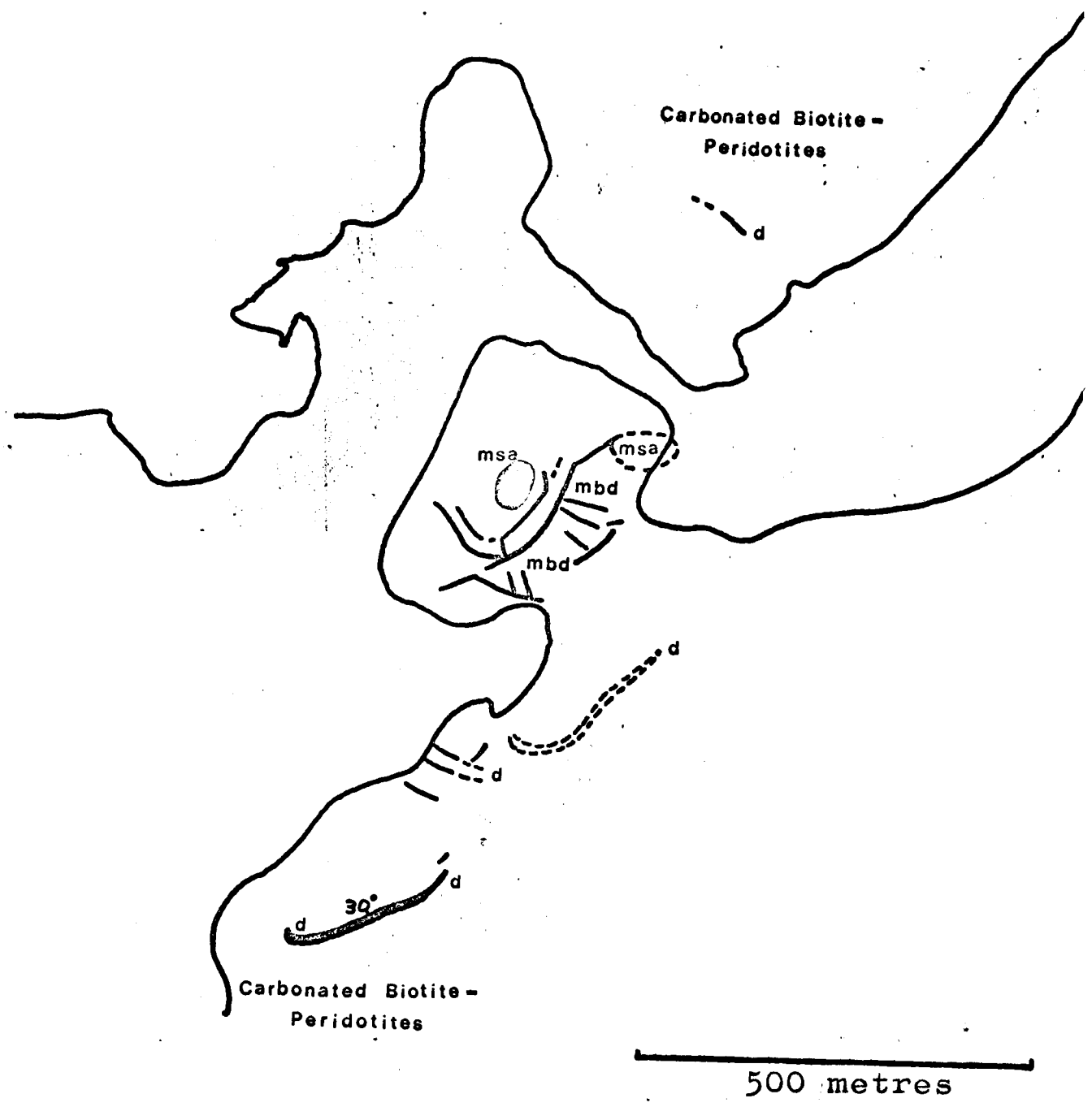
Apatite occurs in the matrix with granular quartz. It invariably forms rosettes of stubby crystals (presumably in spheres). This texture has been described by Wyllie, Cox and Biggar (1962) from synthetic carbonatite melts, where it occurs during quenching only with a hydrous vapour phase. Quench liquids precipitate the normal hollow acicular habit.

Around the rim of the plug, there is microgranite for 5-10m, the inner 3m of which shows a strong, vertical, concentric flow foliation, defined by sheared platy albite and platy quartz. This flow texture precedes the formation of the pipe for fragments of gneiss are caught up in the breccia. The intense shearing in these marginal rocks, the coarse nature of the phenocrysts, the rounding of the xenoliths, and the form of the apatite, suggest that the pipe material was intruded as a magma, rising under high volatile pressure in the manner of a salt dome, followed by explosive decompression, quenching due to loss of volatiles, oxidation of ankerite and degradation of biotite to serpentine. Such process of doming and fracture may explain the radial and cone sheet dolomite dykes which surround the vent.

DOLOMITE DYKES. In the immediate vent vicinity (c.100m), these dykes are equivalent magnetite-biotite-quartz dolomites. Many show chilling, in

FIG 7 - 1 SKETCH MAP OF THE CONE SHEETS AND RADIAL DYKES SURROUNDING THE DOLOMITIC BRECCIA PIPE

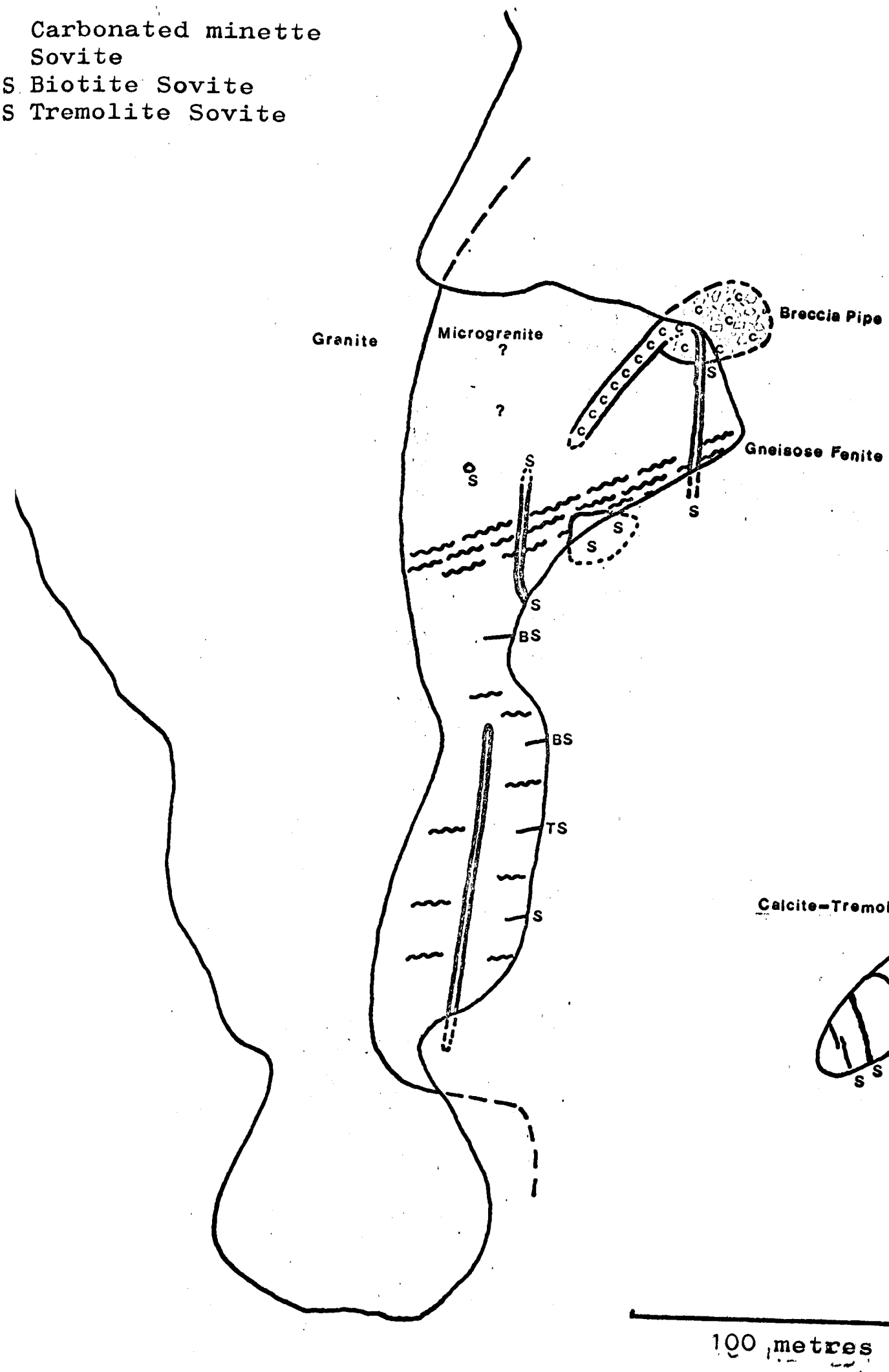
msa Magnetite-serpentine-ankerite carbonatite
mbd Magnetite-biotite-dolomite carbonatite
d Dolomite Carbonatite



The area marked Carbonated-Biotite-Peridotites is intruded by narrow dykes of that character filling a reticulate fracture pattern in the granodiorite.

FIG 7 - 2 **SKETCH MAP OF THE DISTRIBUTION OF CALCITIC CARBONATITES MARGINAL TO THE BIGSPRUCE ISLAND PEGMATITE CENTRE.**

C. Carbonated minette
S. Sovite
B.S Biotite Sovite
T.S Tremolite Sovite



one case with thin 0.05 x 1 cm curving plates of dolomite growing from the contact The chilled matrix is always composed of magnetite, dolomite and quartz. A typical point count shows

Ferroan dolomite	55%
Serpentine	0.5%
Biotite	35%
Magnetite	4%
Quartz	6%
Apatite	Trace

Beyond 200m the dykes are formed of microcrystalline, white, iron-poor, dolomite. The low angle dyke or sill ($\sim 45^{o}$ inward dip) is a breccia of such fragments, in a matrix of coarse dolomite. The margins of the body show a frothy intergrowth with bleached siliceous granite, rich in introduced stubby apatite. Similar metasomatism and similar veins of dolomite, fracture xenoliths in the pipe.

THE CARBONATED BIOTITE PERIDOTITE.

Within this outer zone, and extending beyond it, are several dark green biotite-dolomite dykes, clearly pseudomorphous after biotite-peridotite, the texture of the porphyritic pyroxenes and olivines being perfectly retained. To the north, at least, these become progressively less carbonated, until they grade into the chilled biotite-peridotite with fresh pyroxene (Chapter VI).

The formation of these replacement carbonatites occurs in two stages. First is the formation of pale green tremolite pseudomorphs, after pyroxene and olivine phenocrysts, and after amphibole in the matrix, and the development of a biotite-calcite-apatite-fluorite matrix, This is followed by the resorptionof tremolite to form dolomite, biotite and quartz.

Abundant oxide and a variable proportion of apatite are preserved in the matrix throughout. Possible reactions involved in this sequence are -

1. 5 Diopside + $3CO_2$ + $1H_2O \rightarrow$ 2 Quartz + 3 Calcite + 1 Tremolite.
2. 11 Diopside + 2 Forsterite + 5 CO_2 + $3H_2O \rightarrow$ 5Calcite + 3 Tremolite
3. 8 Forsterite + 13 Calcite + $9CO_2$ + $1H_2O \rightarrow$ 11 Dolomite + 1 Tremolite.
4. 1 Tremolite + 3 Calcite + $CO_2 \rightarrow$ 5 Dolomite + 8 Quartz + $1H_2O$.

Reactions 1 and 3 have been investigated experimentally, and equilibrium curves given in Winkler (1967) show that above PCO_2 = 0.2 kilobars at 1kb constant PCO_2 + PH_2O, the equilibrium curves for both reactions lie in the range 520 - 550^{o}C for a wide range of PCO_2: PH_2O. The curves are raised by circa 20^{o}C per kilobar. This temperature is in agreement with the lack of perthite in the reddened margins bordering the dolomite, and with the mechanical shattering of the quartz and feldspar.

THE CALCITE CARBONATITES.

The reaction sequence from minette to biotite-calcite carbonatite, differs from that described for dolomite series, in the general absence of tremolite. This difference probably results from the original presence of excess alkali aluminate in the form of orthoclase, and hence the substitution of reactions 5 and 6 for reactions 1 and 4.

5. 3 Diopside + 1 Orthoclase + 3 CO_2 + $1H_2O$ ⟶ 1 Biotite + 3 Calcite + 6 Quartz.

6. 3 Tremolite + 5 Orthoclase + $6CO_2$ + $2H_2O$ ⟶ 6 Dolomite + 5 Biotite + 12 Quartz.

On carbonation, the matrix is composed of biotite, quartz, and calcite, enclosing 30-50% of biotite and calcite pseudomorphs, after euhedral pyroxene phenocrysts. The form of the original oscillatory zoning is enhanced by the enrichment of the original titanaugite zones in biotite, presumably due to the entry of Ti, Fe^{3+}, and Al into the biotite structure. The carbonate is a ferroan calcite, as shown by staining.

The field relationship of the minette, breccia pipe, and calcite carbonatite, is shown in Fig 7-2. The texture of the "carbonated minette" dyke which is gradational into the vent, shows that it was intruded, and chilled, with a primary carbonatitic matrix. It possesses a light grey microcrystalline margin, composed of fine grained calcite, magnetite, biotite and apatite enclosing 10-15% of 1-2mm hexagonal biotite phenocrysts. Partially resorbed, rounded xenoliths, of minette or biotite pyroxenite are common (1 - 10% of the rock). The vent rock is similar to the chill, but is poorer in biotite phenocrysts, and contains a few percent of calcite pseudomorphs after pyroxene. It forms the matrix to unsorted round, angular, and disaggregated xenoliths of granodiorite, microgranite, northern foyaite chill, minette and biotite-carbonatite, suggesting a similar explosive origin to the dolomite pipe. Biotite is partially replaced by vermiculite, Both biotite and calcite have exsolved oxide.

A comparison of the modes of biotite-carbonatite (2,3) and carbonated minette (1) is given below.

	1.	2.	3.
Biotite	58.7	55.0	66.9
Magnetite	10.7	5.2	Trace
Calcite	20.3	34.2	25.4
Apatite	1.0	4.2	6.2
Fluorite	Trace	Trace	1.5
Sphene	9.2	Trace	Trace
Quartz	Trace	1.3	Trace
Zircon	tr	tr	tr
Pyrite	tr	tr	tr
Bastnasite	tr	tr	tr
Feldspar	tr	-	-

The carbonatite dykes are narrow (10cm - 2m) with very varied mineral proportions the commonest assemblages being

1. Biotite Sovite

Biotite	30 - 60%
Fluorite	2 - 10%
Apatite	1 - 8%
Calcite	25 - 60%
Magnetite	0 - 8%
Pyrite	Trace

Bastnasite, Allanite, Zircon, Hematite, Perovskite.

2. Bastnasite sovite

Bastnasite	1 - 5%
Biotite	0 - 5%
Calcite	80 -95%
Quartz	Trace - 3%

Allanite, Fluorite, Zircon, Magnetite, Hematite, Apatite pyrite.

3 Fluorite sovite

Fluorite	5 - 20%
Magnetite	2 - 5%
Quartz	Trace - 2%
Calcite	75 - 95%

Allanite, Bastnasite, Pyrite, Biotite.

Typically they are foliated, with aligned platey biotite, acicular apatite, or thin strings of allanite, bastnasite, fluorite or quartz. Sometimes this foliation has been contorted by post-crystallization shearing, or the biotite has recrystallized across the foliation. They show well developed chills against the granodiorite. Generally the dykes are homogeneous but the leucocratic sovites particularly, may show segregations of apatite at the walls, with poikilitic euhedral zircons and acmitic aegirine.

THE MINERALOGY.

a) Calcite: Calcite forms clear elongate interlocking rhombic crystals of iron poor composition. In sheared carbonatites it may show undulose extinction, multiple twinning, and ferroan calcite rims. There is no dolomite exsolution.

b) Biotite: Biotite forms thin plates pleochroic from khaki to pale yellow. In biotite sovites sometimes three generations of biotite may be seen; zoned hexagonal phenocrysts, thin irregular platey crystals in the foliation, and small plates at right angles to the foliation.
In the sovites and flourite sovites, it is segregated with bastnasite, allanite, and magnetite, but is rare and pale green in colour.

c) Fluorite: Typically fluorite is segregated into bands parallel to the foliation, and has a rounded, irregular, blebby outline. In association with bastnasite it shows a mauve discolouration. Blebs of fluorite in calcite and calcite in fluorite suggest co-tectic crystallization.

d) Bastnasite: Bastnasite ($(Ce,La,Dy)FCO_3$) is present in the heavy mineral concentrates of all the calcite carbonatites. It occurs as minute pale brown weakly pleochroic granules concentrated in the mafic or quartz laminae. In the biotite sovites it pseudomorphs an acicular mineral - ? allanite - or a larger mineral of rectangular cross-section - ? monazite. The bastnasite sovites with up to 5% of the mineral show strings of granules alone, or in quartz-tremolite-bastnasite lenticles.

e) Opaque Minerals: Magnetite, titanium poor, occurs as small cubes and octahedra in the apatite rich chilled biotite-sovites, particularly the breccias, and the fluorite sovites. Hematite, as thin plates, is pro-



PLATE 7 - 10 Biotite - sövite breccia. The blocks are dominantly rounded fragments of shattered granodiorite, but include biotite-pyroxenite (lower left) and chilled foyaite (upper right). Breccia pipe transitional into chilled dyke. Spec. locality 68068.

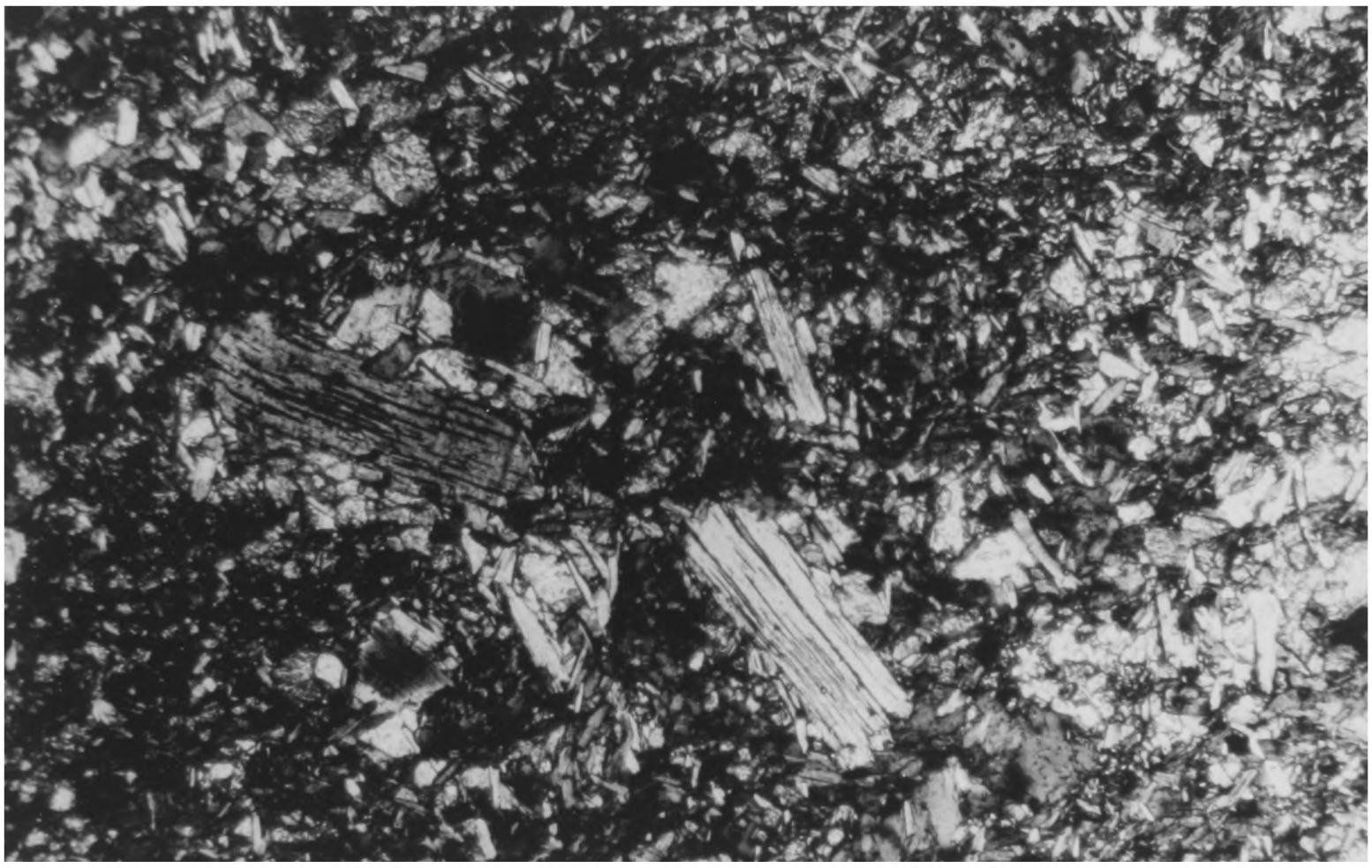


PLATE 7 - 11 Biotite phenocrysts in a biotite sövite dyke. 50cm dyke in S. foyaite. Spec. 67228 x 6.



PLATE 7 - 12 Quartz veins in a bastnäsite sövite mass. The bordering granodiorite is not fenitized. Shore west of Bigspruce island.

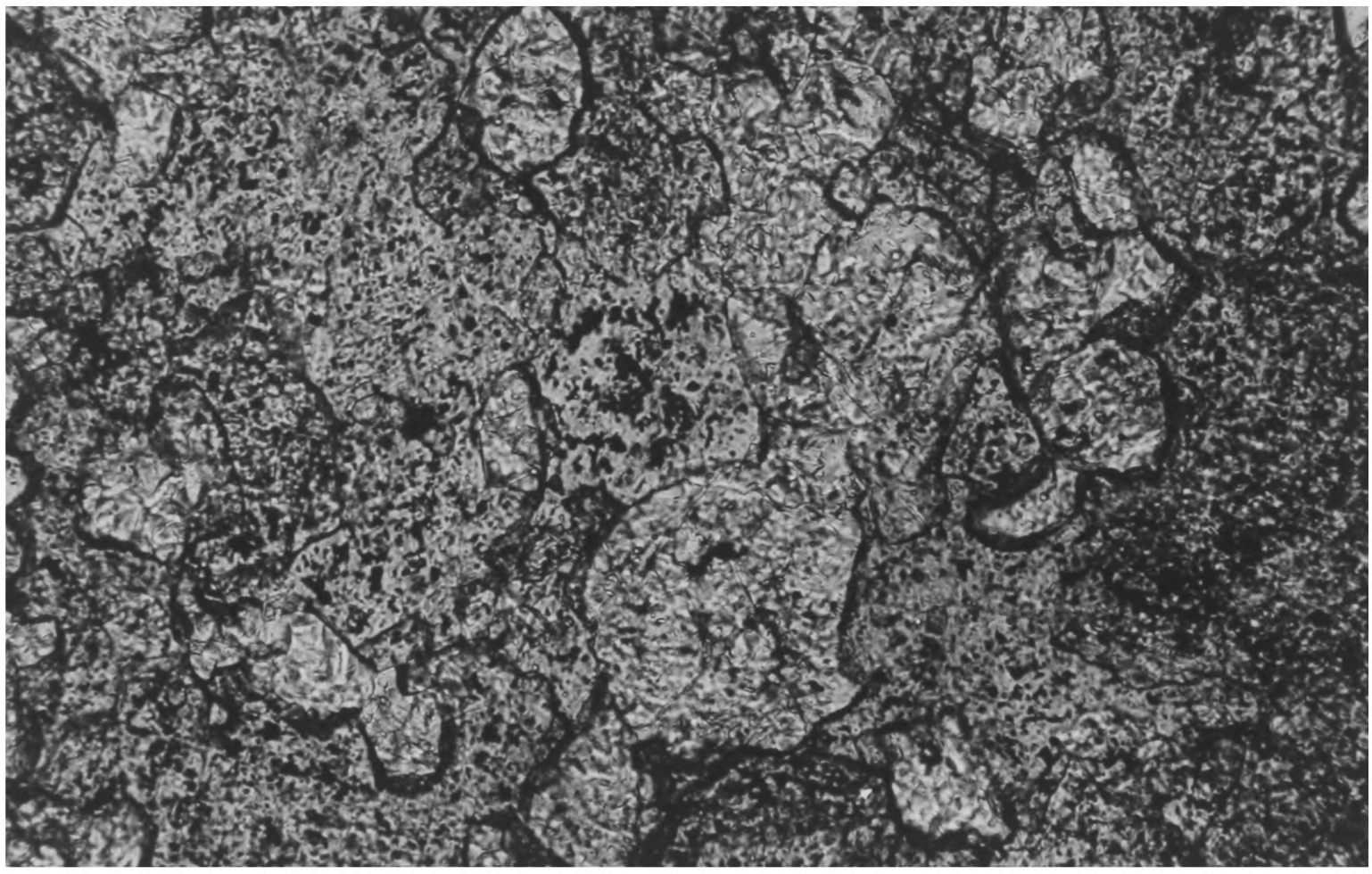


PLATE 7 - 13 Globular intergrowths of fluorite and calcite in a fluorite-sovite. 1m dyke, N.E. corner of Snare River outlet. x 20.

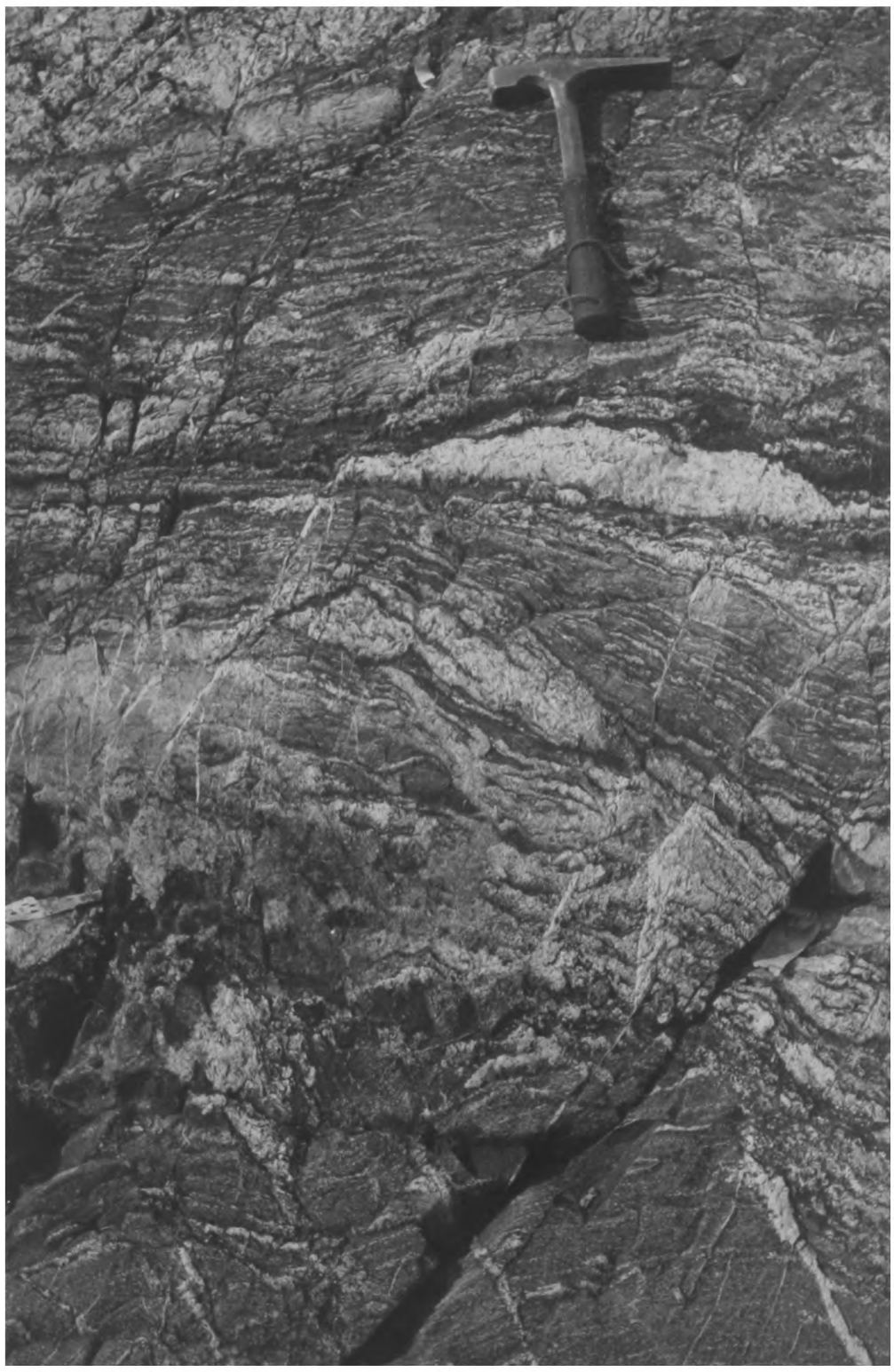


PLATE 7 - 16 Quartz-sericite gneissose fenite. The fenite occupies shear zones radiating from the sövite pegmatite centre, in the microgranite fenite (see fig 7-2).

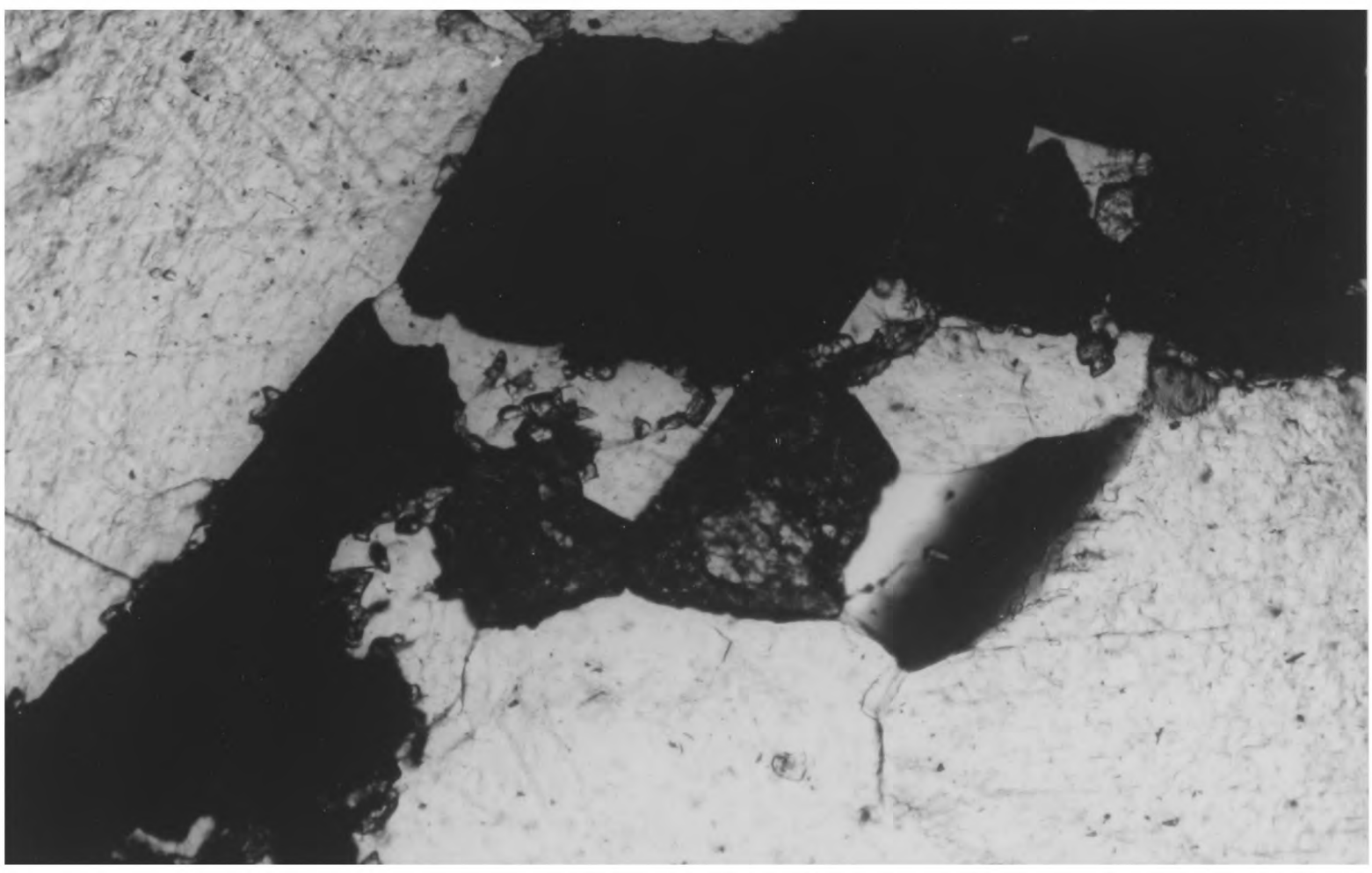


PLATE 7 - 17 Pyrochlore bordering titanomagnetite. Biotite - magnetite - calcite pegmatite, Bigspruce island x 40.

bably secondary. Rutile is exsolved by biotite and included in the bastnasite-sovite quartz. Pyrite is a rare but universal accessory.

f) Amphibole. Pale blue-green tremolite, as euhedral acicular crystals embedded in calcite forms the major phase of the few tremolite-pink sphene-calcite carbonatites. Tremolite, as minute needles, is a rare accessory, generally associated with quartz, in the bastnasite sovite.

g) Apatite: Apatite decreases in quantity progressively from the biotite-sovite breccia to the bastnasite sovite. It occurs as short stubby crystals. The ratio of length to breadth increases sharply in carbonatite chills. Many chilled crystals have a central channel filled with calcite. Clots of apatite parallel to the foliation are common. Evidence of early crystallization and strong crystal settling is given by the layered vesicles in the biotite-peridotite fenite, and by vesicles in the carbonated minettes, found on reefs west of Bigspruce island.

h) Quartz: Quartz is a primary constituent of all the carbonatites owing to the breakdown of the calc-silicates during carbonatite formation. It is most abundant in the biotite sovite breccia, and in the bastnasite carbonatite It forms small clear grains with included tremolite bastnasite, calcite and oxide and with exsolved rutile.

i) Dolomite: Although many specimens have been examined using stained acetate peels no exsolution textures have been observed. Small pebbles of carbonatite composed of 1-3cm curved dolomite plates (75%) in a matrix of poikilitic calcite (25%) have been washed up on the north-east shore of Bigspruce and Littlespruce islands. The source of this carbonatite is unknown but may lie within the area of the closed aeromagnetic minimum northwest of Littlespruce island.

j) Trace Minerals: Zircon, apatite, tremolite, quartz, magnetite and pyrite are found in all heavy mineral concentrates. Allanite has been tentatively identified from the biotite sovites in the x-ray powder pattern.

THE BIGSPRUCE ISLAND PEGMATITES.

The Bigspruce island carbonatites are nowhere well exposed, the outcrop being confined to a few shore sections, and a few overgrown trenches inland. It is regarded as the centre of the sovite activity by virtue of its fracture pattern, the intense metasomatism, and the zoned pegmatites.

THE METASOMATISM.

The carbonatite centre is intruded entirely into the northern foyaite near its western margin. Unaltered foyaite occurs around the eastern, northern, and western sides and in a cancrinitized form on the south side also. With the exception of well defined shear zones, where cancrinite rocks are found, the foyaite passes directly into the metasomatised area without carbonation of the nepheline.

The transition occurs over a broad ill-defined zone with the formation of euhedral poikilitic porphyroblasts of aegirine growing around nepheline, and the loss of orthoclase through corrosion and resorption. The feldspar



PLATE 7 - 1

Aerial photograph of Bigspruce island (pre-flooding). The carbonatite pegmatite, cone - sheet and radial - dyke centre of Bigspruce island, and the cone - fracture pattern of the gas - escape vent B, are readily apparent. Note the densely forested nature of the complex.



is replaced by sericite, or nepheline, or aggregates of nepheline and aegirine. The rock therefore passes from a foyaite into an ijolite and then through further growth of the coarse aegirine, and resorption of the enclosed nepheline, into malignite with up to 85% pyroxene. Magnetite which invades the foyaites as solid magnetite veinlets, grows in the metasomatized rocks as cubic porphyroblastic crystals forming aegirine-magnetite-nepheline rocks - jacupirangites - or magnetite-nepheline rocks.

The metasomatised ijolites may be distinguished from the ijolite breccias by their coarser irregular grain size, and large 1-5cm porphyroblastic aegirines and magnetites. Nepheline phenocrysts are absent from the metasomatic rocks.

The greatest intensity of replacement - malignites and jacupirangites - occurs just to the west of the diamond shaped centre to the pegmatite fracture pattern (see aerial photograph).

THE CARBONATITE PEGMATITES.

The fracture pattern is outlined by steep sided 30 - 60m cuts crossing the island at close to lake level. Where these cross the shore, beach sands of biotite, aegirine and magnetite are formed around protuding reefs of aegirine - biotite - magnetite - calcite pegmatite.

The latter show a crude zonation, with, margins composed of coarse 3 - 20cm bladed aegirine, and thick books of 1 - 3cm biotite, in a fine white calcite matrix, and coarse 5 - 10cm white calcite containing lenticles of magnetite at the centre. Several of the outcrops show evidence of multiple intrusion with biotite rimmed magnetite masses at the pegmatite margins and crosscutting calcite veinlets.

The magnetite in the pegmatites is strongly zoned with a titanian core.

The calcite in the aegirine - biotite marginal zone coexists with a primary orthoclase rich perthite. The pegmatites are bordered by a zone of scapolitization of nepheline and cancrinite.

The presence of unexsolved primary orthoclase perthite, the coarse mineralogy and the extensive replacement reactions suggest a higher temperature of intrusion for these carbonatites than for those in the outlying areas. The zoning of the magnetite, the zonation of the pegmatites, the multiple intrusion and the replacement reactions suggest that they may have crystallized over a considerable temperature interval.

The zonation of the rock types on Bigspruce island presents many similarities to the concentric zonation found in the classical type of carbonatite ring intrusion. This may be idealized as -

rim	1.	Foyaite
	2.	Ijolite
	3.	Malignite + Jacupirangite
core	4.	Carbonatite.

It is clear that in this case the zonation results from replacement reactions from the foyaite country rock, and that the foyaite is a much earlier, separate, igneous intrusion and is not a fenite.

TABLE 7 - 1. TRACE ELEMENT CONTENT OF CARBONATITES.

	68401	68140	68020	68068	68117	67228	68133	67199		67163	68047	68116	2716		68165	68159	68110	68114	68223
TiO_2	2.23	-	2.37	2.16	0.598	0.660	0.116	0.0131		0.0010	0.010	0.003	0.004		4.35	2.73	2.75	0.003	0.062
MnO	0.20	-	0.20	0.64	-	0.58	-	-		1.27	1.7	-	-		0.26	0.21	0.71	1.24	-
P_2O_5	0.65	-	1.68	-	-	-	-	-		-	-	-	-		0.41	0.39	-	-	-
La	275	-	173	547	938	561	485	680		1,980	7,230	1,650	1,300		150	72	636	1,820	2 300
Ce	138	-	383	1,295	2,160	1,480	1,280	1,720		6,450	12,500	6,110	4,300		140	50	1,750	4,540	7,720
Y	29	-	39	71	11	162	44	117		118	83	188	197		25	< 2	73	172	601
Rb	230	201	173	212	179	514	260	5		< 5	< 5	< 5	< 5		48	35	19	< 2	26
Sr	941	929	1,069	1,483	3,250	5,440	5,290	6,070		2,770	2,010	15,910	19,320		408	465	680	411	921
Zr	253	309	165	299	224	514	460	130		129	<2	719	325		242	163	155	158	705
Nb	33	26	24	86	196	110	200	80		193	49	<2	< 2		40	21	104	20	79
Ba	2,280	-	3,089	1,187	2,680	1.350	643	614		373	643	422	267		1,094	581	259	12	230
Sr87/86	On separated calcite									0.7027								0.7021	
K/Arage	On separated biotite					1810	1835												

68401. Minette centre 4.
68140. Minette centre 1.
68020. Biotite·pyroxenite centre 4.
68068. Carbonated minette dyke linked to breccia pipe.
68117. Carbonated minette breccia.
67228. Biotite-sovite dyke.
68133. Biotite fluorite-sovite.
67199. Fluorite sovite.
67163. Bastnasite sovite.
68047. Bastnasite sovite.
68116. White covite vein.
2716. White sovite vein.
68165. Chilled Biotite Peridotite.
68159. Coarse Biotite peridotite.
68110. Dolomite breccia from pipe.
68114. White dolomite dyke.
68223. Quartz-apatite replacement after dolomite dyke.

THE CHEMISTRY OF THE CARBONATITES.

Table 7 - 1 summarises the trace element concentrations determined on the groups of carbonatite rocks and the rock types from which they are believed to be derived.

The carbonatites and the high potassic rocks are characterised by high to very high Ce, La, Sr and Ba. Y, Rb, Zr and Nb are relatively concentrated in most, but not all, of the rocks. These enrichments are typical of many carbonatites, kimberlites, and high potassic rocks in general but most atypical of sedimentary limestones, or of most other rock types in the complex. Thus those rock types in the complex that are enriched in Sr and Ba are depleted in Ce, La, Y, Rb and Nb, and vice-versa.

Within each series the carbonated breccia shows a similar composition to the unaltered biotite-pyroxenite or biotite-peridotite, and there is a consistent gradational increase in La, Ce (La/Ce: 1/3 constant), Y, Sr and Mn, and decrease in Ba and Rb. Each group of carbonatites; biotite sovites, fluorite sovites or bastnasite sovites shows only a small range of composition. These features are thought to indicate a lack of significant country rock contamination.

The S_r isotopic composition on separated non-magnetic residues consisting of calcite, fluorite, and minor quartz and apatite give the very low values of 0.7021 ± 0.0024 and 0.7027 ± 0.0024 despite the low concentration of Sr (411 ppm) in the lower of these two rocks. These values are consistent with the average $Sr\frac{87}{86}$ for world carbonatites of 0.7032 (Powell *et al* 1966). The calculated $Sr\frac{87}{86}$ in the country rock granodiorites at the time of intrusion (1800 m.y. approx.) is circa 0.734. The concentration of Sr in these is circa 150 ppm. Significant contamination of the carbonatite by the granodiorite can therefore be practically ruled out. Since the carbonatites possess similar or greater concentrations of Ce, La, Sr Ba, Y, Rb, Zr and Nb to the high potassic rocks, and are believed to be derived from them, there seems to be strong reason to reject the hypothesis that the high potassic rocks have been derived by the blending in appropriate amounts (or partial melts) of granitic country rock (providing Si, K, Rb, Ba) and carbonatite (providing Sr,La, Ca, Cr, Ni, Mg, V and Ti) as suggested by Holmes (1950), and Higazy (1954). A similar hypothesis using monchiquite in place of carbonatite to produce high potassic rocks has been suggested by Williams (1936), and suffers from the same objection.

Origin: Recent reviews on the occurrence and origin of carbonatites have been given by Pecora (1956), Smith (1956) King and Sutherland (1960), Garson (1965), Tuttle and Gittins (1966) and Heinrich (1966). Experimental data bearing on their origin has been summarised by Wyllie (1966). As a result carbonatites have become accepted as a widespread, low temperature magmatic phenomena associated with continental alkaline igneous complexes. Their regional association with high potassic rocks, particularly kimberlites, has generally been noted.

Four main types of theory for their origin have been proposed -

a) Carbonatite magmas are primary, and possibly alkaline, and of mantle origin (Dawson 1964, Holmes 1950, von Eckermam 1948).

b) Carbonatite magmas are differantiates produced by fractional crystallization of an alkaline ultrabasic magma rich in volatiles (King 1965 Erickson and Blade 1963, James 1959, Saether 1958).

c) Carbonatite magmas are immiscible fractions of an ultrabasic peridotite, ijolite or melilite basalt magma (Koster van Groos 1967, von Eckermann 1961.).

d) Carbonatite magmas are generated through a series of crystal-liquid-fluid reactions from carbonated ultrabasic magmas (Heinrich 1966, Kukharenko and Dontsova 1964, Tomkeieff 1961).

The CO_2 is generally accepted as being of mantle origin in agreement with Roedder's (1965), observation that liquid CO_2 inclusions are common in the minerals from deep seated nodules. The parent magma is generally thought to be either a kimberlite, or an alkali peridotite or a melilite basalt on the basis of field or petrologic or petrochemical observations.

Wyllie 1966) has demonstrated (a) the existence of low temperature (800- 550^{o}C) synthetic carbonatite liquids comparable to the observed carbonatites,

(b) the existence of a limited miscibility gap between alkali silicic and alkali carbonate liquids;

(c) the possibility of alkali subsilicic liquids giving rise to carbonate liquids through the fractionation of olivine, biotite and pyroxene. An alkali carbonate liquid once generated could persist without reaction with the surrounding silicic phases.

There is strong field evidence at Bigspruce lake in the form of dykes and xenoliths that the parent magma was of biotite-peridotite or biotite-pyroxenite composition. The presence of fluid inclusions within the pyroxenes indicates the volatile-rich nature of these magmas. Rounded calcite vesicles within the chill of the biotite-peridotite, similar to those described from Alno by von Eckermann (1966) suggest the separation of a calcite rich liquid without reaction during the early stages of crystallization. The low viscosity of this liquid is indicated by the settling of apatite, (and oxide) in the vesicles from the biotite-pyroxenite, minette, and associated fenites. This liquid persisted and crystallized without reaction with the silicates in these rocks.

The presence of vesicles need not imply immiscibility, since the carbonate fraction would be expected to persist to lower temperatures, after the crystallization of the majority of the silicate minerals.

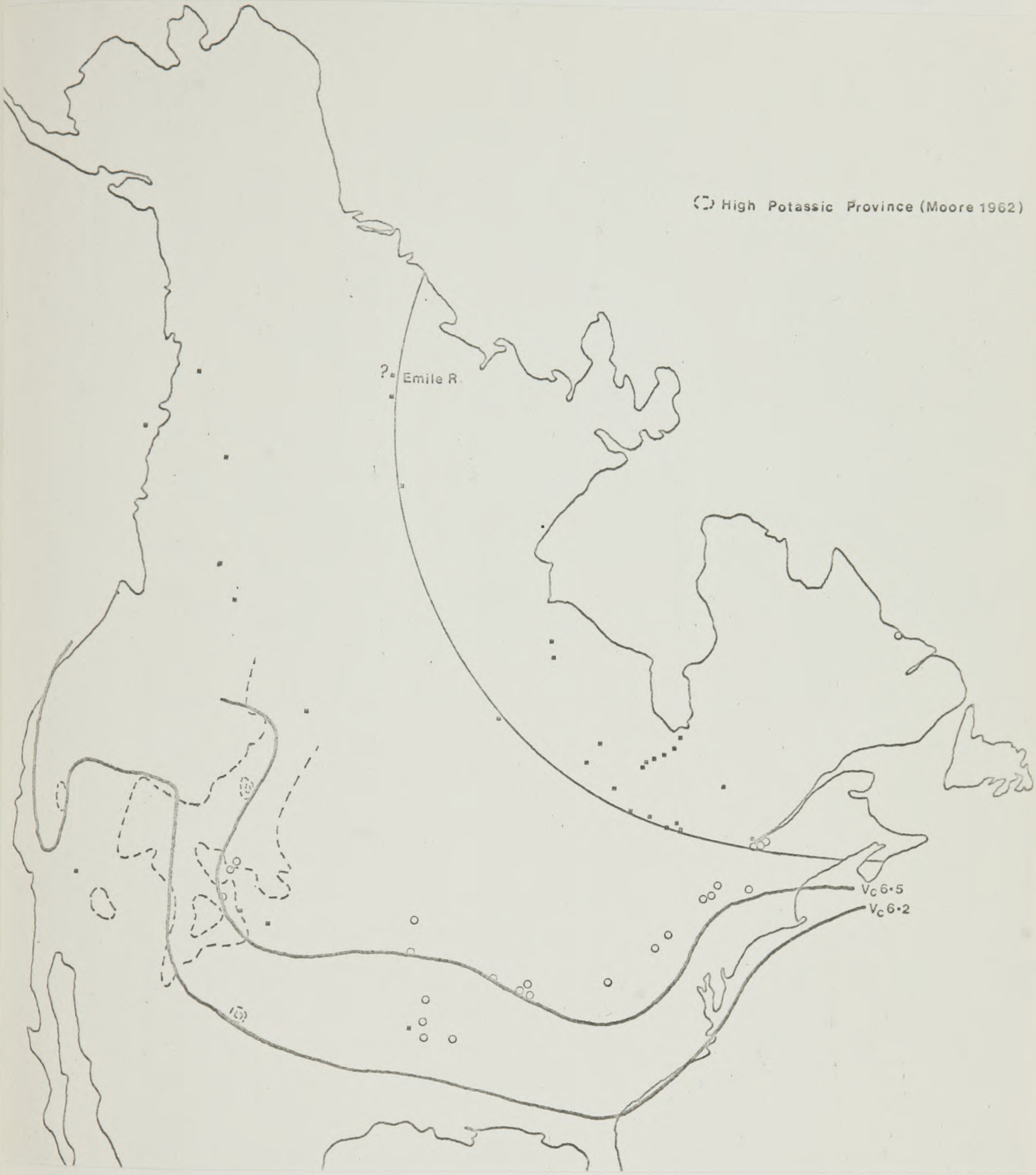
In the presence of excess CO_2 and H_2O, if this carbonate liquid is retained within the structure of the crystalline rock, below 550-600^{o}C, crystal-liquid-vapour reactions involving the formation of biotite, tremolite and calcite are likely to take place. These reactions are believed to result in the formation of secondary carbonatites as are

FIG 7 - 3 DISTRIBUTION OF THE NORTH AMERICAN CARBONATITES AND KIMBERLITES



Data compiled from Gittins (1966), Heinrich (1966), Watson (1967) and Gittins (1967).

FIG 7 - 4 DISTRIBUTION OF NORTH AMERICAN CARBONATITES AND KIMBERLITES IN COMPARISON WITH THE REGION OF HIGH MEAN CRUSTAL VELOCITY.



The mean lower crustal velocities are from Pakiser and Zietz (1965).
The carbonatites appear to lie along three main zones:

(a) Just within the Vc 6.5 km/sec contour
(b) Along the Kupaskasing arch (Gittins 1967)
(c) Along the North side of the St. Lawrence & Great Lakes;
Possibly along a Laurentian rift system (Kumarepelli and Saull 1966)

These zones crosscut age-province and formation boundaries.

found in the ankerite-dolomite and biotite + calcite to calcite + bastnasite carbonatite series. The resulting carbonatites contained derived xenocrysts but were true liquid magmas capable of chilling. Relative to the earlier carbonatites they are enriched in Ba and Nb, contain biotite, and lack significant aegirine or allanite.

Age and location: Potassium-argon ages of 1810 ± 22 m.y. and 1835 ± 32 m.y. have been obtained from biotites from the biotite-sovites (Lambert pers comm). With the possible exception of Palabora, which Holmes and Cahen (1957) have tentatively placed at 2060 m.y.,this is the oldest known carbonatite complex. Gittins (1967) has noted that the carbonatite ages from Eastern Canada fall into four major groupings at 1700 m.y, 1075 m.y, 565 m.y, and 125 m.y, the oldest two of which correspond approximately to the Churchill and Grenville province ages respectively. Ginzburg (1962) has noted that the age of alkalic bodies in the marginal parts of shields is commonly close to the age of the folded areas bordering them, and that many such intrusions are emplaced in the marginal seams, or faults, which bound the platforms. Map8-13 shows that the Bigspruce lake intrusion lies on the Snare lineament. This is a 175 mile transcurrent fault, which forms a major structural feature at the Slave-Bear province boundary (Wilson 1941).

The age of granites intruding the Bear province is circa 1850 m.y. (Stockwell 1964), and hence similar to the age of the complex.

Fig. 7-4 shows the distribution of carbonatites and kimberlites in the North American continent. It can be seen that both are strongly grouped into curvilinear belts.

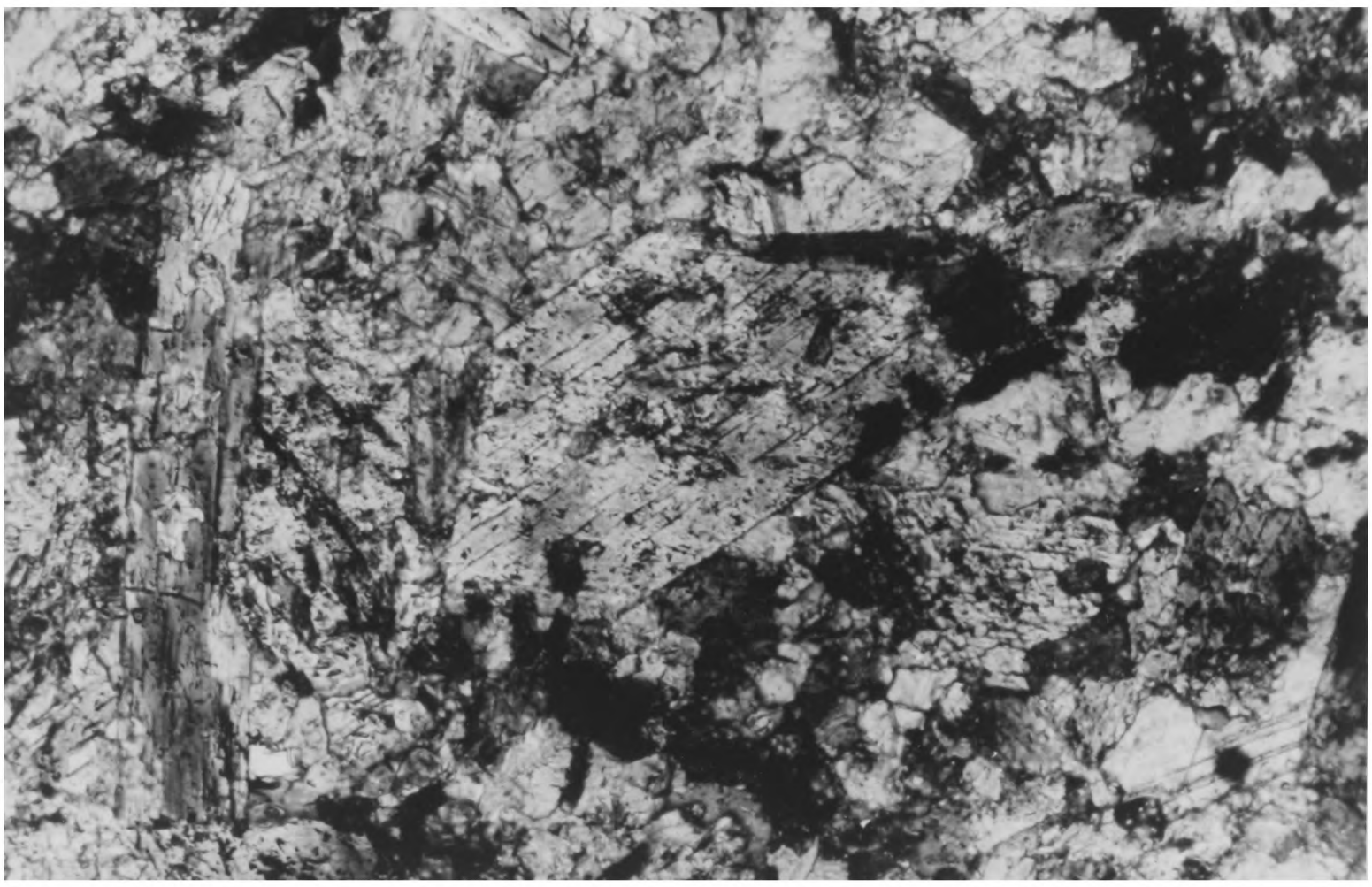
The more recent, mostly post Jurassic, American kimberlites, and high potassic provinces (Moore 1962) bound the "shield" area as outlined by the outer limit of the area of high mean crustal seismic velocity determined by Pakiser and Zietz (1966). A narrow line of carbonatites follows the axis of the Kupaskasing gravity and magnetic high from near Kupaskasing to James Bay (Gittins 1967). A third zone runs approximately east-west from Oka to Prairie Lake along the north shore of the Great Lakes.

Gittins has pointed out that these belts crosscut the structural province boundaries and contain carbonatites from several of his age groupings, in a single line. Similar persistent characteristics are known from the Kola peninsular, and the East African rift. They suggest that the location of these complexes results from deep zones of flexure or fracture bordering continental blocks, extending into the lower crust or upper mantle.

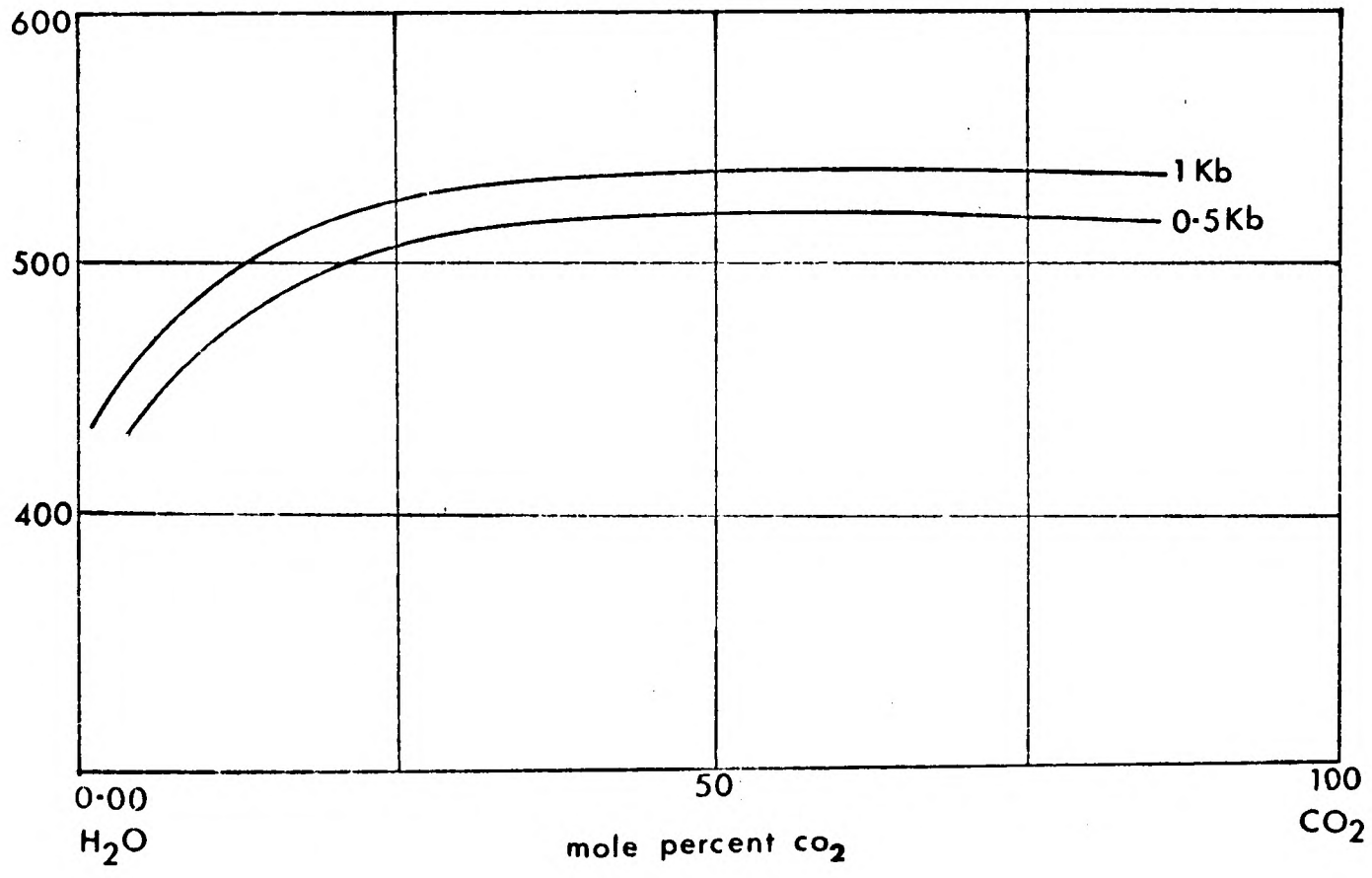
The location of Bigspruce Lake on the Snare lineament at the margin of the Slave province would seem sufficient reason for its presence. However, Lambert (pers comm) has pointed out that the complex lies near the extrapolation of the east-west carbonatite belt. In fact an arc may be drawn through this belt and through Bigspruce Lake on which lie the carbonatites of Nissikatch Lake, and Red Lake and a small isolated limestone body (? an undescribed carbonatite) west of the Emile river. This arc is

FIG 7 - 5 EQUILIBRIUM CURVES FOR THE COEXISTING MINERALS

TREMOLITE + CALCITE + QUARTZ



Euhedral tremolite in the tremolite carbonatite. The matrix is calcite with 3-4% quartz. The dark material is dominantly sphene. The co-existance of calcite, tremolite and quartz gives a maximum temperature of formation at 1Kb of 540°C.



EQUILIBRIUM CURVES FOR THE REACTION

$$1\ \text{Tremolite} + 3\ \text{Calcite} + 2\ \text{Quartz} \rightleftharpoons 5\ \text{Diopside} + 3CO_2 + 1H_2O$$

From Winkler (1961). The maximum temperature for this reaction at 1Kb (at 75% CO_2) is 540°C.

subparallel to a second arc linking the Western Canadian carbonatites. Such gross extrapolations can only be confirmed if further exploration locates more carbonatites in the largely unexplored area near the centre of the arc.

CHAPTER VIII.

THE REGIONAL GEOLOGY, GEOCHEMISTRY, AND GENERAL TOPICS.

Brief mention of the high degree of structural control involved in the location of the alkaline intrusion has been given in chapter VII. This structural environment can here be considered in more detail.

GENERAL. Within a region bounded on the North by the Arctic coast, on the West by the Palaeozoic sediments, and to the South and East by the Great Slave and Bathurst lineaments Jolliffe (1948) and Wilson (1948) have recognised four structural and metallogenic subprovinces. From North to South these are: -

1. The Great Bear subprovince: Proterozoic formations - Snare, Coppermine, and Arctic sedimentary and volcanic series; North-east trending dextral faults; U-Ag-Cu-Ni-Co mineralization.

2. The Yellowknife subprovince: Archean formations - Yellowknife sedimentary and volcanic series; North and North-west sinistral faults; Au mineralization.

3. The East Arm subprovince: Proterozoic formations over Archean formations - Wilson and Et-Then sediments and lavas, in a graben bounded by; North-east dextral faults; Cu-Co-Ni-Au mineralization.

4. The Taltson subprovince: Archean and reworked Archean formations - Tazin and Nonacho sedimentary and volcanic series; North and North-west sinistral faults; Ag - Pb - Au mineralization.

Stockwell (1964) has distinguished the East Arm and Taltson subprovinces from the Slave subprovince on the grounds that although the batholiths, sediments and volcanics are largely of Yellowknife age these have dominantly been modified by a later event to yield (K-Ar) ages similar to those of the Churchill province (c.1750 m.y.).

The Great Bear subprovince may be subdivided so as to distinguish the Coppermine region with its undeformed series of shallow water sediments and its volcanics, from the metamorphic basement.

The Yellowknife subprovince (Slave province).

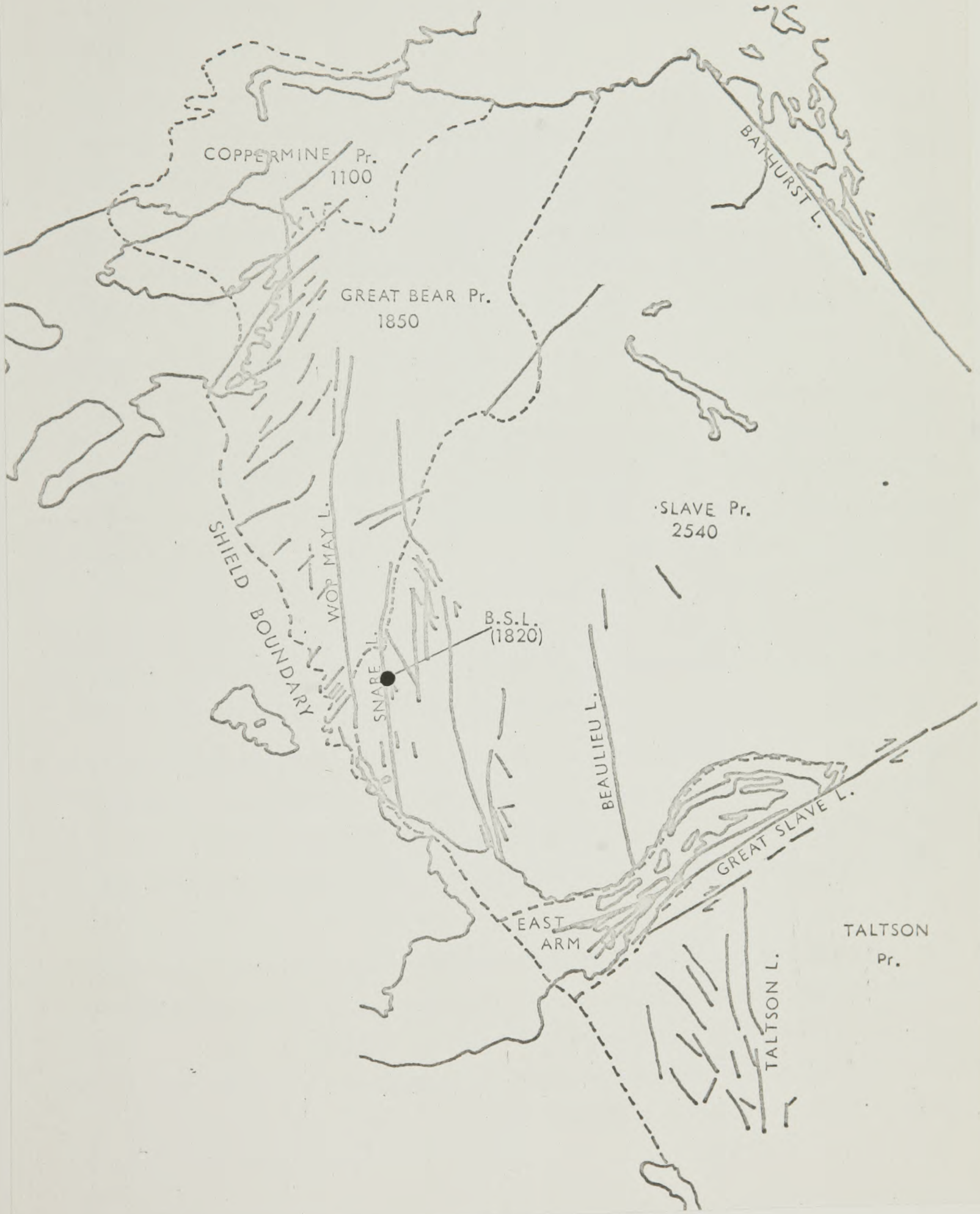
The Yellowknife subprovince is composed of regionally metamorphased sediments and volcanics of the Yellowknife series, and of intrusive batholiths of granodiorite composition. The Yellowknife series is composed of a lower sequence of volcanics, and an upper sequence of sediments. It typically forms irregular strips up to 100 miles across, separated and intruded by the batholiths. The volcanic sequence commonly forms discontinuous narrow lenticles at the margins of the sedimentary regions.

The Yellowknife series near the type locality has been described by Henderson and Brown (1952) and Baragar (1966). The lower part consists of a thick series of calc-alkaline and tholeitic pillow lavas passing upwards into intermediate lavas and pyroclastics in two cycles, with a total thickness of at least 40,000 ft (c.12,000m). This is overlain with regional conformity, by a thick sequence of graded greywackes

MAP 8 - 1 FAULTS, LINEAMENTS AND STRUCTURAL PROVINCES IN THE NORTHWEST CANADIAN SHIELD

STRUCTURAL ENVIRONMENT OF BIGSPRUCE LAKE

Showing the major faults and lineaments (after Jolliffe 1948)



The ages of the provinces are from Stockwell (1964). Note how the intrusion lies on the Snare lineament and is slightly younger than age of uplift of the Great Bear province.

silts and shales of turbidite character. Towards the northeast the sequence thins to 7,000 ft (2,100m) and the acid horizons become less abundant. Towards the south-east the sequence passes into the Wilson island group whose cross-bedded orthoquartzites, conglomerates, and sub-arkoses appear to be of fluviatile origin. Beneath this series occur dolomites and argillites. The Wilson island group may thus be a shelf equivalent of the eugeosynclinal Yellowknife series (Hoffman 1968).

The basement on which the Yellowknife series was laid down is nowhere exposed. Although Baragar (1966) presumes a gneissic basement, Green (1967) has pointed out that the primitive (0.7022 ± 0.0023) $Sr^{87/86}$ isotopic ratios of the lavas, combined with the close geochemical similarities to circumoceanic Tertiary and Quaternary lavas in areas lacking a sialic crust (e.g. Marianas and Aleutians) suggest a derivation from mantle material without significant crustal contamination.

Green has interpreted the Yellowknife event in terms of the gradual development of a segment of sialic crust. The oldest lavas (2625m.y Rb-Sr, 2615 K-Ar) were laid down on oceanic crust possibly as part of an island arc system. They were followed by geosynclinal sediments, in part cannibalistic on the early formed lavas and on early granodioritic intrusions (2610 m.y. Rb-Sr). A period of folding was accompanied by the intrusion of quartz diorites and monzonites with low $Sr^{87/86}$ ratios and by the extrusion of acidic lavas. - A second period of folding accompanied by partial melting in the pile of basic lavas gave rise to the true granites with high $Sr^{87/86}$ ratios (2,540 Rb-Sr).

The Yellowknife series has undergone regional amphibolite facies metamorphism. Around the margins of many of the batholiths quartz-mica schists, hornfels, and "knotted schists" containing metacrysts of andalusite, garnet, staurolite, and cordierite have developed (Folinsbee 1941, Lord 1942, Ross 1966).

The basement in the Slave province has been only weakly affected by the Hudsonian orogeny yielding biotite K-Ar ages in the range 1800-2200 m.y., whilst retaining muscovite ages in the region of 2460 m.y. (Stockwell 1964) It thus appears to have formed part of the shield before the Snare event and cannot have been overlain by a great thickness of sediment at that time.

Two main periods of faulting may be distinguished. The earlier period is syntectonic and forms the Au and sulphide mineralized chlorite shear zones. The later period is represented by north and northwest sinistral faults. Some of these are intruded by diabase dykes presumed to be synchronous, and previously supposed to be of the Mackenzie dyke swarm (1,315 m.y. K-Ar). However, similar north sinistral faults belonging to the same system show pre- and syn- Bigspruce lake intrusion displacement, and south of Ghost lake one diabase dyke in such a fault gives an age of 2,100 m.y.

One consequence of the work at B.S.L. is that these faults can now be referred back to at least the 2,200 m.y., north-south Yellowknife dyke swarm (Fahrig and Wanless 1963).

The Great Bear subprovince (Bear Province).

The Great Bear subprovince shows much similarity to the Yellowknife subprovince. It consists of a thick series of geosynclinal sediments lying to the west of the shield (Slave province), and shows Buchan type metamorphic aureoles around an interlocking pattern of granodiorite and monzonite batholiths. No basement is exposed west of the zone of offlap from the Slave province.

The Snare sedimentary sequence consists of basal conglomerates, white orthoquartzites and algal dolomites, succeeded by a thick series of laminated black shales, silts and thin graded greywackes (Lord 1942, Wilson 1965, Ross 1966). Volcanics are only of local extent, consisting of andesites, and dacites. They occur predominantly in the upper part of the sequence.

The present Slave-Snare contact runs approximately north-south along the extension of the shelf-eugeosynclinal facies transition exposed along the Arctic coast and for 100km south. The boundary is therefore thought to lie close to the continental shelf margin at the time of deposition of the Snare sedimentary series.

In the East Arm subprovince, continental, fluviatile and shelf sediments including oolites, red shales, and evaporite horizons pass southwest into basinal facies as the southern continuation of this trend (Hoffman 1968).

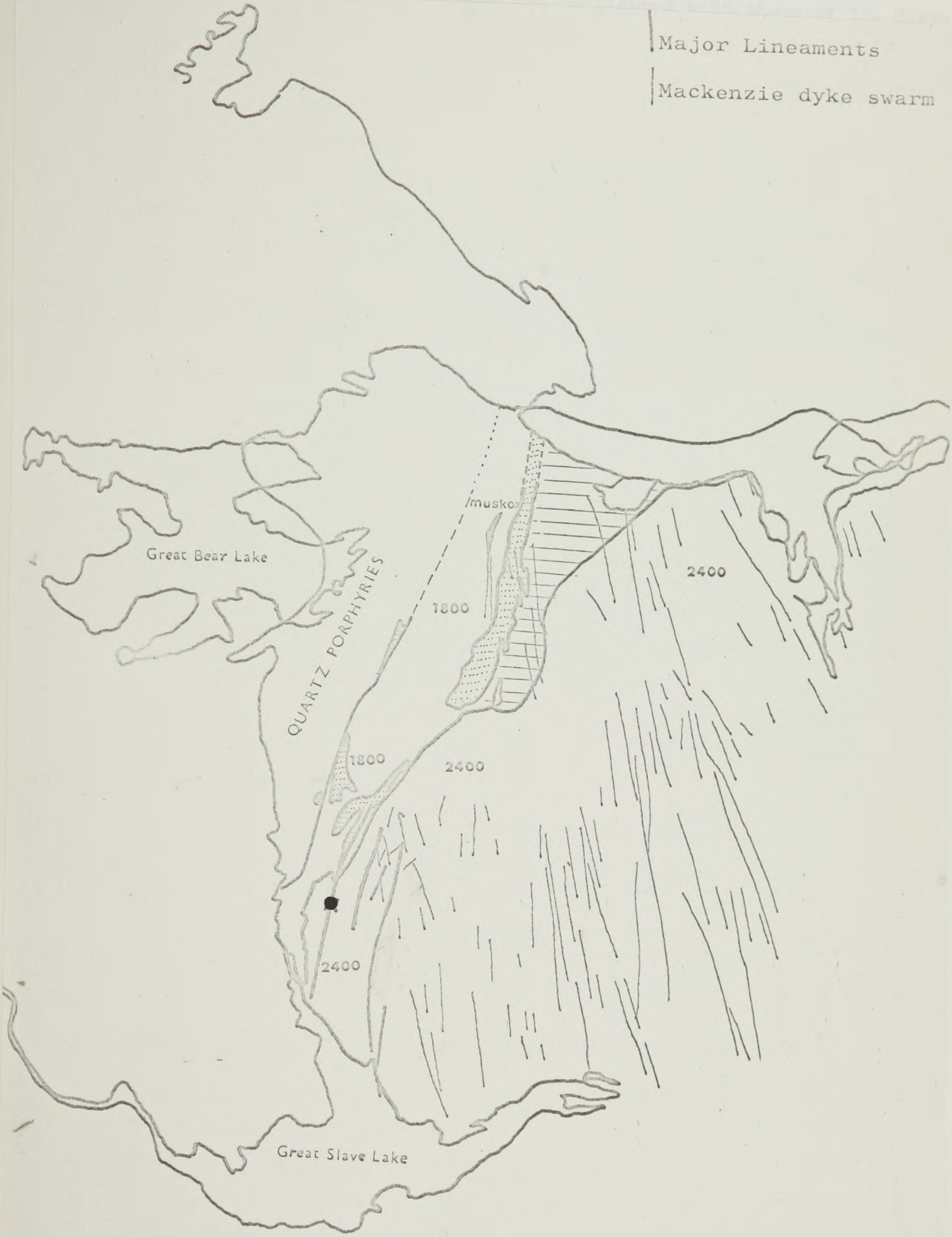
A north-south axis for the Snare geosynclinal belt is further supported by the presence of a 25km broad zone of feldspar and quartz porphyry intrusions running from inliers within the Ordovician cover at Tomi lake northwards to the east edge of the Great Bear Lake. This zone is also the area of pitchblende, copper and cobalt mineralization (Kidd 1936, Lord 1942).

The intrusions consist of 1-2km stocks, sills, and flows of rhyolite, dacite and quartz latite, and are associated with extensive hydrous metasomatism, epidotization and silicification. They form the only extensive post-orogenic volcanic activity of the Snare belt. They are of similar age both to the Snare granodiorites, and to Bigspruce lake.

The batholiths occupy 65% of the area of the Great Bear subprovince and are indistinguishable from the porphyritic granodiorites, diorites and monzonites of the Slave province. They also include late potassic tourmaline-pegmatite rich granite bodies. The associated thermal aureoles include silliminite, andalusite, cordierite, and garnet.

The regional grade is low greenschist facies and decreases south and east in the direction of Bigspruce lake so that unaltered sediments overlie the Yellowknife series around the dome of granite into which the complex is intruded.

MAP 8 - 2 SKETCH MAP OF THE STRUCTURE AND FACIES OF THE SNARE METASEDIMENTARY BELT



Shelf sediments ruled, eugeosynclinal sediments stippled. Shelf and continental sediments also occur in the East Arm sub-province (Map 8 - 1). Note that the complex lies close to the extrapolated shelf--eugeosyncline transition. The axis of the belt runs approx. N.N.E.

Two periods and trends of faults may be distinguished. The earlier forms north-south sinistral faults such as the Wop - May, and Snare River Emile River lineaments. These are continuous with those of the Slave province and probably represent reactivated basement trends. The second set runs north-east parallel to an 875 m.y. dyke swarm and cuts the Coppermine River sediments.

Around the contact between the Snare sediments and Slave province a narrow zone of structural conformity has developed in which the fold systems of both provinces have been rotated to form a steeply plunging isoclinal pattern parallel to the contact (Ross 1966). According to Wilson (1948) this contact zone is also a region of slide planes and high angle reverse faults, one of which forms the Snare lineament.

It is this lineament which passes as a series of N-S faults through the centre of Bigspruce Lake. It extends from Russel lake to the Emile River at least a distance of 170km, with, typically, a sinistral displacement of 0.7 - 1km.

Post Snare Geology.

Post orogenic conglomerates, sandstones, and quartzites of the Hornby group overlie Snare sediments in the region of the Great Bear Lake.

This sequence is cut by dykes of the Mackenzie swarm (1,315 m.y.) which stretches for 1,600 km from the Churchill, to the Slave and Bear provinces. The swarm is focused on the Coppermine River area and representatives of this swarm are present in the country rock around the B.S.L. alkaline complex.

Within the dyke focus, also, lies the basic and ultramafic tholeitic Muskox intrusion (1,120m.y.) and the thick little deformed sequence of tholeitic Coppermine lavas (c.1,100 m.y.).

These lavas are overlain by 12,000m of conglomerate sandstone and sandy shale forming the Coppermine sedimentary series.

The Relationship of Bigspruce lake to the regional geology.

Map figs. 2-2, 8-1, & 8-2 illustrate the relationship of the alkaline intrusion to the faulting, Bear-Slave boundary and Snare facies belts. Four features stand out -

1. The intrusion lies on the extrapolation of the Snare lineament, a major transcurrent fault within the basement.

2. It lies at the intersection of this lineament with another major East-West or Northeast-Southwest lineament.

3. It lies close to the western margin of the Slave province within a lobe of granitic rock which projects across the trend of the Bear-Slave boundary.

4. The age of the intrusion ($1820^{+}_{-}20$m.y.), is only slightly younger than the age of uplift of the Snare granites and metasediments.

The Snare lineament as traced from the aerial photographs is not a single fault plane but a series of bifurcating faults of which the Main fault

A-A, the east coast lineament B-B, and Snare fault C-C, form a part. Although the fault displaces Snare sediments south of Kwejinne Lake (N. end of Map fig 2-1) it is evident that part of the displacement on this fault system was synchronous with the intrusion of the alkaline complex. The evidence for this is -

1. The fault A-A bisects centre 1. It displaces the gabbro, diorite and some of the olivine-magnetite-pyroxenites but does not displace the ring syenite 3. It is intruded by magnetite-pyroxenites and biotite-peridotites.
2. The East coast lineament B-B also displaces the diorite and pyroxenites but it is intruded by a series of en-echelon dolomite dykes. The margins of the fault have suffered riebeckite-pyrochlore metasomatism from the carbonatite which stands out on the aeromagnetic map. The plane of the fault is paralleled by a series of peralkaline syenite pegmatites in centre 2.
3. The Snare fault shows sinistral displacement of the country rock but displaces the syenite-granite contact dextrally.
4. The fault A-A exactly bisects centre 1. The fault C-C exactly bisects centres 2 and 3.

These faults, then, appear to have controlled the location of each phase of the intrusion. Displacement on the faults seems to have been closely related to shift of the intrusive centre, from centre 1 to centre 2, and again from centre 2 to centre 3. It must be regarded as probable that the differentiating magma chambers were located within the shattered rock at the intersection of the two-fault systems.

In addition to bisecting the intrusion the two fault systems bisect the lobe of Slave granodiorites. Because of the rim of Yellowknife age sediments and volcanics, and because of the undeformed Snare sediments which overlap on to that series, this pattern is interpreted as a post-Snare doming of the basement. The central location of the alkaline intrusion, and of the synchronous faults implies a causal relationship, possibly through the addition of much differentiated basic material to the surrounding lower crust. A similar doming is found around the intrusion of Napak and other alkaline-carbonatite bodies where it has been explained as due to the intrusion of tabular basic bodies, or to the addition of material during fenitization (in Heinrich 1966).

Ginzburg (1962) and Heinrich (1966) have stressed that alkaline-carbonatite complexes are frequently associated with faulted continental marginal flexures (e.g. East Greenland), and of similar age to the bordering metamorphic terraine. In addition such intrusions are often located at fault intersections. King and Sutherland (1960), and Bailey (1964) have commented on the close association of the African examples with arching, doming, and faulting, and also with reactivated basement structural trends (as is the Snare lineament). Such doming and faulting appears to be a necessary requirement for the concentration and release of volatiles which are an essential characteristic of these types of intrusion.

The situation has some analogies to oil reservoirs. The mantle is the source of the magma, the CO_2, H_2O and other volatiles; the doming and flexure of the geosynclinal margin has produced a trap, and the synchronous faulting, and fault intersection has provided a conduit.

Geochemical trends and the magma series.

The geochemical and petrological relationships of the units within each centre, and of the centres with each other, has been discussed in chapters 3, 4, 5, 6, 7. A summary of the probable differentiation trends based on the chilled whole-rock compositions of each intrusive unit is given on the CaO-Na_2O-K_2O and MgO - FeO- $Na_2O + K_2O$ triangular diagrams Figs 8-1 and 8-2.

Three dominant trends may be defined:

1. High potassic trend; Biotite-pyroxenite to shonkinite
2. Alkali saturated trend; Alkali gabbro-alkali diorite-quartz free syenite (Larvikite) - quartz syenite-comendite.
3. Alkali undersaturated trend; Alkali gabbro-quartz free syenite (Lardalite) - foyaite - tinguaite.

As has been stressed earlier these trends do not represent successive stages in the differentiation of single magma chambers because the sequence of intrusion particularly of the porphyry dykes indicates the co-existence of many of the magmas; for instance, the co-existence of the pyroxenite, gabbro, diorite, syenite, and lardalite magmas, and of the foyaite and comendite magmas. Rather the trends are made up of short segments representing the fractionation of the gabbro, diorite, quartz free syenite, quartz syenite or undersaturated syenite magmas isolated within independent magma chambers and indicate the generalized pattern of a family of fractionation paths.

The alkali saturated trend.

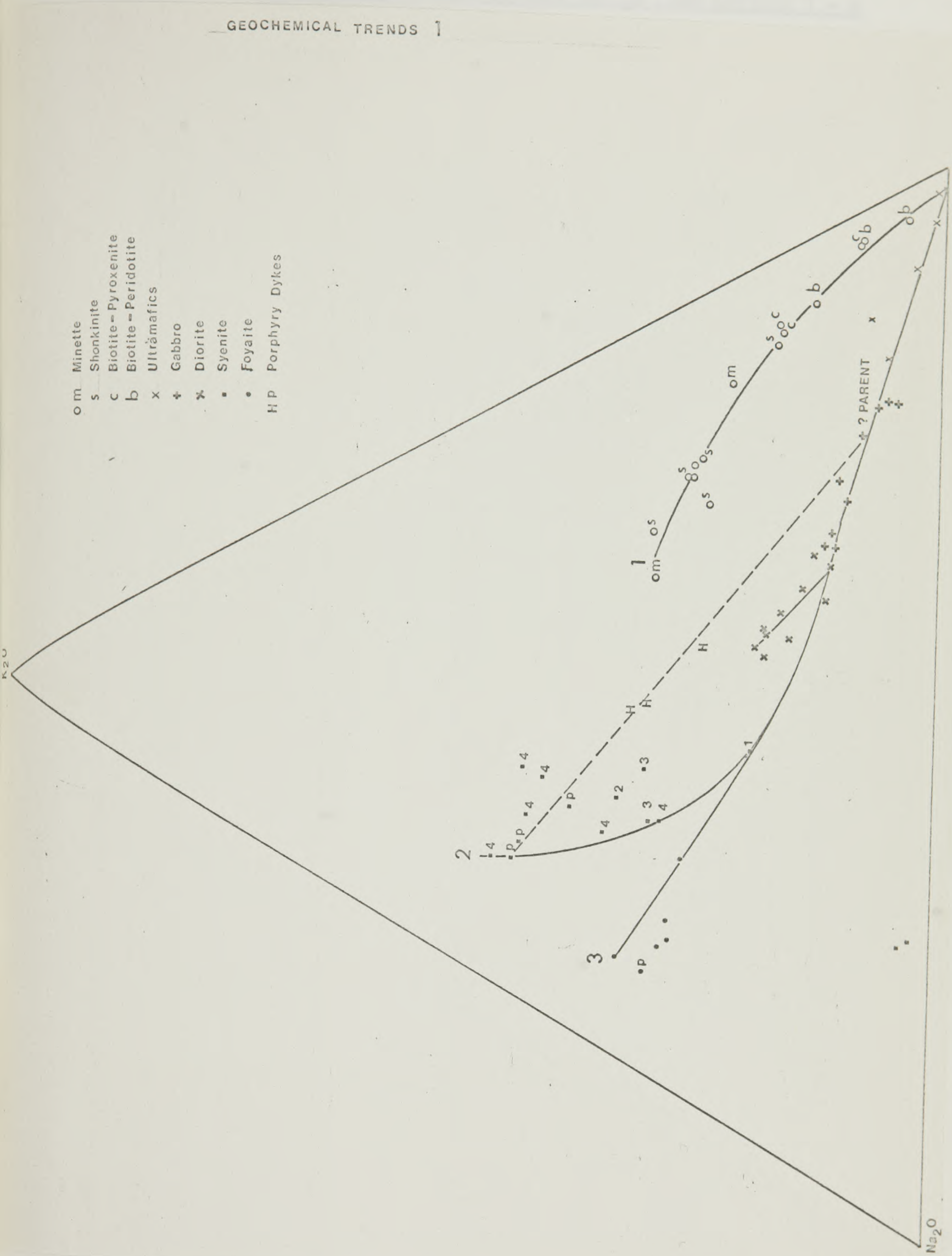
This is particularly true of the alkali saturated trend in which there are a series of short linear fractionation paths representing the feldspar porphyries, gabbros, diorites and quartz syenites breaking away towards the directions of SiO_2, $Na_2O + K_2O$, and K_2O enrichment from the basic trend representing by the non-phenocrystic chilled rocks. This parent trend follows an initial course of calcium depletion with soda enrichment accompanied by only a slight increase in the Fe : Fe + Mg ratio and in the K: K + Na ratio. The phenocryst phases in the basic porphyries, chilled gabbro, chilled diorite and syenite S_1, show that the dominant fractionating phase over this part of the trend was pyroxene together with minor olivine and calcic plagioclase. On intrusion, however, in each case, plagioclase zoned to alkali feldspar became the main fractionating phase, and amphibole appeared corroding or rimming pyroxene. In consequence the residual liquids show an enrichment in potassium relative to sodium and in silica.

At the composition of the soda rich quartz free syenite S_1, this trend is peaked, and thereafter follows a course of potash enrichment. The separation of alkali feldspar which is the dominant phenocryst

FIG 8 - 1

SUMMARY OF THE GEOCHEMICAL TRENDS FROM CENTRES 1 - 4

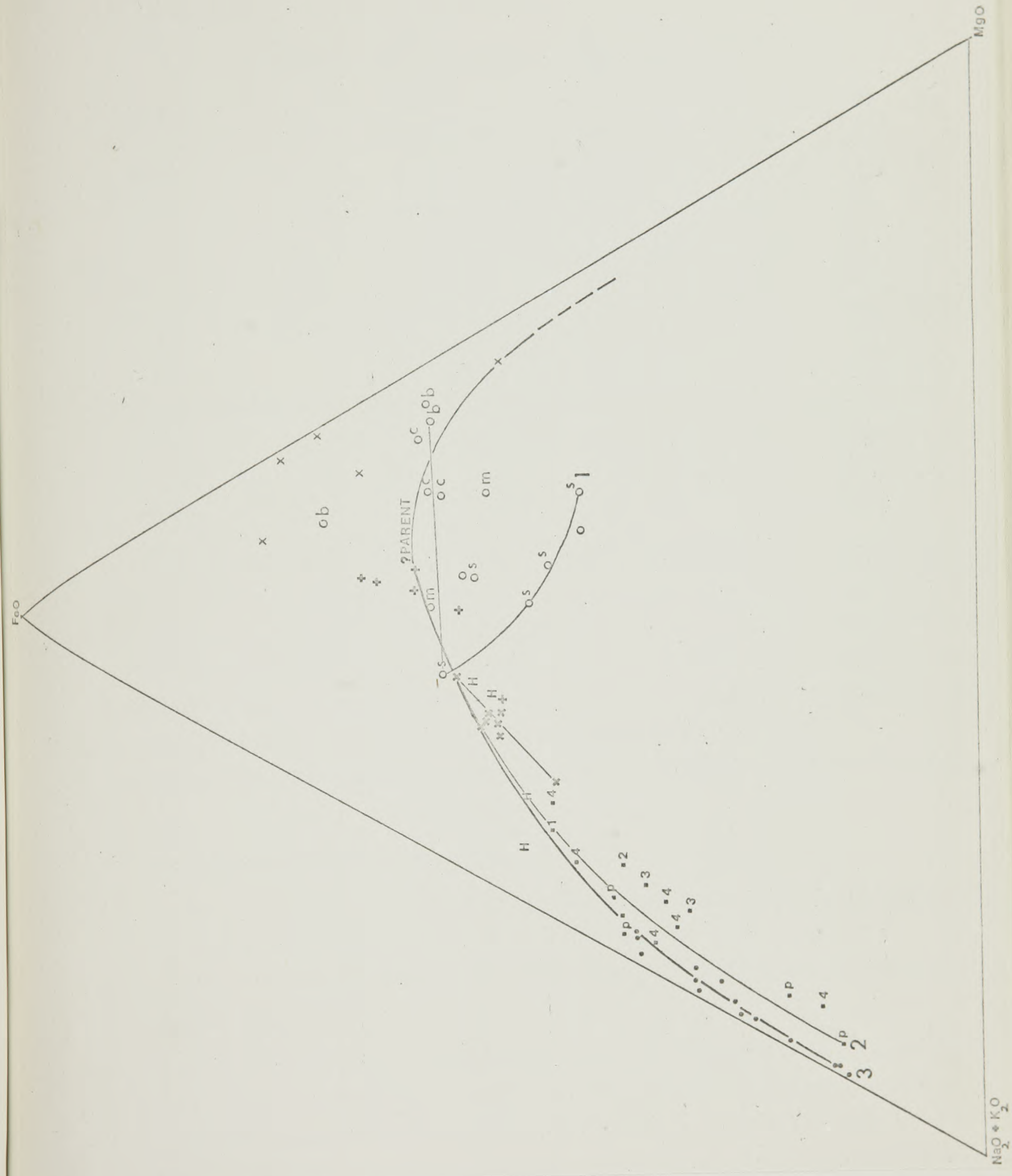
$CaO-Na_2O-K_2O$ DIAGRAM



Trend 1. High potassic rocks; Trend 2. saturated alkaline series; Trend 3. undersaturated alkaline series. Note how the porphyry dykes and the diorites, lie along linear paths divergent from the main trend, and how the saturated and undersaturated trends converge towards a composition slightly more basic than the S_1, syenite.

FIG 8 - 2 SUMMARY OF THE GEOCHEMICAL TRENDS FROM CENTRES 1 - 4

$MgO-FeO-(Na_2O + K_2O)$ DIAGRAM



"Trend" 1. High potassic rocks; Trend 2. saturated alkaline series; Trend 3. undersaturated alkaline series.

phase in all the other syenites is followed by an abrupt decrease in the Ba : K ratio. Throughout there is a progressive parallel increase in the zirconium and niobium concentrations and a decrease in strontium. The most sensitive index of the stage of fractionation is the strong decrease in the ratio Mg : Mn.

The parameters of this sequence are :-

	$\frac{Ca}{Ca+Na+K}$	$\frac{Fe}{Fe+Mg}$	$\frac{K}{K+Na}$	$\frac{Mg}{Mn}$	$\frac{K}{Ba}$	Nb+Zr	Sr
67293	0.59	0.55	0.20	73	9	107	1,870
67340	0.36	0.65	0.26	38	5	139	1,600
68360	0.25	0.75	0.23	21	3	267	1,020
67327	0.16	0.69	0.31	30	43	167	1,020
67103	0.17	0.71	0.30	28	69	773	460
67267	0.09	0.70	0.40	14	-	278	257
67199	0.08	0.88	0.42	-	-	508	113
67R38	0.14	0.90	0.39	10	194	1,170	105
These compare with the foyaite trend parameters of							
67374	0. 7	0.99	0.27	0.59	25	207	1,060
68051	0.15	0.89	0.25	4.10	12	1,000	1,340
2835	0.06	0.68	0.25	15.43	33	806	1,700

The position of S_1(68360) at the convergence of the sodic undersaturated and saturated trends on figs 8-1, 8-2, and 5-1 is in agreement with the low K : Ba ratio and with its composition close to the thermal saddle in the normative Qtz - Ne - Ks projection (fig 5-1). However, on the evidence of the porphyry dykes which respectively contain 0.5% quartz and 2% normative nepheline at intermediate compositions in the two trends, the true divergence is believed to stem from a gabbroic composition.

The alkali undersaturated trend.

On the $CaO-Na_2O-K_2O$ projection the sodic undersaturated series continues the trend of calcium depletion with constant K: K+Na ratio seen in the saturated trend but the Fe: Fe + Mg ratio increases more rapidly and to a higher degree.

Pyroxene, apatite and oxide remain fractionating phases in the porphyry dykes up to the appearance nepheline and sanidine phenocrysts at a "foyaite" composition. As in the saturated series the course of fractionation as represented on the Qtz - Ne - Ks projection follows a thermal trough, towards a minimum melting composition, from the albite-orthoclase tie line.

The high potassic trend.

Although the extrapolations of the saturated and undersaturated trends converge at a common gabbroic composition, the extrapolation of the potassic series is towards a parent composition equivalent to the biotite peridotite, greatly enriched in Ca: Na + K + Ca, and Mg: Mg + Fe relative to the gabbro. The trend of the series is practically linear indicating the depletion of calcium with only a slight increase in the

Fe: Fe + Mg ratio. This is somewhat surprising if the source of the feldspar in the shonkinite has indeed been through the fractionation of olivine/in place of biotite as suggested for the Western Rift high potassic rocks (Holmes and Harwood 1932), and implies an olivine with a Mg: Fe ratio comparable to the liquid.

In view of the fused granitic xenoliths described from such rocks, for instance in the Western Rift, and in the Navajo area (Williams 1936) and the hybridization of the shonkinite in the breccia pipes, the assimilation of feldspar from the granodiorites must be considered plausible. This addition, however, cannot initiate the characteristic enrichment in K, Ba, Sr, Rb, Nb, Zr, La, Ce, or Rb: K, or K: K+Na, since the xenoliths are in fact enriched in these (Holmes and Harwood 1932). Such assimilation is in agreement with the relatively high $Sr^{87/86}$ and low Sr, Nb and Zr found for the feldspathic potassic rocks by Bell and Powell (1969).

The latent heat of fusion of the assimilated granite can only be accounted for by the precipitation of co-existing mafic phases, possibly of the type found in the olivine-biotite-pyroxenite xenoliths. It is considered probable that the source of the shonkinites lies between the alternative paths.

Biotite-peridotite → Shonkinite + olivine cumulate + volatiles
(e.g.Buell Park)

Granite + Biotite-peridotite → Shonkinite + biotite - pyroxenite.

Physical conditions of intrusion.

a) Volatiles. It is evident from the abundance of amphibole, biotite, apatite, calcite and fluorite that all the magmas were rich in volatiles on intrusion.

Within centres 1, 2 and 3 these volatiles were dominantly H_2O and F, now contained within, amphibole, biotite and fluor - apatite. The absence of these phases from the olivine-biotite-pyroxenites and from the foyaites does not imply a volatile deficiency since the former is surrounded by a broad fringe of sericitization and is marginally amphibolitized whilst the foyaites are rimmed by fenites.

Within centres 4 and 5 the dominant volatiles are H_2O, F and CO_2, reflected in the abundance of biotite, calcite, fluorite and zeolite, and in the fluid vesicles in pyroxene. In the carbonatites the abundance of F results in the presence of fluor-apatite, fluor-biotite, cerium fluor-carbonate and fluorite; water has produced the hydration of nepheline to gieseckite, zeolite, analcite or cancrinite; the presence of chlorine is indicated by scapolite, and sodalite.

The effect of dissolved F and Cl is to lower the viscosity, and melting temperature of the magmas, and to greatly increase the solubility of H_2O, in the magma. A second effect is to increase the solubility of alkali silicates in a possible aqueous vapour phase (van Groos 1966).

Van Groos has demonstrated that in a silica poor volatile rich system three fluid phases may co-exist.

a) an alkali-silicate melt rich is dissolved volatiles.

b) a carbonate rich melt rich in volatiles especially water.

c) a vapour phase consisting mainly of H_2O and CO_2 but with alkali silicates in solution.

This situation may be represented in the biotite-peridotites in which are found calcite vesicles, and in the biotite-pyroxenites in which the fenites contain the vesicles. The vapour phase provides a possible fenitizing agent.

The source of the volatiles is believed to be the mantle, in particular the fluid inclusions noted by Roedder (1965) in peridotite nodules which may be mantle xenoliths. The release of these volatiles, present only to the extent of 60 - 500ppm, may be through shearing produced during transcurrent movement along the Snare lineament.

b) Depth. There is no direct method by which an estimate of the contemporary thickness of overlying rock can be obtained. However, the intrusive style is of high leval subvolcanic type with ring dykes, small layered intrusions, breccia pipes, and cone sheets. There is a close correspondence between the oversaturated and undersaturated trends and the 1kb pH_2O synthetic systems. A tentative upper limit is given by the fact that north and south of Bigspruce lake at the margin of the Slave province the K-Ar ages of biotite are slightly lowered whilst those of muscovite are unaffected. Taking a geothermal gradient of 30°C/km and a blocking temperature of 180°C this gives an upper limit of 6km.

c) Temperature. The temperatures deduced for the intrusive phases are strongly influenced by the assumption of a typically high volatile content and a total vapour pressure of 1kb. By analogy to the relevant synthetic systems these temperatures are believed to be in the vicinity of

Olivine-magnetite-pyroxenite	1100 - 1200°C
Quartz-free syenites	870 - 970°C
Comendite	720 - 800°C
Foyaites	750 - 800°C
Fluorite-calcite carbonatite	575 - 600°C
Dolomite carbonatite	520 - 570°C

Limiting conditions are given by the presence of mesoperthite Or_{37} in in the fenites of both foyaites, biotite-pyroxenite and gas-escape vents - circa 620°C at 1kb, and its absence from the carbonatite margins; by the presence of cryptoperthite Or_{50} in the shonkinites; by the incongruent melting of aegirine at 990°C for the ijolites, tinguaites, foyaites and comendites, by the replacement reactions in the dolomite breccias with upper limits of 520 - 570°C.

The magnetite-pyroxenite, syenite S_1, comendite, foyaites, ijolite and fluorite-sovite correspond closely in composition to the minima in the

systems Ol - Cpx - Iron oxide 1300°C (Presnall 1966). 1kb $Ab-Or-H_2O$ 865°C (Tuttle and Bowen 1958), $Ab-Or-Qtz-Ac-H_2O$ 720°C (Carmichael and Mackenzie 1963), $Ne-Ks-Qtz-H_2O$ 750°C (Hamilton and Mackenzie 1965), $Ne-Ac-Na_2O.4SiO_2$ 908°C (Bailey and Schairer 1966), $Ap-Ca(OH)_2 - CaF_2 - CaCO_3$ 575°C (Wyllie 1966).

Comparisons with other alkaline provinces.

The Bigspruce lake complex falls within the normal pattern of subvolcanic ring complexes and layered intrusion complexes found in the alkaline provinces of Quebec, West Greenland, and South-west Africa. In each there are alkali gabbros, syenites, quartz syenites and foyaites similar in composition to those of Bigspruce lake. In addition each contains representative carbonatite and high potassic rocks which form only a small proportion of the intrusive rocks.

In the Monteregian province, in particular, a series of small bodies composed of plugs, ring dykes and cone sheets within cylindrical conduits are arranged along the axis of a northwest trending arch (Gold 1967). The parent magma is believed to be a nepheline normative olivine-titan-augite gabbro, and three fractionation trends are recognised by Gold. Firstly a saturated trend leading to quartz syenites and alkali gabbros, secondly a saturated trend leading to syenites, and thirdly an under-saturated trend leading to foyaites. Diatremes and breccia pipes associated with alnoites and kimberlites are common in the vicinity of the carbonatite complex of Oka.

Magnetite-pyroxenites are present in the Monteregian province (Yamaska), and Gardar province (Narssaq) but differ in that the field evidence appears to suggest an origin through crystal accumulation.

The provinces also differ in possessing a more basic magnesian early gabbro phase which in the Monteregian province is undersaturated, and in the Damaraland province is dominantly tholeitic. In the Gardar province both the gabbros and syenites have very much lower iron oxidation ratios and are relatively impoverished in volatiles. Fayalite-augite syenites and fayalite foyaites are common, and the differentiation trends show a much greater enrichment in iron.

Bigspruce lake differs from individual intrusions in these provinces in containing a far wider variety of rock types and in being an isolated intrusion outside any known province.

On structural grounds other similar intrusions might be expected along the Snare lineament, or along the Snare-Slave boundary where the two are separated. There are no comparable aeromagnetic highs, nor bodies of igneous rock known along these directions.

The subsiduary complex of high potassic feldspathic rocks is also on a larger scale and distinct in composition from the alnoites, kimber-

lites and lamprophyres of the above provinces. It is however closely comparable in form and composition to the dyke and pipe intrusions of the Navajo area.

The olivine-magnetite-pyroxenites in their chilling lamination, concentric zonation and association with saussuritized gabbro are closer to the Alaskan zoned complexes than to the metasomatic or cumulate jacupirangites associated with cone-form carbonatites. For, the ring complexes such as Magnet Cove, Afrikanda or Jacupiranga typically contain nepheline-rich rocks such as urtites, malignites, or ijolites, and the pyroxenites are rich in apatite, and surrounded by fenites.

Possibly partial fusion in the mantle, fractionation of the derivative magmas, and assimilation of shattered country rock at a variety of levels along the Snare lineament fault plane accounts for this diversity, and the doming of the basement may have brought together magma types which would otherwise have formed independent contrasted complexes.

Certainly this fault has had a controlling influence over the complex in the release of volatiles, the location of magma chambers, and the triggering of new intrusive phases.

APPENDIX 1 METHODS OF ANALYSIS.

a) WHOLE ROCK ANALYSIS

In order to adequately cover the very extensive range of rock types found within the intrusion it was necessary to analyse at least 100 rocks. For this reason, and because the same method was applicable to both the major and trace elements, x-ray fluorescence analysis was chosen in preference to chemical methods. The greater degree of error inherent in the analysis of the major elements in comparison with classical chemical analysis was accepted as a consequence of selecting a rapid method.

Details of the technique and of the sources of error have been exhaustively described by Liebhafsky et al (1960), Adler (1966) and Norrish and Chappell (1967).

The major element analyses were made in three batches using a standard Phillips PW 1540 spectrograph 1KW, 2KW, and PW 1212 automatic spectrograph respectively. The machine conditions used have therefore varied but comparison of triplicate analyses shows that results obtained are extremely similar. The trace element analyses were all made using the PW 1540 spectrograph.

The samples were first reduced in size by jaw-crusher, the larger samples divided into six or three, and powdered in a Tema agate swing mill to a uniform grain-size entirely less than 200 mesh. The undiluted powders were mixed with 2-4 drops of aqueous Mowiol cement solution, and briquetted at 4 tons into 2.5 cm tablets without containing rims. The minimum weight of powder used was 3-4g giving a minimum tablet thickness of 3-4mm. The same tablet was used for major and trace element analysis.

The method relies on the fact that subject to certain assumptions concerning the sample and excitation conditions (see Norrish and Chappell pp 183-4) the intensity of the fluorescent

radiation 'I' is proportional to the concentration of the analysed element 'C' divided by the mass absorption coefficient of the sample U

$$\text{viz} \qquad I = \frac{KC}{U}$$

since the absorption coefficients of a sample depend dominantly on the major elements present, if the fluorescent intensities of all the major elements are measured then using an iterative calculation it is possible to determine the mass absorption of a sample at a given wavelength and hence the actual concentration. The mass absorption at any wavelength U is calculated according to the equation.

$$\Sigma U = U_{\lambda a} \times Ca + U_{\lambda b} \times Cb + \ldots\ldots\ldots\ldots$$

Where $U_{\lambda a}$ is the mass absorption coefficient of element a at wavelength λ, and Ca is the concentration of element a.

A computor programme devised for this calculation (Holland and Brindle 1966) was kindly loaned by Dr. J.G. Holland.

For trace element analysis the total mass absorption U may be determined directly by measuring the attenuation of the x-ray beam through a thin film of the rock powder. Details of this method as used have been given by Pankhurst (1968). These measured mass absorptions were determined in duplicate and are reproducible to within $\pm$ 1%. Since no major absorption edges are crossed in the wavelength range Fe K_α - Ba K_α the measured mass absorptions are proportional over this range (R. Goodman pers comm). The mass absorptions were therefore determined at the Sr K_α wavelength at the centre of the range and the same values used for the traces Ni, Zn, Rb, Y, Sr, Zr, Nb, La, Ce, Ba. Using these mass absorptions and accurately analysed standards determined by independant methods a linear calibration, passing through the origin was obtained for each of these elements. A W tube and Li 110 crystal was used in each case and an empirical correction of the form.

$$\text{Background } Bp = I_L + K\,(B_H - B_L)$$

Ip = Background beneath the peak

B_L, I_H = The lower and higher backgrounds on either side of the peak

used to correct for non linearity of the background. The results for La are semi-quantative only due to interference. The results for Y and Zr have been corrected for interference from the Rb K_β (16% RbK_α), and Sr K_β (11% Sr K_α) respectively. For Rb, Y, Sr, Zr, Nb and Ba (over 50ppm) the results are reproducible to within $\pm$ 3% in the range 10-500ppm.

In major element analysis many sources of error become more significant. The chief sources of these are

1. Mass absorption
2. Grain size
3. The mineral matrix
4. Statistical counting error

The most important is probably the lack of accurately known mass absorption coefficients. The accuracey of the tables available is only about 2-5% which means that the accuracey of the method cannot be better than this. Of these, the tables of Birks and Heinrich have been found to give comparable results significantly better than the older tables of Liebhafsky. The source of this difference lies in the very much higher absorption coefficients of the elements Fe, Ti and Mn at long wavelengths determined by Heinrich which markedly improves the concentrations determined for SiO_2, Al_2O_3 and MgO.

The grain size of the sample is critical in determining the homogeneity to x-rays of the tablet particularly at long wavelengths where excitation is essentially a surface phenomenum. It can be shown that for long wavelengths it is not possible to grind most samples sufficiently finely to eleminate a strong grain-size: intensity

relationship. It is therefore important that all samples including the standards should have similar grain size and grain size distribution.

A similar problem is that of grain orientation, in which for instance micas tend to become orientated parallel to the tablet surface during compression and hence present an above average surface area. This effect is reduced by fine grinding, and fortunately in these samples no difficulty in grinding mica rich rocks has been encountered.

Matrix effects result either from the enhancement of one element's fluorescent intensity by another for instance Fe by Zn, or from a peak shift due to the coordination site or valency of an element. Enhancement effects are probably slight, and could be considered as negative absorption. Peak shift may be a source of the very significant errors sometimes found in the analysis of Al, and necessitates closely comparable mineralogy between the unknown and standards.

For most elements the count rates and peak to background ratios are sufficient keep statistical counting error at a very low level. For Na, Mg, and P in the absence of a Ge crystal to eliminate CaK_{α_2} interference, statistical counting error is significant.

All these sources of error have been kept at a minimum by using a consistent grinding method, fine grain size, and standards of comparable composition and mineralogy.

The standards used were rocks from the Gardar province, East Greenland alkali province, Ascension island and Skye.

An estimate of the quality of the analyses may be grained by comparison of the chemical and X.R.F. analyses of rocks from Scourie, Bigspruce Lake and elsewhere.

As may be seen from the asterisks, errors in the chemical analyses of the standards may often be a very significant source of error. This error is reduced but not eliminated by using 16-30 W.R. standards.

COMPARISON OF CHEMICAL AND XRF ANALYSES

	67-30		40430		65-12		65-179	
	c	x						
SiO_2	45.76	47.24	44.19	44.95	48.72	48.26	47.26	46.36
Al_2O_3	12.26	13.00	13.00	16.04	15.38	15.54	7.81	8.48
FeO	21.46	20.98	16.47	15.91	12.43	13.05	11.51	11.18
MgO	5.55	5.09	3.19	3.21	8.26	8.26	21.38	21.87
CaO	9.75	9.20	7.76	7.27	10.33	10.29	8.35	8.19
Na_2O_3	-	-	-	-	-	-	-	-
K_2O	0.06	0.07	2.28	2.22	0.32	0.41	0.13	0.14
TiO_2	2.06	2.05	3.38	3.35	1.04	1.05	0.35	0.36
MnO	-	-	0.27	0.24	-	-	-	-
P_2O_5	-	-	2.88	2.73	-	-	-	-

	14377		65-18		67-66		12955	
	c	x						
SiO_2	53.34	53.82	57.54	58.52	62.13	62.84	72.24	72.88
Al_2O_3	18.79	19.30	19.51	18.10	16.60	15.66	13.79	13.20
FeO	9.19	9.21	5.67	5.53	5.57	5.70	2.76	2.75
MgO	4.01	3.27	2.76	3.14	2.79	2.93	0.47	0.44
CaO	9.00	8.97	6.64	6.96	6.48	6.60	1.30	1.44
Na_2O	-	-	-	-	-	-	-	-
K_2O	0.47	0.44	0.89	0.93	0.50	0.55	5.12	4.91
TiO_2	0.91	0.94	0.96	0.99	0.78	0.79	0.36	0.41
MnO	0.20	0.23	-	-	-	-	0.03	0.02
P_2O_5	0.-9	0.09	-	-	-	-	0.07	0.05

Bigspruce Lake Samples

SiO_2	51.48[x]	54.84	62.76	62.79	49.09	51.18	50.41	51.69
Al_2O_3	17.44[x]	14.87	14.49	14.81	21.13	22.92	13.43	13.47
FeO	9.16	9.90	5.36	8.21	4.86	5.28	12.27	12.36
MgO	3.86	3.78	0.90	1.19	0.28	0.27	4.17	4.01
CaO	6.16	6.19	3.05	2.73	3.74	3.06	8.09	7.49
Na_2O	-	4.80	-	-	10.79	10.89	3.18	3.26
K_2O	-	2.62	5.30	5.24	6.97	5.35	4.29	3.73
TiO	2.17	2.05	0.63	0.66	0.21	0.40	2.48	2.66
MnO	0.14	0.19	0.13	0.12	0.16	0.19	0.20	0. 24
P_2O_5	0.38	0.39	0.09	0.10	0.95[x]	0.10	0.75	0.75

	67336	67106	67351	68021

The calibration for each element is computed, in the above programme, by fitting a least squares quadratic to the mass absorption corrected intensity: concentration values of the standards.

b) NEPHELINES

An estimate for the Na:K ratio in the separated nephelines was obtained by x-ray powder photography. The mineral was extracted with a drill from thin slices of rock, taking unalterred crystals or zones of crystals. The samples were powdered under acetane with one third added silicon powder as an internal standard and mounted in a fine capillary CuK_α filtered radiation was used. Both the $21\bar{3}0$ and $20\bar{2}2$ reflections for each nepheline sample were measured using the internal standard line at 28.4 65 Å, and a vernier scale with an interval of $0.01^{\circ}20$.

As the nephelines were believed to have crystallized in a volatile rich system in the presence of feldspar at a temperature of 700 - 750°c and at a pressure of 0.5 - 1.5 kb the calibration curve of Hamilton and Mackenzie (1960) for silica saturated nephelines at 700°c and 1.5kb PH_2O was used in preference to that of Smith and Sahama. The results obtained are:

			% Ne
2821	Coarse s. foyaite	core	72.1
		rim	72.1
67130	Chilled s. foyaite		68.9
2835	Nepheline-sandine porphyry		72.7
2701	Ijolite	core	72.0
67283	Ijolite		73.4
67001	Urtite; S. foyaite		73.6

c) FELDSPARS

The K: Na + Ca ratio of separated alkali feldspars was also determined by x-ray powder photography. Because even the optically homogeneous feldspars of the shonkinites were found to be cryptoperthites, all the feldspar powders, have been heated at 106[illegible]°c

for 24 hrs, in Pt capsules, in a Johnson Mathey tube furnace, prior to x-ray analysis. In a very few cases fusion at the grain boundaries was found, and a lower temperature and a new sample was used.

The samples were mixed in the proportion 1:10 with $KBrO_2$ before mounting in a fine capillary. The composition was obtained using the position of the $\bar{2}01$ reflection (Orville 1958, Wright 1968), and corrected for structural state (Wright 1968). The internal standard line at 20.205° and a vernier scale of 0.01°2θ were used.

The results obtained are.

		% Or
67007	Tinquaite phenocryst	Or 66
2821	Coarse foyaite, plate	Or 73
67003	" " "	Or 65
67195A	Chill foyaite; plate	Or 72
67312	Contact fenite	Or 58
67190	Inner fenite zone	Or 47
67195B	Syenite fenite	Or 31
67134	Syenite fenite vein	Or 37
68037	Aegirine-syenite fenite	Or 36
68394	Coarse shonkinite	Or 52
68010	Coarse shonkinite	Or 48
67103	Nordmarkite phenocryst	Or 33
67327	Syenite phenocryst	Or 37
67148	Peralkaline dyke	Or 37
67R38	Comendite dyke	Or 41

REFERENCES CITED

Adler, I.	1966	X-Ray emission spectrography in Geology. Elsevier, 257 pp.
Baragar, W.R.A.	1966	Geochemistry of the Yellowknife volcanic rocks. Can. J. Earth Sci., 3, 9-30.
Bailey, D.K. & Schairer, J.F.	1964	The peralkaline residua system: Na_2O - Al_2O_3 - Fe_2O_3 - SiO_2. Carnegie Inst. Washington, Ann. Rept. Direct. Geophys. Lab. 1963-1964, pp 74 - 79.
Bailey, D.K. & Schairer, J.F.	1966	The system Na_2O - Al_2O_3 - Fe_2O_3 - SiO_2 at 1 atmosphere. J. Petrol. V.7. 114-170.
Bearth, P.	1959	On the alkali massif of the Werner Bjerge in East Greenland. Medd om Gronland, Bd.153, Nr.4, pp 1-62.
Bell, R.	1900 (1902)	Geol. surv. Can. Annual Rept. v.12. rept A p.103.
Bhattacharji, S.	1967	Scale model experiments on flowage differentiation in sills. In ultramafic and related rocks. Wyllie (ed), Wiley, New York. p. 69.
Bhattacharji, S. & Smith, C.H.	1964	Flowage differentiation. Science, 145, 150-153.
Bowes, D.R. & Wright, A.E.	1961	An Explosion - Breccia Complex at Back Settlement, Near Kentallen, Argyll. Trans. Edin. Geol. Soc. v.18. 293-314.
Bowes, D.R. & Wright, A.E.	1967	The Explosion - Breccia pipes near Kentallen, Scotland, and Their Geological Setting. Roy. Soc. Edin. Trans. v.67. No. 5. 109-143
Brögger, W.C.	1921	Die Eruptivgesteine des Kristianiagebietes. IV Das Fengebiet in Telemarken, Norwegen. Norske Videns. Skrift Mat - Naturv. Kl. 1920 No.9.
Brögger, W.C.	1933	Die Eruptivgesteine des Oslogebietes. pt. VII Die chemische Zusammensetzung der Eruptivesteine des Oslogebietes. Skrifter av det Norske viden. oslo No.1 8-147
Carmichael, I.S.E.	1967	The mineralogy and petrology of the volcanic rocks from the Leucite Hills Wyoming. Contrib. Min. and Pet. v.15.

Carmichael, I.S.E. & Mackenzie, W.S.	1963	Feldspar - liquid equilibria in pantellerites: an experimental study. Amer. J. Sci. v. 261. pp. 382-396.
Daly, R.A.	1933	Igneous Rocks and the Depths of the Earth. McGraw-Hill, New York.
Dawson, J.B.	1962	Sodium carbonate lavas from oldoinyo Lengai, Tanganyika. Nature, 195, 1075-1076.
Dawson, J.B.	1964	An aid to prospecting for kimberlites. Econ. Geol. 59, pp 1385-1386.
Deer, W.A, Howie, R.A. & Zussman, J.	1962	Rock-forming minerals. v.1-5. Longmans. London.
Dresser, J.A. & Denis, T.C.	1944	Geology of Quebec, vol. 11. Quebec Dept. Mines Geol. Rept.20
Drever, H.I. & Johnston,R.	1967	Picritic minor intrusions. In ultramafic and related rocks. Wyllie (ed). Wiley. New York. p.71-76
Von Eckermann, H.	1948	The process of nephelinization. Intern. Geol. Congr. 18th Sess. Great Britain, 111, 3-6.
Von Eckermann, H.	1948	The genesis of the Alnö alkaline rocks. Intern. Geol. Congr. 18th Sess. Great Britain, 111, 94-101.
Von Eckermann, H.	1966	Progress of Research on the Alnö Carbonatite. In Tuttle and Gittins (ed) 1966. Carbonatites. Wiley. New York. p. 3-31.
Edwards, A.B.	1938	Tertiary lavas from the Kerguelen Archipelago, B.A.N.Z. Antarctic Expedition (D. Mawson) 1929-1931, Rept, Rept., ser. A, pt 5, pp. 72-100, No.2, 1938.
Erickson, R.L. & Blade, L.V.	1963	Geochemistry and petrology of the alkalic igneous complex at Magnet Cove, Arkansas. U.S. Geol. surv. Prof. Paper 425.
Fahrig, W.F. & Wanless, R.K.	1963	Age and significance of diabase dyke swarms of the Canadian shield. Nature, 200 (4910), 934.
Faust, G.T.	1949	Dedolomitization, and its relation to a possible derivation of a magnesium - rich hydrothermal solution. Amer. Min. v.34, 789-803

Fudali, R.F.	1957	On the origin of pseudoleucite. Reviews and abstracts, Trans. Amer. Geophys. Union. v.38.p.391.
Fudali, R.F.	1963	Experimental studies bearing on the origin of pseudoleucite and associated problems in alkalic igneous rock systems. Geol. Soc. Amer. Bull. 74. 1101-1126.
Garson, M.S.	1965	Carbonatites in Southern Malawi. Malawi Geol. Surv. Bull. 15.
Ginzburg, A.I., ed.	1962	Geology of Rare-element Deposits, 17. Geological structure and Mineralogical characteristics of Rare-Metal Carbonatites. Gosgeoltekhizat, Moscow.
Gold, D.P.	1967	Alkaline ultrabasic rocks in the Montreal area, Quebec. In ultramafic and related rocks. Wyllie (ed). Wiley, New York p.228-297.
Green, D.C. Badsgaard, H. & Cumming, G.L.		Geochronology of the Yellowknife area, Northwest Territories, Canada. Can. J. Earth Sci. v,5. 725-735
Koster van Groos, A.F.	1966	The effect of NaF, NaCl, and Na_2CO_3 on the phase relationships in selected joins of the system Na_2O - CaO - Al_2O_3 - SiO_2 - H_2O at elevated temperatures and Pressures. Unpublished D. Phil thesis University of Leiden.
Hamilton, D.L. & Mackenzie, W.S.	1960	Nepheline solid solution in the system Na $AlSiO_4$ - $KALSiO_4$ - SiO_2. J. Pet. 1.pp56-72.
Hamilton, D.L. & Mackenzie, W.S.	1965	Phase-equilibrium studies in the system Na $ALSiO_4$ (nepheline) - $KALSiO_4$ (Kalsilite) - SiO_2 - H_2O. Min. Mag. 34. 214-231
Hargreaves, R.B.	1962	Petrology of the Allard Lake Anorthosite Suite, Quebec. In Petrologic studies. Buddington volume. Geol. Soc. Amer. p.163-190.
Heinrich, E.W.	1966	The Geology of carbonatites, Rand McNally. Chicago. 555 pp.
Henderson, J.F. & Brown, I.C.	1952	The Yellowknife greenstone belt. Geol. Surv. Can., Paper 52-28.
Higazy, R.A.	1954	Trace elements of volcanic ultrabasic potassic rocks of Southwestern Uganda and adjoining part of the Belgian Congo. Bull. Geol. Soc. Am. 65 pp 39-70.

Hoffman, P.F.	1968	Precambrian stratigraphy sedimentalogy, palaeocurrents and palaeoecology in the East Arm of Great Slave Lake, District of Mackenzie Can. Geol. surv. Paper 68-1, part A pp 140-142.
Holland, J.G. & Brindle, D.W.	1966	A self-consistent mass absorption correction for silicate analysis by x-ray fluorescence. spectrochim. Acta 22 (12), 2083-93.
Holmes, A.	1950	Petrogenesis of katungite and its associates. Am. Mineral., 35, 772-792
Holmes, A & Cahen, L.	1957.	Geochronologie Africaine 1956. Accad. Roy. Sci. Coloniales (Brussels) classe Sci. Med. Mem. in 8°, N.S., 5.
Holmes, A & Harwood, F.	1932	Petrology of the volcanic fields east and southeast of Ruwenzori, Uganda. Quart. J. Geol. Soc. 88, 370-442.
Holmes, A. & Harwood, F.	1937	The petrology of the volcanic area of Bufumbira. Geol. Surv. Uganda Mem. 3. Pt.2.
Hori, F.K.	1964	On the role of water in heat transfer from a cooling magma. Tokyo Univ., Coll. Gen. Education, Sci. Papers, v.14, p.121-127.
Irvine, T.N.	1963	Origin of the ultramafic complex at Duke Island, Southeastern Alaska. Mineralog. Soc. American Spec. Paper 1, p.36-45
Irvine, T.N.	1967	The Duke Island ultramafic complex, southeastern Alaska. In ultramafic and related rocks. Wyllie (ed) Wiley. New York. p.84-96
James, T.C.	1959	Carbonatite investigation - progress report. Tang. Geol. surv. Rec. V11 (1957), 65.
Jolliffe, A.W.	1948	The North-west part of the Canadian Shield. Int. Geol. Congr. v.3 pp 141-149.
Kempe, D.R.C.	1966	The mineralogy of the kangerdlugssuaq alkaline intrusion, East Greenland. Unpublished D.Phil. Thesis. University of Oxford 266 pp.
Kesler, S.E. & Heath, S.A.	1968	The effect of dissolved volatiles on magmatic heat sources at intrusive contacts. Amer J. Sci. v. 266 824-839.

Kidd, D.F.	1933	Great Bear Lake Area, Northwest Territories. Geol. Surv. Canada, Sum. Rept. 1932 pt.C. 1-36.
Kidd, D.F.	1936	Rae to Great Bear Lake, Mackenzie District, N.W.T. Geol. Surv. Canada, Mem. 187.
King, B.C.	1965	Petrogenesis of the alkaline igneous rock suites of the volcanic and intrusive centres of eastern Uganda. J. Petrol. v.6, 67-100.
King. B.C. & Sutherland, D.S.	1960	Alkaline rocks of eastern and southern Africa pt 1-111 Sci. Progr., 48, 298-321, 504-524, 709-720.
Knill, D.C.	1969.	The Permian igneous rocks of Devon. Bull. Geol. Surv. Great Britain. No.29 p.115-138.
Kukharenko, A.A. & Dontsova, E.I.	1962	A contribution to the problem of the genesis of carbonatites. Recon. Geol. USSR, 1,(3-4) 31-46 (English translation 1964).
Lambert, R. st. J.	1964	The Bigspruce Lake Nepheline - Syenite complex, Snare River, Northwest Territories: a preliminary report. Unpublished report to the Boreal Institute 9 pp.
Larsen, S.E. & Pardee, J.T.	1929	The stock of alkaline rocks near Libby Montana. J. Geol. v.37, pp 97-112.
Leech, G.B. Lowdon, J.A. Stockwell, C.H. & Wanless, R.K.	1963	Age determinations and geological studies (including isotopic ages - report 4) Can. Dept. Mines. Tech. Surv. Can. Paper 63-17.
Liebhafsky, H.A., Pfeiffer, H.G. Winslow, E.H. & Zemany, P.E.	1960	X-Ray absorption and emission in analytical chemistry. Wiley, 357 pp.
Lord, C.S.	1942	Snare River and Ingray Lake Map-areas, Northwest Territories. Can. Dept. Mines and Resources. Geol. surv. Mem 235. 55 pp.
Luth, W.C.	1967	Studies in the System $KAlSiO_4$ - Mg_2SiO_4 - SiO_2 - H_2O: I Inferred Phase Relations and Petrologic Applications. J. Petrol. v.8 p.372-416.
Martin, H. Mathias, M. & Simpson, E.S.W.	1960	The Damaraland sub volcanic ring complexes in South-West Africa. 21st Intern. Geol. Congr. Copenhagen, Repts. 13, 156-174.

Mathias, M.	1956	The Petrology of the Messum Igneous Complex, South-West Africa. Trans. Geol. Soc. S. Afr., v. 59 pp 1-35.
Moore, J.G.	1962	K/Na ratio of cenozoic igneous rocks of the western United States. Geochem. cosmochim. Acta, v.26, 101-130.
Noble, J.A. & Taylor, H.P. Jr.	1960	Correlation of the ultramafic complexes of southeastern Alaska with those of other parts of North America and the world. 21st Intern. Geol. Congr. Copenhagen, Rept. 13, 188-197.
O'Hara, M.J.	1965	Primary magmas and the origin of basalts. Scot. J. Geol. V.1. 19-40.
O'Hara, M.J. & Yoder, H.S.Jr.	1967	Formation and fractionation of basic magmas at high pressures. Scot. J. Geol. v.3. pp 67-117
Orville, P.M.	1958	Feldspar investigations. Ann. Rep. Dir. Geophy. Lab. Carnegie Inst. Washington, p.206.
Oxburgh, E.R.	1964	Petrological evidence for the presence of amphibole in the upper mantle and its petrogenetic and geophysical implications, Geo. Mag. 101, 1-19.
Pakiser, L.C. & Zietz, I.	1965	Transcontinental Crustal and upper-mantle structure. Rev. Geophys, 3, 505-520.
Pankhurst, R.J.	1968	Strontium isotape and age studies in N.E. Scotland. Unpublished D.Phil thesis, University of Oxford.
Pecora, W.T.	1956	Carbonatites, a review. Bull. Geol. Soc. Am., 1537-1556.
Powell, J.L. Hurley, P.M. & Fairbairn, H.W.	1966	The Strontium isotopic composition and origin of carbonatites. In Tuttle and Gittins (ed) 1966. Wiley. New York. p. 365-378.
Presnall, D.C.	1966	The join forsterite - diopside - iron oxide and its bearing on the crystallization of basaltic and ultramafic magmas. Amer. J. Sci. 264 pp 763-809.
Roedder, E.	1965	Liquid CO_2 inclusions in olivine bearing nodules and phenocrysts from basalts. Am. Mineral, 50 1746-1782.

Ross, J.V.	1966	The structure and metamorphism of Mesa Lake Map area, District of Mackenzie Geol. Surv. Can. Bulletin 124. 39 pp.
Ruckmick, J.C. & Noble, J.A.	1959	Origin of the ultramafic complex at Union Bay, southeastern Alaska. Geol Soc. Amer. Bull. v.70 981-1018.
Saether, E.	1958	The alkaline rock province of the Fen area in Southern Norway. Kong. Norskevidensk. Skrifter, 1957, No. 1.
Shand, S.J.	1939	On the staining of feldspathoids and on zonal structure in nepheline. Amer. Min., 24, 508-513.
Shaw, D.M.	1968	A review of K-Rb fractionation trends by covariance analysis. Geochim et Cosmochim. Acta. v.32 573-601.
Simkin, T.	1967	Flow differentiation in the picritic sills of North Skye, in ultramafic and related rocks. Wyllie (ed) Wiley, New York. p.64-68.
Simpson, E.S.W.	1954	The Okenjeje Igneous Complex, south -west Africa. Trans Geol. Soc. S. Afr. 57, 125-172.
Smith, W.C.	1956	A review of some problems of African carbonatites. Quart J. Geol. Soc. London, 112, 189-219.
Sörensen, H.	1960	On the agpaitic rocks. Intern. Geol. Congr. 21st Sess., Pt XIII, pp 319-327
Stockwell, C.H.	1964	Fourth report on structural provinces, orogenies, and time-classification of the Canadian Precambrian Shield; In Age determinations and geological studies, Geol. surv. Can., Paper 64-17, pt. II pp 1-21.
Streckeisen, A.	1952	Das Nephelinsyenit - Massif von Ditro (siebenbürgen). Schweiz. Miner und Petrog. Mitt. v. 32. 251-302.
Taylor, H.P. Jr.	1967	The zoned ultramafic complexes of southeastern Alaska. In ultramafic and related rocks. Wyllie (ed) Wiley New York p.97-118.
Tilley, C.E.	1958	Problems of alkali rock genesis. Quart J. Geol. Soc. London, 11, 323-360.
Tomkeieff, S.I.	1961	Alkalic ultrabasic rock and carbonatites in the U.S.S.R. Intern. Geol. Rev. 3 (9), 739-758.

Turner, F.J. & Verhogen, J.	1960	Igneous and Metamorphic Petrology. 2nd Ed. McGraw - Hill, New York.
Tuttle, O.F. & Bowen, N.L.	1958	Origin of granite in the light of experimental studies in the system $NaAlSi_3O_8$ - $KAlSi_3O_8$ - SiO_2 - H_2O. Geol. Soc. Am. Mem. 74.
Tuttle, O.F. & Gittins, J. (Editors)	1966	Carbonatites. Wiley - Interscience, London and New York.
Upton, B.G.J.	1960	The structure and petrology of the Kungnat syenite complex, S.W. Greenland. Unpublished D. Phil thesis, University of Oxford.
Upton, B.G.J.	1967	Alkaline pyroxenites.In ultramafic and related rocks, Wyllie (ed), Wiley. New York, P. 281-288.
Vacquier V. Steenland, N.S. Henderson, R.G. & Zietz, I.	1952	Interpretation of aeromagnetic maps. Geol. Soc. Amer. Mem. 47. 151 pp.
Verhoogen, J.	1962	Distribution of titanium between silicates and oxides in igneous rocks. Amer J. Sci v. 260, 211-220.
Wager, L.R.	1965.	The form and internal structure of the alkaline kangerdlugssuaq intrusion, East Greenland. Miner. Mag. 34, 487-97.
Wager, L.R. & Wadsworth, W.J.	1960	Types of igenous cumulates. J. Petrol., 1, 73-85.
Watson, K.D.	1967	Kimberlites of eastern North America. In ultramafic and related rocks. Wyllie (ed). Wiley New York. p.321-322.
Williams, H.	1936	Pliocene volcanoes of the Navajo - Hopi country. Bull. Geol. Soc. Am., 47, 111-172.
Wilson, J.T.	1941	Structural features in the North-west Territories, Amer J. Sci., v. 239 pp 493-502.
Wilson, J.T.	1948	Some aspects of geophysics in Canada with special reference to structural research in the Canadian Shield, Pt. 2. Trans. Amer Geophys. Union, v. 29, pp 691-726.
Washington, H.S.	1917	Chemical analyses of igneous rocks. U.S. Geol. Surv. Prof. Pap. 99.

Watts, W.S. 1966 Chemical analyses from the Gardar igneous province south Greenland. Grön. Geol. undersögelse. Rpt. 6. 92 pp.

Wyllie, P.J. 1966 Experimental studies of carbonatite problems. The origin and differentiation of carbonatite magmas. In Tuttle and Gittins (ed) 1966. Carbonatites. Wiley. New York p.311-352.

Wyllie, P.J. Cox, K.G. & Biggar, G.M. 1962 The habit of apatite in synthetic systems and igneous rocks. J. Petrol., 3, 238-243.

ADDENDUM

Bailey, D.K. 1964 Crustal warping - a possible tectonic control of alkaline magmatism. Geophys. Research, v.6. p.1103-1111

Bell, K. & Powell, J.L. 1969 Strontium isotopic studies of alkalic rocks: The potassium-rich lavas of the Birunga and Toro-Ankole regions East and Central Equatorial Africa. J. Petrol. v.10 p.536-572.

Birks, L.S. 1963 Electron probe microanalysis. Wiley- Interscience, New York.

Clark, S.P. (ed.) 1966 Handbook of physical constants. Revised edition. Geol. Soc. Am. Mem. 97.

Folinsbee, R.E. 1941 The chemical composition of garnet associated with cordierite. Am. Min. v.26 p.50-53.

Gittins, J. 1966 World distribution of carbonatites in "Carbonatites" Tuttle and Gittins (ed) Wiley-Interscience, London and New York.

Gittins, J. Macintyre, R.M. & York, D. 1967 The ages of carbonatite complexes in Eastern Canada. Can. J. Earth Sci. v.4 p.651-655

Green, D.C. 1967 Age and isotope studies on the Prosperous Lake granites. Unpublished Ph.D. thesis University of Alberta, Edmonton.

Griffin, W.L. & Murthy, V.R. 1969 Distribution of K, Rb, Sr, and Ba in some minerals relevant to basalt genesis. Geochim. Cosmochim. Acta, v.33 p.1389-1414.

Gunn, B.M. 1965 K/Rb and K/Ba ratios in Antarctic and New Zealand tholeiites and alkali basalts. J. Geophys. Research 70. p.6241-6247.

Harris, P.G. 1957 Zone refining and the origin of potassic basalts. Geochim. Cosmochim. Acta v.12 p.195-208

Heinrich, S. 1966 X-ray absorption uncertainty. In "The electron microprobe" p. 296. Wiley New York.

Kumarapeli, P.S. & Saull, V.A. 1966 The St. Lawerence valley system: A North American equivalent of the East African rift valley system. Can.J. Earth. Sci v.3 p.639-658.

Larsen, E.S. 1940 Petrographic province of Central Montana Bull. Geol. Soc. Am. v.51 p.887-948.

Morse, S.A. 1962 The Kiglapait layered intrusion coast of Labrador, Canada. Miner. Assoc. Canada 7th Ann. meeting p.1-12.

Norrish, K. & Chappell, B.W. 1967 X-ray fluorescence spectrography In "Physical methods in determinative mineralogy" J. Zussman (ed) Academic Press. London. p. 161-214

Shand, S.J. 1931 The granite-syenite-limestone complex of Palabora, eastern Transvaal and its associated apatite deposits. Trans. Geol. Soc. South Africa v.34 p.81-105.

Wade A. & Prider, R.J. 1940 The leucite-bearing rocks of the west Kimberly area, western Australia. Quart. J. Geol. Soc. London. v.96 p.39-98.

Wager, L.R. & Brown, G.M. 1968 Layered igneous rocks. Oliver & Boyd.

Wilson, M.E. 1965 The Precambrian of Canada: The Canadian Shield. In "The Precambrian" v.2 Rankama (ed). Wiley-Interscience. London p.263-418.

Winkler, H.G.F. 1967 Petrogenesis of metamorphic rocks. Revised 2nd edition. Springer-verlag Berlin.